Titre: Title:	Development of Microwave Heating-Assisted Catalytic Reaction Process: Application for Dry Reforming of Methane Optimization
Auteur: Author:	Sepehr Hamzehlouia
Date:	2017
Type:	Mémoire ou thèse / Dissertation or Thesis
Référence: Citation:	Hamzehlouia, S. (2017). Development of Microwave Heating-Assisted Catalytic Reaction Process: Application for Dry Reforming of Methane Optimization [Ph.D. thesis, École Polytechnique de Montréal]. PolyPublie. https://publications.polymtl.ca/2750/

URL de PolyPublie: PolyPublie URL:	https://publications.polymtl.ca/2750/
Directeurs de recherche: Advisors:	Jamal Chaouki
Programme: Program:	Génie chimique

UNIVERSITÉ DE MONTRÉAL

DEVELOPMENT OF A MICROWAVE HEATING-ASSISTED CATALYTIC REACTION PROCESS: APPLICATION FOR DRY REFORMING OF METHANE OPTIMIZATION

SEPEHR HAMZEHLOUIA

DÉPARTEMENT DE GÉNIE CHIMIQUE

ÉCOLE POLYTECHNIQUE DE MONTRÉAL

THÈSE PRÉSENTÉE EN VUE DE L'OBTENTION

DU DIPLÔME DE PHILOSOPHIAE DOCTOR

(GÉNIE CHIMIQUE)

AOÛT 2017

UNIVERSITÉ DE MONTRÉAL

ÉCOLE POLYTECHNIQUE DE MONTRÉAL

Cette thèse intitulée:

DEVELOPMENT OF A MICROWAVE HEATING-ASSISTED CATALYTIC REACTION PROCESS: APPLICATION FOR DRY REFORMING OF METHANE OPTIMIZATION

présentée par : HAMZEHLOUIA Sepehr

en vue de l'obtention du diplôme de : Philosophiae Doctor

a été dûment acceptée par le jury d'examen constitué de :

M. PERRIER Michel, Ph. D., président

M. CHAOUKI Jamal, Ph. D., membre et directeur de recherche

M. DOUCET Jocelyn, Ph. D., membre

M. DE LASA Hugo Ignacio, Ph. D., membre

DEDICATION

To Mom and Dad who showed me how to live, and to Sina who lived it by my side

ACKNOWLEDGEMENTS

I would like to express my most sincere gratitude to my research supervisor, Prof. Jamal Chaouki, for his boundless mentorship, guidance, and support in both professional and personal levels as well as generous financial support for the duration of this research. The completion of this thesis would have not been possible without his enormous contributions.

I would like to reserve special thanks to my parents who supported me both financially and emotionally through all the pains and happiness, to make me be believe I have the potential to fulfill my dreams. Also, special tribute to my twin brother, who always challenged me to reach my hidden potentials and gave me hope to direct my endeavors to the way of a better future.

I would also like to thank my PhD thesis committee, Prof. Hugo de Lasa, Prof. Michel Perrier and Dr. Jocelyn Doucet for their careful review of my work and constructive input. Moreover, I would like to express my gratitude to Prof. Lahcen Saydy for representing the director of the graduate studies.

Furthermore, I would like to thank Natural Sciences and Engineering Research Council of Canada (NSERC), Total-NSERC chair, Polytechnique Montreal Department of Chemical Engineering and Centre d'Entrepreneuriat Poly-UdeM for providing their generous financial support.

Moreover, I would like to thank our industrial partners at Total, especially Dr. Shaffiq Jaffer for investing countless hours reviewing my work and providing invaluable input.

Additionally, I would like to extend my gratuities to all my colleagues in the Process Engineering Advanced Research Lab (PEARL), in particular Dr. Mohammad Latifi, Dr. Jaber Shabanian, Dr. Majid Rasouli, Dr. Sherif Farag and Mr. Philippe Leclerc for sharing their personal and professional experience with me as well as their valuable advices and assistance. I would also like to thank Mr. El Mahdi Lakhdissi for his much-appreciated assistance with translating the abstract of the thesis to French. Furthermore, I would like to acknowledge Dr. Ali Kashani for the revision of the scientific articles. I would like to further acknowledge Dr. Rahmat Sotudeh-Gharebagh, Dr. Navid Mostoufi and Dr. Reza Zarghami for their endless scientific support and constructive advices.

In addition, I would like to express my gratitude to Mr. Sylvain Simard-Fleury, Mr. Daniel Pilon and Mr. Robert Delisle for the technical support and the development of the experimental setups.

Moreover, I would like to thank Mr. Gino Robin, Ms. Martine Lamarche and Mr. Jean Huard for their endless support with the chemicals and gases purchasing.

Finally, I would like to thank Mr. Diego del Angel Salas, Ms. Selima Ben Khelifa, Ms. Ghita Bouanane El Edrisi, MS. Helena Miata-Bouna Ms. Abidah Bachoo, Mr. Sami Chaouki and Ms. Aya Kanso for their assistance with the experimental aspect of the study through various internship programs.

RÉSUMÉ

Les ressources conventionnelles de combustibles à base de pétrole sont en train de subir une période transitoire de déclin à cause des préoccupations environnementales liées à l'extraction, le traitement, l'application et aussi à l'épuisement irrépressible des réserves disponibles. Actuellement, le pétrole constitue le vecteur énergétique prédominant qui contrôle 33% du marché mondial d'énergie tandis que 1697.6 milliards barils estimés globalement comme réserves disponibles vont couvrir à peine la demande universelle en énergie pour les 50 prochaines années. Par conséquent, le secteur énergétique est rapidement inspiré de chercher une feuille de route alternative pour la perspective de la demande mondiale. Le gaz naturel, mélange de hydrocarbures légers dominé par le méthane comme constituant principal a été délibéré comme candidat robuste grâce à sa distribution mondiale, sa disponibilité et aussi ses diverses applications. Ainsi, grâce à la forte croissance de l'offre et à la conformité avec les politiques environnementales mondiales strictes, le gaz naturel a été fortement considéré comme l'énergie la plus croissante et le ressource de la production chimique. Toutefois, la distribution générale des ressources de gaz naturel sous forme d'hydrate dans les régions éloignées, les zones désertes et au fond des océans a suscité une controverse liée à l'accessibilité, le transport et les activités de manipulation.

La conversion du méthane en produits chimiques à valeur ajoutée a été fortement considérée pour remédier aux déficiences associées en conséquence au transport, à la manipulation et à la distribution des composants gazeux. Or, le procédé proéminent menant à la conversion du méthane au gaz de synthèse a été mis en évidence comme une approche substantielle pour préserver un cycle d'énergie carboneutre pour la perspective prospective d'énergie. Le gaz de synthèse, un mélange gazeux vraisemblablement dominé par l'hydrogène et le monoxyde de carbone est une matière première robuste pour une multitude de procédés de fabrication de produits chimiques et aussi énergivores. Subséquemment, plusieurs approches scientifiques ont été implémentée pour convertir le méthane en gaz de synthèse, substantiellement, les procédés du vaporeformage (SRM), l'oxydation partielle (POx) et le reformage à sec du CO_2 (DRM). Simultanément, le procédé DRM a été renommé comme la méthode de conversion du méthane la plus avantageuse grâce aux avantages environnementaux, au ratio de composition du produit (H_2/CO) et la flexibilité du procédé. Initialement étudié par Fischer et Tropsch, le reformage à sec du méthane est une réaction endothermique menant à un ratio H_2/CO proche de l'unité et ainsi offrant une possibilité stimulante de convertir le gaz de synthèse en produits chimiques, en méthanol, et des hydrocarbures à longue

chaine particulièrement à travers le procédé de Fischer-Tropsch. De plus, le mécanisme du DRM permet de réaliser la conversion des deux composants clés des gaz à effet de serre à savoir CO_2 et CH_4 et permettant ainsi d'établir un avantage environnemental instantané. Toutefois, et à cause des multiples équilibres thermodynamiques, le procédé de reformage à sec DRM est fortement affecté par la production de sous-produits indésirables associée aux réactions secondaires en phase gazeuse à savoir la dégradation thermique du méthane, la réaction de la conversion à la vapeur d'eau et la dismutation du monoxyde de carbone. L'évolution de la réaction secondaire en phase gazeuse diminue drastiquement la sélectivité des composants du gaz de synthèse et mène ainsi à un produit de mauvaise qualité. Par conséquent, plusieurs études concentrées principalement sur le développement d'un système catalytique à haute performance ont été rapportées. Cependant, l'application industrielle du reformage à sec a été bloquée à cause de la non disponibilité d'un catalyseur efficace et économique et aux grands besoins en énergie. Bien que plusieurs études portant sur le design et l'optimisation du catalyseur pour résoudre le problème de sélectivité ont été rapportées dans la littérature, le manque d'études portant sur l'effet de la méthode de chauffage est évident.

Le développement des sources d'énergie renouvelables à savoir l'énergie solaire et éolienne a été reconnu comme une opportunité remarquable pour répondre aux exigences du marché énergétique et en même temps être conforme à la réglementation environnementale stricte pour protéger la planète contre une destruction irrémédiable. Or, les progrès récents concernant les techniques de production et de récolte, la dégradation et l'épuisement des réserves de combustibles fossiles, les procédés en série et la disponibilité spontanée des matières premières ont développé des critères pour diviser les ressources d'énergie renouvelable en ressources non rentables économiquement et à des ressources largement accessibles. Par conséquent, l'avènement des ressources d'énergie renouvelable rentable économiquement et écologiques prévoit une opportunité appréciée pour produire rapidement une électricité propre et accessible. Ainsi, l'opportunité d'obtenir une électricité renouvelable abordable offre une perspective exceptionnelle d'effectuer des réactions chimiques via des méthodes de traitement électromagnétiques à savoir, le chauffage par induction, le chauffage par ultrasons et le chauffage à micro-ondes.

Ainsi, pour remédier aux déficiences susmentionnées et relatives au procédé du reformage à sec DRM et plus généralement relatives aux conséquences liées aux réactions gaz-solide, la présente étude propose l'application du chauffage à micro-ondes pour l'optimisation des réactions

catalytiques gaz-solide. Les avantages majeurs de la méthode de chauffage à micro-ondes comprennent le chauffage sélectif, uniforme et volumétrique, une densité de puissance élevée, un contrôle de température instantané, une consommation d'énergie réduite, une sélectivité de réaction élevée, moins de limitations liées au transfert de chaleur, la flexibilité du procédé et la portabilité de l'équipement. Toutefois, la caractéristique clé de la méthode de chauffage à micro-ondes est associée au mécanisme exclusif de chauffage sélectif. Quand les matériaux sont exposés aux radiations micro-ondes, leur niveau d'énergie interne est augmenté en fonction des leurs propriétés diélectriques projetées et qui sont liées aux caractéristiques physiques et structurels. Cependant, le matériau principal le plus utilisé à savoir les composés gazeux échouent à projeter une interaction significative avec les micro-ondes à cause de l'insuffisance de leurs propriétés diélectriques. Par conséquent, et contrairement aux méthodes conventionnelles de chauffage, le mécanisme de chauffage à micro-ondes établit un gradient de température significatif entre la phase solide diélectrique et la phase gazeuse pour les réactions catalytiques gaz-solide. Ainsi, la température locale élevée sur les sites actifs du solide favorise la réaction catalytique tandis que la température faible du gaz permet de limiter la perspective des réactions secondaires en phase gazeuse. Par conséquent, le présent travail de recherche est classifié en trois sections principales :

1) La préparation de l'activateur du catalyseur/récepteur des micro-ondes : le récepteur des micro-ondes a été développé dans un réacteur à lit fluidisé pour le dépôt chimique en phase vapeur (FBCVD). Ainsi, le carbone a été déposé sur un substrat de sable de silice en utilisant le méthane dans un équipement de chauffage par induction. L'effet des conditions opératoires à savoir la température et le temps de réaction sur les propriétés de la couche de revêtement a été déterminé. Ainsi, la composition, l'épaisseur et la morphologie de la couche de revêtement en carbone a été examinée pour plusieurs conditions opératoires. Finalement, la performance des particules de sable de silice revêtues en carbone (C-SiO_2) a été évaluée dans un lit fluidisé utilisant le chauffage à micro-ondes à l'échelle laboratoire. Il a été démontré que les particules C-SiO_2 présentent une interaction exceptionnelle avec les micro-ondes grâce à leurs propriétés diélectriques significatives. Les particules C-SiO_2 développées ont été recommandées pour leur application comme récepteur à micro-ondes et support/activateur de catalyseur pour les réactions catalytiques gaz-solide.

2) L'importance du mécanisme de chauffage : l'effet du mécanisme de chauffage à micro-ondes sur la réaction d'oxydation sélective gaz-solide a été étudié par la simulation de la

conversion du *n*-C_4 en MAN sur le catalyseur VOP dans un réacteur à lit fluidisé à l'échelle industrielle. Il a été démontré qu'en fonction des propriétés diélectriques des composants, un gradient de température persiste entre le gaz et le solide. A cause de l'incapacité de mesurer directement le profil de température du gaz, les profils de température de la surface du solide et le profil de température du mélange ont été obtenu à l'aide des méthodes de radiométrie et thermométrie dans un réacteur à lit fluidisé chauffé à micro-ondes à l'échelle laboratoire. Ainsi, l'effet des conditions opératoires de la température et la vitesse superficielle du gaz sur les profils de température associés a été étudié. En outre, des corrélations ont été proposées pour estimer le profil de température de gaz à travers le lit en utilisant les données expérimentales et le bilan énergétique. Les profils de température du gaz, du solide et du mélange ont été utilisés après pour comparer le chauffage conventionnel et à micro-ondes pour la conversion de *n*-C_4 et la sélectivité du MAN dans l'étude de simulation. Les résultats ont révélé que le chauffage à micro-ondes est supérieur en terme de la productivité de la réaction.

La réaction catalytique assistée par micro-ondes : le reformage à sec du méthane dans un réacteur à lit fluidisé chauffé à micro-ondes à l'échelle laboratoire a été effectué pour étudier l'effet du mécanisme de chauffage sur l'évolution des produits. Ainsi, l'effet de la température de fonctionnement sur la conversion des réactifs et la sélectivité des produits désirés, H_2 et CO a été rigoureusement étudié. Il a été conclu que le chauffage à micro-ondes favorise les réactions catalytiques tout en limitant les réactions secondaires en phase gazeuse indésirables.

ABSTRACT

Conventional petroleum-based fuel resources are undergoing a transition decline period due to the environmental concerns associated with the extraction, processing and application, and the irrepressible depletion of the available reserves. Presently, oil has been the predominant energy vector, regulating 33% of the global energy market, while the 1697.6 thousand million barrels globally estimated available reserves will barely cover the universal energy demands for the next 50 years. Consequently, the energy sector is promptly inspired to pursuit alternative roadmap for the global demand outlook. Natural gas, a mixture of light hydrocarbons dominated by methane as the principal constituent, has been deliberated as a robust candidate due to the global distribution and availability, and the diverse applications. Accordingly, due to the strong supply growth and compliance with the strict global environmental policies, natural gas has been highly regarded as the fastest growing energy and chemical production resource. However, the general distribution of the natural gas resources in the hydrate format in remote regions, the deserted areas and the ocean beds, has aroused controversy associated with the accessibility, transportation and handling activities.

The conversion of methane to value-added chemicals has been highly regarded, to address the deficiencies associated with the transportation, handling and distribution of the gaseous components, correspondingly. Whereas, the prominent processes leading to the conversion of methane into syngas has been highlighted as a substantial approach to preserve a carbon-neutral energy cycle in the prospective energy outlook. Syngas, a gaseous mixture presumably dominated by hydrogen and carbon monoxide is a robust feedstock for multiple energy intensive and chemical production processes. Subsequently, numerous scientific approaches have been implemented to convert methane into syngas, substantially, steam reforming (SRM), partial oxidation (POx), and CO_2 (dry) reforming processes (DRM). Meanwhile, the DRM process has been renowned as the most advantageous methane conversion method due to the environmental benefits, product composition ratio (H_2/CO) and the process flexibility. Initially investigated by Fischer and Tropsch, the dry reforming of methane is an endothermic reaction concluding a H_2/CO ratio close to unity, providing a stimulating possibility to convert syngas to chemicals, methanol, and long-chain hydrocarbons particularly, through the Fischer-Tropsch process. Moreover, the DRM mechanism accomplishes the conversion of the two key greenhouse gas components, CO_2 and CH_4, establishing an instantaneous environmental advantage. However, due to multiple thermodynamic

equilibria, the DRM process is heavily affected by the production of the undesired by-products associated with the secondary gas-phase reactions, namely, thermal degradation of methane, water gas shift reaction and carbon monoxide disproportionation. The evolution of the secondary gas-phase reactions drastically diminishes the selectivity of the syngas components and concludes a lower quality product, respectively. Hence, various studies, majorly concentrated on the development of a high performance catalytic system, have been reported. However, the industrial application of dry reforming has been stalled due to the scarcity of an effective and economical catalyst and high energy requirements. Although various investigations regarding the catalyst optimization and design has been reported in the literature, to address the selectivity issue, the lack of studies demonstrating the effect of the heating method is evident.

The development of the renewable energy resources, namely, solar and wind power, have been acknowledged as a remarkable opportunity to maintain the demanding energy market, while comply with strict environmental regulation to persevere the planet from further irretrievable destruction. Whereas, the recent advances in the production and harvesting methods, depletion and exhaustion of the fossil fuel reserves, mass production processes and spontaneously available feedstock has developed renewable energy criteria from economically unfeasible to highly affordable and accessible resources. Consequently, the advent of the economically feasible and environmental friendly renewable energy resources stipulates an esteemed opportunity to promptly produce clean and affordable electricity. Therefore, the expediency of the affordable renewable electricity provides an exceptional prospect to preform chemical reactions via electromagnetic processing methods, namely; induction heating, ultrasound heating and microwave heating, correspondingly.

Thus, to address the aforementioned deficiency with the DRM process, and the correlated consequence for the gas-solid reactions in general, the present study proposes the application of microwave heating for the gas-solid catalytic reactions optimization. Major advantages of the microwave heating method have been underlined as, uniform, selective, and volumetric heating, high power density, instantaneous temperature control, reduced energy consumption, high reaction selectivity, less heat transfer limitations, process flexibility and equipment portability. However, the key feature of the microwave heating method is associated with the exclusive selective heating mechanism. While materials are exposed to microwave radiation, their internal energy level is enhanced based on the projected dielectric properties, associated with the physical and structural

characteristics. However, most common material, namely, gaseous components, fail to project significant microwave interaction due to the lack of sufficient dielectric properties. Consequently, unlike the conventional heating methods, microwave heating mechanism establishes a significant temperature gradient between the dielectric solid phase and the gas phase in the gas-solid catalytic reactions. Hence, the higher local temperature on the solid active sites promotes the catalytic reactions while the lower gas temperature restricts the prospect of the secondary gas-phase reactions, correspondingly. Therefore, the present research study is classified into three major sections correspondingly:

1) Microwave Receptor/Catalyst Promoter Preparation: A microwave receptor has been developed by fluidized bed chemical vapor deposition (FBCVD) of carbon using methane over silica sand substrate material in an induction heating setup. The effect of the operating conditions, namely temperature and reaction time, on the properties of the coating layer was attained. The composition, thickness and morphology of the developed carbo-coating layer for multiple operating conditions were further investigated, accordingly. Ultimately, the performance of the developed carbon-coated silica sand particles (C-SiO_2) in a lab-scale microwave heating-assisted fluidized bed reactor was thoroughly evaluated. It was demonstrated that the C-SiO_2 particles exhibited exceptional microwave intractability according to significant dielectric properties of the material. The developed C-SiO_2 particles were further recommended for application as microwave receptor and catalyst support/promoter in gas-solid catalytic reactions.

2) The Significance of Heating Mechanism: The effect of microwave heating mechanism on a gas-solid selective oxidation reaction was investigated by simulation of *n*-C_4 conversion to MAN on the VOP catalyst in an industrial-scale fluidized bed reactor. It was exhibited that based on the dielectric properties of components a temperature gradient endures between the gas and the solid phases accordingly. Due to the inability for direct measurement of the gas temperature profile, the solid surface and bulk temperature profiles were demonstrated with the assistance of radiometry and thermometry methods in a lab-sale microwave heated fluidized bed reactor. Hence, the effect of operating conditions, temperature and superficial gas velocity, were investigated on the associated temperature profiles. Furthermore, correlations were proposed to estimate the gas temperature profile with the bed employing experimental data and an energy balance. The temperature profile

of solids, bulk and gas were further deployed to compare (conventional vs microwave heating) the conversion of *n*-C_4 and selectivity of MAN in the simulation study. The results revealed microwave heating was superior in terms of the reaction productivity.

3) Microwave-Assisted Catalytic Reaction: The dry reforming of methane in a lab-scale microwave heating-assisted fluidized bed reactor was performed to study the effect of the heating mechanism on the evolution of the products. Whereas, the effect of the operating temperature on the conversion of the reactants and the selectivity of the desired products, H_2 and CO was thoroughly investigated. It was concluded that microwave heating promoted catalytic reactions while restricting the secondary undesired gas-phase reactions.

TABLE OF CONTENTS

LIST OF TABLES

LIST OF FIGURES

LIST OF SYMBOLS AND ABBREVIATIONS

B.E.	Binding energy of the corresponding atomic orbitals
CVD	Chemical vapour deposition
DRM	Dry reforming of methane
EDX	Energy dispersive X-ray spectroscopy
FBCVD	Fluidized bed chemical vapour deposition
FIB	Focused ionized beam
GC	Gas chromatographer
MAN	Maleic anhydride
n-C_4	Normal butane
PEA	Poly ethyl acrylate
RWGS	Reverse water-gas shift reaction
SEM	Scan electron microscopy
S.F.	Sensitivity factor of the corresponding atomic orbital
TDM	Thermal degradation of methane
TGA	Thermogravimetric analysis
VPO	Vanadium phosphorus oxide
WGS	Water-gas shift reaction
wt%	Total weight percentage

XPS	X-ray photoelectron spectroscopy

CHAPTER 1 INTRODUCTION

The environmental concerns associated with the application of petroleum-based resources and the irrepressible depletion of available reserves has inspired the energy sector to pursuit alternative roadmap for the global demand outlook. In 2011, BP reported that there has been a +5.6% escalation in the global energy consumption, which is regarded as the strongest growth since 1973 with China leading the market share by 20.3% (BP, 2011). According to a report published by BP in 2016, oil has been the predominant vector, accounting for 33% of the global energy consumption. Furthermore, the total available oil reservoirs on the planet were estimated to be 1697.6 thousand million barrels. Thus, based on the current production rate and capacity, considering the reserves to production ratio (R/P), the accessible reservoirs will scarcely cover the global energy requirements for the next half decade (BP, 2016b).

Through the quest to seek an alternative to petroleum-based resources, natural gas has been signified as a robust candidate. Natural gas, a gaseous mixture of light hydrocarbons dominated by methane as the principal constituent, is globally distributed comparable to oil and coal reserves, although majorly confined in hydrate format throughout remote regions. Therefore, major studies on natural gas processes concentrate on methane as the predominant component, exclusively (A. P. York, T. Xiao, & M. L. Green, 2003). Natural gas has been denoted as the fastest growing energy resource, based on the strong supply growth, particularly due to US shale gas and liquefied natural gas (LNG) reserves and strict environmental policies. Consequently, natural gas has been considered as the dominant energy resource surpassing coal, due to the decline in production and rigorous environmental regulations, and merely approaching the petroleum level in the global energy outlook (BP, 2016a; IEA, 2016).

Due to the low accessibility of the available reserves and transportation deficiencies associated with the gaseous components, conversion of methane to value-added chemicals with improved transportation capacities have aroused prominent interest by the commercial sector. Conversion of methane into syngas has been highlighted as a substantial approach to preserve a carbon-neutral energy cycle in the advanced energy outlook. Synthetic gas, commonly known as syngas, is a complex conformation of gaseous products dominated by hydrogen and carbon monoxide (Wilhelm, Simbeck, Karp, & Dickenson, 2001). Major applications of syngas have been underlined as co-firing (Wu et al., 2004), energy production in gas turbines (Gadde et al., 2006), gas engines

(Martínez, Mahkamov, Andrade, & Silva Lora, 2012), Stirling engines (Miccio, 2013), fuel cell production (B. C. H. Steele & Heinzel, 2001) and production of value-added chemicals such as methanol, formaldehyde and long-chain hydrocarbons via gas to liquids (GtL) processes, namely Fischer-Tropch synthesis (Dry, 2002; Riedel et al., 1999). Originally, Sabatier and Senderens (Sabatier & Senderens, 1902) developed the reaction mechanism to produce syngas from methane in the presence of steam. Subsequently, numerous scientific approaches have been implemented to convert methane into syngas, substantially, steam reforming (SRM), partial oxidation (POx), and CO_2 (dry) reforming processes (DRM). The critical factor in the prosperous conversion of methane to value added products is to postulate energy to disband the resilient $CH_3 – H$ bond, with a high dissociation energy of 439.3 kJ/mol (Lide, 2004).

Meanwhile, catalytic dry (CO_2) reforming, conversion of hydrocarbons to synthetic gas in the presence of carbon dioxide, of methane has been extensively investigated in the available literature due to the environmental benefits and the process flexibility (M. C. J. Bradford & Vannice, 1999; Fidalgo, Domínguez, Pis, & Menéndez, 2008; Gallego, Mondragón, Barrault, Tatibouët, & Batiot-Dupeyrat, 2006; Guo, Lou, Zhao, Chai, & Zheng, 2004; Khajeh Talkhoncheh & Haghighi, 2015; M.-w. Li, Xu, Tian, Chen, & Fu, 2004; Pakhare & Spivey, 2014; Papp, Schuler, & Zhuang, 1996; Usman, Wan Daud, & Abbas, 2015; S. Wang, Lu, & Millar, 1996). Dry reforming of methane was initially investigated by Fischer and Tropsch at the presence of Ni and Co catalysts in 1928, while they reported severe deactivation of the catalyst due to the unexpected carbon deposition (Fisher & Tropsch, 1928). Comparable to steam reforming, dry reforming of methane is endothermic, thus enhances the energy requirements of the process. Furthermore, the equivalent (1:1) ratio of H_2/CO in the product stream provides a stimulating prospect to convert syngas to chemicals, methanol, and long-chain hydrocarbons particularly, through the Fischer-Tropsch process (Hu & Ruckenstein, 2004). In addition, with the application of CO_2 available in the natural gas reservoirs, dry reforming establishes a procedure to decrease the concentration of two major greenhouse gasses, CO_2 and CH_4, instantaneously through the process (Dyrssen, Turner, Paul, & Pradier, 1994). Unlike steam reforming and partial oxidation, which require cost-effective steam and oxygen production respectively prior to the process, dry reforming eliminates any excessive treatment and preparation of the reactants (Rostrup-Nielsen, Sehested, & Nørskov, 2002). However, the industrial application of dry reforming has been stalled due to the scarcity of an effective and economical catalyst and high energy requirements (Puskas, 1995). Although, the

pursuit of identifying a justifiable catalyst has been promptly under investigation (Ashcroft, Cheetham, & Green, 1991). It should be noted the major drawback of methane conversion to syngas in general, is associated with the complex and divers thermodynamic equilibria. Whereas, due to possibility of gas-phase reactions namely, thermal degradation (TDM), water-gas shift reaction (WGS) and carbon monoxide disproportionation, the reaction mechanism leads to the production of undesired products(Christian Enger, Lødeng, & Holmen, 2008; Hu & Ruckenstein, 2004; Pakhare & Spivey, 2014). Hence, the selectivity of the syngas components is drastically declined. Although various investigations regarding catalyst optimization and design has been reported in the literature to address the selectivity issue (Usman et al., 2015), the lack of studies demonstrating the effect of the heating method is evident.

Renewable energy resources have been acknowledged as noteworthy possibilities to maintain the ever-growing energy market, while comply with strict environmental regulation to persevere the planet from further irretrievable destruction (Turner, 1999). Application of renewable energy resources in transportation, electricity and power generation, and industrial processes have been highly regarded as the coherent alternative to economically unfeasible carbon dioxide sequestration endeavours (Pimentel & Patzek, 2008). Recent developments and breakthroughs in production and harvesting methods, depletion and exhaustion of the fossil fuel reserves, mass production processes and spontaneously available feedstock has developed renewable energy criteria from economically unfeasible to highly affordable and accessible resources (Timmons, Harris, & Roach, 2014). In 2015, U.S. Department of Energy reported a 4% growth in the global investments in renewable energy market for a total sum of $329 billion (Beiter & Tian, 2016). Consequently, the advent of the economically feasible and environmental friendly renewable energy resources stipulates an esteemed opportunity to promptly produce clean and affordable electricity (Carrasco et al., 2006). Moreover, a significant production, maintenance and distribution cost decline trend for solar and wind based electricity has been evidenced during the last 3 decades (Saidur, Islam, Rahim, & Solangi, 2010; Solangi, Islam, Saidur, Rahim, & Fayaz, 2011; Timilsina, Kurdgelashvili, & Narbel, 2012; Wiser et al.). Consequently, the convenience of affordable renewable electricity which projects substantially lower carbon footprint and CO_2 emission during the production, distribution and application stages provides a unique potential to preform chemical reactions via electromagnetic processing methods, namely; induction heating, ultrasound heating and microwave heating, correspondingly.

Thus, to address the present deficiencies discussed earlier regarding the catalytic reactions, the present study proposes the application of microwave heating for the gas-solid catalytic reaction optimization. Hence, dry reforming of methane has been contemplated as a case study to optimize catalytic reactions to simultaneously increase the conversion of methane and the selectivity of syngas constituents, and minimize the production of undesired by-products via secondary gas-phase reactions. Microwave heating represents numerous advantages over conventional methods namely, uniform, selective, and volumetric heating, high power density, instantaneous temperature control, reduced energy consumption, high reaction selectivity, less heat transfer limitations, process flexibility and equipment portability (Dominguez, Menendez, et al., 2007; Doucet, Laviolette, Farag, & Chaouki, 2014; Sherif Farag & Chaouki, 2015; S. Farag, Sobhy, Akyel, Doucet, & Chaouki, 2012; Khaghanikavkani & Farid, 2013; Metaxas, 1988; Motasemi & Afzal, 2013; Sobhy & Chaouki, 2010).

A major advantage of microwave heating over conventional methods is the distinctive temperature distribution scheme generated inside the reactor. While in conventional heating methods, the heat is provided by an external source, the microwave heating mechanism is governed by the interaction of the electromagnetic wave with the dielectric material within the reaction zone. Consequently, the temperature throughout the dielectric material is significantly higher than the bulk temperature. Moreover, due to the neutral dielectric properties of gasses in general, there will be no interaction between the gas phase components and the microwave radiation. This exceptional mechanism provides a worthwhile opportunity for the gas-solid catalytic reactions. Whereas, the higher local temperature on the active sites promotes higher selectivity and yield of the catalytic reactions, while lower bulk temperature and negligible microwave interaction of the gaseous components restricts the prospect of the undesired gas phased reactions.

1.1 References

Ashcroft, A. T., Cheetham, A. K., & Green, M. (1991). Partial oxidation of methane to synthesis gas using carbon dioxide. *Nature, 352*(6332), 225-226.

Beiter, P., & Tian, T. (2016). 2015 Renewable Energy Data Book: National Renewable Energy Laboratory.

BP. (2011). BP Statistical Review of World Energy 2011. London, UK: BP.

BP. (2016a). BP Energy Outlook 2016 Edition. London, UK: BP.

BP. (2016b). BP Statistical Review of World Energy 2016. London, UK: BP.

Bradford, M. C. J., & Vannice, M. A. (1999). CO2 Reforming of CH4. *Catalysis Reviews, 41*(1), 1-42. doi: 10.1081/cr-100101948

Carrasco, J. M., Franquelo, L. G., Bialasiewicz, J. T., Galvan, E., PortilloGuisado, R. C., Prats, M. A. M., . . . Moreno-Alfonso, N. (2006). Power-Electronic Systems for the Grid Integration of Renewable Energy Sources: A Survey. *IEEE Transactions on Industrial Electronics, 53*(4), 1002-1016. doi: 10.1109/tie.2006.878356

Christian Enger, B., Lødeng, R., & Holmen, A. (2008). A review of catalytic partial oxidation of methane to synthesis gas with emphasis on reaction mechanisms over transition metal catalysts. *Applied Catalysis A: General, 346*(1–2), 1-27. doi: http://dx.doi.org/10.1016/j.apcata.2008.05.018

Dominguez, A., Menendez, J. A., Fernandez, Y., Pis, J. J., Nabais, J. M. V., Carrott, P. J. M., & Carrott, M. M. L. R. (2007). Conventional and microwave induced pyrolysis of coffee hulls for the production of a hydrogen rich fuel gas. *Journal of Analytical and Applied Pyrolysis, 79*(1-2), 128-135. doi: Doi 10.1016/J.Jaap.2006.08.003

Doucet, J., Laviolette, J.-P., Farag, S., & Chaouki, J. (2014). Distributed microwave pyrolysis of domestic waste. *Waste and Biomass Valorization, 5*(1), 1-10. doi: 10.1007/s12649-013-9216-0

Dry, M. E. (2002). The Fischer–Tropsch process: 1950–2000. *Catalysis Today, 71*(3–4), 227-241. doi: http://dx.doi.org/10.1016/S0920-5861(01)00453-9

Dyrssen, D., Turner, D., Paul, J., & Pradier, C. (1994). Carbon Dioxide Chemistry: Environmental Issues: Athenaeum Press, Cambridge.

Farag, S., & Chaouki, J. (2015). A modified microwave thermo-gravimetric-analyzer for kinetic purposes. *Applied Thermal Engineering, 75*, 65-72. doi: http://dx.doi.org/10.1016/j.applthermaleng.2014.09.038

Farag, S., Sobhy, A., Akyel, C., Doucet, J., & Chaouki, J. (2012). Temperature profile prediction within selected materials heated by microwaves at 2.45GHz. *Applied Thermal Engineering, 36*, 360-369. doi: Doi 10.1016/J.Applthermaleng.2011.10.049

Fidalgo, B., Domínguez, A., Pis, J. J., & Menéndez, J. A. (2008). Microwave-assisted dry reforming of methane. *International Journal of Hydrogen Energy, 33*(16), 4337-4344. doi: http://dx.doi.org/10.1016/j.ijhydene.2008.05.056

Fisher, F., & Tropsch, H. (1928). Conversion of methane into hydrogen and carbon monoxide. *Brennst.-Chem., 9*.

Gadde, S., Wu, J., Gulati, A., McQuiggan, G., Koestlin, B., & Prade, B. (2006). *Syngas capable combustion systems development for advanced gas turbines.* Paper presented at the ASME Turbo Expo 2006: Power for Land, Sea, and Air.

Gallego, G. S., Mondragón, F., Barrault, J., Tatibouët, J.-M., & Batiot-Dupeyrat, C. (2006). CO2 reforming of CH4 over La–Ni based perovskite precursors. *Applied Catalysis A: General, 311*, 164-171. doi: http://dx.doi.org/10.1016/j.apcata.2006.06.024

Guo, J., Lou, H., Zhao, H., Chai, D., & Zheng, X. (2004). Dry reforming of methane over nickel catalysts supported on magnesium aluminate spinels. *Applied Catalysis A: General, 273*(1–2), 75-82. doi: http://dx.doi.org/10.1016/j.apcata.2004.06.014

Hu, Y. H., & Ruckenstein, E. (2004). Catalytic Conversion of Methane to Synthesis Gas by Partial Oxidation and CO2 Reforming *Advances in Catalysis* (Vol. Volume 48, pp. 297-345): Academic Press.

IEA. (2016). *Energy and Air Pollution*. Paris, France: Inetrational Energy Agency.

Khaghanikavkani, E., & Farid, M. M. (2013). Mathematical Modelling of Microwave Pyrolysis. *International Journal of Chemical Reactor Engineering, 11*. doi: 10.1515/ijcre-2012-0060

Khajeh Talkhoncheh, S., & Haghighi, M. (2015). Syngas production via dry reforming of methane over Ni-based nanocatalyst over various supports of clinoptilolite, ceria and alumina.

Journal of Natural Gas Science and Engineering, 23, 16-25. doi: http://dx.doi.org/10.1016/j.jngse.2015.01.020

Li, M.-w., Xu, G.-h., Tian, Y.-l., Chen, L., & Fu, H.-f. (2004). Carbon Dioxide Reforming of Methane Using DC Corona Discharge Plasma Reaction. *The Journal of Physical Chemistry A, 108*(10), 1687-1693. doi: 10.1021/jp037008q

Lide, D. R. (2004). *CRC handbook of chemistry and physics* (Vol. 85): CRC press.

Martínez, J. D., Mahkamov, K., Andrade, R. V., & Silva Lora, E. E. (2012). Syngas production in downdraft biomass gasifiers and its application using internal combustion engines. *Renewable Energy, 38*(1), 1-9. doi: http://dx.doi.org/10.1016/j.renene.2011.07.035

Metaxas, A. C. (1988). *Industrial Microwave Heating Power and Energy* (pp. 1 online resource (376 p.)).

Miccio, F. (2013). On the integration between fluidized bed and Stirling engine for micro-generation. *Applied Thermal Engineering, 52*(1), 46-53. doi: http://dx.doi.org/10.1016/j.applthermaleng.2012.11.004

Motasemi, F., & Afzal, M. T. (2013). A review on the microwave-assisted pyrolysis technique. *Renewable & Sustainable Energy Reviews, 28*, 317-330. doi: 10.1016/j.rser.2013.08.008

Pakhare, D., & Spivey, J. (2014). A review of dry (CO2) reforming of methane over noble metal catalysts. *Chemical Society Reviews, 43*(22), 7813-7837. doi: 10.1039/c3cs60395d

Papp, H., Schuler, P., & Zhuang, Q. (1996). CO2 reforming and partial oxidation of methane. *Topics in Catalysis, 3*(3), 299-311. doi: 10.1007/bf02113856

Pimentel, D., & Patzek, T. W. (2008). Biofuels, solar and wind as renewable energy systems. *Benefits and risks. New York: Springer*.

Puskas, I. (1995). Natural gas to syncrude: Making the process pay off. *CHEMTECH, 25*(12).

Riedel, T., Claeys, M., Schulz, H., Schaub, G., Nam, S.-S., Jun, K.-W., . . . Lee, K.-W. (1999). Comparative study of Fischer–Tropsch synthesis with H2/CO and H2/CO2 syngas using Fe- and Co-based catalysts. *Applied Catalysis A: General, 186*(1–2), 201-213. doi: http://dx.doi.org/10.1016/S0926-860X(99)00173-8

Rostrup-Nielsen, J. R., Sehested, J., & Nørskov, J. K. (2002). Hydrogen and synthesis gas by steam- and C02 reforming *Advances in Catalysis* (Vol. Volume 47, pp. 65-139): Academic Press.

Sabatier, P., & Senderens, J.-B. (1902). New synthesis of methane. *CR Acad. Sci. Paris, 134*, 514-516.

Saidur, R., Islam, M. R., Rahim, N. A., & Solangi, K. H. (2010). A review on global wind energy policy. *Renewable and Sustainable Energy Reviews, 14*(7), 1744-1762. doi: http://dx.doi.org/10.1016/j.rser.2010.03.007

Sobhy, A., & Chaouki, J. (2010). Microwave-assisted Biorefinery. *Cisap4: 4th International Conference on Safety & Environment in Process Industry, 19*, 25-29. doi: Doi 10.3303/Cet1019005

Solangi, K. H., Islam, M. R., Saidur, R., Rahim, N. A., & Fayaz, H. (2011). A review on global solar energy policy. *Renewable and Sustainable Energy Reviews, 15*(4), 2149-2163. doi: http://dx.doi.org/10.1016/j.rser.2011.01.007

Steele, B. C. H., & Heinzel, A. (2001). Materials for fuel-cell technologies. *Nature, 414*(6861), 345-352.

Timilsina, G. R., Kurdgelashvili, L., & Narbel, P. A. (2012). Solar energy: Markets, economics and policies. *Renewable and Sustainable Energy Reviews, 16*(1), 449-465. doi: http://dx.doi.org/10.1016/j.rser.2011.08.009

Timmons, D., Harris, J. M., & Roach, B. (2014). The economics of renewable energy. *Global Development And Environment Institute, Tufts University*, 52.

Turner, J. A. (1999). A Realizable Renewable Energy Future. *Science, 285*(5428), 687-689. doi: 10.1126/science.285.5428.687

Usman, M., Wan Daud, W. M. A., & Abbas, H. F. (2015). Dry reforming of methane: Influence of process parameters—A review. *Renewable and Sustainable Energy Reviews, 45*, 710-744. doi: http://dx.doi.org/10.1016/j.rser.2015.02.026

Wang, S., Lu, G. Q., & Millar, G. J. (1996). Carbon Dioxide Reforming of Methane To Produce Synthesis Gas over Metal-Supported Catalysts: State of the Art. *Energy & Fuels, 10*(4), 896-904. doi: 10.1021/ef950227t

Wilhelm, D. J., Simbeck, D. R., Karp, A. D., & Dickenson, R. L. (2001). Syngas production for gas-to-liquids applications: technologies, issues and outlook. *Fuel Processing Technology, 71*(1–3), 139-148. doi: http://dx.doi.org/10.1016/S0378-3820(01)00140-0

Wiser, R., Bolinger, M., Barbose, G., Darghouth, N., Hoen, B., Mills, A., . . . Widiss, R. 2015 Wind Technologies Market Report. *Energy Efficiency and Renewable Energy*.

Wu, K. T., Lee, H. T., Juch, C. I., Wan, H. P., Shim, H. S., Adams, B. R., & Chen, S. L. (2004). Study of syngas co-firing and reburning in a coal fired boiler. *Fuel, 83*(14–15), 1991-2000. doi: http://dx.doi.org/10.1016/j.fuel.2004.03.015

York, A. P., Xiao, T., & Green, M. L. (2003). Brief overview of the partial oxidation of methane to synthesis gas. *Topics in Catalysis, 22*(3-4), 345-358.

CHAPTER 2 LITERATURE REVIEW

This chapter delivers a comprehensive literature review emphasizing on the significance of natural gas in the future global energy market, available conversion methods to value-added chemicals, partial oxidation of methane particularly, the effect of the renewable energies and the principles of microwave heating as an innovative processing method for material treatment.

2.1 Energy Resources

Carbon dioxide has been regarded as the premier source of greenhouse gas emission in the world. In 2014, United States Environmental Protection Agency (EPA) reported that 81% of the total greenhouse gas emission in US were associated with the carbon dioxide discharge and evolution represented in Figure 2-1 (EPA, 2015). Accordingly, the global level of carbon dioxide concentration has drastically increased by 90 ppm during the last 200 years, summarized in Table 2-1 (Omae, 2006).

Table 2-1: The variation of CO_2 in the atmosphere during the last 1000 years (Omae, 2006)

Years	Period (years)	Concentration (ppm)	Increase (ppm)	Increase rate (ppm/year)
1000 - 1800	800	270 - 280	10	0.01
1800 - 1950	150	280 - 310	30	0.2
1958 - 1975	17	315 - 330	15	0.9
1955 - 2002	27	330 - 370	40	1.5

The environmental concerns associated with the combustion and processing of petroleum-based resources, namely, sulfur dioxide, nitrogen oxides, carbon monoxide, carbon dioxide and particulate matter, have emerged the governments to mandate strict policies to control the emission crisis (IEA, 2016). Whereas, fossil fuels have severely contributed to the global warming discharging 70 - 75% of annual carbon dioxide via combustion reactions (Hoel & Kverndokk,

1996). Furthermore, the irrepressible depletion of available dominant energy resource reserves, oil, and coal, has inspired the energy sector to pursuit alternative roadmap for the global demand outlook (Shafiee & Topal, 2009). In 2011, BP reported that there has been a +5.6% escalation in the global energy consumption, which is regarded as the strongest growth since 1973 with China leading the market share by 20.3% (BP, 2011).

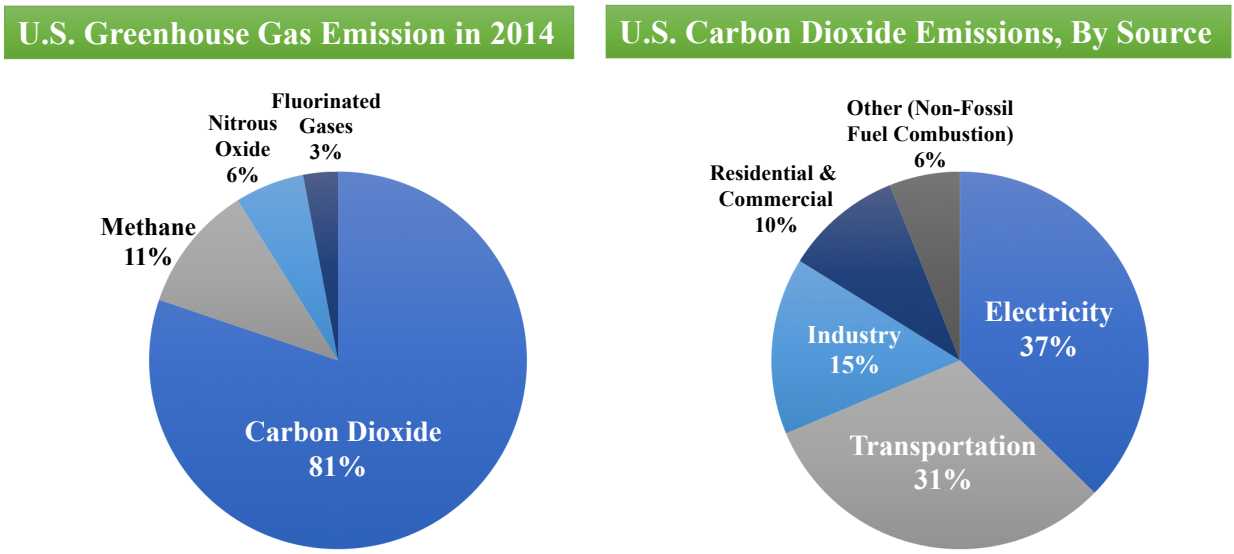

Figure 2-1: The total greenhouse gas emission and CO_2 emission in United states in 2014 breakdown reproduced from (EPA, 2015)

It has been estimated that the global energy demands would increase at an average rate of 1.1% per annum, from 500 quadrillion Btu in 2006 to 701.6 quadrillion Btu in 2030 (Shafiee & Topal, 2008). According to a report published by BP in 2016, oil has been the predominant vector, accounting for 33% of the global energy consumption. Furthermore, the total available oil reservoirs on the planet were estimated to be 1697.6 thousand million barrels. Thus, based on the current production rate and capacity, considering the reserves to production ratio (R/P), the accessible reservoirs will scarcely cover the global energy requirements for the next half decade (BP, 2016b). Figure 2-2 illustrates the petroleum consumption profile and proved reserves based on global regions for the last 30 years.

Meanwhile, the unprecedented decline of the conventional energy market on the one hand, and the environmental concerns associated with extraction, transportation and application of the established fissile fuel based energy on the other hand has urged the industrial sector to investigate for sustainable, innovative and alternative resources to satisfy the global energy market demands.

Consequently, renewable energy resources have been acknowledged as noteworthy possibilities to maintain the ever-growing energy market while comply with strict environmental regulation to persevere the planet from further irretrievable destruction (Turner, 1999). Application of renewable energy resources in transportation, electricity and power generation, and industrial processes have been highly regarded as the coherent alternative to economically unfeasible carbon dioxide sequestration endeavours (Pimentel & Patzek, 2008). Renewable energy in generally defined as a resource independent from viable and independent of restricted fossil reserves, namely, hydro-electricity, geothermal, hydrogen, biomass, solar and wind (Salameh, 2003).

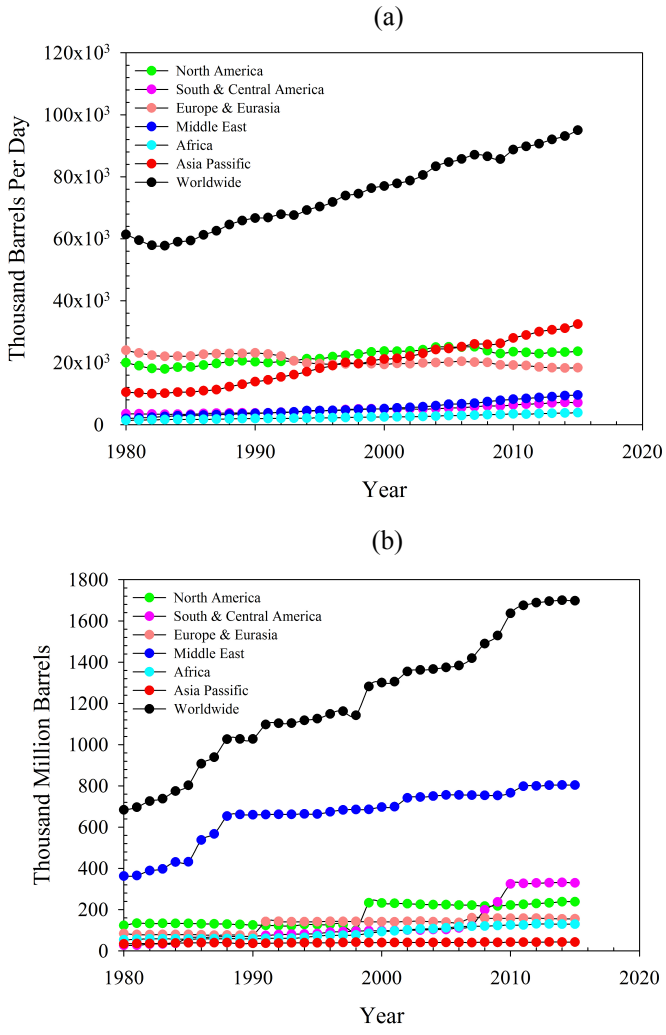

Figure 2-2: The representative data of worldwide (a) Oil consumption profile and (b) Verified oil reserves for various global regions from 1980 to 2015. (Image reproduced from data provided by (BP, 2016b)).

Moreover, solar energy has been regarded as the preliminary resource for all renewable energy segments contemplating that every supplementary format has been principally established and driven by the energy transmitted from the sun. Recent developments and breakthroughs in production and harvesting methods, depletion and exhaustion of the fossil fuel reserves, mass production processes and spontaneously available feedstock has developed renewable energy criteria from economically unfeasible to highly affordable and accessible resources (Timmons et al., 2014). In 2015, U.S. Department of Energy reported a 4% growth in the global investments in renewable energy market for a total sum of $329 billion (Beiter & Tian, 2016). Consequently, the advent of the economically feasible and environmental friendly renewable energy resources stipulates an esteemed opportunity to promptly produce clean and affordable electricity (Carrasco et al., 2006). Moreover, a significant production, maintenance and distribution cost decline trend for solar and wind based electricity has been evidenced during the last 3 decades (Saidur et al., 2010; Solangi et al., 2011; Timilsina et al., 2012; Wiser et al.). Consequently, the convenience of affordable renewable electricity which projects substantially lower carbon footprint and CO_2 emission during the production, distribution and application stages provides a unique potential to preform chemical reactions via electromagnetic processing methods, namely; induction heating, ultrasound heating and microwave heating, correspondingly.

2.1.1 Natural Gas Prospect

Contemplating the deficiencies of conventional resources, the energy sector has promptly maintained endeavors to identify complementary solutions, thus natural gas has been signified as a robust candidate. Natural gas is a combustible mixture of low-chain and light hydrocarbons structurally dominated by methane as the major component and minor proportions of ethane, propane, butane, pentane and acid gasses (S. Lee, 1996). Table 2-2 has summarized the conventional composition of natural gas according to the structural compounds. The major advantages of the application of natural gas over conventional dominant energy resources, oil and coal, are the clean burning, significantly lower carbon footprint, lower contribution to the worldwide emission and evolution of lower level of CO_2, an influential factor in global warming (Christian Enger et al., 2008).

Due to the dominant proportions of methane in the structure of natural gas, major studies emphasize on the methane processes and reaction mechanisms (A. P. E. York, T. Xiao, & M. L. H. Green,

2003). Natural gas has been highlighted as the fastest growing energy resource, while oil and coal are suffering from a declining transition period, specifically due to the escalation in US shale gas and liquefied natural gas (LNG) production rate, strict environmental policies reinstated by the governments and the significant elevation of demands from emerging economies with China, India and the Middle East leading the market shares (BP, 2016a). Early predictions have concluded natural gas to surpass coal as the second dominant energy vector, majorly based on the decline in the production and rigorous environmental regulations, and further reach the petroleum dominance level in the short-term energy outlook (Birol & Argiri, 1999; BP, 2016a; IEA, 2016). Figure 2-3 provides a representative profile of primary energy resources from 1980 to an estimated trend up to 2035.

Table 2-2: Approximate Structural Data of Methane in Wet and Dry States (Speight, 1993).

	Composition (vol %)	
Constituents	**Wet**	**Dry**
Hydrocarbons		
Methane	84.6	96.0
Ethane	6.4	2.0
Propane	5.3	0.6
Isobutane	1.2	0.18
n-Butane	1.4	0.12
Isopetane	0.4	0.14
n-Pentane	0.2	0.06
Hexanes	0.4	0.10
Heptanes	0.1	0.08
Nonhydrocarbons		
CO	0 – 5	
He	0 – 0.05	
H_2S	0 – 5	
N_2	0 – 10	
Ar	0 – 0.05	
Radon, Krypton, and Xenon	Traces	

The distribution of natural gas has been identified similar to oil and coal reserves. However, natural gas is majorly confined in hydrate form allocated in remote regions and deep ocean environments. Clathrates of gas and water, commonly known as gas hydrates, are solid and non-stoichiometric compounds generate by contact between small guest molecules, namely, methane and carbon monoxide at minimal sizes (< 0.9 nm) with water at ambient temperature and moderate pressures higher than 0.6 Mpa (Sloan, 2003).

Presently, methane has been an indispensable component of various industrial applications including, energy supply for power plants and electricity generation, automotive fuels, syngas production, and production of various value added chemicals including hydrogen cyanide, chloromethane and carbon disulfide (R. Edwards, Mahieu, Griesemann, Larivé, & Rickeard, 2004; Eriksson et al., 2006; Folkins, Miller, & Hennig, 1950; Hickman & Schmidt, 1993; Koberstein, 1973; Murray, Tsai, & Barnett, 1999; Podkolzin, Stangland, Jones, Peringer, & Lercher, 2007). Figure 2-4 illustrates various applications and conversion processes of methane to energy and value-added chemicals.

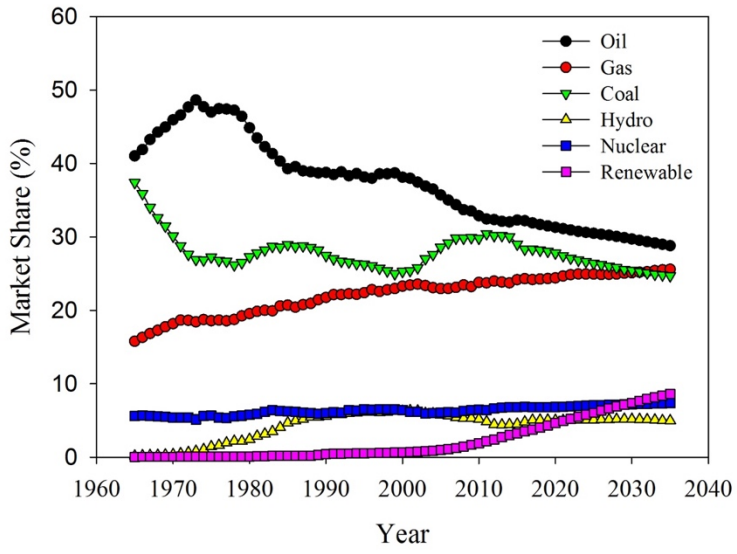

Figure 2-3: Global energy market share profile from 1965 to an estimated trend up to 2035 (Image reproduced from data provided by (BP, 2016a)).

2.2 Methane Conversion to Syngas

Deliberating the critical accessibility issues associated with the discovered reserves and the general complexity accompanying the transportation of gaseous components, conversion of methane resources to value-added chemicals have been promptly perused (C. A. Jones, Leonard, & Sofranko, 1987). Conversion of methane aims to address the transportation deficiencies while economically justifies the processing for the energy sector (Rostrup-Nielsen, 1994). Meanwhile, conversion of methane into syngas has aroused prominent interest to preserve a carbon-neutral energy cycle on the future industrial outlook. Synthetic gas, commonly referred as syngas, is a complex gas mixture majorly dominated by hydrogen, carbon monoxide and carbon dioxide and traces of sulfur compounds as impurities (Hu & Ruckenstein, 2004; Wilhelm et al., 2001).

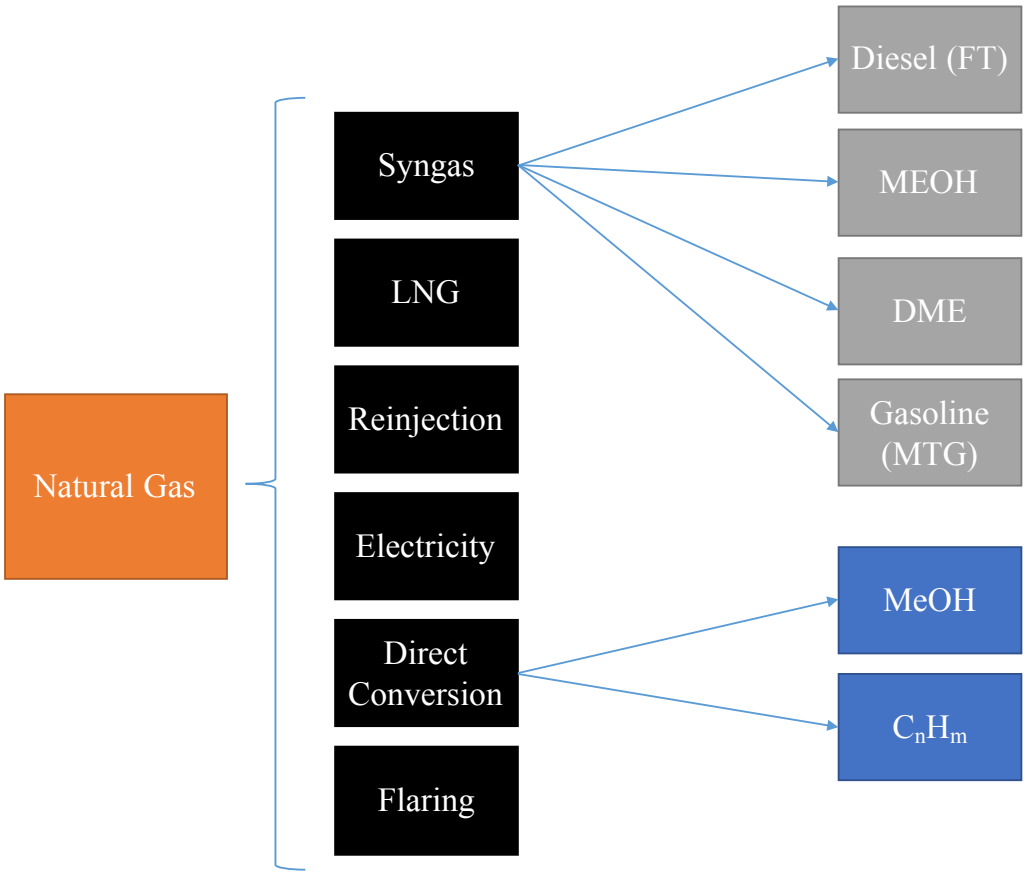

Figure 2-4: Various conversion mechanisms and applications of natural gas.

The production of syngas from various resources including natural gas, coal, biomass or various hydrocarbon feedstock has been investigated in the literature using multiple oxidizing components namely, steam and oxygen, denoting the versatility of the feedstock and the flexibility of the processes (Aasberg-Petersen et al., 2001; Rostrup-Nielsen, 2000). Major applications of syngas have been underlined as co-firing (Wu et al., 2004), energy production in gas turbines (Gadde et al., 2006), gas engines (Martínez et al., 2012), Stirling engines (Miccio, 2013), fuel cell production (B. C. H. Steele & Heinzel, 2001) and production of value-added chemicals such as methanol, formaldehyde and long-chain hydrocarbons via gas to liquids (GtL) processes, namely Fischer-Tropch (FT) synthesis (Dry, 2002; Riedel et al., 1999). The direct conversion of CH_4 to methanol (MeOH) with a relatively high selectivity of 80% presents a very low conversion of 7% which leads to scale-up issues such as high recycling rate and complex separation processes (Yarlagadda, Morton, Hunter, & Gesser, 1990). In contrary, the commercial production of methanol from syngas provides 50% conversion and the selectivity can reach as high as 99% (Aasberg-Petersen et al., 2001). Figure 2-5 provides a graphical review of various syngas production routes and applications.

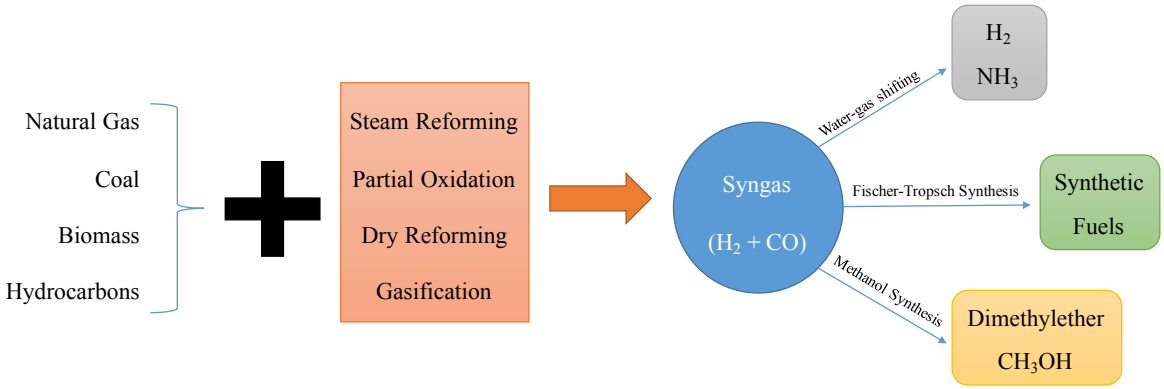

Figure 2-5: A schematic review of syngas production and further conversion to value-added chemicals.

Originally, Sabatier and Senderens developed the mechanism of conversion of methane into syngas in the presence of steam in 1902 (Sabatier & Senderens, 1902). Since then multiple state-of-the-art processes have been developed to convert methane into syngas based on the final application of the products (Christian Enger et al., 2008; Hu & Ruckenstein, 2004). However, the most prominent processes have been acknowledged as steam reforming (SRM), dry (CO_2) reforming (DRM) and catalytic partial oxidation (POx). The critical factor in the prosperous conversion of methane to value added products is to provide energy to disband the resilient CH_3 – H bond, with a high

dissociation energy of 439.3 kJ/mol (Lide, 2004). The following sections will investigate the properties of each syngas production method with the emphasize on the catalytic partial oxidation process.

2.3 Dry Reforming

Dry reforming of methane is the conversion of methane in the presence of carbon dioxide (CO_2) and energy to carbon monoxide and hydrogen, commonly known as syngas. Though:

$$CH_4 + CO_2 \rightarrow 2CO + 2H_2 \qquad \Delta H^0_{298} = +247\ kJ\ mol^{-1} \qquad (2.1)$$

$$\Delta G^o = 61770 - 67.32T$$

The dry reforming process in principle is extremely endothermic, thus requires enormously high temperatures to attain high conversion of reactants to the dominant product, syngas, based on the thermodynamic equilibrium (Brungs, York, Claridge, Márquez-Alvarez, & Green, 2000; S. Wang et al., 1996).

Dry reforming of methane was initially investigated by Fischer and Tropsch at the presence of Ni and CO catalysts in 1928 while they reported severe deactivation of the catalyst due to the unexpected carbon deposition (Fisher & Tropsch, 1928). However, the carbon deactivation problem was later addressed by Reitmeier *et al.* in 1949 (Reitmeier, Atwood, Bennett, & Baugh, 1948). Consequently, a general solution for elimination of carbon deposition problem in dry and steam reforming of hydrocarbons was proposed by clarification of a correlation between the reactants composition and the amount of carbon produced. The investigation ultimately lead to major design criteria of reactants composition, reactor scheme, and process operating conditions to a high ratio of syngas production ($0.5 < H_2/CO < 3$) while significantly eliminating the carbon deposition obstacle. At the same year, Lewis et al. proposed a general approach for reforming of the hydrocarbons to syngas (Lewis, Gilliland, & Reed, 1949). The process was maintained on Cu oxide supported catalyst with a sub-stoichiometric oxygen supply to achieve selective oxidization of hydrocarbons to CO and H_2. The dual stage process known as *stoichiometric control method* consisted of partial oxidization of hydrocarbons to syngas and regeneration of the Cu oxide supported catalyst. However, low reaction rate and considerable carbon deposition prevented the

commercialization of the process. The method for methane reforming catalyst synthesis was initially proposed by Rostrup-Nielson through a patent in 1974. The process was based on co-precipitation of aluminum hydroxide, magnesium hydroxide, and nickel hydroxide to form a spinel structure of Al and Mg upon calcination at 800 – 1100 ^{o}C. Moreover, the excess Mg residual on the surface of the catalysts proceeded as a promoter to activate CO_2 whereas limiting the formation of carbon deposition over the catalyst layer. However, the mechanism which promoters promptly restricted carbon deposition and catalyst deactivation was not thoroughly investigated (Pakhare & Spivey, 2014). The application of metal promoters to restrict carbon deposition concerns has been further investigated accordingly in the available literature. In 1979, Sodesawa *et al.* investigated silica supported Ni catalyst for carbon dioxide reforming of methane (Sodesawa, Dobashi, & Nozaki, 1979). It was concluded that Ni/SiO_2 catalyst amended higher selectivity of CO at relatively low temperature, markedly suppressing the carbon deposition issue compared to the earlier studies. In 1988, Gadalla *et al.* studied the effect of alumina supported Ni catalyst on restricting the undesired carbon deposition throughout the dry reforming of methane (Gadalla & Bower, 1988). The investigation revealed that the carbon deposition would be inhibited by increasing the CO_2/CH_4 ratio. However, the thermodynamic studies revealed an optimum operating temperature for each CO_2/CH_4 ratio which would derive the carbon deposition mechanism to the production of nickel carbide. Later in 1993, Rostrup-Nielsen and Hansen investigated the effect of multiple transition metal catalysts, namely, Ni, Ru, Rh, Pt, Ir and Pd on the conversion, reforming activity and carbon deposition for dry reforming of methane with satisfactory results obtained (Rostrup-Nielsen & Hansen, 1993). Ultimately in 1994, Choudhary *et al.* proposed a simultaneous reforming of methane with CO_2 and O_2 over NiO/CuO catalyst which under controlled operating conditions facilitated low H_2/CO ratio, high conversion of methane and significant selectivity of CO and H_2, without deactivation of the catalyst due to the minimal carbon formation through an auto-thermal reaction (Choudhary, Rajput, & Prabhakar, 1995). Recently, the concept of mix reforming, a combination of dry reforming, partial oxidation, and steam reforming have been proposed and investigated to address the inadequacies of each process individually (Choudhary et al., 1995; Teuner, 1987; Udengaard, 1992). First, such a process provides the opportunity to achieve a CO/H_2 ratio in the range of 1 to 3 depending on the reaction conditions and the $CO_2/H_2O/O_2$ feed ratio. Second, due to the exothermic characteristics of the partial oxidation process, the excess oxygen will compromise for the high-energy requirements of dry and steam

reforming reactions. Finally, the oxygen and steam in the feed will inhibit the formation of carbon due to methane decomposition or carbon monoxide disproportionation via gasification and oxidation mechanisms, though:

$$H_2O + C_{(S)} \leftrightarrow CO + H_2 \qquad \Delta H^0_{298} = 31.14\ kJ\ mol^{-1}C_{(S)} \quad (2.2)$$

$$xO_2 + C_{(S)} \leftrightarrow (1-x)CO + (2x-1)CO_2 \qquad 94.1 \geq \Delta H^0_{298} \geq -26.4\ kJ\ mol^{-1}C_{(S)} \quad (2.3)$$

The advantages of dry reforming of methane over other syngas production methods have been thoroughly investigated in the literature. Considering the economic aspects of the process, Rose has concluded that dry reforming of methane is maintained at 20% lower operating cost compared to the other reforming methods (Ross, 2005). From the environmental perspective, dry reforming of methane has been regarded as a prosperous method to convert two predominant constituents of greenhouse gas emissions, CH_4, and CO_2, to commercial chemical products, explicitly if the thermal requirements of the reaction is provided by a carbon-neutral source, namely, nuclear or solar energy (Budiman, Song, Chang, Shin, & Choi, 2012; Lavoie, 2014; Usman et al., 2015). Furthermore, dry reforming of methane facilitates biogas utilization for value-added chemicals production and riases the opportunity to engage natural gas sources with high carbon dioxide to syngas through a robust process (Usman et al., 2015). From the process standpoint, dry reforming of methane grants lower yield of syngas ratio (H_2/CO=1) compared to the other methane reforming methods stipulating the possibility to produce methanol, oxygenated products and longer chained hydrocarbons through Fischer-Tropsch synthesis (Oyama, Hacarlioglu, Gu, & Lee, 2012; Wurzel, Malcus, & Mleczko, 2000). Moreover, syngas product maintained by dry reforming of methane can be utilized to store solar or nuclear energy through the chemical energy transmission system (CETS) where the syngas can be transferred to energy-deprived regions and release the absorbed energy via backward reactions (Chubb, 1980; Fraenkel, Levitan, & Levy, 1986). Table 2-3 presents a comprehensive summary of available reforming processes for methane

Table 2-3: Summary of methane conversion processes to syngas (Hu & Ruckenstein, 2004; York et al., 2003)

Process	Reaction Mechanism	ΔH^0_{298} (kJ mol^{-1})	$\frac{H_2}{CO}$
Steam Reforming	$CH_4 + H_2O \rightarrow CO + 3H_2$	206	3
Dry Reforming	$CH_4 + CO_2 \rightarrow 2CO + 2H_2$	247	1
Partial Oxidation	$CH_4 + \frac{1}{2}O_2 \rightarrow CO + 2H_2$	- 36	2

2.3.1 Reaction Mechanism and Carbon Deposition

The major disadvantage of dry reforming of methane, as discussed earlier, is associated with the carbon deposition (coking) deficiency, which leads to the deactivation and sintering of the catalyst (Hu & Ruckenstein, 2004; Lavoie, 2014; Nikoo & Amin, 2011; Pakhare & Spivey, 2014; Usman et al., 2015). Generally, carbon formation is maintained by two dominating mechanisms of CH_4 decomposition and CO disproportionation referred as Boudouard reaction. Whereas:

$$CH_4 \leftrightarrow C + 2H_2 \qquad \Delta H^0_{298} = 74.9\ kJ\ mol^{-1} \qquad (2.4)$$

$$\Delta G^o = 2190 - 26.45T$$

$$2CO \leftrightarrow C + CO_2 \qquad \Delta H^0_{298} = -172.4\ kJ\ mol^{-1} \qquad (2.5)$$

$$\Delta G^o = -39810 + 40.87T$$

Due to lower O/C and H/C ratios for DRM, 1 and 2 respectively, a higher tendency towards carbon deposition is observed compare to steam reforming and partial oxidation reactions (J. H. Edwards & Maitra, 1995). In order to address the carbon deposition phenomena, thermodynamic investigations have suggested the application of high CO_2/CH_4 ratio, well above unity, at high

temperatures (~1000 K) (Gadalla & Bower, 1988; Reitmeier et al., 1948; G. A. White, Roszkowski, & Stanbridge, 1975). Although low CO_2/CH_4 (near unity) ratio at low temperatures is typically favored by the industry (M. C. J. Bradford & Vannice, 1999; Hu & Ruckenstein, 2004). This necessitates the application of a reforming catalyst which incorporates the kinetics of carbon formation and deposition while the thermodynamics of such deposition is favorable by the reaction mechanism.

Multiple species of carbon formation have been reported by dry reforming reactions; namely, α - C, β - C, and γ - C. In the case of Ni/Al_2O_3, it was concluded while α - C assisted the formation of carbon monoxide, the less active carbon species, β - C, and γ - C, derive the deactivation of the catalyst (Z. L. Zhang & Verykios, 1994). A similar study temperature programmed hydrogenation (TPH) on Ni/MgO revealed that while less active carbon species highly contribute to the catalyst deactivation, the active species is increased by proceeding the DRM reaction, acting as an intermediate class (Y.-G. Chen, Tomishige, & Fujimoto, 1997). Ultimately, XPS investigation on DRM using $NiO/\gamma\text{-}Al_2O_3$ revealed the presence of both amorphous and filamentous morphologies on the surface. While the latter is accounted for the deactivation problem due to lower activity which leads to resistance to oxidation and reduction reactions (X. Chen, Honda, & Zhang, 2005).

Moreover, dry reforming of methane is a system of multiple reactions based on the thermodynamic equilibria. Although the aim for DRM process is the production of syngas components, H_2 and CO, however, multiple parallel or secondary gas phase reactions occur which interfere with the selectivity and yield of the principally desired products. These secondary gas phase reactions predominantly lead to the production of long-chained hydrocarbons, water vapor, carbon dioxide and carbon formation, which the latter, as stated before, disrupts the reaction kinetics by deactivating the reforming catalyst.

Table 2-4 has summarized all major reactions associated with the dry reforming of methane. One of the Major DRM side reactions has been highlighted as reverse water-gas shift (RWGS) reaction given as:

$$CO_2 + H_2 \leftrightarrow CO + H_2O \qquad \Delta H^0_{298} = 41.2\ kJ\ mol^{-1} \qquad (2.6)$$

$$\Delta G^o = -8545 - 7.84T$$

where reduces the syngas yield to $H_2/CO < 1$. Thermodynamic studies have exposed lower tendency of spontaneous reactions at temperatures below 640. Dejonovic *et al.* proposed the application of high temperatures (> 750 ^oC) or intensified CH4/CO2 ratio, higher than unity, to dismiss the contribution of RWGS reaction (Eq. 6). Although such reaction conditions lead to operational complexities such as extreme production of carbon and outstanding of large scales of excess methane in the system (Djinović, Osojnik Črnivec, Erjavec, & Pintar, 2012).

Additionally, the methane decomposition, and carbon monoxide disproportionation, which lead to the production and deposition of carbon, have been denoted as other undesired secondary reactions in the DRM process which have been discussed earlier. Thermodynamic studies revealed these reactions are driven at a significant rate between 633 and 700 ^oC temperatures, however the application of higher temperatures (<700) although diminishes the effect of side reactions, but simultaneously leads to the blockage of the reactor and sever reduction in activity. Therefore, Figure 2-6 is a graphical representation of the effect of temperature on the equilibrium value of major dry reforming reactants and products in the presence and absence of carbon forming reactions. Furthermore, Nematollahi *et al.* have investigated the effect of operating pressure and reactants ratio on the conversion of reactants and evolution of products maintained a thermodynamic analysis using Gibbs energy minimization method (Nematollahi, Rezaei, Lay, & Khajenoori, 2012).

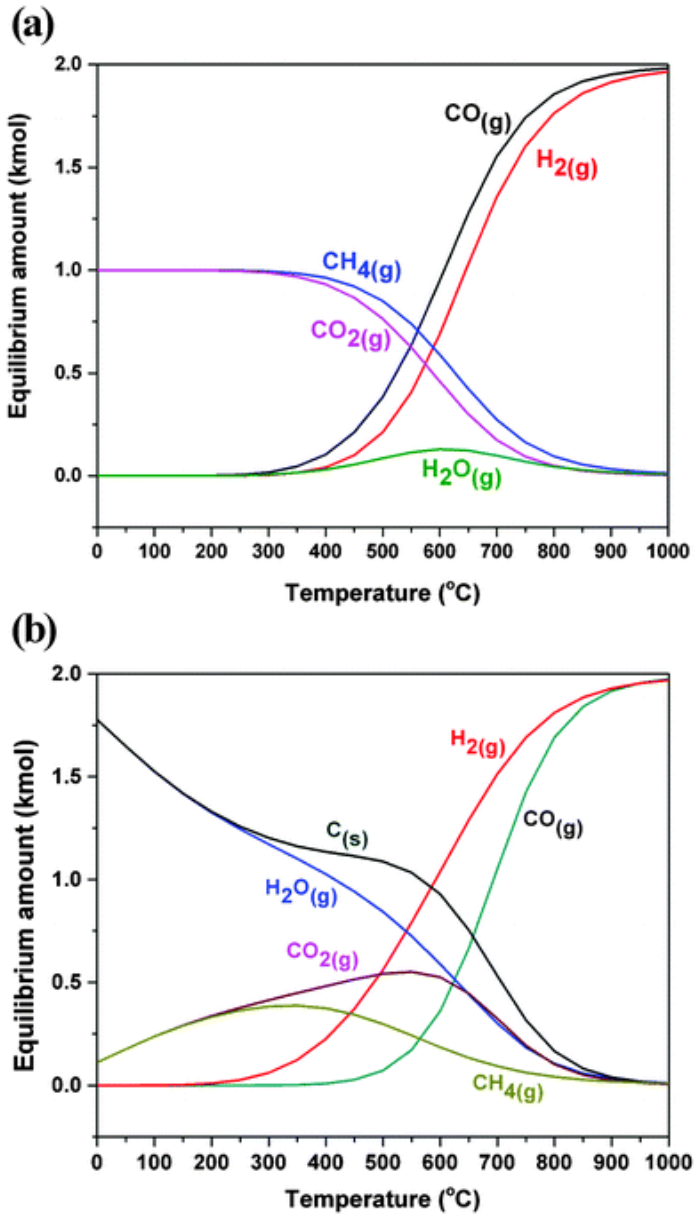

Figure 2-6: Thermodynamic equilibrium plots for DRM as a function of temperature at 1 atm and at inlet feed ratio of CO2/CH4 = 1 (a) Assuming no carbon formation occurs, (b) assuming carbon formation occurs (Pakhare & Spivey, 2014)

It has been concluded that high operating temperature and reactant ratio (CO/CH_4) is required to minimize the carbon deposition issue while low operating pressures are essential to attain high conversion of reactants and syngas yield (Pakhare & Spivey, 2014).

Table 2-4: Complete reaction mechanism pathways for dry reforming of methane (Nikoo & Amin, 2011)

Reaction #	Reaction	ΔH_{298}(kJ/mol)
1	$CH_4 + CO \leftrightarrow CO + 2H_2$	247
2	$CO_2 + H_2 \leftrightarrow CO + H_2O$	41
3	$2CH_4 + CO_2 \leftrightarrow C_2H_6 + CO + H_2O$	106
4	$2CH_4 + 2CO_2 \leftrightarrow C_2H_4 + 2CO + 2H_2O$	284
5	$C_2H_6 \leftrightarrow CH_4 + H_2$	136
6	$CO + 2H_2 \leftrightarrow CH_3OH$	-90.6
7	$CO_2 + 3H_3 \leftrightarrow CH_3OH + H_2O$	-49.1
8	$CH_4 \rightarrow C + 2H_2$	74.9
9	$2CO \rightarrow C + CO_2$	-172.4
10	$CO_2 + 2H_2 \leftrightarrow C + 2H_2O$	-90
11	$H_2 + CO \leftrightarrow H_2O + CO$	-131.3
12	$CH_3OCH_3 + CO_2 \leftrightarrow 3CO + 3H_2$	248.4
13	$3H_2O + CH_3OCH_3 \leftrightarrow 2CO_2 + 2H_2$	136
14	$CH_3OCH_3 + H_2O \leftrightarrow 2CO + 4H_2$	204.8
15	$2CH_3OH \leftrightarrow CH_3OCH_3 + H_2O$	-37
16	$CO_2 + 4H_2 \leftrightarrow CH_4 + 2H_2O$	-165
17	$CO + 3H_2 \leftrightarrow CH_4 + H_2O$	-206.2

2.3.2 Catalyst Selection

It should be signified that supported metal catalysts are susceptible to high temperatures which may lead to sintering of the catalyst or irreversible reaction with the support which both lead to irretrievable deactivation of the active sites (Hou, Chen, Fang, Zheng, & Yashima, 2006). Consequently, developing the catalytic system is the most critical stage of the DRM process to assure high conversion of reactants at lower temperatures, high selectivity of desired products and minimizing irrelevant secondary reactions which lead to the formation of long-chained hydrocarbons and carbon deposition on the active sites, and, resist sintering and deactivation at high temperatures (Gallego, Batiot-Dupeyrat, Barrault, Florez, & Mondragón, 2008; M. García-

Diéguez et al., 2010; Hou et al., 2006; Luo, Yu, Ng, & Au, 2000). It is noteworthy that the general performance of the catalytic system and carbon resistance is associated with the properties of the material used for active and support phase, the surface area of the support phase material, the particle size of the active phase components, the possibility of the interaction between active and support phase, and the preparation and activation method (Avetisov et al., 2010; Ballarini, de Miguel, Jablonski, Scelza, & Castro, 2005; Usman et al., 2015). Various, noble metals, transition metals and crystalline oxides with multiple support combinations have been investigated in the literature as a quest to identify a compatible catalyst system for the DRM process accordingly (Pakhare & Spivey, 2014).

2.3.2.1 Transition Metal Catalysts

Transition metals, namely, iron (Fe), nickel (Ni) and cobalt (CO), have been significantly studied for DRM catalytic reaction due to high reactivity characteristics with methane. From an economical perspective, the application of transition metals for DRM catalytic reaction is extremely profitable however, thermodynamic investigations have disclosed the vulnerability of these type of metal catalysts to carbon deposition which consequently leads to deactivation of the active sites (Gadalla & Bower, 1988). Two major parameters to inhibit carbon deposition on the catalyst surface have been highlighted as surface structure and surface acidity (Hu & Ruckenstein, 2002). The effect of surface structure on carbon resistance of the catalyst has been verified by comparing results obtained by the application of multiple morphologies of nickel for the DRM process. In 1982, Bartholomew investigated the effect of carbon deposition on steam reforming and concluded that the deposition affects the catalyst structure by fouling of the metal surface, blockage of catalysts pores and voids (active site) and physical disintegration of the catalyst support (Bartholomew, 1982). Ultimately, it was concluded that Ni (111) projects higher resistance to carbon deposition compared to Ni (100) and Ni (110) verifying the effect of surface structure on the phenomenon. Later, Rostrup – Nielsen, justified the effect of surface structure by investigating the effect of the size of the ensembles of metal atoms on the surface of the catalyst concluding that the ensembles required for carbon formation are significantly larger than species compulsory for methane reforming (Rostrup-Nielsen, 1991). Hence, the carbon deposition can be restricted by adjusting the metal particle size accordingly. Furthermore, sulfur passivation has been introduced as a commercial stage of SPARG process to influence the ensemble size and suppression of carbon

deposition (Dibbern, Olesen, Rostrup-Nielsen, Tottrup, & Udengaard, 1986). Sulfur passivation facilitates the elimination of carbon formation stage by predominantly eliminating larger ensembles on the metal surface(Rostrup-Nielsen & Hansen, 1993). Moreover, attenuation and suppression of carbon formation on metal surface catalyst has been reported by the application of a metal oxide catalyst support with robust Lewis basicity (G. J. Kim, Cho, Kim, & Kim, 1994; Z. L. Zhang & Verykios, 1994). The high Lewis basicity associated with the metal oxide support contributes to the suppression of the carbon formation by increasing the ability of the metal surface to chemisorb CO_2 in reforming reactions and converting carbon to CO in the concomitant secondary reactions (Horiuchi et al., 1996; Yamazaki, Nozaki, Omata, & Fujimoto, 1992).

Hou *et al.* compared the application of transition metal catalysts (Ni and CO) and noble metal catalysts (Ir, R, Rh, Pd and Pt) over alumina support and concluded higher activity of the non-noble metals while noble metals exhibited minimal carbon deposition (Hou et al., 2006). Crisaulli *et al.* proposed multiple strategies to overcome the carbon deposition issue with transition metal catalysts, namely, addition of alkali and alkaline (basic) dopants, application of basic support material and distribution of the metals in a highly-dispersed formation (Crisafulli, Scirè, Minicò, & Solarino, 2002).

2.3.2.2 Noble Metal Catalysts

Furthermore, the application of noble metals, namely, palladium (Pd), platinum (Pt), Rhodium (Rh) and Ruthenium (Ru) have been studied due to high DRM activity and resistance to carbon deposition. Unlike common transition metals, namely, nickel, noble metals project significantly higher carbon deposition resistance while simultaneously restrict the formation of carbon on the surface of the metal. However, extremely high cost has been regarded as the major barrier from commercialization of these type of catalysts (Hu & Ruckenstein, 2004; Pakhare & Spivey, 2014). Accordingly, Inui and Spivey, and Rostrup – Nielsen *et al.* have presented a ranking sequence for carbon deposition resistance of metal catalysts whereas (Inui & Spivey, 2002; Rostrup-Nielsen & Hansen, 1993);

$$Ni \gg Rh > Ir = Ru > Pt \cong Pd \qquad \text{At 773 K} \qquad (2.7)$$

$Ni \gg Rh > Ir = Ru > Pt \cong Pd$ At 923 K

emphasizing on the superiority of noble metals for carbon deposition restriction, nevertheless the phenomenon is not utterly inevitable. It has been accentuated that catalyst support has an indispensable role on enforcing the restriction of carbon formation on the metal surface (Ashcroft, Cheetham, Green, & Vernon, 1991). Hou *et al.* investigated the effect of multiple alumina supported noble metal catalysts, namely, Ir, R, Rh, Pd and Pt, and concluded that this category show high activity, stability and ke resistance (zero coke formation for all tested noble metals except minor deposition on Pd) with the activity sequence given as

$$Rh/\alpha - Al_2O_3 > Ru/\alpha - Al_2O_3 > Ir/\alpha - Al_2O_3 > Pd/\alpha - Al_2O_3 > Pt/\alpha - Al_2O_3 \quad (2.8)$$

Tsyganok *et al.* investigated the performance of the same noble metal catalyst supported on Mg – Al layer double hydroxides and reported a similar outcome of the activity and coke resistance of these catalyst species using morphological and surface analysis techniques, namely, X-ray diffraction (XRD) and transmission electron microscopy (TEM). Although noble metals project high activity and extreme coke formation resistance, however, the commercialization of such catalyst systems has been prevaricated due to prohibitive costs and unfavourable economy (Crisafulli et al., 2002).

2.3.2.3 Bimetallic Catalysts

Ultimately, in order to benefit from both metal groups simultaneously, promoting transition metal catalyst with noble metals have been promptly studied to compromise for the activity, stability, resistivity and economy of the catalyst system. Hou *et al.* investigated the performance Rh over Ni catalyst to determine the effect of noble and non-noble metal catalyst combination. While the independent application of Ni as catalyst demonstrated higher coke formation (17.2 mg coke/mg(Ni) h) and lower reactant conversion, 62% and 68% for methane and CO_2 respectively, addition of minor traces of Rh exhibited higher catalyst activity and entirely diminished coke formation (Hou et al., 2006). Furthermore, Garcia *et al.* investigated the catalytic effect of bimetallic Pt – Ni system ($0.4Pt - Ni/\gamma - Al_2O_3$) and concluded that the bimetallic catalyst exhibited a higher activity compared to monometallic $4Ni/\gamma - Al_2O_3$and $0.4Pt/\gamma - Al_2O_3$ in terms of metal conversion with 69%, 60% and 65% respectively. The higher activity of the

bimetallic catalyst was further associated with the formation of Pt – Ni alloy which leads to the deposition of fine Pt particles on the surface. Moreover, significantly lower carbon formation was reported for the bimetallic case compared to the monometallic catalyst, 6 Wt% to 45 Wt% correspondingly (García-Diéguez, Finocchio, Larrubia, Alemany, & Busca, 2010). Usman *et al.* have reported a discreet review on various monometallic and bimetallic catalytic systems reported in the literature and furthered compared the activity and carbon deposition results (Usman et al., 2015). It was concluded that contemplating the unfavorable economy, despite the exceptional carbon deposition resistance, application of monometallic catalysts or bimetallic systems with extremely low traces of noble metals, is favoured by the industry. Although multiple studies reported higher catalyst activity and coke resistance with the application of bimetallic catalysts. Consequently, various other parameters such as, catalyst support, promoters, preparation techniques and activation methods have been considered to develop active, resistant and feasible catalyst systems. Table 2-5 has summarized the performance of multiple mono and bimetallic systems investigated in the literature for dry reforming reactions.

Table 2-5: Catalyst performance summary for multiple monometallic and bimetallic systems recreated from (Usman et al., 2015)

Metal	Support	W	P	RC		Reactor	Conversion	
				T	t		CH_4	CO_2
Ni	Al_2O_3	10	IMP	800	30	FBR	63.0	69.0
			SG		48	FIBR	94.0	93.0
	CeO_2	10	IWIMP	550	7	FBR	11.7	29.7
	ZrO_2	5	IWIMP	750	10	FBR	65.0	-
	MgO - SiO_2	5	IMP	700	-	FBR	58.3	-
	SiO_2	5					55.0	-
	CeZr	5	IMP	750	70	FBR	41.0	-
	$Ce_{0.75}Zr_{0.25}O_2$	14	IMP	750	17	FBR	5.8	8.3
	$Ce_{0.75}Zr_{0.25}O_2$	2.1	CP	850	9	FBR	92	95
	$Ce_{0.8}Zr_{0.2}O_2$	15	CP	800	42	FBR	78.0	77.0
	MCM-41	1.2	DHT	750	30	FBR	70.0	-

		0.04						
	MCM-41	0.19[b]	DHT	600	4	FBR	20.0	38.0
	MCM-41	0.22	DHT	600	4	FBR	28.0	39.0
	SBA-15	12.5	IMP	800	720	FBR	43	70
	SiO_2	4.5	IWIMP	750	11	FBMR	47.0	60.0
Ni -CeO_2	ZrO_2	5	IWIMP	700	50	FBR	59.0	-
NiO	MgO	13.1	IMP	800	5	FBR	93.0	95.0
Ni-Rh		14- 0.7					6.9	11.8
Ni -MgO		15-10			200		95.0	96.0
Ni Rh					14		29.0	39.0
Ni Mo	SBA-15	5-25	IWIMP	800	120	FBMR	84.0	96.0
Ni-Ce	SiO_2	10-5	IWIMP	800	30	FBR	81.4	87.5
Co	γ-Al_2O_3	20	SG	700	20	FBR	32.0	39.0
					20	FIBR	66.0	71.0
	MgO	12	IMP	900	0.5	FBR	91.9	93.9
Pt	ZrO_2	1	IMP	700	4	FBR	79.0	86.0
	Al_2O_3	1	IMP	800	97	FBR	46.0	62.0
	ZrO_2						83.0	94.0
Pt -Ni		0.01-5					80.7	-
Pt-CeO_2 ZrO_2	MgO	0.8-3.0-3.0	IMP	800	24	FBR	69.0	80.0
Rh	CeO_2	0.5	IMP	800	50	FBR	50.7	63.2
	ZrO_2						65.9	74.2
	SiO_2	0.5	IMP	800	50	FBR	71.9	77.2
Rh@Ni		1.0			1		31.0	41.0
Ru	Al_2O_3	3	IMP	750	20	FBR	46.0	48.0
	CeO_2	2					52.0	60.0
	Al_2O_3	5	IMP	750	-	FBR	91.0	90.0
	CeO_2	5			-		90.0	96.0
Ru Ce	Al	2O3			-		97.0	97.0

Mg@Rh@Ni		1.0			1		38.0	40.0
$La_{0.8}Sr_{0.2}Ni_{0.8}Cu_{0.2}O_3$	-	4.9	SG	800	24	MR	75	60
$La_{0.8}Sr_{0.2}Ni_{0.8}Fe_{0.2}O_3$		4.1					80	81
AC	-	-	CM	700	-	FBR	4.0	8.3
AC-HNO_3			CM				4.0	8.3
AC-$NaNO_3$			IMP				17.7	29.7

2.4 Microwave Heating

The idea of the application of microwave as an industrial heating source goes back to the Second World War with the advent of the magnetron. However, the technology was later implemented for peaceful purposes such as industrial and research applications. The lack of adequate equipment and the knowledge of dielectric properties were regarded as the major obstacles to the deployment of the microwave technology for heat generation in the industry. Von Hippel *et al.* at MIT university obtained valuable experimental data on the dielectric properties of various organic and inorganic material in the frequency region of $100 < f < 10^{10}$ Hz (Von Hippel, 1954). The outcome of this study, in collaboration with the prospered investigations by their predecessors, has been regarded as a reliable scientific and industrial source for the dielectric properties of material up-to-date. Moreover, the recent technological advances in the field of microwaves such as significant developments in the magnetron and power source designs have gradually introduced the microwave heating technology as a reliable heating resource for industrial and scientific applications (Metaxas & Meredith, 1983).

In the frequencies bellow 100 MHz, where the conventional open-wire circuits are used, the industrial application is referred as radio frequency heating. However, for frequencies higher than 500 MHz, the current is guided into the applicator instead of the open circuit wires, which is referred as microwave heating. Moreover, in the frequency range of 100 – 500 MHz, the two techniques blend and occur simultaneously, triggering complexity to differentiate the leading method which is referred as the dielectric or high-frequency heating, generally highlighted as the preferred method in the industry. The combination of the two techniques is illustrated in Figure 2-7.

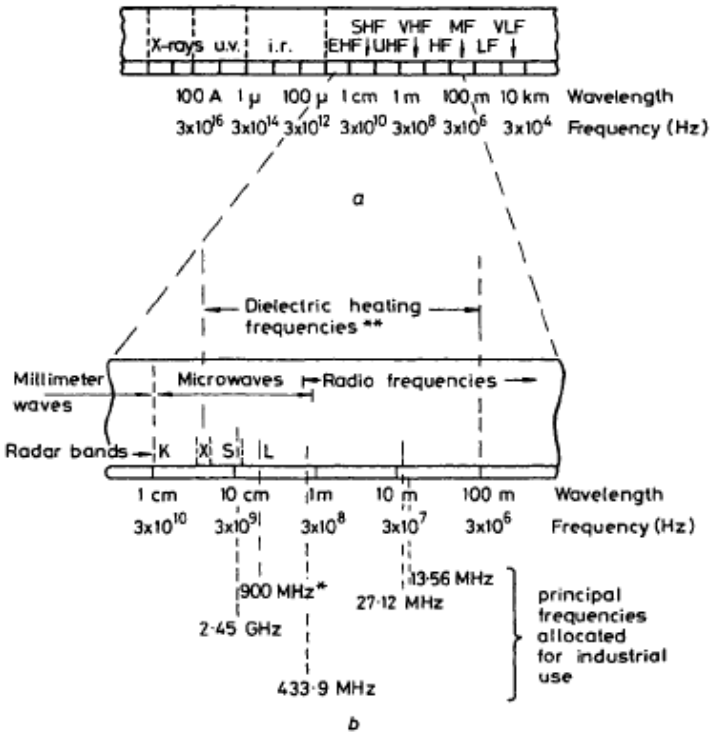

Figure 2-7: Electromagnetic Wave Classification (Metaxas & Meredith, 1983)

2.4.1 Dielectric Loss

The polarization of the insulating material and the inability of the divergence to keep up with the exceptionally rapid reversals of the electric field while exposed to the high-frequency electromagnetic field is the basis of the dielectric heating method. In a high-frequency exposure, the polarization vector (P) halts the applied electric field causing the originated current ($\partial P/\partial t$) to comprise a phase component with the enforced electric field leading to the distribution of power through the insulated material. The polarization could be accompanied by the direct conduction effects, majorly in a mixture of heterogeneous material, due to the redistribution of charged particles in association with the externally applied electric field (Daniel, 1967; Debye, 1929; Fröhlich, 1958; Hasted, 1973; Hill, Vaughan, Price, & Davies, 1969).

The interaction of dielectric and electric field originates the response of the charged particles to the implemented field causing displacement of the particles from the equilibrium state to induced dipoles. This induced polarization is derived by the *electronic polarization,* the displacement of the electrons around the nuclei or by the *atomic polarization*, the relative displacement of the atomic

nuclei due to the heterogeneous charge distribution in the molecular structure. Other polarization methods are polar dielectrics reorientation and Maxwell-Wagner polarization depicted in Figure 2-8. The aforementioned mechanisms, in addition to the d.c. conductivity is the basis of the high-frequency heating.

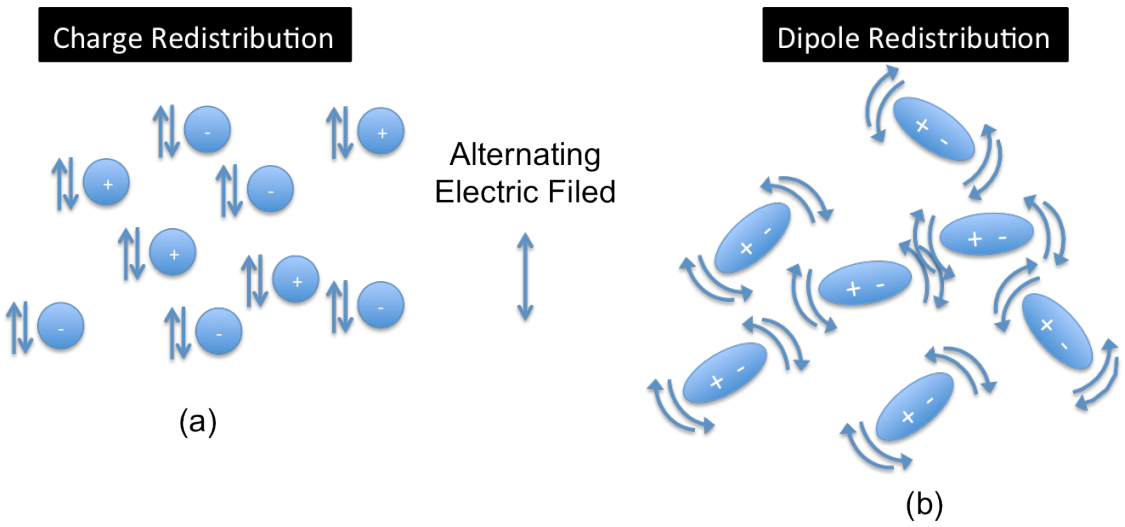

Figure 2-8: (a) Interfacial and (b) Reorientation Polarization (Metaxas & Meredith, 1983)

Later, Mosotti derived an equation to represent the relationship between the externally applied electric field on the system (E) and the local field applied to the individual dipole (E') given by (Zheludev & Tybulewicz, 1971):

$$E' = \frac{E}{3}(\varepsilon' + 2) \tag{2.9}$$

where ε' is the relative dielectric constant which is commonly referred as the dielectric constant in the literature. However, Eq. (2.9) is exclusively applicable for gases and non-polar liquids.

It is commonly acknowledged that the dielectric constant has a real dielectric value. However, when taking the losses into account, it develops a complex format expressed by:

$$\varepsilon^* = \varepsilon' - j\varepsilon'' \tag{2.10}$$

where the imaginary part (ε") is termed as the loss factor. However, the real loss factor should reflect the cumulative loss taking the conductive, dipolar, atomic and Maxwell-Wagner loses into account, expressed as the effective lost factor ($\varepsilon_{eff}^{"}$) given by

$$\varepsilon_{eff}^{"} = \varepsilon_{d}^{"}(\omega) + \varepsilon_{e}^{"}(\omega) + \varepsilon_{a}^{"}(\omega) + \varepsilon_{MW}^{"}(\omega) + \sigma/\varepsilon_0\omega \\ = \varepsilon^{"}(\omega) + \sigma/\varepsilon_0\omega \quad (2.11)$$

where the subscripts *d*, *e*, *a* and *MW* represent dipolar, electronic, atomic and Maxwell-Wagner respectively, σ is the conductivity of the medium, ε_0 is the dielectric constant of free space and ω is the corresponding general angular frequency. Substituting the effective loss factor for the loss factor in Eq. (2.9) gives:

$$\varepsilon^* = \varepsilon' - j\varepsilon_{eff}^{"} \quad (2.12)$$

Moreover, the ratio of the effective loss factor to the dielectric constant is called the effective loss tangent, including the effects of d.c. conductivity and the angle between the total current density vector (J_e) and the vertical axis as schematically illustrated in Figure 2-9, where J_p is the current associated to the polarization mechanism exclusively and J_e is the current due to both polarization and d.c. conductivity effects given by

$$J_e = j\omega\varepsilon_0[\varepsilon' - j(\varepsilon" + \sigma/\varepsilon_0\omega)]E \quad (2.13)$$

which all types of losses are comprised (Metaxas & Meredith, 1983).

2.4.2 Dielectric Properties

The knowledge of the dielectric properties of material is an integral and essential part of the microwave heating process. Dielectric properties are dominated by temperature, moisture content, and density of the material. Hence, the theoreticians have been striving to apprehend an enhanced understanding of the heterogeneous dielectric material and the effect of the combination of various dielectrics on the microwave heating parameters by introducing innovative methods to acquire the relevant data.

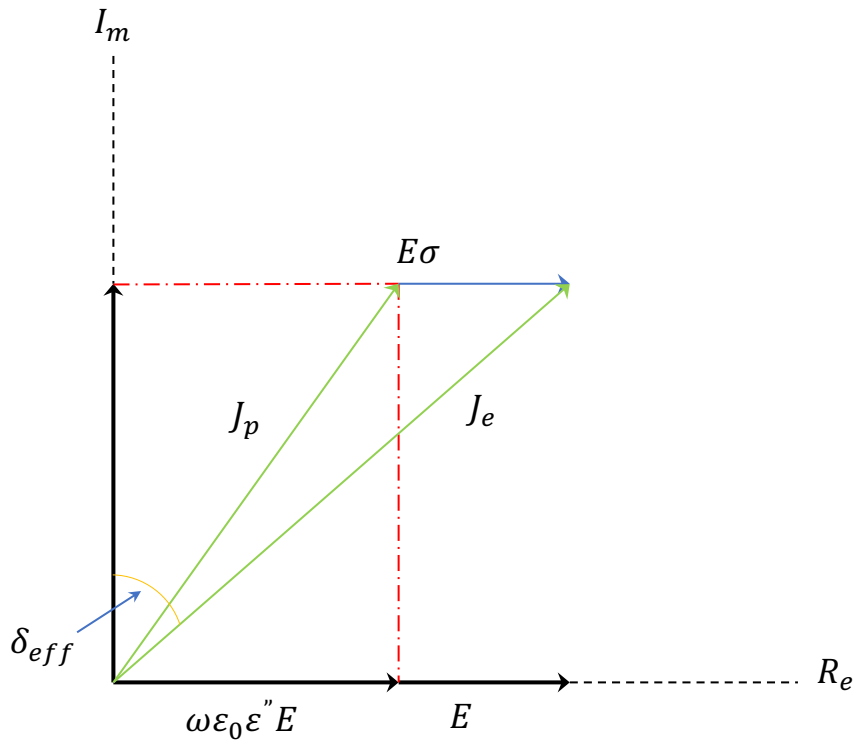

Figure 2-9: Current Density and Applied Electric Vectors Recreated From (Metaxas & Meredith, 1983)

The mathematical form of the dielectric property of material is earlier presented as the complex permittivity, ε^*, by equation 4. It should be acknowledged that both ε^* and $\varepsilon^{"}_{eff}$ are frequency and temperature dependent. As already stated, Von Hippel *et al.* tabulated the dielectric properties of various inorganic materials (crystals, ceramic, glasses and water) and organic materials (crystals, simple non-crystals, plastics, natural resins, asphalts and cements, waxes and woods) for the frequency and temperature range of $100 < f < 10^{10}$ (Hz) and $-12 < T < 200$ (^oC) respectively (Von Hippel, 1954). The data provided by Van Hippel *et al.* has since been expanded by other researches (Tinga and Nelson for food and biological substances) and is utilized as a reference in order to predict the behavior of different dielectric material while exposed to high frequency waves (W. R. Tinga & Nelson, 1973).

As discussed earlier, some substances incorporate permanent dipole moments through their molecular structure, which is associated with the molecular dimensions and symmetry. Molecules containing a center of charge symmetry through their structure, namely, methane (CH_4), carbon tetrafluoride (CF_4) and propane (C_3H_8), exhibit zero polar moments and are identified as non-polar

molecules. On the other hand, molecules like water (H_2O) or proteins such as gelatin and hemoglobin are considered as polar molecules since they endorse no charge symmetry in their structure and exhibit strong polar moments. However, the loss factor of polar material depends on the relaxation time, τ, in addition to the polar moments based on the equation introduce by Debye, for the total loss factor of a mixture of polar solute into a non-polar solution given by (Debye, 1929):

$$\varepsilon_d^{"}(\omega) = \frac{C_0(\varepsilon' + 2)}{k_b T}\mu^2 + \frac{\omega\tau}{1 + (\omega\tau)^2} \tag{2.14}$$

where C_0 depends on the relevant concentration, μ is the dipole moment, k_b is the Boltzmann's constant and T is the corresponding temperature. The interpretation of such dipole moments based on the molecular parameters considering the total losses, $\varepsilon_{eff}^{"}$, for various dipolar materials has been studied by Hill *et al.* (Hill et al., 1969). An extended list of various organic and inorganic materials dielectric properties is presented by Von Hippel *et al.* at various corresponding frequencies (Von Hippel, 1954).

2.4.2.1 Measurement Techniques

The frequency which is commonly employed for the industrial heating purposes is in the range of $400 < f < 3000$ MHz, where the bands are classified as 433.9 ± 0.87 MHz, 896 ± 10 MHz, 915 ± 13 MHz (US) and 2450 ± 50 MHz which the latter is the most conventional frequency for the industrial and municipal microwave heating purposes (Gupta & Wong, 2007). The dielectric property measurement is performed by exhilarating a waveguide in the coaxial conductors' format, where the test material is employed as part of the dielectric medium separating the conductors. The primary parameter identified during the dielectric measurement method is propagation constant (γ) given by:

$$\gamma^2 = (2\pi/\lambda_c) - \omega^2\mu_a\varepsilon_a = (\alpha + j\beta)^2 \tag{2.15}$$

where λ_c is the cutoff wavelength of the wave guide. Measurement of the propagation constant of the electromagnetic wave through the material (γ_1) and through the empty transmission line (γ_2) enables the calculation of the dielectric constant, ε^*, by reducing the Eq. (2.15) for the coaxial line ($\lambda_c = \infty$) to

$$\varepsilon_a = \varepsilon_0 \varepsilon^* = \varepsilon(\gamma_2/\gamma_1)^2 \quad (2.16)$$

Hence, to determine the dielectric constant values, the attenuation constant, α, and the phase constant, β, of the electromagnetic wave signal, are required. In this regard, three methods of *Robert and von Hippel Method, X-band Techniques* and *Cavity Perturbation Techniques* are exploited for calculation and measurement of the dielectric properties of different materials.

1. Robert and von Hippel method

The method introduced by Robert and von Hippel is regarded as the most experimentally simple and commercially accessible technique for the measurement of the γ_2 values (Von Hippel, 1954). Initially presented for the application with solids, the method was later extended to the lossy liquids (Metaxas & Meredith, 1983). However, the major drawback of the Robert and von Hippel method is the dependency on the experimental data and resolution of transcendental equations for the calculation of the dielectric properties of the material. Although this deficiency has been surpassed by advancements of the computational techniques (Metaxas & Meredith, 1983; W. R. Tinga & Nelson, 1973)

The basis of the measurements is the termination of the standing waves in the waveguide by the section field using the dielectric material. Figure 2-10 illustrates the apparatus and mechanism of the Robert and von Hippel technique. The relationship between input impedance of the dielectric filled section, Z_{in}, and γ_2 is given by:

$$Z_{in} = Z_{02} \tanh(\gamma_2 d) \quad (2.17)$$

$$\frac{\tanh(\gamma_2 d)}{\gamma_2 d} = \frac{S - j\tan(\beta_1 x_0)}{(1 - jS\tan(\beta_1 x_0))} j\beta_1 d \quad (2.18)$$

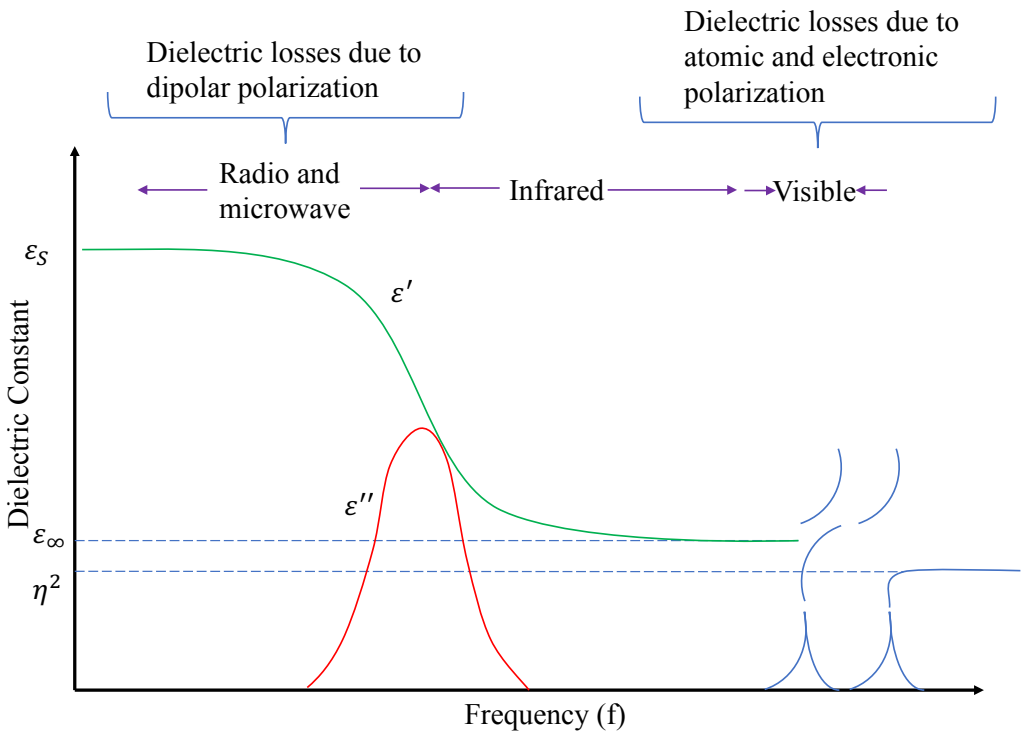

Figure 2-10: The dielectric Constant as a Function of the Frequency in the Region of Dipolar and Distortion Absorption (Metaxas & Meredith, 1983)

where d is the dielectric specimen length, S is the voltage standing wave ratio (VSWR), x_0 is the distance from the interface, and β_1 is the phase constant. The determination of the $\frac{tanh(\gamma_2 d)}{\gamma_2 d}$ enables the calculation of x_0, S, d and λ_0' (the wave length in the empty coaxial line). Solving Eq. (2.18) and substituting the results into Eq. (2.17) reveals multiple possible solutions for the dielectric properties. Subsequently, repeating the experiment at a different length of the dielectric specimen and comparing the results ultimately leads to the elimination of the unsatisfactory values and the unique dielectric property value is eventually obtained. However, the short-circuited technique, the modified von Hippel method, in the industry consists of the measurement of the debilitation of a lunched microwave wave signal to the dielectric material located as a thin film inside a TE_{10} waveguide with the advantage of directly revealing the property of interest value to the system designers, eliminating the complex computational steps and errors.

2. X-band techniques

The idea of the application of x-band (8-10 GHz) was primarily introduced in the design and manufacturing of the industrial moisture meters. The employment of the x-band techniques for the

microwave property measurement of the material is barely considered as the most microwave operations are performed at 2.45 GHz frequency. However the application of the x-bands in the heating industry has been studied (Metaxas & Meredith, 1983)

Although deliberated as a short-circuited technique, Time Delay Refractory (TDR) and strapline have been widely used for the dielectric property and moisture measurements of various material for the commercial purposes (Iskander & Stuchly, 1972; D. J. Steele & Kent, 1978). Moreover, the application of x-bands in the moisture gauging of numerous material such as aquametric has been occasionally reported (Kalinski, 1978; Kraszewski, 1980). The application of x-bands for measuring the dielectric properties of the material is based on the attenuation, α, of the wave signal as a function of the moisture content of the tested material, M.

3. Cavity perturbation techniques

The application of methods based on electromagnetic field perturbation of a resonant cavity employing a small sample of the insulating material in it has been extensively reported for the measurement of the dielectric properties of the low-loss material (Metaxas & Meredith, 1983). The technique obliges the measurement of the shift of the cavity resonance to the new frequency of ω_0, from the original unperturbed frequency value of $\omega_0^{'}$. The similar requirement withstands for the cavity Q – factor (quality factor) values. The dimensions of the sample are selected considerably smaller compared to the cavity to induce a diminutive frequency shift, thus verifying the validity of the perturbation theory. Furthermore, the correct positioning of the sample through the cavity should be acknowledged to preserve the symmetry of the system.

The complex frequency shifting caused by the insertion of an insulated small sample in the negligible magnetic field region to the cavity has been described and formulated by Altman for the perturbation derived from Maxwell's equation expressed as (Altman, 1964):

$$\frac{\widehat{\omega}_0 - \widehat{\omega}_0'}{\omega_0} = -\varepsilon_0(\varepsilon^* - 1)\frac{\iiint E^* E_0 dV}{4U} \tag{2.19}$$

where E and E_0 are the perturbed and unperturbed peak electrical field in the region of the dielectric sample, U is the total energy stored in the cavity and V is the total volume of the cavity. Moreover, the complex angular frequency of the perturbed cavity can be expressed as

$$\widehat{\omega}_0 = \omega_0 + j(\omega_0/2Q) \tag{2.20}$$

where ω_0 represents the resonance-frequency measured on an impedance basis. Substituting the resonance frequency for perturbed and unperturbed complex frequency in Eq. (2.19) gives:

$$\frac{\Delta\omega}{\omega_0} + j\left(\frac{1}{2Q_0} - \frac{1}{2Q_0'}\right) = -\varepsilon_0(\varepsilon^* - 1)\frac{\iiint E^* E_0 dV}{4U} \tag{2.21}$$

where Q_0 and $Q_0^{'}$ are the loaded unperturbed and perturbed Q – factors of the cavity respectively. Hence, the dielectric properties of the material can be determined by the measurement of the resonance frequency shifting and the fluctuation of the Q – factors.

2.4.3 Dielectric Properties Dependency

As previously stated, the dielectric properties of material comprehensively depend on the moisture content of the components, process temperature, and frequency where the effects are concisely discussed in the following section.

2.4.3.1 Moisture Content

The dielectric properties data presented in the literature generally correspond to the equilibrium moisture content state. However, many industrial processes such as paper, textile, wood, and leather, engage the elimination of the moisture content of the material. Hence, the variation of ε^* and $\varepsilon_{eff}^{"}$ specifically, with the moisture content performs a considerable role in designing the microwave heating systems. Consequently, major studies have been devoted to determination and analysis of the effect of the moisture content fluctuations on the dielectric properties of the material in order to extend the eventual results to the design of the microwave applicators (Metaxas & Meredith, 1983).

Liquid water has a strong polar structure, which interacts extensively with microwave as it absorbs the wave and further transforms it to heat. Liquid water, when contacted with another material is regarded as absorbed water, which in this case the dielectric properties considerably differ by the liquid water itself. The principle relaxation (maximum loss factor) of water arises at 18 GHz, while other minor relaxations occur over the infrared frequency range (Hasted, 1972). Moreover, the

relaxation peaks arise at frequencies considerably below 18 GHz. Subsequently, based on the high-frequency field exposure, water demonstrates diverse microwave interactive behavior, thus affecting the microwave absorption of the adjacent material (Hasted, 1973).

The absorbed water content of the wet material is classified under two principle states (Metaxas & Meredith, 1983):

- *Free Water*: Residing in the capillaries and cavities.
- *Bound Water*: Chemically combined with other materials in the component structure or physically absorbed on the surface of the dry material.

Figure 2-11 illustrates the loss factor variations corresponding to the moisture content, *M*, fluctuations of a regular wet solid. The water principle states could be related to the various regions, defined by the slope ($d\varepsilon''_{eff}/dM$), of the ε''_{eff} vs *M*. The graphical analysis depicts that the minor slope is originally related to the bound water territory (region I) whereas the considerably sharp slope is majorly affected by the presence of the free water (region II) inside the system. The phenomena could be addressed by the limited rotation of the in-bound water content on the molecular surface compared to the water residing freely in the capillaries or cavities. Consequently, the free water composition of the material extensively controls the dielectric loss property of the components (Metaxas & Meredith, 1983). Moreover, the critical moisture content, M_c, is located at the point where the slope shift occurs. The critical moisture content of the highly hygroscopic material typically occurs in the region of 10 – 14 % whereas the value is allocated approximately at 1% for the non-hygroscopic components (Stuchly, 1970).

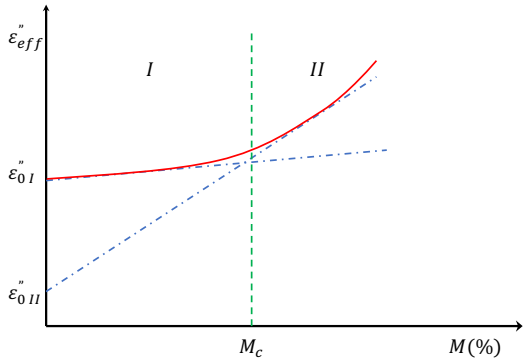

Figure 2-11: The Effective Loss Factor as a Function of the Moisture Content Recreated From (Metaxas & Meredith, 1983)

The mathematical relationship between the moisture content and loss factor is commonly required for the optimization and design of the microwave applicators and engagement of the $\varepsilon_{eff}^{"}$ vs *M* data for computational purposes. Employing the linear regression methods to linearize the response of the $\varepsilon_{eff}^{"}$ vs *M,* the equations for various regions of the Figure 2-11 gives:

$$\varepsilon_{eff}^{"} = \varepsilon_{0I}^{"} + \left(\frac{d\varepsilon^{"}}{dM}\right)_{I} M \qquad \text{(Region I)} \qquad (2.21)$$

$$\varepsilon_{eff}^{"} = \varepsilon_{0II}^{"} + \left(\frac{d\varepsilon^{"}}{dM}\right)_{II} M \qquad \text{(Region II)} \qquad (2.22)$$

where $\varepsilon_{0I}^{"}$ and $\varepsilon_{0II}^{"}$ are constants and $(d\varepsilon^{"}/dM)$ corresponds to the slope of the dual regions. Alternatively, the empirical equation reflecting the best fitting of the experimental data is presented as

$$\varepsilon_{eff}^{"} = \varepsilon_{0}^{"} + \frac{AM^{3}}{M_{\infty} - M} \qquad (2.23)$$

where $\varepsilon_{0}^{"}$, *A* and M_{∞} are selected to best fit the data according to the curve.

2.4.3.2 Temperature

Various studies have been presented in the literature, investigating the variation of the dielectric properties with the system temperature (Bengtsson & Risman, 1971; Rzepecka & Pereira, 1974). In 1969, Tigana illustrated the variation of the loss factor with the temperature at various moisture levels on Douglas fir (Figure 2-12) (Wayne R. Tinga, 1970). Based on this study, the loss factor increases with temperature, at low moisture contents since the physical structure reduces; thus, the dipoles are provided higher freedom to reorientation. However, the loss factor decreases with temperature elevation at hydrations of above 25%.

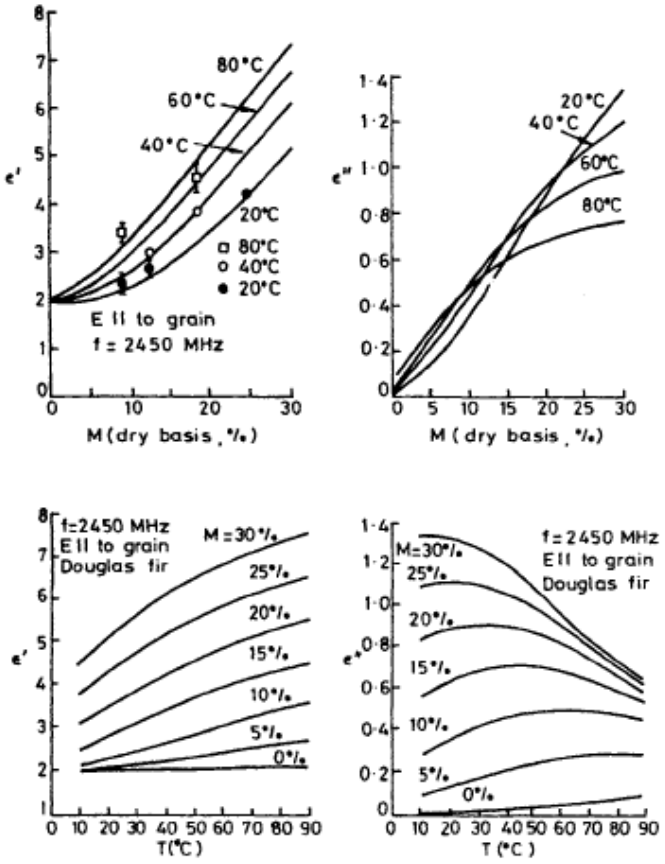

Figure 2-12: Electric Properties vs. Moisture Content & Temperature in Douglas Fir (Wayne R. Tinga, 1970)

In 1974, To *et al.* investigated the effect of temperature variations on the dielectric factor and dielectric loss for various feedstock (To, Mudgett, Wang, Goldblith, & Decareau, 1974). It was highlighted that initially the diminution in dipolar losses is neutralized by the escalation in the conductivity losses while elevating the temperature at 2.8 GHz, which practically leads to a constant ε''_{eff} versus temperature variations. However, at frequencies below 1000 MHz, conductivity losses dominate the dipolar losses; hence, ε''_{eff} increases by rising the temperature.

Runaway heating, the uncontrolled temperature rise in the material consequence to the positive slope of $+d\varepsilon''/dT$ of the ε''_{eff} versus temperature response, is a diagnosed issue with the microwave heating which may lead to damages to the material. Based on the study by Huang after an initial temperature rise, the effective loss factor increases which subsequently leads to a further elevation in the temperature of the system (Huangt, 1976). The possible solutions to address the runaway

heating issue is interrupting the microwave energy or removing the material from the hot zone. Further studies have investigated the effect of runaway heating on the microwave heating process (Couderc, Giroux, & Bosisio, 1973; Terselius & Ranby, 1978). Moreover, the microwave applicator design severely affects the runaway heating effects.

2.4.4 Volumetric Heating

2.4.4.1 Average Dissipated Power

The power dissipated by the microwave generator inside the dielectric material is associated with the electric field imposed on the system. The energy is transported as electromagnetic waves through space and eventually converted to heat. The power through a closed surface area is calculated by the integration of the Poynting vector where:

$$p = E \times H \qquad w/m^2 \tag{2.24}$$

Thus the power is calculated as (Johnk, 1975):

$$\int_{S'} (E \times H^*).dS' \tag{2.25}$$

Consequently, employing the Maxwell law given by:

$$\nabla \times H = J + j\omega\varepsilon_0\varepsilon^* E \tag{2.26}$$

Moreover, by the application of the appropriate substitutions for the parameters and taking the integration yields:

$$P_{av} = \omega\varepsilon_0\varepsilon''_{eff}E^2_{rms} \tag{2.27}$$

Substituting ε_0= 8.8 $\times 0^{-12}$ F/m and $\omega = 2\pi f$ yields:

$$P_{av} = 0.556\times10^{-10} f\varepsilon''_{eff}E^2_{rms}VW \tag{2.28}$$

where E_{rms} is the imposed electric field (V/m), f is the frequency (Hz), V is the volume (m^3) and W is the weight (Kg). Moreover, if the dielectric material projects magnetic loss through the process, Eq. (2.28) will be further developed to:

$$P_{av} = \omega\varepsilon_0\varepsilon''_{eff}E^2_{rms} + \omega\mu_0\mu''_{eff}H^2_{rms}V \tag{2.29}$$

Also, Eq. (2.28) could be identically derived by employing the *lossy capacitor* method (Metaxas & Meredith, 1983)

2.4.4.2 Penetration Depth

The penetration depth (D_p) is defined as the depth which the electromagnetic wavelength could penetrate through the dielectric material. Employing the Maxwell's equations and Von Hippel's equation and the application of the proper parameters substitutions calculates the penetration depth as (Von Hippel, 1954):

$$D_p = \frac{1}{2\omega}\left(\frac{2}{\mu'\mu_0\varepsilon_0\varepsilon'}\right)^{1/2}\left[\left(1+\left(\varepsilon''_{eff}/\varepsilon'\right)^2\right)^{1/2}-1\right]^{-1/2} \tag{2.30}$$

where μ' and μ_0 are the real and free space permeability respectively. Eq. (2.31) can be rearranged in the terms of free space wavelength

$$D_p = \frac{\lambda'_0}{2\pi(2\varepsilon')^{1/2}}\left[\left(1+\left(\varepsilon''_{eff}/\varepsilon'\right)^2\right)^{1/2}-1\right]^{-1/2} \tag{2.31}$$

In the case of low loss dielectrics where $\left(\varepsilon''_{eff}/\varepsilon'\right) \ll 1$, Eq. (2.31) is further simplified to:

$$D_p = \frac{\lambda'_0(\varepsilon')^{1/2}}{2\pi\varepsilon''_{eff}} \tag{2.32}$$

where λ'_0 is the free space wavelength. Eq. (2.30) and (2.31) highlight that the penetration depth is proportional to the wavelength, hence, increases by decreasing the frequency. At the microwave frequency range, the penetration depth values are small and in the order of the treated material dimensions. Thus, in the case of wet materials, may lead to an extremely uninform temperature distribution through the dielectric material. In 1974, Ohlsson *et al.* studied the relationship between

the penetration depth and the temperature at the three major industrial frequencies (Ohlsson, Bengtsson, & Risman, 1974).

The power requirement to raise the temperature of a mass M_a (Kg) of the material from T_0 to T in designated period, t (s) is expressed as:

$$p = \frac{Q_h}{t} = \frac{M_a c_p (T - T_0)}{t} \tag{2.33}$$

where c_p is the specific heat capacity of the material. Substituting Eq. (2.28) in equation (2.33) and further rearranging yields:

$$(T - T_0)/t = \frac{0.556\times10^{-10} f \varepsilon''_{eff} E^2_{rms}}{\rho c_p} \qquad ℃\ s^{-1} \tag{2.34}$$

where ρ is the density (kg/m^3) and c_p is the specific heat of the dielectric material ($J/kg\ ^oC$). Hence for a fixed frequency, the temperature-rise value is proportional to the $\varepsilon''_{eff} E^2_{rms}$, which is a function of the temperature itself.

The electric field is regarded as the principle parameter in the microwave heating process, which performs as a link between the electromagnetic energy and the treated material. Determination of the penetrated electric field in the dielectric material is the challenging task, commonly performed by the perturbation techniques. However, rearranging Eq. (2.34) is considered as a practical method to address the electric field distribution through the dielectric material given by

$$E_{rms} = \left(\frac{\rho c_p (T - T_0)/t}{0.556\times a0^{-10} f \varepsilon''_{eff}} \right)^{1/2} \qquad V/m \tag{2.35}$$

However, Eq. (2.35) is not applicable to the case which the electric field distribution is not constant. In this case, various alternative field equations are presented in the literature to be substituted with the constant electric field parameters in Eq. (2.27) and (2.35) (Bleaney & Bleaney, 1965; Francis, 1960; MacLatchy & Clements, 1980; J. R. White, 1970).

2.5 Heat and Mass Transfer

As already stated, the heat generation inside a microwave system is the result of the electromagnetic waves interaction with the dielectric material employed in the process. Contemplating the temperature fluctuations, Perkin has described the high-frequency microwave drying in three steps, illustrated in Figure 2-13 (Perkin, 1979):

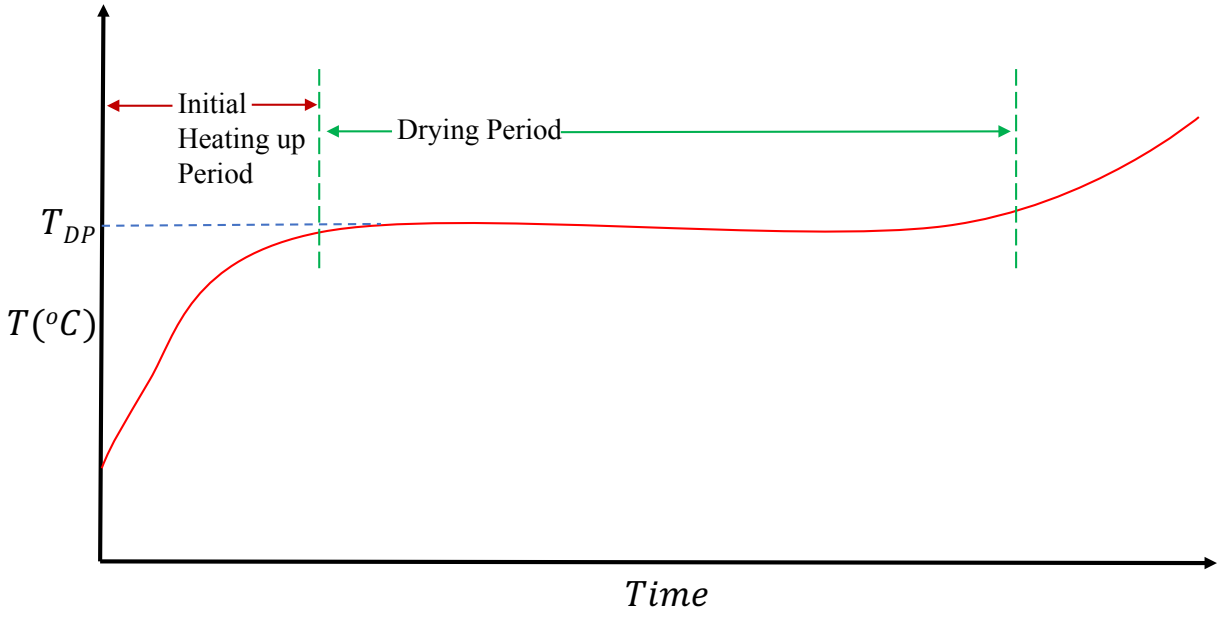

Figure 2-13: Rate of Rising Temperature During High-Frequency Drying (Perkin, 1979)

The solid is rapidly heated to the moisture content (liquid phase) boiling temperature where thereafter $\partial T/\partial t \cong 0$.

The temperature increases through the drying process due to the boiling point of the liquid phase material not attained.

The solid is heated up to a critical temperature below the boiling point of the liquid components and force cooled accordingly. This category is applicable to the heat sensitive material.

Furthermore, Perkin and Luikov developed an equation system to mathematically express the mass transfer, heat transfer and momentum transfer behavior inside a microwave heating system, given as (Luikov, 1964; Perkin, 1979):

Mass Transfer:

$$\frac{\partial M}{\partial t} = \alpha_m \nabla^2 M + \alpha_m \delta_T \nabla^2 T + \alpha_m \delta_p \nabla^2 P \tag{2.36}$$

Heat Transfer:

$$\frac{\partial T}{\partial t} = \alpha_T \nabla^2 T + \frac{\varepsilon_v}{c_p} L_h \frac{\partial M_l}{\partial t} + \frac{\delta P}{\rho c_p} \tag{2.37}$$

Momentum Transfer:

$$\frac{\partial p}{\partial t} = \alpha_p \nabla^2 P - \frac{\varepsilon_v}{c_a} \frac{\partial M_l}{\partial t} \tag{2.38}$$

where δP is the localized power density, L_h is the hydraulic length of the dielectric material, α_m, α_T and α_p are the mass, temperature and pressure diffusivities respectively, p is the total pressure, ∇T and ∇P are the thermal and pressure gradient coefficients respectively, c_a is the specific moisture capacity of vapor phase, M is the total moisture content where:

$$M = M_l + M_v \tag{2.39}$$

where M_l *and* M_v are the mass content of the liquid and vapor phase respectively and ε_v is the ratio of the vapor flow to the total moisture flow. In 2011, Farag *et al.* presented a three dimensional model to address the heat transfer equations for the microwave heating (S. Farag et al., 2012). Deploying the definition of the loss tangent, the ratio between the loss factor and the electric constant which is regarded as ability of dielectric material to convert the absorbed wave energy and transform it to heat, Eq. (2.27) is rearranged to Eq. (2.40) valid for the non-magnetic material:

$$P_{av} = 2\pi f \varepsilon' tan\delta \; E_{rms}^2 \tag{2.40}$$

where:

$$tan\delta = \frac{\varepsilon^{"}}{\varepsilon'} \tag{2.41}$$

The schematic representation of the heat balance of a cubic dielectric material exposed to a microwave heating system is illustrated in Figure 2-14.

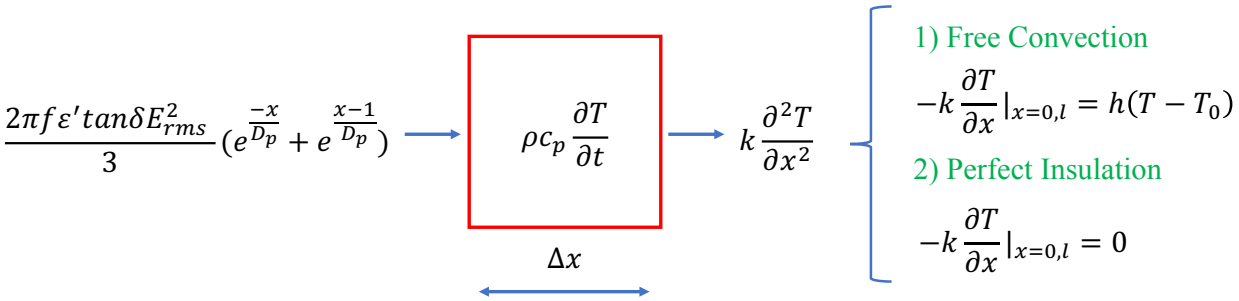

Figure 2-14: Schematic representation of the thermal balance on a dielectric element in the system (S. Farag et al., 2012)

Application of the energy balance on the designated element leads to the heat transfer equation on a cubic dielectric material exposed to the high-frequency electromagnetic waves given by:

$$k\nabla^2 T + \frac{P_0}{3}\sum_i \left[e^{\frac{-i}{D_p}} + e^{\frac{i-1}{D_p}}\right] = \rho c\frac{\partial T}{\partial t} \qquad (2.42)$$

where k is the conductivity coefficient, P_0 is the specific power derived from Lambert's equation, describing the power penetration in one direction of the Cartesian system (S. Farag et al., 2012), l is the dimension of the cube, and i refers to the Cartesian coordinates: *x, y & z.* Various heat transfer investigation through the microwave heating system has been studied and presented in the literature (Campañone & Zaritzky, 2005; Ciacci, Galgano, & Di Blasi, 2010; Pandit & Prasad, 2003).

2.5.1 Wave Applicators

An electromagnetic wave travels through empty space at 3×10^8 m/s velocity, irrespective of the frequency based on two major principles:

- The electric field (*E*) in *V/m*
- The magnetic field (*H*) in *A/m*

In practice, metal conductors are employed to transmit the electromagnetic wave from the generator to the load material for heating purposes through waveguides or microwave ovens. It is verified that the electromagnetic field propagates inside metal tubes and resonates inside metal boxes. The

characteristics of the field are defined by multiple plane waves, a sinusoidal alternating electric field vertically polarized with a horizontal magnetic field which corresponds to a sinusoidal lag phase with the electric field, where the geometry is depicted in Figure 2-15.

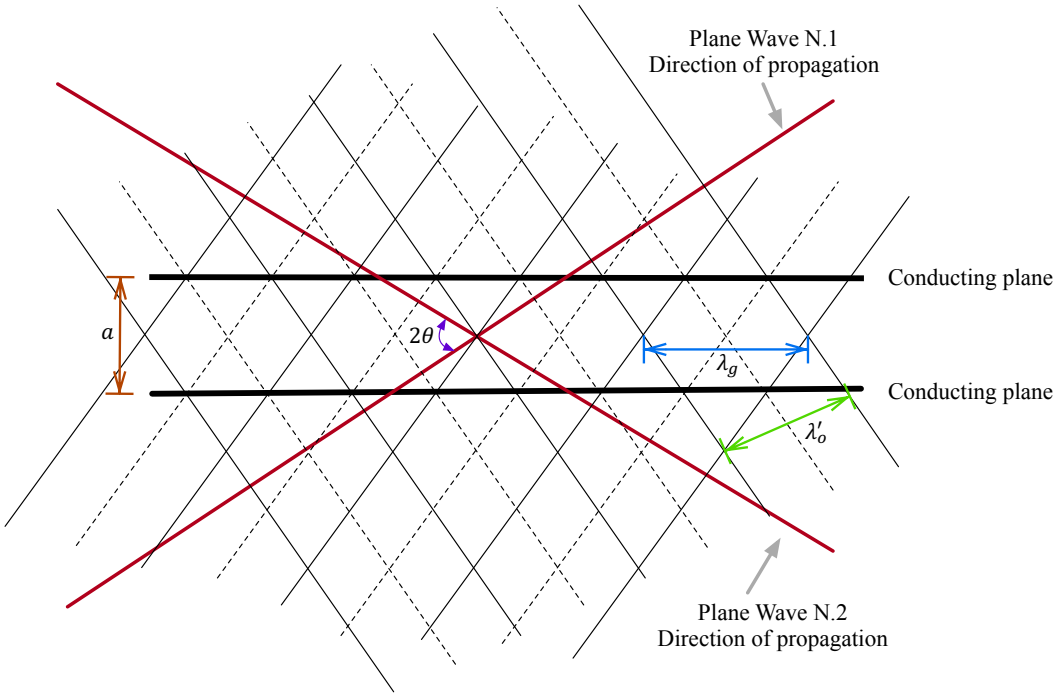

Figure 2-15: Synthesis of a Guided Wave Between Conducting Planes by Two Coherence Plane Waves (Metaxas & Meredith, 1983)

For microwave heating purposes, two major waveguide propagation properties are considered in principle:

The magnitude of the electric field as the premier component involved in heating

The distribution of the induced current in the walls of the waveguide to prevent wave leakage leading to energy loss and hazard.

The relationship between the power flow and the peak field propagated through a rectangular waveguide is expressed as (Dicke, Montgomery, & Purcell; Harvey & Harvey, 1963):

$$E = \left(\frac{4P\lambda_g}{\lambda_0'}\frac{1}{ab}\left(\frac{\mu_a}{\epsilon_a}\right)^{0.5}\right)^{0.5} \tag{2.43}$$

where P is the power flow (watts) and a and b are the broad and narrow faces dimensions respectively.

Microwave applicators, in general, are classified under two major categories:

- *Traveling wave applicators:* the dissipated power is transmitted from the magnetron through a chamber, which ultimately is absorbed by the dielectric load. The efficiency highly depends on the dielectric properties and the cross-sectional area of the workload. The balanced symmetry, which is commonly deliberated in the design criteria of such applicators, minimizes the leakage risk and energy losses. Traveling waveguide applicators are not recommended for the processing of low loss material, as the length of the applicator will inconveniently increase. Various types of traveling wave applicators have been presented in the literature namely; the axial traveling wave applicators and Meander traveling wave applicators (Dunn, 1967; Heenan, 1968; Puschner, 1966). Table 2-6 has summarized the comparison of the structural material employed for the traveling wave applicators manufacturing.
- *Multimode oven applicators:* This type of applicators dominates the industrial applications of microwaves by an enormous margin. Multimode oven applicators are widely employed for oven boxes, low power, and high power industrial applications. Although highly feasible due to the simple structure, the major challenge is to maintain the uniform heating through the process. The design of the multimode applicators in principle is a box, sufficiently large (a couple of wavelengths) in at least two dimensions, coupled with a magnetron. The multimode oven applicators are commonly employed for municipal microwave heating purposes. The power volume density (kW/m^3) is the principal design parameter for this type of applicators where the limitations expressed as:
- Dielectric interruption of the air or gas (vapor) mixture.
- Possible destructive damage to the workload depending on the employed material.

Table 2-6: Comparison of construction materials (Metaxas & Meredith, 1983)

Parameter	Stainless steel	Aluminum	Mild steel aluminum coated	Copper	Brass
Wall loss	High	Low	Moderate	Low	Moderate
Hygiene	Good	Moderate	Poor	Moderate	Moderate
Corrosion	Good	Moderate	Fare	Moderate	Moderate
Thermal Conductivity	Poor	High	Moderate	Moderate	Moderate
High temperature ^{o}C	Up to 600	80 Max	250 Max	300	300
Thermal expansion	Moderate	High	Moderate	-------	--------

2.5.2 Leakage and Safety

Due to the invisibility of the high-frequency electromagnetic waves and the lack of public knowledge, a constant safety concern during the application of microwave technology endures. The hazardous effects of the microwave are commonly classified into two major categories:

- The thermal effects caused to the internal human body organs
- The non-thermal effects comprised on the nervous system further classified as temporary and permanent damages.

However, a global safety code to address the possible microwave hazardous effects associated with the leakage or constant exposure is yet to be concluded due to the insufficient data and the inability to reproduce the exact conditions. A practical guide and a precise review over the possible high-frequency and microwave exposure have been published by the Environmental Health Directorate of Canada (Metaxas & Meredith, 1983) limiting the maximum exposure of 100 W/m^2. The studies have highlighted that the human body tissues are highly receptive to microwave radiation, hence, should be protected from the excessive exposure.

Moreover, the human body is regarded as a heterogeneous dielectric, with exclusive sections namely, eyes and testicular area, are more prone to damages by the microwave radiation. In 1977, Dodge and Glaser studied the microwave exposure standards for various developed countries.

However, due to the microwave wavelength at 2.45 GHz, thermal concerns over the human body have been dismissed. The possible leakage sources and practical solutions have been presented in the literature for various application scenarios (Metaxas & Meredith, 1983).

2.5.3 Economics and Future Trends

Considering the efficiency of the conversion of conventional fuel resources to the electricity about 30% followed by the transformation of the electricity to heat to be approximately 65%, the overall efficiency is calculated in the region of 20%. Comparing to the data available for the conventional heating methods, microwave heating is regarded as a more efficient process for the highly dielectric material particularly. The generation of the higher heating rate through the dielectric material is the principle advantage of the microwave heating over the conventional methods. Moreover, microwave heating provides considerably higher efficiency regarding the moisture-drying process. Various studies concentrated on the economic analysis of the microwave heating process have been presented in the literature (Ishii, 1974; Jolly, 1972, 1976) emphasizing on the energy savings and increased throughput concepts. The studies have highlighted the economical and energy saving advantages of the microwave heating process over the conventional methods in terms of capital investment, capital revenue, energy saving criteria and maintenance costs.

The availability of the affordable renewable electricity, and the economical and energy saving aspects of the microwave technology, on the other hand, are regarded as the major factors to sketch the future of the microwave heating technology. The technology advances have led to the gradual reduction of the microwave equipment prices, which will considerably affect the future insight of the technology. The advantages of the application of the microwave heating over the conventional methods are regarded as (Sobhy & Chaouki, 2010):

- Strong selective heating of the water content
- Selective heating of the material or phases according to the dielectric properties
- Avoiding the heat loss in the heating components and enclosure of the reaction chamber
- Maximum conversion efficiency of electricity into microwave (about 95%)
- Maximum heat conversion of microwave to heat within the dielectric material (almost 85%)
- Beneficial for locations where electricity is available and low-priced

The major parameter in microwave intractability of material is the dielectric properties. In cases where the microwave absorption of the substances is considered insufficient, microwave receptors, high permittivity material such as char is added to the system in order to produce the required heating source and transfer it through the material employing conventional heat transfer methods (convection and conduction).

2.6 References

Aasberg-Petersen, K., Bak Hansen, J. H., Christensen, T. S., Dybkjaer, I., Christensen, P. S., Stub Nielsen, C., . . . Rostrup-Nielsen, J. R. (2001). Technologies for large-scale gas conversion. *Applied Catalysis A: General, 221*(1–2), 379-387. doi: http://dx.doi.org/10.1016/S0926-860X(01)00811-0

Altman, J. L. (1964). *Microwave circuits*: Van Nostrand Reinhold.

Ashcroft, A. T., Cheetham, A. K., Green, M. L. H., & Vernon, P. D. F. (1991). Partial oxidation of methane to synthesis gas using carbon dioxide. *Nature, 352*(6332), 225-226.

Avetisov, A. K., Rostrup-Nielsen, J. R., Kuchaev, V. L., Bak Hansen, J. H., Zyskin, A. G., & Shapatina, E. N. (2010). Steady-state kinetics and mechanism of methane reforming with steam and carbon dioxide over Ni catalyst. *Journal of Molecular Catalysis A: Chemical, 315*(2), 155-162. doi: http://dx.doi.org/10.1016/j.molcata.2009.06.013

Ballarini, A. D., de Miguel, S. R., Jablonski, E. L., Scelza, O. A., & Castro, A. A. (2005). Reforming of CH4 with CO2 on Pt-supported catalysts: Effect of the support on the catalytic behaviour. *Catalysis Today, 107–108*, 481-486. doi: http://dx.doi.org/10.1016/j.cattod.2005.07.058

Bartholomew, C. H. (1982). Carbon Deposition in Steam Reforming and Methanation. *Catalysis Reviews, 24*(1), 67-112. doi: 10.1080/03602458208079650

Beiter, P., & Tian, T. (2016). 2015 Renewable Energy Data Book: National Renewable Energy Laboratory.

Bengtsson, N. E., & Risman, P. D. (1971). Dielectric properties of foods at 3 GHz as determined by cavity perturbation technique. *J. Microwave Power, 6*(2).

Birol, F., & Argiri, M. (1999). World energy prospects to 2020. *Energy, 24*(11), 905-918.

Bleaney, B. I., & Bleaney, B. (1965). *Electricity and magnetism* (Vol. 236): Clarendon Press Oxford.

BP. (2011). BP Statistical Review of World Energy 2011. London, UK: BP.

BP. (2016a). BP Energy Outlook 2016 Edition. London, UK: BP.

BP. (2016b). BP Statistical Review of World Energy 2016. London, UK: BP.

Bradford, M. C. J., & Vannice, M. A. (1999). CO2 Reforming of CH4. *Catalysis Reviews, 41*(1), 1-42. doi: 10.1081/cr-100101948

Brungs, A. J., York, A. P. E., Claridge, J. B., Márquez-Alvarez, C., & Green, M. L. H. (2000). Dry reforming of methane to synthesis gas over supported molybdenum carbide catalysts. *Catalysis Letters, 70*(3), 117-122. doi: 10.1023/a:1018829116093

Budiman, A. W., Song, S.-H., Chang, T.-S., Shin, C.-H., & Choi, M.-J. (2012). Dry Reforming of Methane Over Cobalt Catalysts: A Literature Review of Catalyst Development. *Catalysis Surveys from Asia, 16*(4), 183-197. doi: 10.1007/s10563-012-9143-2

Campañone, L. A., & Zaritzky, N. E. (2005). Mathematical analysis of microwave heating process. *Journal of Food Engineering, 69*(3), 359-368. doi: http://dx.doi.org/10.1016/j.jfoodeng.2004.08.027

Carrasco, J. M., Franquelo, L. G., Bialasiewicz, J. T., Galvan, E., PortilloGuisado, R. C., Prats, M. A. M., . . . Moreno-Alfonso, N. (2006). Power-Electronic Systems for the Grid Integration of Renewable Energy Sources: A Survey. *IEEE Transactions on Industrial Electronics, 53*(4), 1002-1016. doi: 10.1109/tie.2006.878356

Chen, X., Honda, K., & Zhang, Z.-G. (2005). CO2CH4 reforming over NiO/γ-Al2O3 in fixed/fluidized-bed multi-switching mode. *Applied Catalysis A: General, 279*(1–2), 263-271. doi: http://doi.org/10.1016/j.apcata.2004.10.041

Chen, Y.-G., Tomishige, K., & Fujimoto, K. (1997). Formation and characteristic properties of carbonaceous species on nickel-magnesia solid solution catalysts during CH4CO2 reforming reaction. *Applied Catalysis A: General, 161*(1), L11-L17. doi: http://dx.doi.org/10.1016/S0926-860X(97)00106-3

Choudhary, V. R., Rajput, A. M., & Prabhakar, B. (1995). Energy efficient methane-to-syngas conversion with low H2/CO ratio by simultaneous catalytic reactions of methane with carbon dioxide and oxygen. *Catalysis Letters, 32*(3), 391-396. doi: 10.1007/bf00813234

Christian Enger, B., Lødeng, R., & Holmen, A. (2008). A review of catalytic partial oxidation of methane to synthesis gas with emphasis on reaction mechanisms over transition metal catalysts. *Applied Catalysis A: General, 346*(1–2), 1-27. doi: http://dx.doi.org/10.1016/j.apcata.2008.05.018

Chubb, T. A. (1980). Characteristics of CO2-CH4 reforming-methanation cycle relevant to the solchem thermochemical power system. *Solar Energy, 24*(4), 341-345. doi: http://dx.doi.org/10.1016/0038-092X(80)90295-9

Ciacci, T., Galgano, A., & Di Blasi, C. (2010). Numerical simulation of the electromagnetic field and the heat and mass transfer processes during microwave-induced pyrolysis of a wood block. *Chemical Engineering Science, 65*(14), 4117-4133. doi: http://dx.doi.org/10.1016/j.ces.2010.04.039

Couderc, D., Giroux, M., & Bosisio, R. G. (1973). Dynamic High-Temperature Microwave Complex Permittivity Measurements on Samples Heated via Microwave Absorption. *J. Microwave Power, 8*, 69.

Crisafulli, C., Scirè, S., Minicò, S., & Solarino, L. (2002). Ni–Ru bimetallic catalysts for the CO2 reforming of methane. *Applied Catalysis A: General, 225*(1–2), 1-9. doi: http://doi.org/10.1016/S0926-860X(01)00585-3

Daniel, V. V. (1967). *Dielectric relaxation* (Vol. 967): Academic Press London.

Debye, P. J. W. (1929). *Polar molecules* (Vol. 172): Dover New York.

Dibbern, H. C., Olesen, P., Rostrup-Nielsen, J. R., Tottrup, P. B., & Udengaard, N. R. (1986). Make low H/sub 2//CO syngas using sulfur passivated reforming. *Hydrocarbon Process.;(United States), 65*(1).

Dicke, R. H., Montgomery, C. G., & Purcell, E. M. Principles of microwave circuits, 1948: McGraw-Hill.

Djinović, P., Osojnik Črnivec, I. G., Erjavec, B., & Pintar, A. (2012). Influence of active metal loading and oxygen mobility on coke-free dry reforming of Ni–Co bimetallic catalysts. *Applied Catalysis B: Environmental, 125*, 259-270. doi: http://doi.org/10.1016/j.apcatb.2012.05.049

Dry, M. E. (2002). The Fischer–Tropsch process: 1950–2000. *Catalysis Today, 71*(3–4), 227-241. doi: http://dx.doi.org/10.1016/S0920-5861(01)00453-9

Dunn, D. A. (1967). Slow wave couplers for microwave dielectric heating systems.

Edwards, J. H., & Maitra, A. M. (1995). The chemistry of methane reforming with carbon dioxide and its current and potential applications. *Fuel Processing Technology, 42*(2), 269-289. doi: http://dx.doi.org/10.1016/0378-3820(94)00105-3

Edwards, R., Mahieu, V., Griesemann, J.-C., Larivé, J.-F., & Rickeard, D. J. (2004). Well-to-wheels analysis of future automotive fuels and powertrains in the European context: SAE Technical Paper.

EPA. (2015). Overview of Greenhouse Gases. from https://www.epa.gov/ghgemissions/overview-greenhouse-gases

Eriksson, S., Wolf, M., Schneider, A., Mantzaras, J., Raimondi, F., Boutonnet, M., & Järås, S. (2006). Fuel-rich catalytic combustion of methane in zero emissions power generation processes. *Catalysis Today, 117*(4), 447-453.

Farag, S., Sobhy, A., Akyel, C., Doucet, J., & Chaouki, J. (2012). Temperature profile prediction within selected materials heated by microwaves at 2.45GHz. *Applied Thermal Engineering, 36*, 360-369. doi: Doi 10.1016/J.Applthermaleng.2011.10.049

Fisher, F., & Tropsch, H. (1928). Conversion of methane into hydrogen and carbon monoxide. *Brennst.-Chem., 9*.

Folkins, H. O., Miller, E., & Hennig, H. (1950). Carbon Disulfide from Natural Gas and Sulfur. Reaction of Methane and Sulfur over a Silica Gel Catalyst. *Industrial & Engineering Chemistry, 42*(11), 2202-2207.

Fraenkel, D., Levitan, R., & Levy, M. (1986). A solar thermochemical pipe based on the CO2-CH4 (1:1) system. *International Journal of Hydrogen Energy, 11*(4), 267-277. doi: http://dx.doi.org/10.1016/0360-3199(86)90187-4

Francis, G. (1960). *Ionization phenomena in gases*: Butterworths Scientific Publications London.

Fröhlich, H. (1958). Theory of dielectrics. *Clarendon, Oxford*.

Gadalla, A. M., & Bower, B. (1988). The role of catalyst support on the activity of nickel for reforming methane with CO2. *Chemical Engineering Science, 43*(11), 3049-3062. doi: http://dx.doi.org/10.1016/0009-2509(88)80058-7

Gadde, S., Wu, J., Gulati, A., McQuiggan, G., Koestlin, B., & Prade, B. (2006). *Syngas capable combustion systems development for advanced gas turbines.* Paper presented at the ASME Turbo Expo 2006: Power for Land, Sea, and Air.

Gallego, G. S., Batiot-Dupeyrat, C., Barrault, J., Florez, E., & Mondragón, F. (2008). Dry reforming of methane over LaNi1−yByO3±δ (B = Mg, Co) perovskites used as catalyst precursor. *Applied Catalysis A: General, 334*(1–2), 251-258. doi: http://dx.doi.org/10.1016/j.apcata.2007.10.010

García-Diéguez, M., Finocchio, E., Larrubia, M. Á., Alemany, L. J., & Busca, G. (2010). Characterization of alumina-supported Pt, Ni and PtNi alloy catalysts for the dry reforming of methane. *Journal of Catalysis, 274*(1), 11-20. doi: http://doi.org/10.1016/j.jcat.2010.05.020

García-Diéguez, M., Pieta, I. S., Herrera, M. C., Larrubia, M. A., Malpartida, I., & Alemany, L. J. (2010). Transient study of the dry reforming of methane over Pt supported on different γ-Al2O3. *Catalysis Today, 149*(3–4), 380-387. doi: http://dx.doi.org/10.1016/j.cattod.2009.07.099

Gupta, M., & Wong, W. L. (2007). *Microwaves and metals*. Singapore: John Wiley & Sons.

Harvey, A. F., & Harvey, A. F. (1963). *Microwave engineering* (Vol. 50): Academic Press London and New York.

Hasted, J. B. (1972). Water: A Comprehensive Treatise. *The Physics and Physical Chemistry of Water, 1*, 255-305.

Hasted, J. B. (1973). *Aqueous dielectrics* (Vol. 17): Chapman and Hall London.

Heenan, N. I. (1968). Travelling Wave Dryers. *Microwave Power Engineering, 2*, 126-144.

Hickman, D. A., & Schmidt, L. D. (1993). Production of syngas by direct catalytic oxidation of methane. *Science-new york then washington-, 259*, 343-343.

Hill, N. E., Vaughan, W. E., Price, A. H., & Davies, M. (1969). *Dielectric properties and molecular behaviour* (Vol. 53): Van Nostrand Reinhold London.

Hoel, M., & Kverndokk, S. (1996). Depletion of fossil fuels and the impacts of global warming. *Resource and Energy Economics, 18*(2), 115-136. doi: http://dx.doi.org/10.1016/0928-7655(96)00005-X

Horiuchi, T., Sakuma, K., Fukui, T., Kubo, Y., Osaki, T., & Mori, T. (1996). Suppression of carbon deposition in the CO2-reforming of CH4 by adding basic metal oxides to a Ni/Al2O3 catalyst. *Applied Catalysis A: General, 144*(1), 111-120. doi: http://dx.doi.org/10.1016/0926-860X(96)00100-7

Hou, Z., Chen, P., Fang, H., Zheng, X., & Yashima, T. (2006). Production of synthesis gas via methane reforming with CO on noble metals and small amount of noble-(Rh-) promoted Ni catalysts. *International Journal of Hydrogen Energy, 31*(5), 555-561. doi: http://dx.doi.org/10.1016/j.ijhydene.2005.06.010

Hu, Y. H., & Ruckenstein, E. (2002). Binary MgO-Based Solid Solution Catalysts for Methane Conversion to Syngas. *Catalysis Reviews, 44*(3), 423-453. doi: 10.1081/cr-120005742

Hu, Y. H., & Ruckenstein, E. (2004). Catalytic Conversion of Methane to Synthesis Gas by Partial Oxidation and CO2 Reforming *Advances in Catalysis* (Vol. Volume 48, pp. 297-345): Academic Press.

Huangt, H. F. (1976). Temperature Control in a Microwawe Resonant Cavity System for lapìd Heating of Nylon Monofilament. *Journal of Microwave Power, 11*(4), 5.4.

IEA. (2016). *Energy and Air Pollution*. Paris, France: Inetrational Energy Agency.

Inui, T., & Spivey, J. J. (2002). *Reforming of CH4 by CO2, O2 and/or H2O* (Vol. 16): The Royal Society of Chemistry: London.

Ishii, T. K. (1974). Theoretical Basis for Decision to Microwave Approach for Industrial Processing. *JMPEE, 9*(4), 355-360.

Iskander, M. F. S., & Stuchly, S. S. (1972). A time domain technique for measurement of the dielectric properties of biological substances. *IEEE J. IM-21, 4*(425).

Johnk, C. T. A. (1975). Engineering electromagnetic fields and waves. *New York, John Wiley and Sons, Inc., 1975. 667 p., 1*.

Jolly, J. A. (1972). Financial techniques for comparing the monetary gain of new manufacturing processes such as microwave heating. *J. Microwave Power, 7*(1), 5-16.

Jolly, J. A. (1976). Economics and Energy Utilization Aspects of the Application of Microwaves: A Tutorial Review. *J. Microwave Power, 11*(3), 233-245.

Jones, C. A., Leonard, J. J., & Sofranko, J. A. (1987). Fuels for the future: remote gas conversion. *Energy & Fuels, 1*(1), 12-16. doi: 10.1021/ef00001a002

Kalinski, J. (1978). An industrial microwave attenuation monitor (MAM) and its application for continuous moisture content measurements'. *J. Microwave Power, 13*, 275-281.

Kim, G. J., Cho, D.-S., Kim, K.-H., & Kim, J.-H. (1994). The reaction of CO2 with CH4 to synthesize H2 and CO over nickel-loaded Y-zeolites. *Catalysis Letters, 28*(1), 41-52. doi: 10.1007/bf00812468

Koberstein, E. (1973). Model Reactor Studies of the Hydrogen Cyanide Synthesis from Methane and Ammonia. *Industrial & Engineering Chemistry Process Design and Development, 12*(4), 444-448. doi: 10.1021/i260048a010

Kraszewski, A. (1980). Microwave aquametry: A review. *J. Microwave Power, 15*(4), 209-220.

Lavoie, J.-M. (2014). Review on dry reforming of methane, a potentially more environmentally-friendly approach to the increasing natural gas exploitation. *Frontiers in Chemistry, 2*, 81. doi: 10.3389/fchem.2014.00081

Lee, S. (1996). *Methane and its Derivatives* (Vol. 70): CRC Press.

Lewis, W. K., Gilliland, E. R., & Reed, W. A. (1949). Reaction of methane with copper oxide in a fluidized bed. *Industrial & Engineering Chemistry, 41*(6), 1227-1237.

Lide, D. R. (2004). *CRC handbook of chemistry and physics* (Vol. 85): CRC press.

Luikov, A. V. (1964). Capillary-Porous Bodies. *Advances in heat transfer, 1*.

Luo, J. Z., Yu, Z. L., Ng, C. F., & Au, C. T. (2000). CO2/CH4 Reforming over Ni–La2O3/5A: An Investigation on Carbon Deposition and Reaction Steps. *Journal of Catalysis, 194*(2), 198-210. doi: http://dx.doi.org/10.1006/jcat.2000.2941

MacLatchy, C. S., & Clements, R. M. (1980). Simple Technique for Measuring High Microwave Electric Field Strengths. *J. Microwave Power, 15*(1), 7-14.

Martínez, J. D., Mahkamov, K., Andrade, R. V., & Silva Lora, E. E. (2012). Syngas production in downdraft biomass gasifiers and its application using internal combustion engines. *Renewable Energy, 38*(1), 1-9. doi: http://dx.doi.org/10.1016/j.renene.2011.07.035

Metaxas, A. C., & Meredith, R. J. (1983). *Industrial microwave heating*. London, UK: P. Peregrinus on behalf of the Institution of Electrical Engineers.

Miccio, F. (2013). On the integration between fluidized bed and Stirling engine for micro-generation. *Applied Thermal Engineering, 52*(1), 46-53. doi: http://dx.doi.org/10.1016/j.applthermaleng.2012.11.004

Murray, E. P., Tsai, T., & Barnett, S. A. (1999). A direct-methane fuel cell with a ceria-based anode. *Nature, 400*(6745), 649-651.

Nematollahi, B., Rezaei, M., Lay, E. N., & Khajenoori, M. (2012). Thermodynamic analysis of combined reforming process using Gibbs energy minimization method: In view of solid carbon formation. *Journal of Natural Gas Chemistry, 21*(6), 694-702. doi: http://dx.doi.org/10.1016/S1003-9953(11)60421-0

Nikoo, M. K., & Amin, N. A. S. (2011). Thermodynamic analysis of carbon dioxide reforming of methane in view of solid carbon formation. *Fuel Processing Technology, 92*(3), 678-691. doi: http://dx.doi.org/10.1016/j.fuproc.2010.11.027

Ohlsson, T. H., Bengtsson, N. E., & Risman, P. O. (1974). The frequency and temperature dependence of dielectric food data as determined by a cavity perturbation technique. *Journal of Microwave Power, 9*(2), 129-145.

Omae, I. (2006). Aspects of carbon dioxide utilization. *Catalysis Today, 115*(1–4), 33-52. doi: http://dx.doi.org/10.1016/j.cattod.2006.02.024

Oyama, S. T., Hacarlioglu, P., Gu, Y., & Lee, D. (2012). Dry reforming of methane has no future for hydrogen production: Comparison with steam reforming at high pressure in standard and membrane reactors. *International Journal of Hydrogen Energy, 37*(13), 10444-10450. doi: http://dx.doi.org/10.1016/j.ijhydene.2011.09.149

Pakhare, D., & Spivey, J. (2014). A review of dry (CO2) reforming of methane over noble metal catalysts. *Chemical Society Reviews, 43*(22), 7813-7837. doi: 10.1039/c3cs60395d

Pandit, R. B., & Prasad, S. (2003). Finite element analysis of microwave heating of potato—transient temperature profiles. *Journal of Food Engineering, 60*(2), 193-202. doi: http://dx.doi.org/10.1016/S0260-8774(03)00040-2

Perkin, R. M. (1979). Prospects of drying with radio frequency and microwave electromagnetic fields. *Capenhurst Electr. Council Res. Centre Rep. ECRC/M 1235, 1979*.

Pimentel, D., & Patzek, T. W. (2008). Biofuels, solar and wind as renewable energy systems. *Benefits and risks. New York: Springer*.

Podkolzin, S. G., Stangland, E. E., Jones, M. E., Peringer, E., & Lercher, J. A. (2007). Methyl chloride production from methane over lanthanum-based catalysts. *Journal of the American Chemical Society, 129*(9), 2569-2576.

Puschner, H. (1966). Heating with microwaves. *Fundamentals, Components, and Circuit Technique, Philips Gloeilampenfabrieken, Eindhoven, Netherlands*.

Reitmeier, R. E., Atwood, K., Bennett, H. A., & Baugh, H. M. (1948). Production of Synthesis Gas by Reacting Light Hydrocarbons Wit Steam and Carbon Dioxide. *Ind. Eng. Chem., 40*, 620-626.

Riedel, T., Claeys, M., Schulz, H., Schaub, G., Nam, S.-S., Jun, K.-W., . . . Lee, K.-W. (1999). Comparative study of Fischer–Tropsch synthesis with H2/CO and H2/CO2 syngas using Fe- and Co-based catalysts. *Applied Catalysis A: General, 186*(1–2), 201-213. doi: http://dx.doi.org/10.1016/S0926-860X(99)00173-8

Ross, J. R. H. (2005). Natural gas reforming and CO2 mitigation. *Catalysis Today, 100*(1–2), 151-158. doi: http://dx.doi.org/10.1016/j.cattod.2005.03.044

Rostrup-Nielsen, J. R. (1991). Promotion by poisoning. *Studies in Surface Science and Catalysis, 68*, 85-101.

Rostrup-Nielsen, J. R. (1994). Catalysis and large-scale conversion of natural gas. *Catalysis Today, 21*(2), 257-267. doi: http://dx.doi.org/10.1016/0920-5861(94)80147-9

Rostrup-Nielsen, J. R. (2000). New aspects of syngas production and use. *Catalysis Today, 63*(2–4), 159-164. doi: http://dx.doi.org/10.1016/S0920-5861(00)00455-7

Rostrup-Nielsen, J. R., & Hansen, J. H. B. (1993). CO2-Reforming of Methane over Transition Metals. *Journal of Catalysis, 144*(1), 38-49. doi: http://dx.doi.org/10.1006/jcat.1993.1312

Rzepecka, M. A., & Pereira, M. (1974). Permittivity of some dairy products at 2450 MHz. *Journal of Microwave Power, 9*(4), 277-288.

Sabatier, P., & Senderens, J.-B. (1902). New synthesis of methane. *CR Acad. Sci. Paris, 134*, 514-516.

Saidur, R., Islam, M. R., Rahim, N. A., & Solangi, K. H. (2010). A review on global wind energy policy. *Renewable and Sustainable Energy Reviews, 14*(7), 1744-1762. doi: http://dx.doi.org/10.1016/j.rser.2010.03.007

Salameh, M. G. (2003). Can renewable and unconventional energy sources bridge the global energy gap in the 21st century? *Applied Energy, 75*(1), 33-42. doi: http://dx.doi.org/10.1016/S0306-2619(03)00016-3

Shafiee, S., & Topal, E. (2008). An econometrics view of worldwide fossil fuel consumption and the role of US. *Energy Policy, 36*(2), 775-786. doi: http://dx.doi.org/10.1016/j.enpol.2007.11.002

Shafiee, S., & Topal, E. (2009). When will fossil fuel reserves be diminished? *Energy Policy, 37*(1), 181-189. doi: http://dx.doi.org/10.1016/j.enpol.2008.08.016

Sloan, E. D. (2003). Fundamental principles and applications of natural gas hydrates. *Nature, 426*(6964), 353-363.

Sobhy, A., & Chaouki, J. (2010). Microwave-assisted Biorefinery. *Cisap4: 4th International Conference on Safety & Environment in Process Industry, 19*, 25-29. doi: Doi 10.3303/Cet1019005

Sodesawa, T., Dobashi, A., & Nozaki, F. (1979). Catalytic reaction of methane with carbon dioxide. *Reaction Kinetics and Catalysis Letters, 12*(1), 107-111. doi: 10.1007/bf02071433

Solangi, K. H., Islam, M. R., Saidur, R., Rahim, N. A., & Fayaz, H. (2011). A review on global solar energy policy. *Renewable and Sustainable Energy Reviews, 15*(4), 2149-2163. doi: http://dx.doi.org/10.1016/j.rser.2011.01.007

Speight, J. G. (1993). *Gas processing: environmental aspects and methods*: Butterworth-Heinemann.

Steele, B. C. H., & Heinzel, A. (2001). Materials for fuel-cell technologies. *Nature, 414*(6861), 345-352.

Steele, D. J., & Kent, M. (1978). *Microwave stripline techniques applied to moisture measurement in food materials.* Paper presented at the Proc. 1978 IMPI Symp. On Microwave Power.

Stuchly, S. S. (1970). Dielectric properties of some granular solids containing water. *J. Microwave Power, 5*(2), 62-68.

Terselius, B., & Ranby, B. (1978). Cavity perturbation measurements of the dielectric properties of vulcanizing rubber and polyethylene compounds. *J. Microwave Power, 13*, 327-335.

Teuner, S. (1987). A new process to make oxo-feed. *Hydrocarbon Process.;(United States), 66*(7).

Timilsina, G. R., Kurdgelashvili, L., & Narbel, P. A. (2012). Solar energy: Markets, economics and policies. *Renewable and Sustainable Energy Reviews, 16*(1), 449-465. doi: http://dx.doi.org/10.1016/j.rser.2011.08.009

Timmons, D., Harris, J. M., & Roach, B. (2014). The economics of renewable energy. *Global Development And Environment Institute, Tufts University*, 52.

Tinga, W. R. (1970). *Multiphase dielectric theory applied to cellulose mixtures.*

Tinga, W. R., & Nelson, S. O. (1973). Dielectric properties of materials for microwave processing-tabulated. *J. Microwave Power, 8*(1), 23-66.

To, E. C., Mudgett, R. E., Wang, D. I. C., Goldblith, S. A., & Decareau, R. V. (1974). Dielectric properties of food materials. *J. Microwave Power, 9*(4), 303-315.

Turner, J. A. (1999). A Realizable Renewable Energy Future. *Science, 285*(5428), 687-689. doi: 10.1126/science.285.5428.687

Udengaard, N. R. (1992). Sulfur passivated reforming process lowers syngas H sub 2/CO ratio. *Oil and Gas Journal;(United States), 90*(10).

Usman, M., Wan Daud, W. M. A., & Abbas, H. F. (2015). Dry reforming of methane: Influence of process parameters—A review. *Renewable and Sustainable Energy Reviews, 45*, 710-744. doi: http://dx.doi.org/10.1016/j.rser.2015.02.026

Von Hippel, A. R. (1954). *Dielectric materials and applications ; papers by twenty-two contributors*. Cambridge New York: Technology Press of M.I.T. ; Wiley.

Wang, S., Lu, G. Q., & Millar, G. J. (1996). Carbon Dioxide Reforming of Methane To Produce Synthesis Gas over Metal-Supported Catalysts: State of the Art. *Energy & Fuels, 10*(4), 896-904. doi: 10.1021/ef950227t

White, G. A., Roszkowski, T. R., & Stanbridge, D. W. (1975). Predict carbon formation.[Synthesis gas and SNG operations]. *Hydrocarbon Process.;(United States), 54*(7).

White, J. R. (1970). Measuring the strength of the microwave field in a cavity. *Journal of Microwave Power, 5*(2), 145-147.

Wilhelm, D. J., Simbeck, D. R., Karp, A. D., & Dickenson, R. L. (2001). Syngas production for gas-to-liquids applications: technologies, issues and outlook. *Fuel Processing Technology, 71*(1–3), 139-148. doi: http://dx.doi.org/10.1016/S0378-3820(01)00140-0

Wiser, R., Bolinger, M., Barbose, G., Darghouth, N., Hoen, B., Mills, A., . . . Widiss, R. 2015 Wind Technologies Market Report. *Energy Efficiency and Renewable Energy*.

Wu, K. T., Lee, H. T., Juch, C. I., Wan, H. P., Shim, H. S., Adams, B. R., & Chen, S. L. (2004). Study of syngas co-firing and reburning in a coal fired boiler. *Fuel, 83*(14–15), 1991-2000. doi: http://dx.doi.org/10.1016/j.fuel.2004.03.015

Wurzel, T., Malcus, S., & Mleczko, L. (2000). Reaction engineering investigations of CO2 reforming in a fluidized-bed reactor. *Chemical Engineering Science, 55*(18), 3955-3966. doi: http://dx.doi.org/10.1016/S0009-2509(99)00444-3

Yamazaki, O., Nozaki, T., Omata, K., & Fujimoto, K. (1992). Reduction of carbon dioxide by methane with Ni-on-MgO-CaO containing catalysts. *Chemistry letters, 21*(10), 1953-1954.

Yarlagadda, P. S., Morton, L. A., Hunter, N. R., & Gesser, H. D. (1990). Temperature oscillations during the high-pressure partial oxidation of methane in a tubular flow reactor. *Combustion and Flame, 79*(2), 216-218.

York, A. P. E., Xiao, T., & Green, M. L. H. (2003). Brief Overview of the Partial Oxidation of Methane to Synthesis Gas. *Topics in Catalysis, 22*(3), 345-358. doi: 10.1023/A:1023552709642

Zhang, Z. L., & Verykios, X. E. (1994). Carbon dioxide reforming of methane to synthesis gas over supported Ni catalysts. *Catalysis Today, 21*(2), 589-595. doi: http://dx.doi.org/10.1016/0920-5861(94)80183-5

Zheludev, I. S., & Tybulewicz, A. (1971). *Physics of crystalline dielectrics* (Vol. 2): Plenum Press New York.

CHAPTER 3 ORIGINALITY AND OBJECTIVES

3.1 Originality

In general, catalytic gas-solid reactions have been thoroughly investigated to study the effect of the reaction conditions and parameters, namely, temperature, feed ratio, pressure and gas superficial velocity, on the prospect of the reactions. Furthermore, investigations have been concentrated on increasing the selectivity of the desired products by restricting the undesired gas-phase reactions, accordingly. The associated endeavours have been expressly observed for the reactions corresponding the conversion of methane to syngas components. H_2 and CO. Whereas, endeavours for optimizing the dry reforming of methane (DRM), the preferential industrial syngas production process, has been widely associated with the optimization of the catalyst system. Such efforts have been widely classified as, the application of transition and noble metals (individually or in pairs), the application of catalyst promoters, investigating the effect of the catalyst support and the general structure of the system, accordingly. However, due to the enhanced carbon production reactions associated with the DRM process, most catalytic systems failed to fulfil the expectations. While, the catalyst systems which projected satisfactory results were rejected by the industry due to the overwhelming economical perspectives. Hence, the lack of endeavours concentrated on the effect of the heating mechanism on the performance of the reactions are widely evident.

According to the recent developments in the field of renewable energies and the exhilarating effect on the production of extremely affordable and environmental friendly electricity, the application of electrical heating methods for material processing is exceedingly justified. Whereas, microwave heating has been highlighted as a stimulating opportunity for chemical processing due to the exclusive selective heating mechanism. However, the application of the microwave heating in the available literature is majorly associated with drying, waste treatment and ceramic synthesis, exclusively. While intermittent instances of microwave-heated catalytic reaction applications reported in the literature have failed to comprehensively address the effect on the performance and the mechanism of the reactions. To the best of our knowledge, no published work to this date has proposed to implement microwave heating mechanism to promote the catalytic reactions and restrict undesired gas-phase side reactions in a gas-solid catalytic reaction, correspondingly.

3.2 Objectives

According to the deficiencies associated with the catalytic gas-solid reactions, namely, dry reforming of methane, and the exclusive selective microwave heating mechanism articulated in the literature review section (Chapter 2), the main objective of this thesis was expressed as:

"Development of a Microwave Heating-Assisted Catalytic Reaction Process: Application for Dry Reforming of Methane Optimization"

Correspondingly, the specific objectives of the present study have been expressed as:

1. To develop a microwave receptor with the assistance of the induction heated fluidized bed chemical vapour deposition method that simultaneously acts as a catalyst promoter/support with promising microwave radiation interaction.
2. To study the effect of the microwave heating mechanism on the evolution of the gas phase and solid phase temperature profiles in a gas-solid fluidized bed reactor and the eventual effect on the reaction performance and mechanism within a simulation investigation.
3. To study the effect of the developed microwave receptors/catalyst promoters and the microwave selective heating mechanism on promoting the catalytic reactions and restricting the undesired gas-phase reactions for dry reforming of methane.

CHAPTER 4 COHERENCE OF THE ARTICLES

The deficiency with the catalytic conversion of methane was thoroughly investigated in the literature review section. Furthermore, the available approach to address the shortcomings with the DRM process has been selectively established. Meanwhile, the principles of the microwave heating and the exclusive effect projected to the material processing has been particularly described. Consequently, it was expected that with the assistance of the microwave selective heating mechanism, the catalytic reactions would be amplified while the secondary gas-phase reactions would be promptly isolated. Hence, Chapters 5 to 9, discuss multiple stages to verify and conclude the specific objectives of the present study to validate the effect of the microwave heating mechanism on the optimization of the dry reforming of methane (DRM), as a representative process for the catalytic gas solid reactions, whereas:

- In Chapter 4, a novel microwave receptor was developed by the induction heating assisted fluidized bed chemical vapour deposition of methane over the silica sand substrates. Most common material fail to project sufficient microwave interaction, due to the insignificant dielectric properties. Accordingly, microwave receptors have been developed to mitigate for the heat generation inside a chemical reactor, exposed to microwave radiation. The novel carbon-coated silica sand (C-SiO_2) receptors were developed to address the temperature gradient established in the bed material due to the destructive segregation effect upon microwave exposure. The effect of the operating conditions and reaction time on the carbon coating layer composition, uniformity and thickness were investigated. Hence, the carbon composition of the coating layer was established by the thermogravimetric analysis (TGA) and combustion infrared carbon detection (LECO). Moreover, the morphology and coating layer thickness were investigated with scan electron microscopy (SEM), X-ray photoelectron spectroscopy (XPS), energy dispersive X-ray spectroscopy (EDX), and focused ionized beam (FIB) milling, correspondingly. Ultimately, the microwave heating performance of the developed C-SiO_2 particles was investigated in a lab-scale microwave heating-assisted fluidized bed reactor at different operating conditions. The results were compared with the microwave heating performance various graphite/sand compositions and the supremacy of the C-SiO_2 particles microwave interaction were confirmed.

Consequently, the application of the developed C-SiO_2 particles was recommended as the microwave receptor/catalyst promoter for the gas-solid catalytic reactions.

- In Chapter 5, the effect of the microwave selective heating mechanism on the performance of a hydrocarbon selective oxidation process was established with the assistance of a simulation analysis. Whereas, partial oxidation of n-butane over the fluidized vanadium phosphorous oxide catalyst to produce maleic anhydride in an industrial-scale fluidized bed reactor was selected as the model reaction. Due to the complexity associated with the direct temperature measurement of the gas-phase, correlations were attained by the experimental data and using a general energy balance. The experimental data were acquired by the radiometry and thermometry of the solid surface (C-SiO_2 receptors) and the bulk temperatures respectively, in a lab-scale microwave-heated fluidized bed reactor. Ultimately, with the assistance of the developed correlations and the available hydrodynamic and kinetic models in the literature, a simulation study to determine the effect of the microwave heating mechanism compared to the conventional heating method on the performance of the model reaction was achieved. The results exhibited the superior performance of the microwave heating mechanism in the terms of the conversion of the reactant and the selectivity of the desired product. Furthermore, the application microwave heating mechanism was further recommended to substantiate between the catalytic and gas-phase reactions and hence, identify the mechanism of the gas-solid catalytic reactions systems, correspondingly.
- In Chapter 6, the effect of the microwave selective heating mechanism on the performance of the dry reforming of methane was performed. Hence, a lab-scale microwave heating-assisted fluidized bed reactor was developed. The C-SiO2 particles were selected as the microwave receptor and catalyst promoter, simultaneously. HiFUEL R110, a nickel based alumina supported industrial catalyst was selected to perform the reactions. It was underlined that the C-SiO2 particles were the exclusive component that projected significant microwave interaction and mitigated for the heat generation inside the reactor. The temperature of the catalyst surface was measured with a thermopile, a radiometry measurement method. Whereas, the gas temperature was estimated with the assistance of the developed correlations. The reaction results demonstrated a very high conversion of the reactants, CH_4 and CO_2, and the selectivity of the syngas components, H_2 and CO.

Accordingly, it was concluded that the microwave heating mechanism promoted the catalytic reactions while restricted the undesired secondary gas-phase reactions.

CHAPTER 5 ARTICLE 1: DEVELOPMENT OF A NOVEL SILICA-BASED MICROWAVE RECEPTOR FOR HIGH TEMPERATURE PROCESSES

Sepehr Hamzehlouia, Mohammad Latifi, and Jamal Chaouki[1]

Department of Chemical Engineering, Polytechnique Montreal, c.p. 6079, Succ. Centre-ville, Montreal, Quebec, H3C 3A7, Canada

5.1 Abstract

A novel silica-based microwave receptor material was developed via a fluidized bed chemical vapor deposition (FBCVD) technique. In this study, the quartz sand particles were successfully coated in an induction heating-assisted stainless steel tubular reactor, with carbon produced from thermal degradation of methane (TDM) as the precursor at 800, 900 and 1000^{o}C and 60-, 120- and 240- minute reaction temperature and time, respectively. The amount of carbon deposition on each sample was investigated using thermogravimetric analysis and combustion infrared carbon detection (LECO) techniques. The morphological analysis of the coated receptors using scan electron microscopy (SEM) revealed that increasing the FBCVD reaction time and temperature elevated the coherence of carbon coating. Moreover, focused ionized beam (FIB) milling of the selected coated particles obtained from longer reaction times combined with SEM observations disclosed the enhancement of the carbon coating layer thickness by increasing the FBCVD temperature. Ultimately, X-ray photoelectron spectroscopy (XPS) and energy dispersive X-ray spectroscopy (EDX) methods enabled quantitative information regarding the effect of TDM reaction time and temperature on the coating layer composition and uniformity. The microwave heating performance of such developed receptors were further investigated in a new single-mode microwave apparatus and was subsequently compared with the microwave heating performance of sand and graphite particle mixtures under different mass ratios. The effects of FBCVD temperature and time on carbon composition and layer uniformity, microwave input power, surficial erosion and microwave heating rate were further investigated to characterize the microwave intractability of the receptor particles. The developed microwave receptor represents four major features: 1) a low level of carbon content and high layer uniformity, 2) an extreme microwave heating rate, 3)

low surficial erosion and high durability, and 4) excellent potential for application in gas-solid fluidized bed reactors as heat generator and catalyst support/promoter simultaneously.

5.2 Introduction

Microwave heating is an innovative thermal processing technique that was expanded to various industrial and commercial sectors with the introduction of the magnetron following World War II (Metaxas & Meredith, 1983). Microwave heating has been applied to various heat intensive processes including drying (Antti & Perre, 1999), polymer synthesis (Wiesbrock, Hoogenboom, & Schubert, 2004), ceramics sintering (Das, Mukhopadhyay, Datta, & Basu, 2009), biomass pyrolysis (Sherif Farag, Fu, Jessop, & Chaouki, 2014; Mushtaq, Mat, & Ani, 2014; Sobhy & Chaouki, 2010), food processing (M. Zhang, Tang, Mujumdar, & Wang, 2006), mineral sintering (Roy, Agarwal, Chen, & Gedevanishvili, 1999), environmental engineering (D. A. Jones, Lelyveld, Mavrofidis, Kingman, & Miles, 2002b), waste treatment (Doucet et al., 2014) and organic/inorganic synthesis (Caddick, 1995). Microwave heating represents numerous advantages over conventional methods namely selective, and volumetric heating (Sherif Farag & Chaouki, 2015; S. Farag et al., 2012; Khaghanikavkani & Farid, 2013; Metaxas & Meredith, 1983; Motasemi & Afzal, 2013), high power density (Khaghanikavkani & Farid, 2013; Metaxas & Meredith, 1983), instantaneous temperature control (Dominguez, Menendez, et al., 2007; Khaghanikavkani & Farid, 2013; Wiesbrock et al., 2004), reduced energy consumption (Doucet et al., 2014; S. Farag et al., 2012; Sobhy & Chaouki, 2010), high reaction selectivity (S. Farag et al., 2012; Khaghanikavkani & Farid, 2013; Sobhy & Chaouki, 2010; Wiesbrock et al., 2004), low heat transfer limitations(Doucet et al., 2014), process flexibility(S. Farag et al., 2012) and equipment portability (Dominguez, Menendez, et al., 2007; S. Farag et al., 2012).

Microwave heating is the result of increased kinetic energy triggered by reorientation of molecular dipoles exposed to an oscillating electric field. The fundamentals of microwave heating have been thoroughly reviewed in the available literature (Clark, Folz, & West, 2000; Sherif Farag & Chaouki, 2015; S. Farag et al., 2012; Gupta & Wong, 2007; Metaxas & Meredith, 1983; Motasemi & Afzal, 2013; Thostenson & Chou, 1999). In microwave heating, *complex permittivity* (ε^*) is the decisive parameter in evaluating the heat generation within an exposed dielectric material:

$$\varepsilon^* = \varepsilon' - j\varepsilon'' \quad (1.1)$$

where the real part of the equation is known as *dielectric constant* (ε'), representing the potential of the exposed material to conserve electric energy. The imaginary part of the equation is called the *loss factor* (ε''), which demonstrates the ability of the exposed material to dissipate microwave energy. The ratio of the loss factor to the dielectric constant, referred to as the *loss tangent*, denotes the amount of dissipated microwave energy converted to thermal energy within a dielectric material (Clark et al., 2000; S. Farag et al., 2012; Gabriel et al., 1998; Metaxas & Meredith, 1983). Mathematical definition of the loss tangent is expressed as:

$$tan\delta = \frac{\varepsilon''}{\varepsilon'} \quad (1.2)$$

Although the loss tangent is the major contributor to the dielectric microwave-heating rate, other parameters including the electric field pattern, heat capacity, and density of the compound affect the heat generation regime significantly (Gabriel et al., 1998).

Knowledge of the dielectric properties of material is an integral part of the microwave heating technique. Dielectric properties are governed by frequency, temperature, moisture content, and density of material (Metaxas & Meredith, 1983). In the early 1950's, von Hippel et al. presented the first dielectric properties database of various common substances, which has since been expanded, trailing the technological advances in the field of microwave heating (W. R. Tinga & Nelson, 1973; Von Hippel, 1954). Conversely, due to their chemical and physical structure, most common compounds such as gases (O_2, N_2 and CO_2), wood residues (lignin, paper and cellulose), plastics (polystyrene, nylon and rubber) and ceramics (quartz, alumina and Pyrex) are transparent or project low intractability with microwave radiation (Metaxas & Meredith, 1983). Consequently, microwave receptors, material with high microwave absorption and intractability, have been utilized to absorb the waves and transform it into thermal energy while exposed to microwave radiation, including, metals (Sherif Farag, Kouisni, & Chaouki, 2014; Hussain, Khan, Basheer, & Hussain, 2011; Hussain, Khan, & Hussain, 2010) and carbonaceous compounds (Menéndez et al., 2010; Russell, Antreou, Lam, Ludlow-Palafox, & Chase, 2012; Tai & Jou, 1999; Undri, Frediani, Rosi, & Frediani, 2014).

An application where microwave heating would provide a great advantage is in endothermic chemical reactors, such as pyrolyzers and gasifiers, which must operate at extremely high temperatures (Dominguez, Fernandez, Fidalgo, Pis, & Menendez, 2007; Sherif Farag, Fu, et al., 2014; Sherif Farag, Kouisni, et al., 2014). Coupling the microwave heating technology with a fluidized bed reactor is particularly advantageous according to the fluidization characteristics, namely, particulates uniform mixing and low temperature gradient (Samih & Chaouki, 2014; Warnecke, 2000). In such a system, the application of an external heating source such as partial combustion of a hydrocarbon would not be required, thus avoiding generating the emission of undesirable gases. However, in the case of low microwave intractability of the bed material such as silica sand, it would be necessary to add microwave receptors such as char or graphite to the fluidized bed to mitigate the microwave heating deficiency. Unfortunately, the introduction of these microwave receptors could lead to disruption to the magnetic field pattern and non-uniform temperature distribution in the bed due to the particles segregation phenomenon resulting from difference in density and size between the bed particles (sand-like material specifically) and the microwave receptors (Gómez-Barea & Leckner, 2013). This segregation could lead to the formation of hot spots in the fluidized bed, deteriorating the uniform temperature distribution of the fluidized bed reactor, by transferring the microwave receptor material to the top or the bottom of the sand bed. Furthermore, in case of fixed bed applications, the non-uniform distribution of receptors in the bed leads to the formation of significant local hot spots and a large temperature gradient.

Consequently, in order to address the non-uniform temperature distribution and segregation issues associated with the application of microwave receptors in fixed and fluidized beds, it is proposed to combine the bed material and microware receptor within single particles as a novel and practical solution. Thus, an induction heating-assisted fluidized bed chemical vapor deposition (FBCVD) reactor was employed to thermally decompose methane and deposit the generated carbon, which is an excellent microwave receptor, on the surface of silica sand particles that were under bubbling fluidization conditions. Consequently, the coupling of sand and carbon led to a uniform distribution of the receptors in the bed, ultimately minimizing the temperature gradient and providing a high heating rate. Accordingly, the following tasks have been performed: 1) The effect of temperature and reaction time on the physical properties (thickness, composition and surficial properties) of the

coated-sand particles have been studied, 2) The effect of the application of graphite and sand mixtures and carbon-coated sand as the bed material on the heating rate and the temperature distribution of the bed has been compared and 3) The effects of surficial erosion on the carbon-coated sand performance and durability in a fluidized bed have been investigated.

5.3 Methodology

5.3.1 Fluidized bed chemical vapor deposition (FBCVD)

Chemical vapor deposition (CVD) involves chemical reactions, thermal decomposition or dissociation of a gas reagent (precursor) close to or on the vicinity of a substrate surface in a thermally activated environment leading to the deposition of stable powder or film-shaped solid products (Archer, 1979; Choy, 2003). The commercial application of CVD traces back to the deposition of tungsten on carbon lamp filaments through the reduction of tungsten tetra-chloride by H_2 reagent (Xu & Yan, 2010). The advantages of CVD have been highlighted as a uniform coating layer, feed flexibility, a relatively low deposition temperature, an adjustable deposition rate and feasible economy (Choy, 2003; Xu & Yan, 2010). The application of CVD has been reported in semiconductors (A. C. Jones & O'Brien, 2008), dielectrics (C. H. Lee et al., 2000), metallic films (Oehr & Suhr, 1988), refractory ceramic materials (Naslain & Langlais, 1986) and the ceramic fibers (Besmann, Seldon, Lowden, & Stinton, 1991) production industry.

The application of the fluidized bed rectors has been extended to the CVD technology due to high-gas-solid contact, particle mixing and reaction control characteristics (Danafar, Fakhru'l-Razi, Salleh, & Biak, 2009). The major advantages of FBCVD technology over fixed bed methods are easy scale-up, lower production expenditure, higher productivity, flexibility, higher space velocity, product homogeneity, purity, process yield and selectivity (Danafar et al., 2009; X. Liu, Sun, Chen, Lau, & Yang, 2008; Philippe et al., 2009; See & Harris, 2008; Vahlas, Caussat, Serp, & Angelopoulos, 2006; Weizhong et al., 2003; Yen, Huang, & Lin, 2008). Therefore, based on the advantages of FBCVD, it was decided to use it for carbon coating of silica sand particles in the present study.

5.3.2 Induction heating

The principles of induction heating as a reliable high heating rate method have been thoroughly presented in the available literature (Davies, 1990; Haimbaugh, 2001; Rudnev, Loveless, Cook, & Black, 2002; Zinn & Semiatin, 1988). The heat distribution within the workpiece is non-uniform and is subject to (1) skin effect, (2) proximity effect, and (3) ring effect depending on the process conditions (Rudnev et al., 2002). Induction heating is dominantly generated on the surface of the workpiece and penetrates to the extent of the *reference depth (d)*, where the intensity of the magnetic field proportional to the eddy currents is reduced by 86% (Davies, 1990; Zinn & Semiatin, 1988). The reference depth has been presented as:

$$d = k\sqrt{\frac{r}{\mu f}}\ ,\ k\text{=constant} \tag{1.3}$$

where f is the frequency of the electrical current, r is the electrical resistivity of the workpiece and μ is the relative magnetic permeability. The surficial heating characteristic of induction heating which eliminates the risk of core distortion is referred to as the skin effect (Rudnev et al., 2002). Furthermore, the reference depth is proportional to the process temperature (Davies, 1990; Latifi & Chaouki, 2015; Rudnev et al., 2002).

The commercial application of induction heating has been underlined as preheating prior to metal working, heat treating, melting, welding and brazing, curing of organic coatings, adhesive bonding, semiconductor fabrication, tin reflow and sintering (Haimbaugh, 2001; Rudnev et al., 2002; Zinn & Semiatin, 1988). Moreover, the major advantages of the application of induction heating over the conventional heating methods have been expressed as faster heating due to the high heating rate, less scale up heat loss, fast startup, energy saving, high production rate, facilitated process automation and control, reduced spatial requirements, and safe, clean and low maintenance operating conditions (Davies, 1990; Haimbaugh, 2001; Rudnev et al., 2002; Zinn & Semiatin, 1988).

The employed FBCVD reactor utilizes the induction heating to supply the required heat at high temperatures. It has been shown that the induction heating provides a uniform temperature profile, a very fast heating rate and heat transfer coefficients in the bed as in the industrial fluidized bed reactors.(Latifi, Berruti, & Briens, 2014; Latifi & Chaouki, 2015)

5.3.3 Thermal decomposition (TDM) of methane

The application of thermal decomposition of methane (TDM) for hydrogen production and decarbonization with elimination of CO_2 emission and minor fractions of aromatic and aliphatic chains production has been reported in the literature (Dunker, Kumar, & Mulawa, 2006; Dunker & Ortmann, 2006; M. Steinberg, 1999):

$$CH_4 \rightarrow C + 2H_2, \qquad \Delta H = 74.5 \text{ kJ/mol } CH_4 \tag{4}$$

Due to the endothermic nature, temperatures above 600°C are required to drive the reaction. Furthermore, lower pressure facilitates higher feedstock conversion while higher pressure maintains higher rates of reaction (M. Steinberg, 1999). Thermal decomposition of methane has been performed using various processing methods, namely, plasma heating (Gaudernack & Lynum, 1998), molten metal bath (Serban, Lewis, Marshall, & Doctor, 2003), solar radiation (Dahl, Buechler, Weimer, Lewandowski, & Bingham, 2004; Dahl et al., 2001) and regular thermal reactors in the absence of catalyst (Meyer Steinberg, 1998), and in the presence of metal (N. Z. Muradov, 1998; Shah, Panjala, & Huffman, 2001) or carbon catalysts (Dunker et al., 2006; N. Muradov, 2001; Nazim Muradov, 2001; N. Muradov, Smith, & T-Raissi, 2005). The major advantages of TDM over steam reforming of methane are (i) decreased CO_2 emission, (ii) less thermal energy requirements for the reaction and (iii) production of carbon as a value-added byproduct (Dunker et al., 2006; Dunker & Ortmann, 2006; N. Muradov et al., 2005).

In 2006, Dunker et al investigated the effect of temperature, residence time, space velocity and various types of carbon catalysts on TDM, based on the hydrogen and carbon production in a fluidized bed reactor (Dunker et al., 2006). It was reported that at high temperatures (approximately 900^oC), even in the absence of catalyst, very rapid gas-phase decomposition of methane is observed, leading to considerable hydrogen and black carbon production. Furthermore, Holmen et al have studied the effect of temperature and reaction time on the product formation, selectivity and the reaction mechanism, affecting the hydrogen and carbon production specifically (Holmen, Olsvik, & Rokstad, 1995). It was highlighted that due to the instability of hydrocarbons at high temperatures, carbon production is considerably increases at high methane concentrations and long reaction times. Thus, methane was selected as the precursor for the induction heating-assisted CVD

of carbon on sand particles in a fluidized bed reactor considering the low cost, high carbon production selectivity and compliance with safety regulations.

5.4 Experimental

5.4.1 Materials

The Geldart's group B industrial silica sand (SiO_2) particles (ρ_p= 2.6 g/cm^3, d_p= 212- 250 μm) as the substrate material for FBCVD process was used. The selected sand particles were stored in containers to prevent moisture and environmental effects. Furthermore, methane (99.92% purity, Canadian Air Liquid) and nitrogen (99.99% purity, Canadian Air Liquid) were used as the carbon precursor component for CVD process and fluidizing gas, respectively. Finally, micro-sized graphite powder (99.99% purity, <150 μm) was purchased from Sigma-Aldrich to compare the microwave heating performance with various coated particle grades at different graphite-sand compositions.

5.4.2 Induction Heating FBCVD Setup

A 10 KW power source with a PID controller by Norax Canada was employed to provide a high frequency and voltage electrical field for induction heating applications. Furthermore, a matching box and a 5-cm OD and 7.6-cm high copper induction coil was designed and manufactured by Norax Canada to induce the electrical current into the workpiece. The induction coil was coated with polymer material in order to prevent harmful electric shocks and comply with the safety regulations. Water was running through the induction coil to maintain the temperature at lower levels. Chemical vapor deposition of methane was performed in a 2.5-cm OD, 0.3-cm width and 30-cm long stainless steel grade 316 tubular reactor. A distributor plate was designed and manufactured in order to disperse the flow uniformly, minimize the risk of flow channeling and support the sand particle substrates inside the reactor. Removable stainless steel caps were deployed for loading, unloading and reactor maintenance on both sides of the tube. The fluidized bed chemical vapor deposition setup for carbon coating of sand particles schematic is shown in Figure 5-1.

For each test, 60 g silica sand was added to the reactor. The particles were initially fluidized with nitrogen flow in a bubbling regime where U/U_{mf} ratio was in the region of 2 to 4. The nitrogen flow

was maintained using a mass flow controller Bronkhorst F-201CV, with initial gas velocity of 10 cm/s. In order to maintain the bubbling fluidization regime throughout the reaction at a fixed U/U_{mf}, using LabView software and a type K thermocouple monitoring the reaction zone temperature, the inlet gas velocity was reduced at elevated temperatures proportional to the initial gas velocity and the initial temperature.

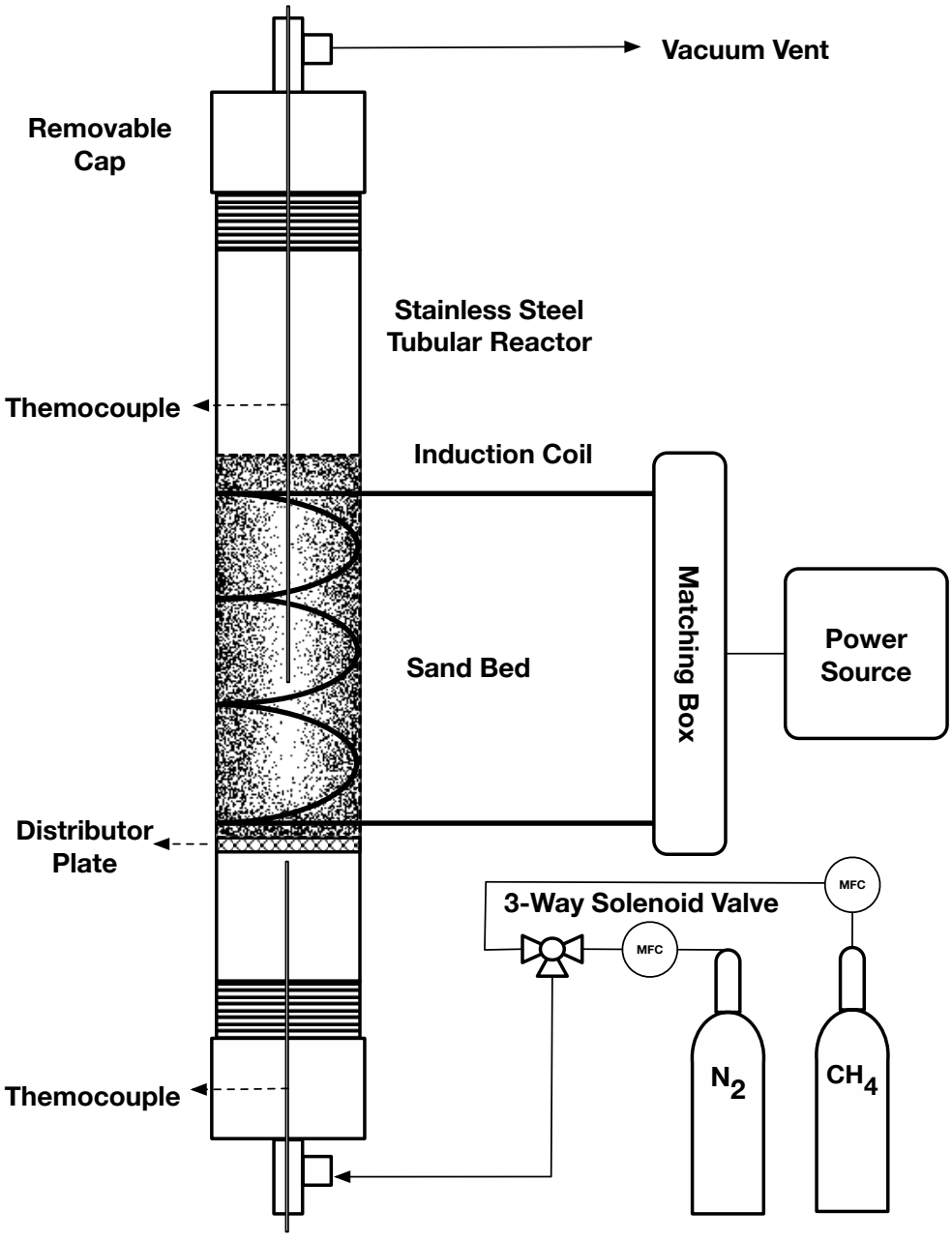

Figure 5-1: Induction heating-assisted fluidized bed CVD experimental setup

The induction power source was programmed through a PID controller interface to approach and maintain the designated reaction temperature. Once the bed temperature reached the setpoint value and stabilized, the flow of carbon precursor, methane, was turned on using an automatic solenoid valve. The methane superficial gas velocity was maintained constant at 2.3 cm/s during the reaction period using a Bronkhorst mass flow controller Bronkhorst F-201CV. The bed and distributor plate temperatures and the gas flow were constantly monitored with LabView software. The FBCVD of carbon over silica sand particles was repeated at 800, 900 and 1000^{o}C temperatures for 60-, 120- and 240 -minute reaction times, where all the experiments were performed at atmospheric pressure. Following the completion of each reaction at the designated temperature and reaction time, the coated particles were unloaded through the removable reactor cap, stored in sealed glass vials and, subjected to a cooling stage under nitrogen purge. Following each test, the reactor and the distributor plate were cleaned to remove all residual carbon deposits using micro brush scrubbers and combustion under air.

5.4.3 Carbon Layer and Surface Characterization

The quantity of carbon deposited on the silica sand particles was assessed by means of thermogravimetric analysis (TGA) using a TA Instruments TGA Q 5000 apparatus in a temperature range of 25 to 1000^{o}C and at a heating rate of 10^{o}C/min under air atmosphere with a flow rate of 20 mL/min and Nitrogen as the purge gas at 20 mL/min. Furthermore, the TGA results investigated the thermal stability of the carbon-coated particles under air at high temperatures. The TGA study was further repeated under nitrogen to verify the effect of moisture and volatile matter presence in the samples.

The morphological characteristics and qualitative and quantitative properties of the carbon coating of the particles at different temperatures and reaction times were conducted by field emission scanning electron microscopy (SEM-FEG; model JSM-7600 TFE, JEOL, Japan) equipped with energy-dispersive X-ray spectroscopy (EDX; Oxford Instruments) and focused ionized beam (FIB; model 2000-A, Hitachi, Japan) microscopic analysis methods. The SEM was operated at 5 kV with LEI imaging mode and a working distance of 15 mm. The samples were vacuum coated for 15 seconds prior to the analysis by gold spattering device to restrict the charging effect of the particles.

Due to the size range of the particles, application of transmission electron microscopy (TEM) was impractical to investigate the status of the carbon coated layer. Hence, focused ionized beam (FIB)

was used to investigate the carbon coating layer thickness and location on selected samples. These samples were vacuum coated with a tungsten layer prior to the milling step in order to minimize the destructive effect of the high-energy ionized beam on the coating surface. Following the selection of appropriate particles, a rectangular area of 30x10 μm^2 was milled on each sample particle to observe the carbon coating thickness and the layer location associated with each sample grade operated at 20 KV. Initial cuts were operated at high currents, and lower currents were employed to clean the site of interest. Ultimately, the milled samples were transferred to the SEM-FEG device, tilted for 30 degrees for proper visibility of the carbon layer, and microscopic images were captured at 3700 and 4300 magnifications. The quality of the coating was verified by EDX at different local spots of each sample. Furthermore, microscopic images of each sample at 50 and 100 magnifications were captured to investigate the effect of temperature and time on the morphology of the carbon-coating layer.

The surface characterization of the coated and the uncoated silica sand was performed by X-ray photoelectron spectroscopic (XPS) analysis carried out on a VG scientific ESCALAB 3 MK II X-ray photoelectron spectrometer using a MG Kα source (15 kV, 20 mA) to investigate the effect of temperature and time on the carbon layer formation. The survey scans were implemented at pass energy of 100 eV and energy step size of 1.0 eV at 10-nanometer penetration depth.

The total carbon content of the coated samples and uncoated silica sand particles was determined by combustion infrared carbon detection technique deploying a LECO CS744 series carbon analyzer with a Lecocel II and an iron chip accelerator. The major advantage of the LECO over TGA is the capability to detect carbon composition exclusively while neglecting other volatile matter components degradation. The accelerator temperature and sample temperature were adjusted at 1800^{o}C and 1400^{o}C, respectively. The amount of 1 mg of each sample was mixed with a volumetric unit of the accelerator prior to each analysis.

5.4.4 Microwave Heating Performance

The heating performance and operational durability of all samples were tested in a fluidized bed microwave heating apparatus. A 2.5 kW, 2.45 GHz Genesys Systems microwave generator, with water-cooling unit, was employed for microwave generation during the heating stage. The generated microwave was transferred from the magnetron to the cavity position through rectangular brass waveguides. A 2.5 cm OD and 8 cm length tubular quartz reactor was designed and

manufactured to transmit the microwave into the reaction zone operating as a transparent medium. In order to eliminate the application of a distributor plate for gas flow dispersion, the quartz reactor was attached to a 6 mm OD and 10 cm length lift tube at the bottom. The lift tube was filled with coarse sand particles, a 700-800 micrometer size range, to uniformly distribute the gas flow to the bed material, restrict gas jet formation and channeling effects, and support the bed material prior to the experiments based on the segregation phenomena. The quartz reactor and bare silica sand projected no interaction with microwave radiation throughout the operation, verifying that the heating effect was solely associated with the carbon coated particles and graphite mixtures. The quartz reactor was positioned inside a brass-copper alloy tubular electromagnetic shield to restrict the microwave leakage within the operating environment and comply with the safety guidelines. A removable cap was mounted on top of the shield tube for sample loading, maintenance and piping purposes. A schematic of the microwave heating setup diagram is presented in Figure 5-2.

All metal parts were located outside of the microwave shielding, eliminating the risk of interaction and arching effects. Initially, 30 g of each sample was loaded through the quartz-fitting opening to the reactor where the fitting was blocked by a quartz cap prior to the microwave heating activation. Next, the magnetron output current was adjusted using the controller knob, adapting the dissipated power, which ultimately led to the heat generation. Nitrogen was used as the fluidizing and carrier gas, while the superficial gas velocity was maintained through a mass flow controller Bronkhorst F-201CV. In order to restrict the fluidization regime to the bubbling region and prevent particle entrainment, as in the FBCVD setup, gas velocity was reduced at elevated temperatures. The particles were heated under constant current of 0.2 Amps from room temperature to 500^{o}C, while the bed temperature, heating time and gas velocity were monitored and recorded by LabView software. Each sample was submitted to three heating experiments to study the effect of surficial erosion on the operational durability of the samples. Moreover, the microwave heating performance of 800, 900 and 1000°C samples at 240 min was furthermore tested at 0.1 and 0.3 Amps magnetron input current respectively to investigate the effect of microwave power on the temperature profile.

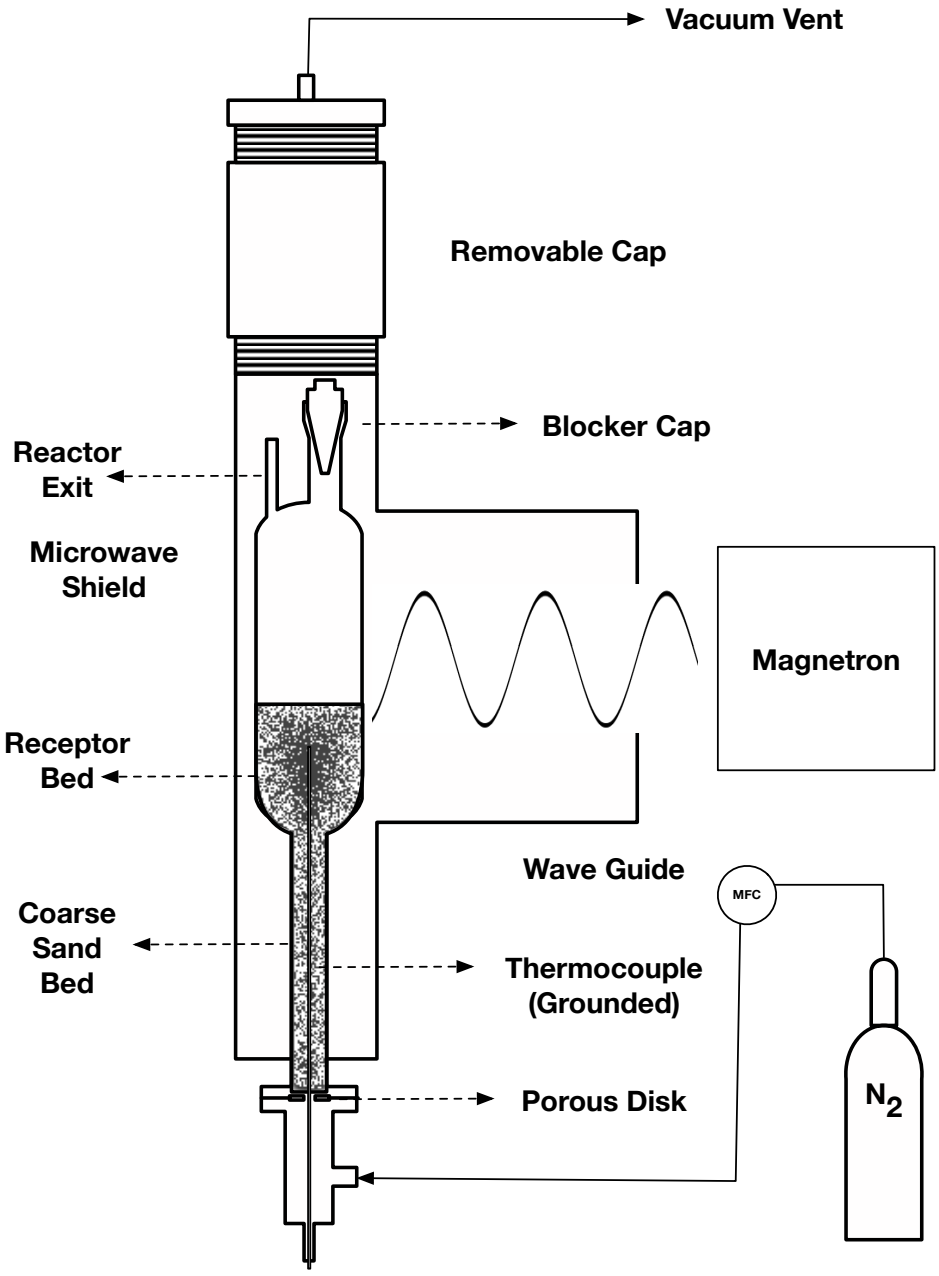

Figure 5-2: Microwave heating fluidized bed setup diagram

The dissipated power and reflected power were continuously monitored during the experiments employing an analog power meter. The reflected power was transferred and dissipated using a one-way air-cooled fin to prevent the magnetron from overheating. The fin temperature was continuously monitored by a type K thermocouple to comply with the safety regulations. To determine the performance capability of the coated samples versus manual mixtures of sand and

graphite, 1%, 5%, 50% and 90% weight fractions of graphite to sand mixtures were prepared and 30 mg of each sample was tested in the microwave setup. Each sample was extensively mixed prior to each experiment individually. The tests were performed at 0.1, 0.2 and 0.3 Amps for each graphite-sand mixture sample accordingly. The quartz reactor was removed and thoroughly cleaned following the cooling down stage under purged nitrogen. The type K thermocouple located inside the reactor was further electrically grounded to eliminate the thermocouple effects and microwave interaction leading to temperature measurement uncertainty (Pert et al., 2001).

5.5 Results and Discussion

5.5.1 Induction Heating FBCVD of Methane on Quartz Sand

The FBCVD carbon coating of silica sand particles in an induction heating reactor was implemented at 800, 900 and 1000^{o}C and 60, 120 and 240 minutes to study the effect of TDM temperature and reaction time on the coating quality and carbon deposition. The observations indicated that at lower temperatures and reaction times the amount and quality of the carbon coating were significantly subordinate even without access to a microscope, due to low thermal degradation of methane and low carbon production. The effect of TDM temperature and time was later verified by microscopic analysis of the particles, which is thoroughly investigated in the next section. In order to maintain similar fluidization regime at all temperatures, the nitrogen flow was continuously re-adjusted according to the bed temperature based on the following equation:

$$U_{adj} = U_0 \times \left(\frac{T_0}{T_R}\right) \tag{5}$$

where U_{adj} is the adjusted gas velocity, U_0 is the initial gas velocity value generally set at 10 cm/s, T_0 the initial reactor temperature, which was equivalent to the laboratory temperature and T_R is the reaction temperature in K constantly monitored by a type K thermocouple during the heating period and the reaction stage.

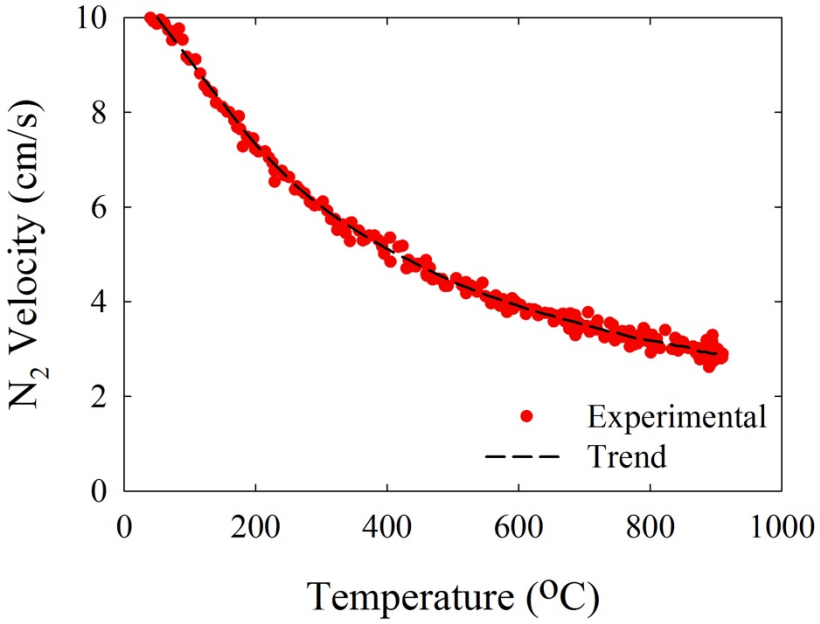

Figure 5-3: Gas velocity profile of nitrogen at feed condition during the heating period

Figure 5-3 illustrates the nitrogen gas velocity profile during the heating and reaction stages. The nitrogen gas velocity was gradually decreased while the temperature increased until the reactor reached the designated temperature value to maintain the bed at bubbling fluidization condition and minimize the temperature gradient issue. Afterwards, the gas flow was switched to the carbon precursor, methane, using an automatic 3-way valve while the nitrogen flow was stopped. After the designated coating time period, the gas flow was switched back to nitrogen while the reactor temperature was decreased prior to the unloading stage.

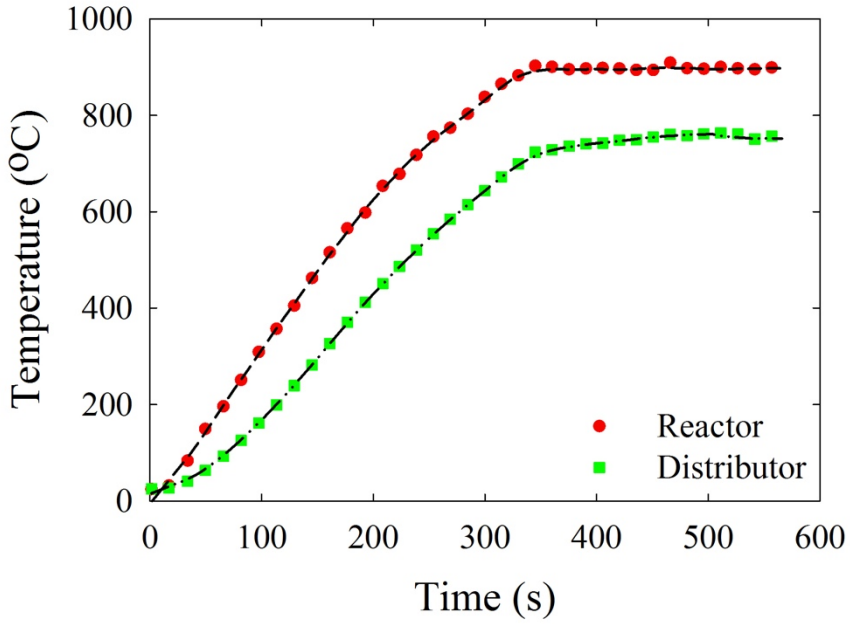

Figure 5-4: Temperature profile of the bed and the distributor plate during heating and reaction stages

Figure 5-4 presents the temperature profile of the middle of the bed and at the bottom of the distributor plate during the heating and FBCVD stages measure with type K thermocouples. It is observed that a temperature gradient of approximately 130°C existed between the bed temperature and the distributor plate. Taking into account the difference between the bed and the distributor plate materials together with the fluidized state of the bed, such a temperature difference inside the reactor would be expected. Furthermore, the distributor plate was located outside of the induction coil to minimize the thermal damages to the welded intersection of the plate and the reactor wall, which also explains its lower temperature. In addition, the reaction zone was insulated with quartz fiber to minimize heat loss risk while the distributor plate was located outside of the insulated area to prevent overheating and consequent damage. Moreover, since the operating temperature was close to the sand sintering temperature, a lower temperature value on the distributor plate diminished the risk of blockage and other problems (Shabanian & Chaouki, 2015).

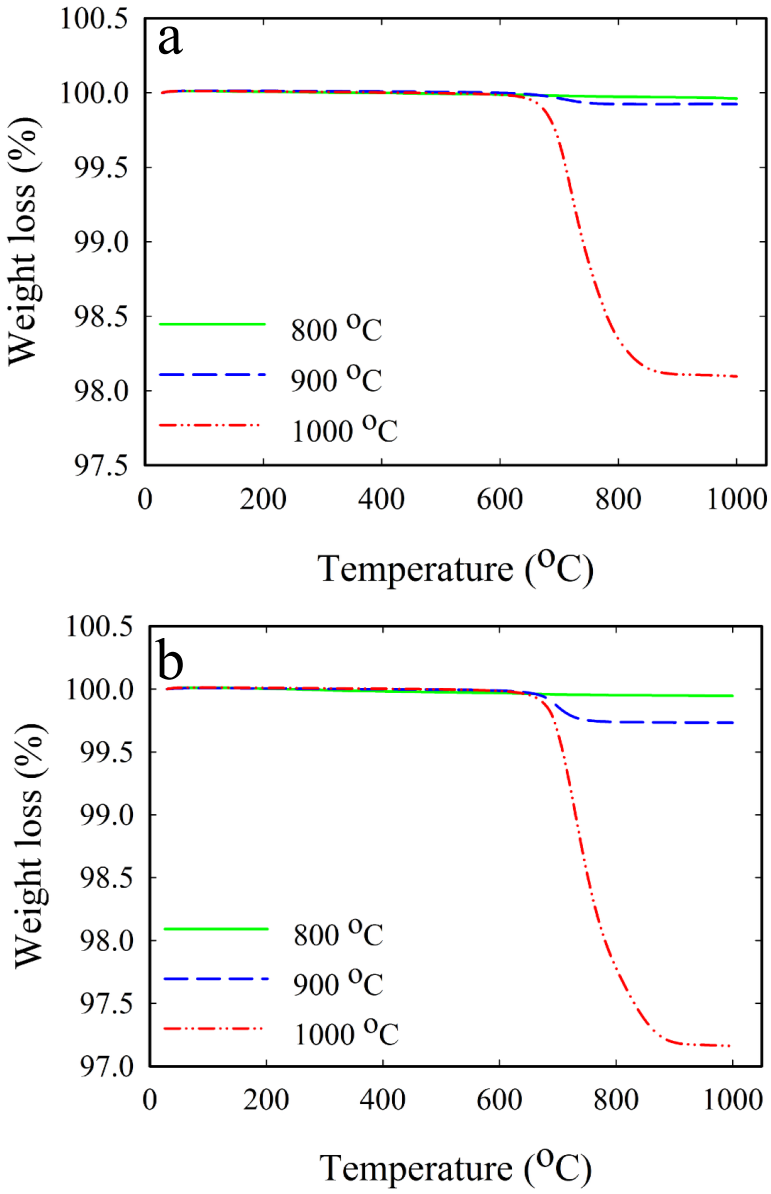

Figure 5-5: Representative TGA results for coated particles produced under different FBCVD temperatures and reaction times: a) 120 mins and b) 240 mins under air

5.5.2 Characterization of the Carbon Coated Sand Particles

The amount of carbon (microwave dielectric material) in the base silica sand material and carbon coated sand particles was determined by means of TGA and LECO tests. The TGA curves under air of the uncoated sand particles and carbon-coated sand particles obtained at different methane thermal decomposition temperatures and reaction times are presented in Figure 5-5 and 6. The major weight loss step of the samples arose at temperatures between 600 and 800°C, which

corresponds to the degradation of carbon-coated material deposited on the sand particles. Figure 5-5 also presents the thermal behavior of the carbon coated sand particles in air, clearly showing that the coated layer of carbon would tend to dissipate if the coated sand were exposed to an oxidative reaction environment at temperatures above 600°C. The TGA results under nitrogen did not reveal any significant weight loss step, which indicates a negligible content of moisture and volatile matter in the samples.

As presented in

Table 5-1, the TGA results have verified that the amount of carbon deposition on the substrate material is a function of reaction time and temperature. Increasing the coating temperature and/or reaction time considerably affects the carbon production and deposition on the sand material, although the effect of temperature is more significant.

Table 5-1 has summarized the carbon content investigation of the prepared samples according to the TGA results.

Furthermore, the carbon composition of base sand material and coated particles produced under different coating times and temperatures was measured using combustion infrared carbon detection technique (LECO). The results were in compliance with the TGA investigation to confirm the effect of time and temperature condition on the final carbon coating composition. The results of combustion infrared carbon detection are compared with equivalent TGA data in

Table 5-1.

Table 5-1: TGA and Combustion Infrared Carbon Detection (LECO) Results for the Original and Coated Particles at Various Coating Times and Temperatures

Reaction Temperature (^{o}C)	Pure Sand	800			900			1000		
Reaction Time (min)	N/A	60	120	240	60	120	240	60	120	240
TGA Carbon (wt%)	0.02	0.04	0.05	0.06	0.05	0.09	0.27	0.31	1.90	2.84
LECO Carbon (wt%)	<0.01	<0.01	<0.01	0.02	0.01	0.1	0.25	0.27	1.83	2.75

The SEM observations for the morphological investigation of the base sand material and coated particles produced under different coating times and temperatures are presented in Figure 5-7. The charging effect on the particles indicates absence or poor presence of carbon on the surface; on the other hand, increased carbon deposition and uniformity of the layer gradually diminishes the reflections gradually. The SEM-FEG results precisely present a graphical analysis of the effect of time and temperature on the quality of the carbon coating on the sand substrate particles. While initially a poor, heterogeneous and negligible coating of carbon on the sand particles was observed for 800^{o}C and 60-min coating temperature and time respectively, the evolution of the coating layer uniformity was gradually observed by increasing the reaction time and temperature.

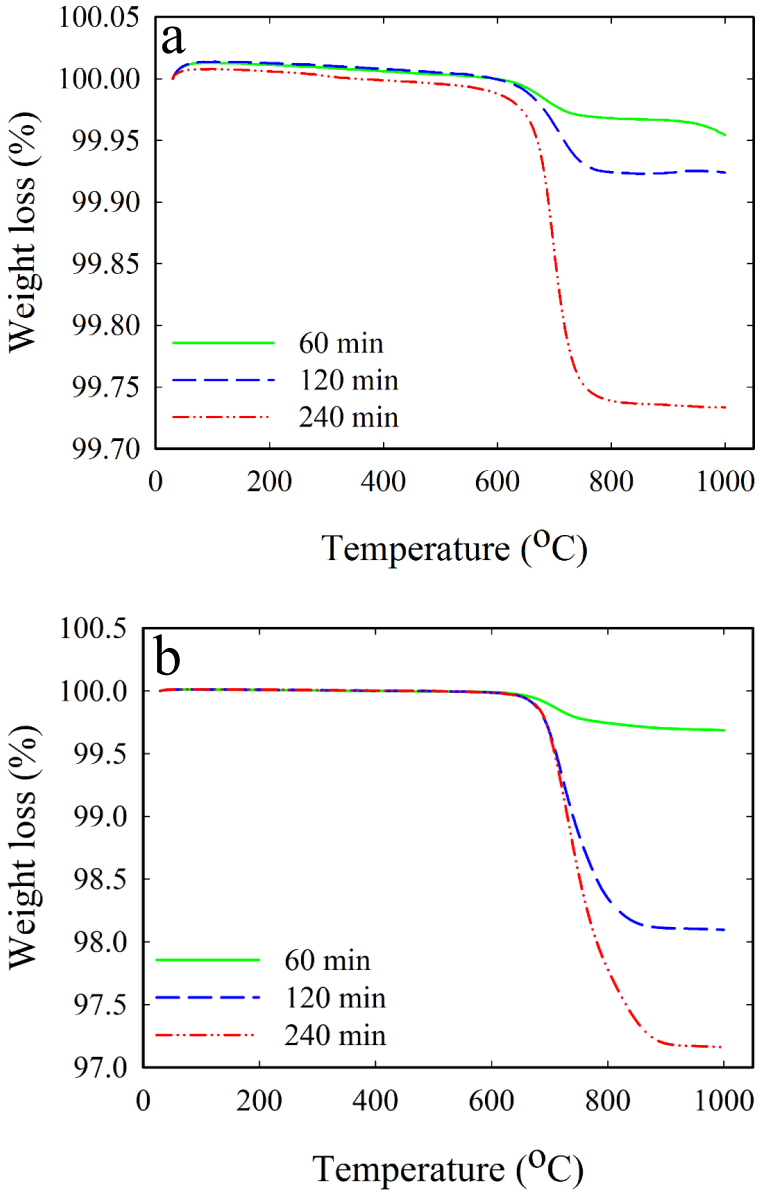

Figure 5-6: Representative TGA results at FBCVD temperatures: a) 900°C and b) 1000°C and different durations

The morphological analysis indicated that the coating quality and uniformity was poor in all samples produced under a temperature of 800°C, indicating the low carbon production through TDM at temperatures below 900°C and in the absence of a catalyst (Dunker et al., 2006).

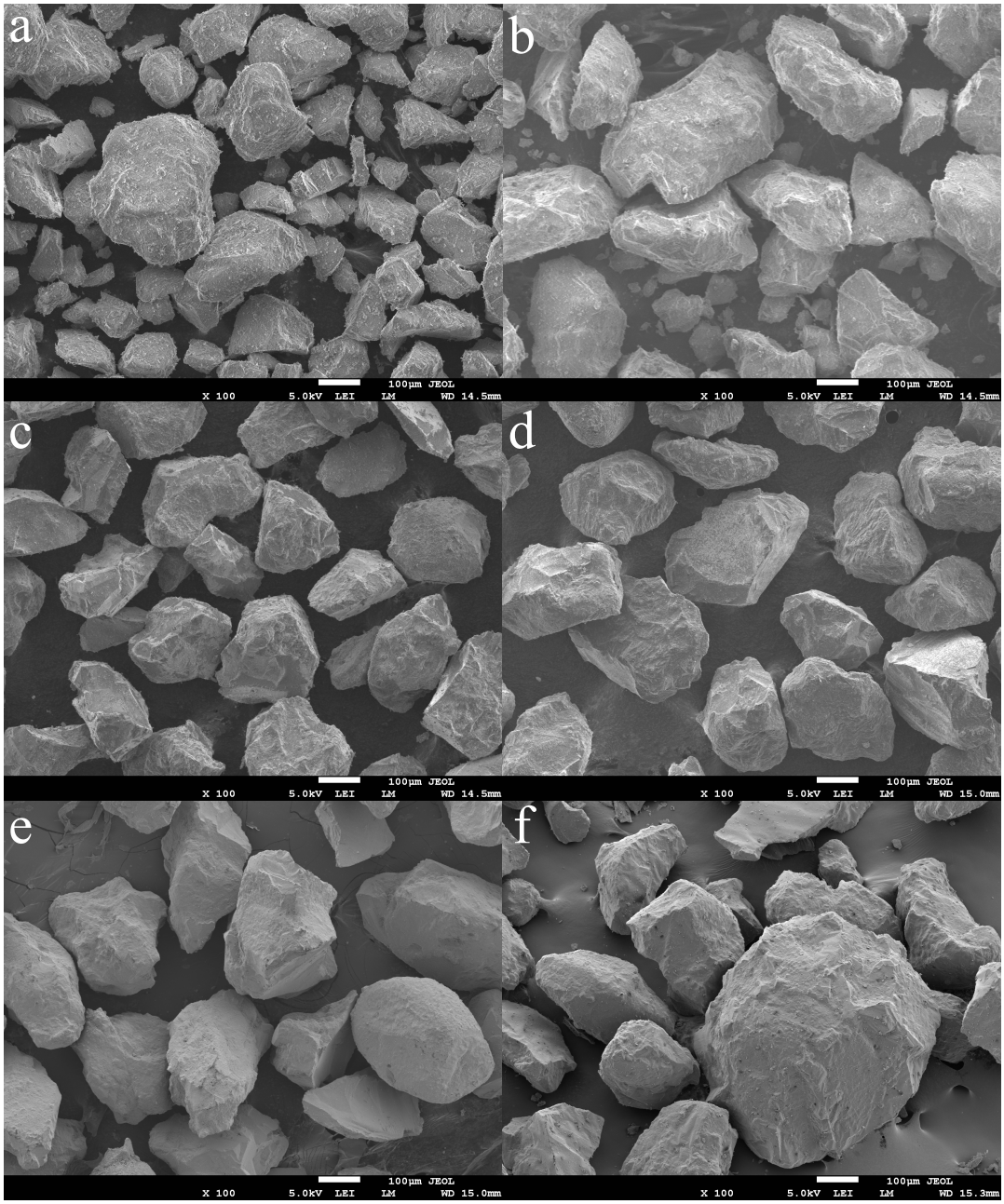

Figure 5-7: Representative SEM observation of the particles: (a) pure sand, (b) coated sand at 800^{o}C and 60 mins, (c) coated sand at 800^{o}C and 120 mins, (d) coated sand at 900^{o}C and 60 mins, (e) coated sand at 900^{o}C and 240 mins and (f) coated sand at 1000^{o}C and 240 mins FBCVD temperature and reaction time

Moreover, all coating grades obtained for 60-minute reaction time, in general, show poor carbon coating, which indicates a strong effect of reaction time on carbon production and deposition during the TDM (Holmen et al., 1995). However, by increasing the reaction temperature to 900^{o}C, the rate

of carbon production and deposition are considerably increased, leading to higher grades of coating due to the higher rate of methane degradation at high temperatures even in the absence of a catalyst.

In addition, increasing the reaction time provides higher methane thermal exposure, which ultimately leads to higher carbon production and deposition on the sand particles. Ultimately, for the samples produced at 1000^{o}C and 240-minute reaction temperature and time, respectively, the rate of carbon production is substantially higher than the rate of carbon deposition leading to the presence of carbon agglomeration particles in the sample, which are evidently observed by the SEM imaging. Observations of the thickness of the carbon coating layer and the location of multiple layers were facilitated by the focused ionized beam (FIB) milling of the samples produced at 800, 900 and 1000^{o}C temperature and 240-minute reaction time. Figure 5-8 illustrates the evolution of carbon as a function of coating layer thickness via temperature by means of FIB milling and SEM imaging. SEM observations noticeably approved the growth of the coating layer in terms of thickness by increasing the TDM temperature from 800 to 1000^{o}C. The mean value of the carbon coating layer thickness at 800, 900 and 1000^{o}C FBCVD temperature and 240-minute reaction time was evaluated by ImageJ software and statistical analysis. Accordingly, 20 measurements were implemented on each SEM image at the FIB milling intersection by ImageJ built in function; the mean values and standard deviation values are highlighted in Figure 5-8, respectively.

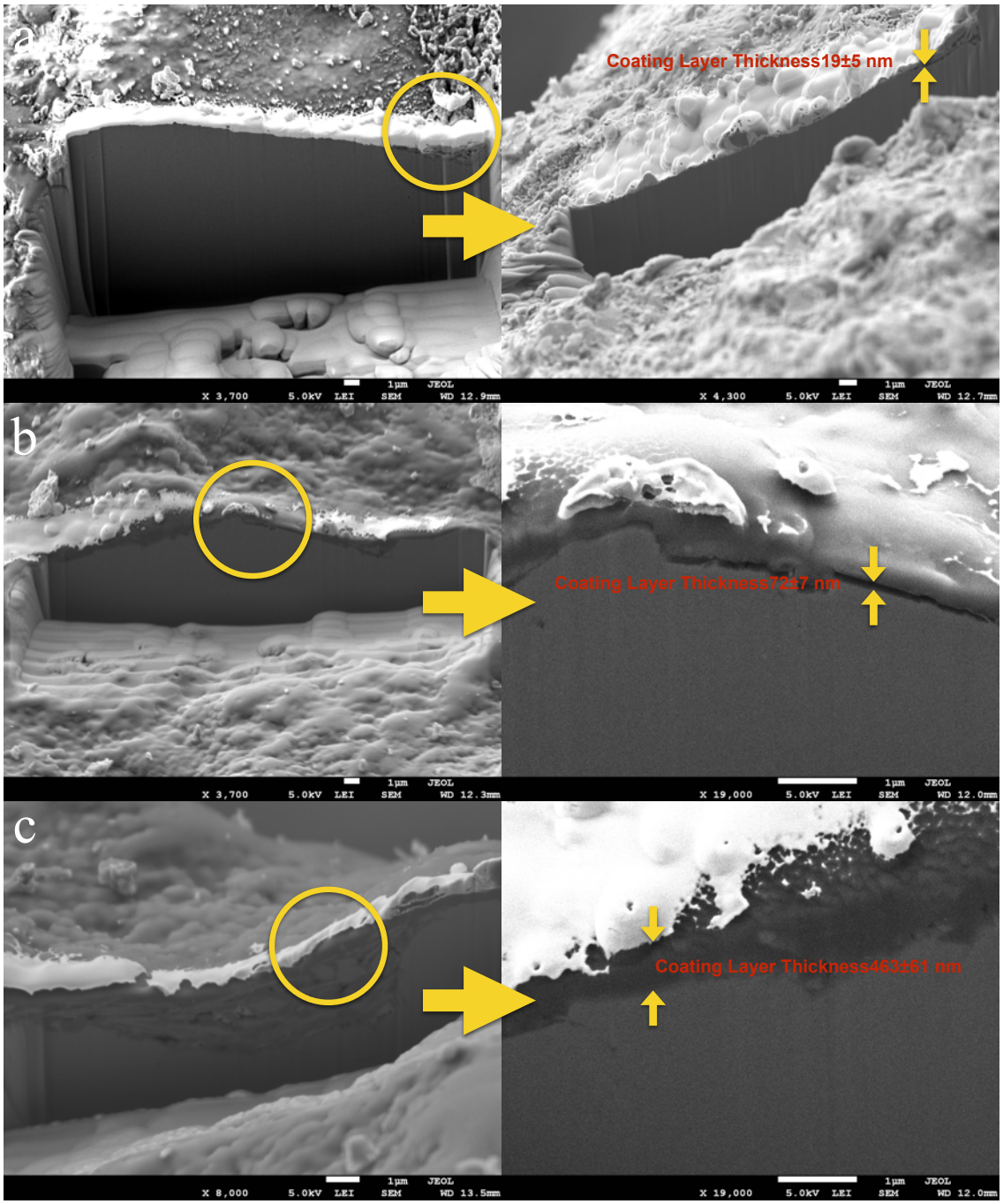

Figure 5-8: Representative SEM images of the evolution of the coating layer thickness using FIB milling of a) 800°C, b) 900°C and c) 1000°C at 240-min FBCVD temperature and time

Ultimately, EDX analysis was used to identify multiple layers at the FIB milling intersection, to investigate the composition and uniformity of coated layers thoroughly.

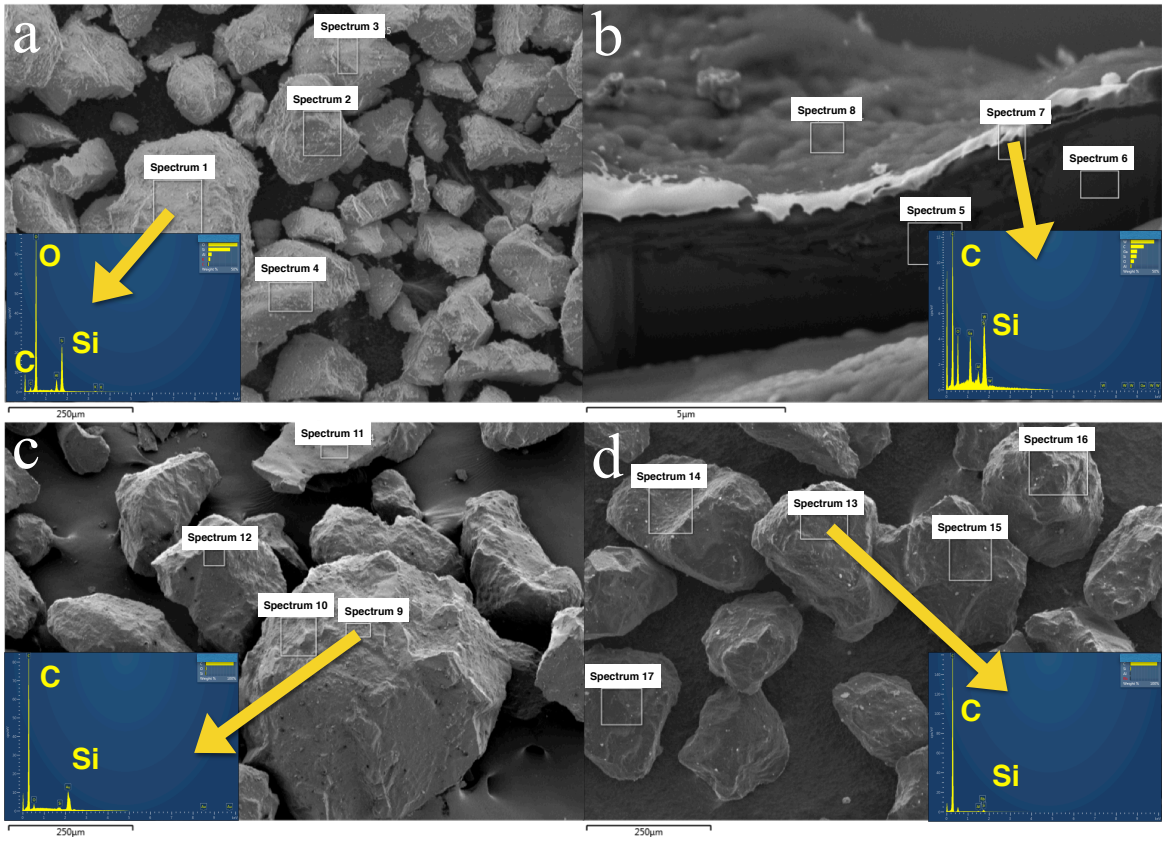

Figure 5-9: EDX results of (a) uncoated sand and coated particles at (b) 800°C and 240 mins, (c) 900°C and 240 mins and (d) 1000°C and 120 mins FBCVD temperature and reaction time

The EDX results revealed that increasing the temperature can extensively increase the carbon content of the coating layer. Moreover, the coating evolves to a more uniform layer as EDX identifies lower traces of Si and O, the principle elements of the core sand material, while elevating the coating temperature from 800 to 1000°C. Figure 5-9 and Table 5-2 present the EDX results and spectrum analysis of multiple local investigations for substrate sand and various coated particles. Table 5-3 compares the surficial elemental analysis of substrate sand material and coated sample grades at 800, 900 and 1000°C reaction temperatures and 60-, 120- and 240- minute reaction times obtained by XPS analysis. The surface analysis of the samples revealed an elevation in the carbon content and a decrease in the Si and O elements while increasing temperature and/or reaction time. However, the influence of the thermal effects is far more dominant. Moreover, the XPS results verified the presence of metals such as Al, in the core sand composition.

Table 5-2**:** Spectrum Analysis of EDX Data According to Figure 5-9 Acquisitions

Composition (%)	Spectrum Number Based on Figure5-9																
	1	2	3	4	5	6	7	8	9	10	11	12	13	14	15	16	17
C	1.6	1.3	1.2	1.6	8.2	3.1	24.1	91	93.9	87.4	95.3	94.3	95.4	91.8	89.7	89.8	89.6
Si	37.7	44.6	42.5	35.8	48.1	83.7	11.5	1.1	2.6	7.2	2.6	2.4	3.3	2.4	3.4	3.8	4.8
O	50	48.4	52.7	50.3	7.9	6.7	7	1	3.5	5.4	2.1	3.2	1	4.9	5.2	5.8	4.9

Table 5-3: XPS Data Analysis for Original and Coated Particles at Various Coating Times and Temperatures

Element	B.E.	S.F.	Pure Sand	800			900			1000		
			N/A	60	120	240	60	120	240	60	120	240
			Relative Atomic Percentage (%)									
AL2p	74.4	0.185	5.3	6.9	6.0	5.7	4.7	1.3	0.3	6.2	0.7	0.7
Si2p	102.9	0.270	17.7	16.8	15.7	15.0	11.0	4.1	1.2	13.7	2.3	1.7
C1s	284.9	0.250	7.6	16.5	25.1	27.3	50.6	78.6	92.9	27.5	89.9	91.4
Ca2p	348.1	1.580	0.6	0.5	0.2	0.1	---	---	---	0.4	---	---
K2s	377.8	0.387	1.4	1.9	1.5	2.0	0.9	---	---	2.0	---	---
N1s	401.7	0.420	0.8	---	---	---	---	---	---	---	---	---
O1s	532.0	0.660	64.3	57.4	50.7	50.0	32.2	15.6	5.5	48.7	6.9	6.2
F1s	688.6	1.000	1.4	---	0.9	---	0.6	---	---	1.5	0.3	0.4
Na1s	1071.6	2.300	0.8	---	---	---	---	---	---	---	---	---

Although the coating quality is noticeably poor at initial 800^{o}C and 60 minutes TDM conditions, confirmed by the core sand elements detection on the surface, namely Si, O, and metals, carbon is

the dominating element on samples obtained at higher temperature and longer reaction time, with values reaching above 90%. The inability of the XPS analysis to detect impurities and core sand composing material indicates a more uniform deposition of the carbon layer on such samples. The characterization observations revealed that very uniform and thorough layers of carbon could be deposited by induction heating FBCVD provided that appropriate reaction temperature and time were applied.

5.5.3 Microwave Heating Performance of the Carbon Coated Sand Receptors

Although low traces of carbon are observed in uncoated sand substrate, as reported in Table 5-3, the substrate did not experience any significant interaction with microwaves; this implies that such a low amount of carbon is not sufficient to counteract the poor dielectric properties of the main constituting elements of sand. The poor interaction of uncoated sand with microwaves emphasizes the importance of developing an effective receptor material for microwave heating applications. Therefore, the significant microwave interaction of carbonic material proves that the produced carbon coated sand particles were considered ideal microwave receptors for a gas-solid reactor, eliminating the necessity for adding excess amount of char or graphite to microwave-assisted high temperature reactions. Figure 5-10 and Figure 5-11 illustrate the heating profile of coated samples from room temperature to 500^{o}C while exposed to microwaves at 0.2 Amps power cycle produced under different TDM reaction times and temperatures. It was initially observed that because of the low coating uniformity and carbon deposition, for samples produced under short reaction times particularly 60 minutes--the receptor material did not compensate for the poor dielectric properties of the core sand particles. Consequently, even at prolonged microwave exposure periods, the temperature failed to reach the designated 500^{o}C value, resulting in a low heating rate and insufficient microwave absorption.

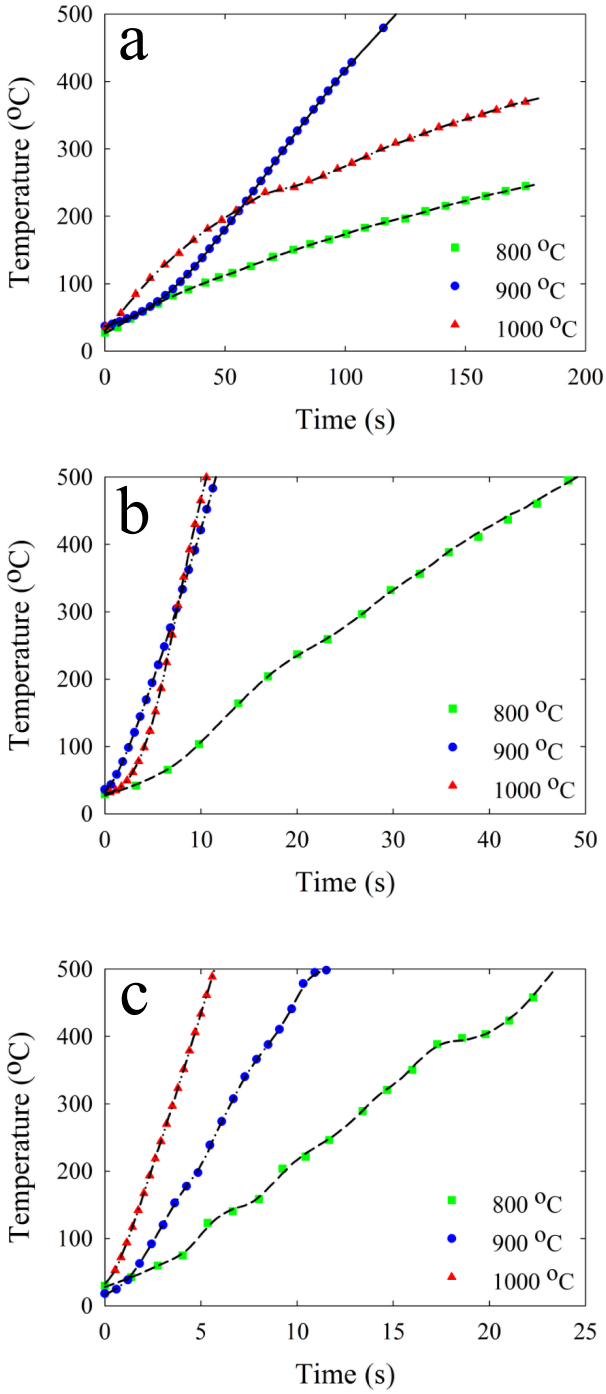

Figure 5-10: Microwave heating performance of coated particles produced at multiple FVCVD temperatures and (a) 60 mins, (b) 120 mins and (c) 240 mins reaction time at 0.2 Amps power cycle

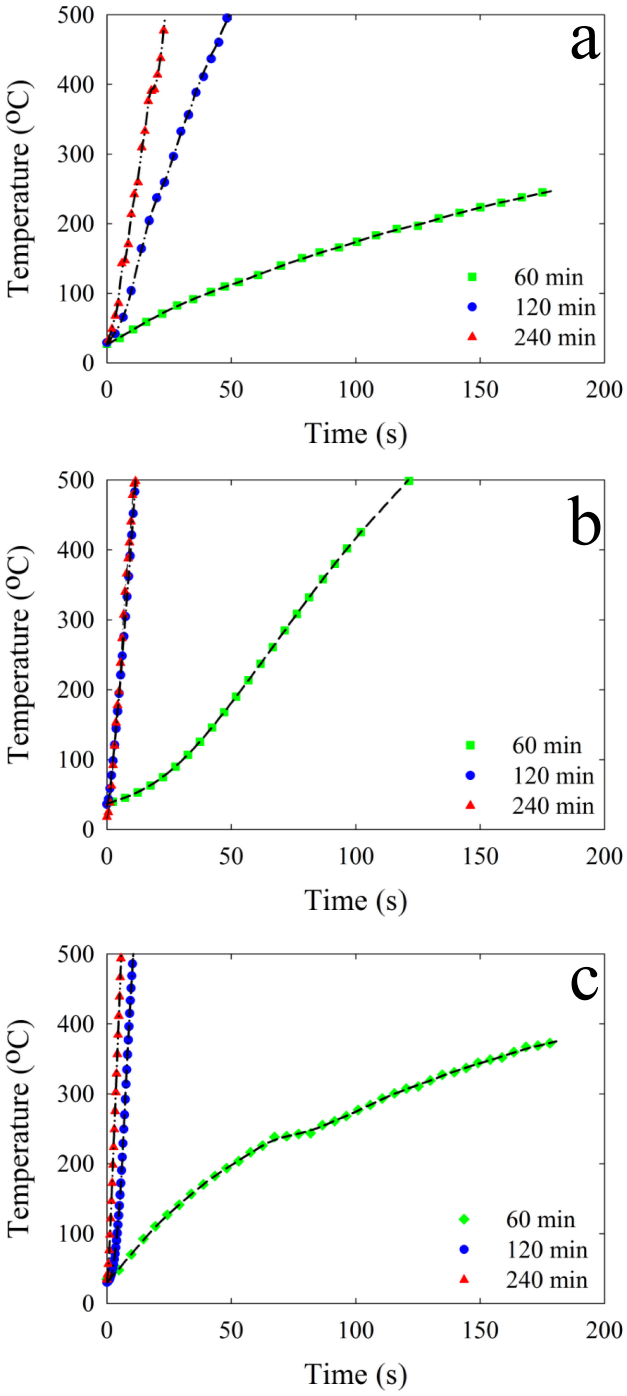

Figure 5-11: Microwave heating performance of coated particles produced at (a) 800°C, (b) 900°C and (c) 1000°C FBCVD temperatures and multiple reaction durations at 0.2 Amps power cycle

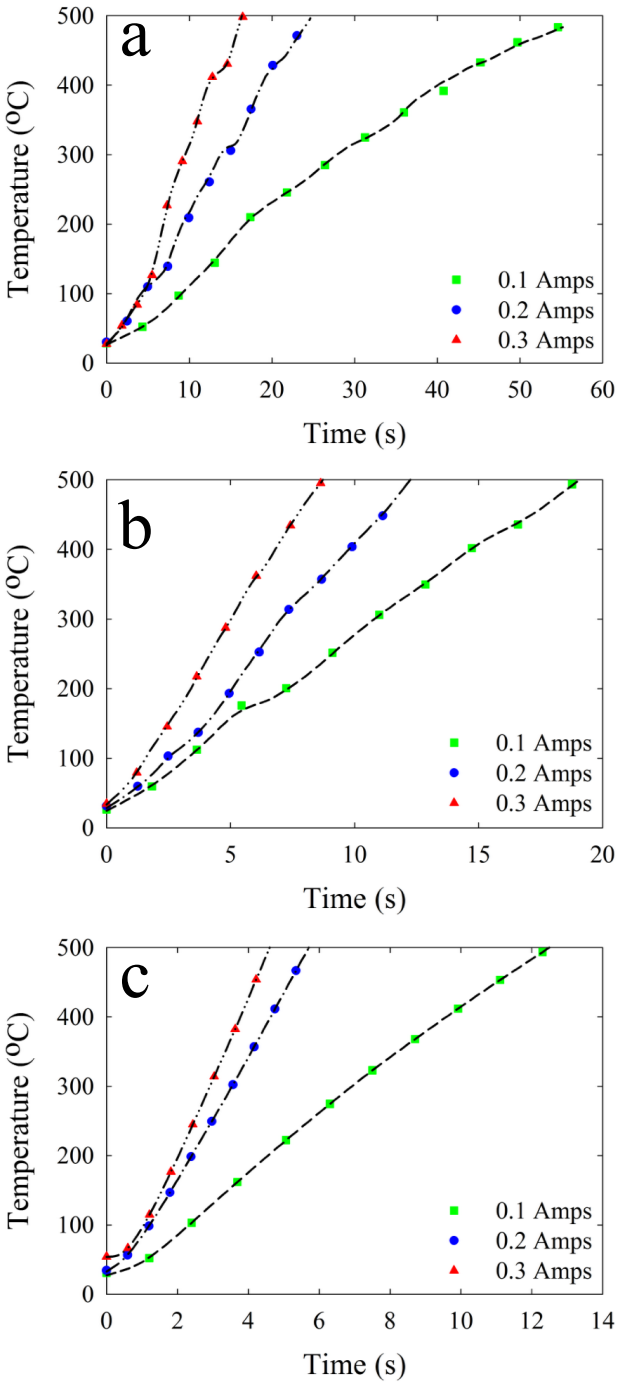

Figure 5-12: Effect of microwave power on heating performance of coated particles produced at (a) 800°C, (b) 900°C and (c) 1000°C FBCVD temperatures and 240-min time at different microwave power cycles

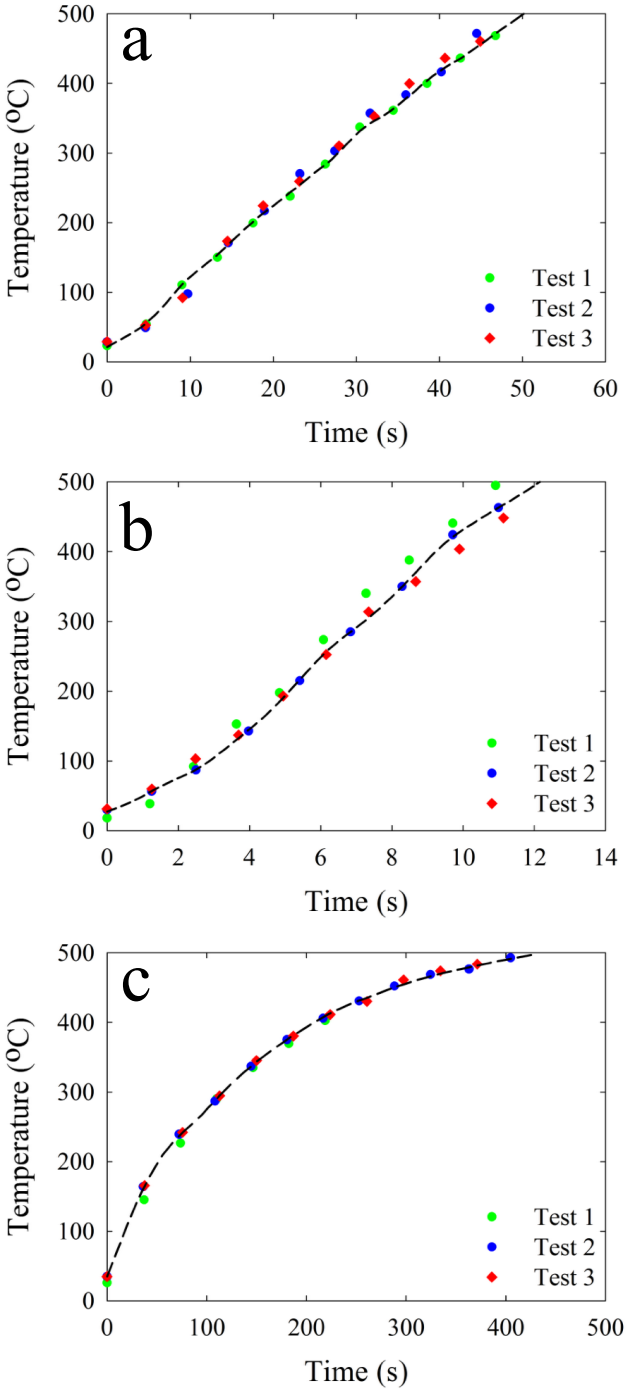

Figure 5-13: Durability and attrition test results for coated particles obtained at (a) 800°C and 120 mins, (b) 900°C and 240 mins and (c) 1000°C and 60 mins FBCVD operational conditions at 0.2 Amps microwave power cycle

However, enhancing the TDM operating conditions and consequently increasing the carbon deposition rate, which was verified by TGA and LECO results and coating thickness and uniformity, demonstrated by SEM, FIB and EDX results, greatly increased the heating rate for a constant microwave power. Furthermore, observed heating profiles for samples produced at FBCVD operating conditions leading to low carbon deposition and poor coating layer uniformity show that the microwave heating was constantly interrupted, as shown by broken lines in Figure 5-10 and Figure 5-11. Consequently, both the amount of carbon and the uniformity of the coating proved to be crucial to promote the microwave heating performance of the receptors. The enhanced and uniform coating at higher TDM temperatures and reaction times not only promotes the dielectric properties of the microwave receptors, but also creates a network of carbon nano-layers which boosts the electron interchange by boosting the conductivity, leading to the superior microwave heating performance of the coated receptors. The same concept has been employed to optimize the conductivity of LFP cathodes for battery production (J. Wang & Sun, 2012).

Furthermore, coated sample grades produced at 800, 900 and 1000^{o}C TDM temperature and 240 reaction time were exposed to microwave at 0.1, 0.2 and 0.3 Amps power cycle to investigate the effect of microwave power on the heating mechanism of the receptor materials. As depicted in Figure 5-12, the results were in compliance with the general rules of microwave heating, i.e. that increasing the microwave power has a significant effect on enhancing the heating rate of the dielectric material. The same trend was observed for all the coated sample grades covering the complete FBCVD production temperature range. In addition, the attrition resistance and durability of the receptor material in a gas-solid fluidized bed while exposed to the microwave was tested thoroughly by repeating the heating performance tests three times for each sample. In each test, the samples were heated to the designated 500^{o}C temperature and subsequently cooled down to 25^{o}C under nitrogen purge, while the bed was fluidized. The results are presented in Figure 5-13. If the receptor material had not been sufficiently resistant to attrition, their microwave heating performance would have deteriorated due to reduction in the cross-linking bridge for electrons to travel within the carbon layer. Also, damaged and detached carbon layers would have segregated to the surface of the fluidized bed, resulting in poor interaction of the bed material with the microwave.

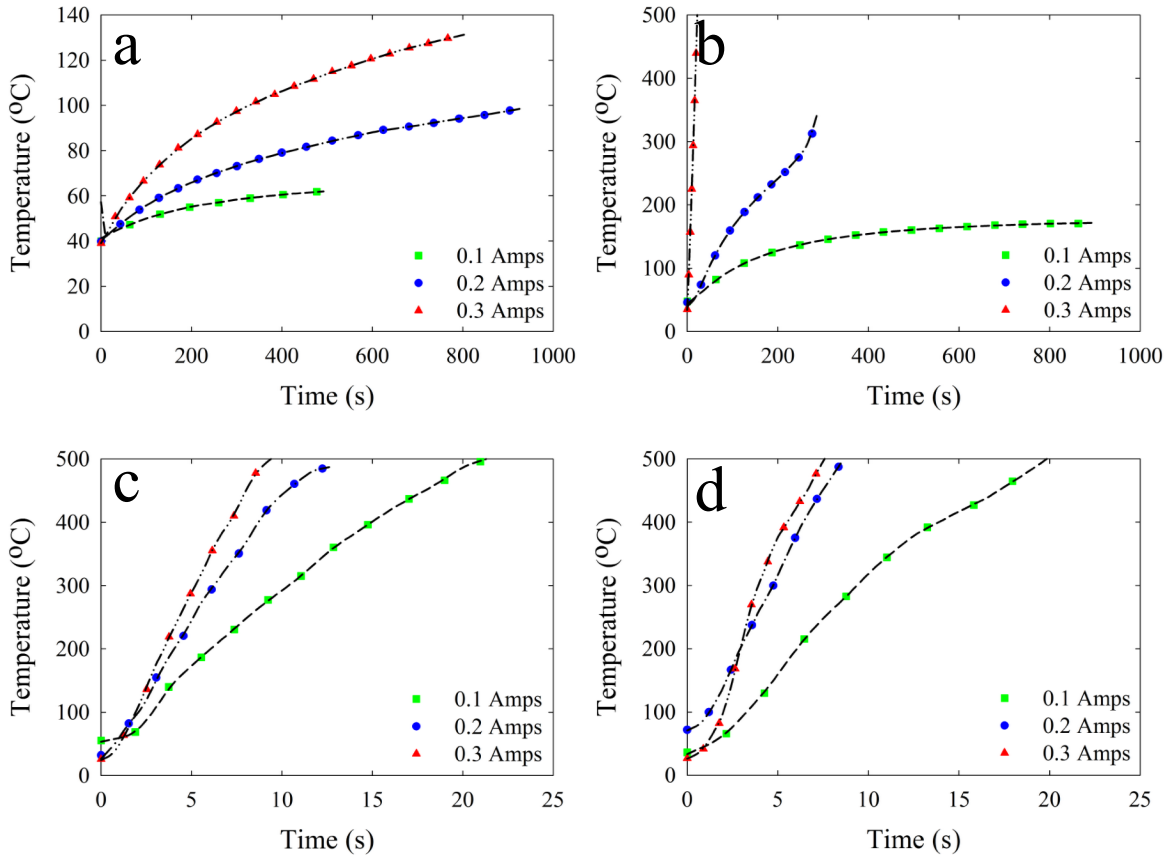

Figure 5-14: Microwave heating performance of (a) 1% (b) 5%, (c) 50% and (d) 90% graphite to sand mixtures at different microwave powers

Following the observations, it was concluded that submitting the receptor material to multiple heating and cooling cycles did not seem to affect the heating capabilities of the coated particles. However, longer exposures with multiple cycles will be carried out to confirm the results.

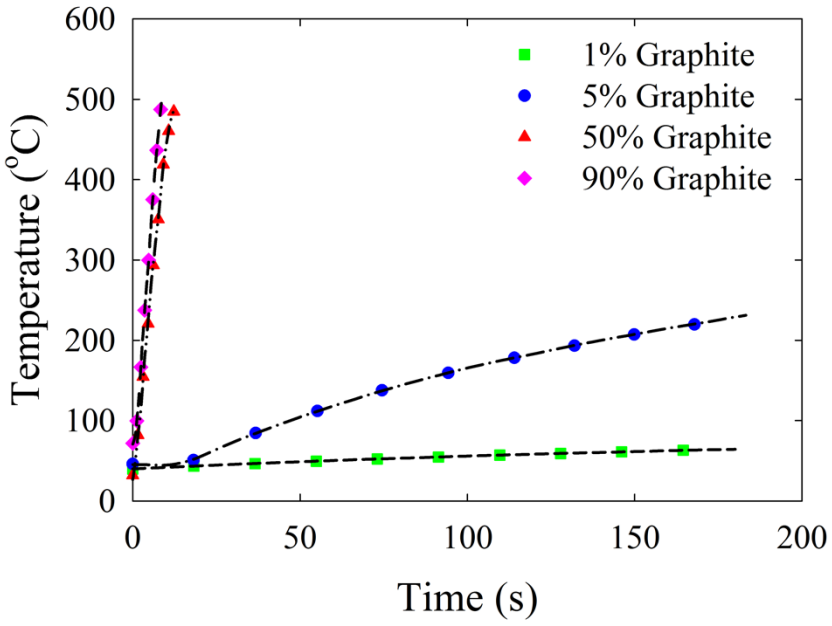

Figure 5-15: Comparative microwave heating performance of different graphite and sand mixtures at 0.2-Amp microwave power

In order to evaluate and compare the heating performance results from the developed microwave receptors, 1%, 5%, 50% and 90% weight fractions of graphite to pure sand mixtures were prepared and exposed to microwave radiation in the fluidized bed. Graphite has been widely regarded as the most outstanding dielectric material with exceptional microwave intractability among the carbon receptor criteria; hence the comparison provides a high level qualitative evaluation of the characteristics and properties of the developed receptor material. All the experiments aimed at heating the bed material from 25 ^{o}C to 500^{o}C. The results are shown in Figure 5-14.

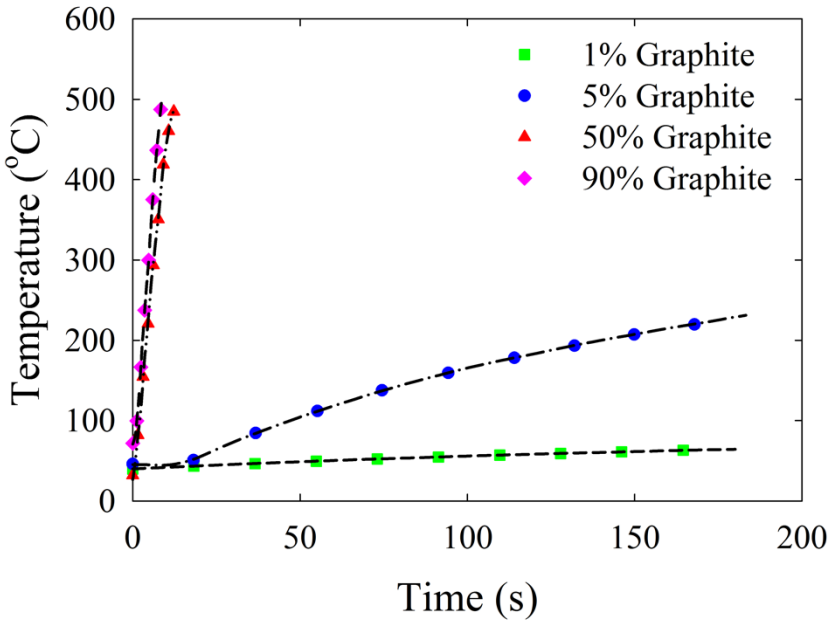

Figure 5-16: Comparative microwave heating performance of 50% and 90% graphite to sand mixtures and coated particles at 800, 900, 1000 °C and 240 mins FBCVD operational conditions

Figure 5-15 presents a comparative microwave heating performance of 1%, 5%, 50% and 90% graphite to sand mixtures exposed to 0.2-Amp power cycle. All the experiments were implemented from 25°C to 500°C correspondingly. The investigation disclosed that at low graphite content namely, 1% and 5%, even by increasing the microwave power, the mixture did not possess satisfactory dielectric properties to enable the bed reach the designated temperature even at prolonged microwave exposure. However, increasing the graphite content of the bed significantly improved the heating performance of the mixtures with comparable outcome to the developed microwave receptors obtained at high FBCVD temperature and reaction time.

It is noteworthy that the best performing graphite/sand mixture contained 90% of carbonic material, while the highest rated carbon coated receptor, obtained at 1000°C temperature and 240-minute period of FBCVD, contained 2.8 wt% of carbon. In addition, the developed receptor still exhibited a higher heating rate compared to graphite/sand mixed bed experiments. Moreover, while the coated sample produced at 900 °C and 240 minutes coating temperature and reaction time, respectively, had a carbon composition below 0.3%, the coated sample still exhibited a significantly higher heating rate while exposed to microwave radiation as compared to the competitive graphite/sand bed mixture material. Figure 5-16 shows the microwave heating performance of

carbon-coated sand receptors at 800, 900 and 1000°C and 240 minutes TDM temperature and time, compared to 1%, 5%, 50% and 90% graphite to sand mixtures at 0.2 Amps microwave power cycle.

From these results it, appears that the effect of coupling the carbon receptor with the bed material has a much more substantial effect than simply increasing the carbon composition of the bed, suggesting there is an enhanced coherence between the carbon layers that facilitate the travel of electrons through vacant orbitals of carbon, thus increasing microwave interaction efficiency. Moreover, pairing the carbon and sand bed material minimizes the risk of segregation, which diminishes the temperature gradient within the bed. Consequently, with a significantly low level of carbon contents of below 3 wt% a coating uniformity that leads to a network of carbon and nano-layers, a coating durability and erosion resistivity, the novel carbon coated sand receptors are remarkably superior to the competitive graphite/sand mixtures in their microwave heating performances.

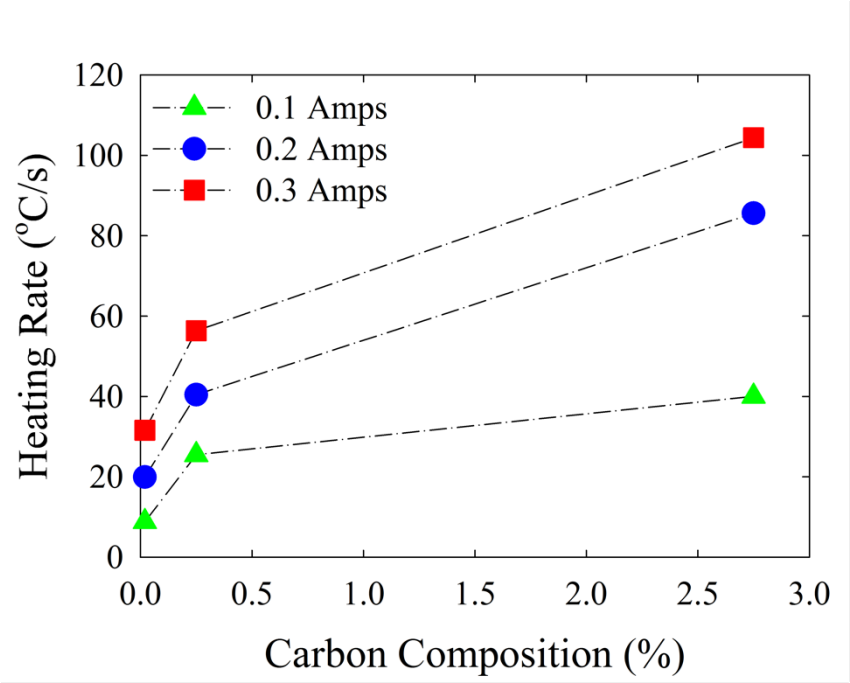

Figure 5-17: Effect of microwave output current and carbon composition on heating rate development of the coated receptors

Moreover, heating rate efficiency of the developed microwave receptor material as a function of carbon content and microwave power, was investigated, and the results are shown in Figure 5-17.

The heating rate data were acquired from Figure 5-12 using a linear curve fitting. Initially, with a microwave power corresponding to 0.1 Amps cycle current, which is a very low output, the measured heating rates are drastically low, highlighting the requirement for a minimum microwave power in order to produce adequate heating rates. However, when the microwave power was increased above 0.2 Amps, all coated samples demonstrated a significantly higher heating rate, which is in compliance with microwave heating principles. Furthermore, an increase in carbon content deposition led to the generation of higher heating rates for receptors while exposed to microwave radiation, which is in accordance with carbonic compounds as substantial dielectric materials for microwave heating purposes. The advantage of the observed extreme heating rates could be exploited in the reduction of process time and improved kinetic rates of endothermic reactions. The thermal requirements of endothermic reactions, biomass gasification and partial oxidation, for instance, lead to an enormous temperature drop in the reaction system. Consequently, a high heating rate technique would compensate for the temperature fluctuations preventing the production of undesired by-products and promoting the selectivity of the desired components. The combination of the specific characteristics of the developed microwave receptor with the negligible interactivity of gaseous components with microwave radiation provides an exceptional opportunity to simultaneously engage the carbon coated particles as catalyst support to optimize gas-solid catalytic reactions.

5.6 Conclusion

In this study, a novel microwave receptor was developed by carbon coating of silica sand particles through fluidized bed chemical vapor deposition (FDCVD) in an induction heating stainless steel reactor. Silica sand (SiO_2) particles as the substrate and methane (CH_4) as carbon precursor were employed for successful coating of the base material. The required carbon was produced through thermal degradation of methane (TDM) in the absence of any catalyst. The reaction was implemented at 800, 900 and 1000^oC temperatures and 60-,120- and 240-minute reaction times to study the effect of operating conditions on the quality and composition of the coated layer. TGA results exposed the carbon content of the coating layer for coated samples produced under a wide range of reaction temperatures and durations. Moreover, TGA results investigated the thermal resistivity of the receptor particles under air and verified the upper threshold of 600^oC. Furthermore, combustion infrared carbon detection (LECO) tests further substantiated the effect of

reaction temperature and time on the carbon composition of the samples, whose outcome was in compliance with the TGA results. It was concluded that increasing both reaction temperature and time significantly affects the deposition of carbon on the silica sand particles, although temperature dominated the coating mechanism, from 0.1% for the base sand material to 2.8% for 1000^{o}C and 240 minutes operating conditions.

The morphological study of the samples with microscopic analysis methods disclosed valuable information regarding the dependence of reaction time and temperature on the coating layer uniformity and thickness. The SEM imaging helped infer the TDM temperature and time impacts on the uniformity of the coated surface. The combination of FIB milling with SEM imaging denoted the effect of CVD operational conditions on the coating layer thickness and quantified carbon deposition on the receptor samples. Eventually, XPS and EDX results provided a discrete analysis of the coating surface composition, revealing the ratio of carbon content to the core sand structural elements, thus quantifying the coating homogeneity of the deposition layer.

The microwave performance of the carbon-coated sand receptors was investigated in a single-mode microwave apparatus. The heat generation mechanism of each sample was studied by microwave exposure from room temperature of 25^{o}C to a designated 500^{o}C temperature, while monitoring the temperature profile. Initially, samples with low TDM temperature and time failed to fulfill the minimum heating rate requirements to reach the designated temperature value. However, samples produced under higher reaction temperatures and times succeeded the microwave heating performance test in a matter of seconds, confirming the effect of FBCVD operating conditions on the dielectric properties of the receptor particles. Furthermore, the effect of microwave power on the heating performance of samples coated at extended 240-minute period was investigated at 0.1-, 0.2- and 0.3- amp microwave power cycles. Moreover, the operational durability of the particles to surficial erosion and attrition was investigated by exposing the samples to repeated cycles of experimental conditions and evaluating the results. The durability tests revealed the significant resistance of the samples to operating conditions, thus validating the use of the receptor particles for multiple applications. Ultimately, the microwave performance of various graphite and sand mixtures at different microwave power values were observed to compare the results with the behaviour of the novel receptors. It was highlighted that while mixtures with low graphite to sand composition failed to fulfill the heating tests, samples with higher graphite compositions (90%) showed a similar performance as our higher-grade coated receptors. Considering the maximum

2.8% carbon content of the coated receptors, the results emphasized the substantial effect of the carbon layer uniformity on the carbon content. Ultimately, the effect of deposited carbon composition and output power on the microwave heating rate was investigated for the novel receptors. It is strongly recommended to engage the developed silica based carbon coated microwave receptors simultaneously as a catalyst support or promoter to optimize gas-solid reactions based on the established characteristics of the particles.

5.7 Acknowledgments

The authors are grateful to the Natural Sciences and Research Council of Canada (NSERC) through discovery grant and NSERC/Total chair for financial support of the project. The authors acknowledge Ms. Ghita Bouanane El Edrisi for her invaluable cooperation during the experiments through the undergraduate internship program.

5.8 Nomenclature

B.E.	Binding energy of the corresponding atomic orbitals
C	Carbon composition of the coated sand receptor, %
d	Reference depth, m
d_p	Diameter of the particles, μm
f	Frequency of the electric current
ΔH	Heat of formation, kj/mol
I_{out}	Microwave output current, Amps
k	Reference depth constant
OD	Outside diameter, cm
r	Electrical resistivity, Ω
R^2	Coefficient of determination
S.F.	Sensitivity factor of the corresponding atomic orbital
T_R	Reaction zone temperature, K

T_0	Initial reactor temperature, K
dT/dt	Microwave heating rate of the receptors $^{o}C/s$
$tan\delta$	Loss tangent
U	Superficial gas velocity, cm/s
U_{adj}	Adjusted gas velocity, cm/s
U_0	Initial gas velocity value, cm/s
U_{mf}	Minimum fluidization gas velocity, cm/s
$WT\%$	Weight percentage, %
ε^*	Complex permittivity
ε'	Dielectric constant
ε''	Loss factor
ρ_p	Density of the particles, kg/m^3
μ	Relative magnetic permeability, m

5.9 Literature Cited

Antti, A. L., & Perre, P. (1999). A microwave applicator for on line wood drying: Temperature and moisture distribution in wood. *Wood Science and Technology, 33*(2), 123-138.

Archer, N. J. (1979). Chemical vapour deposition. *Physics in Technology, 10*(4), 152.

Besmann, T. M., Seldon, B. W., Lowden, R. A., & Stinton, D. P. (1991). Vapor-Phase Fabrication and Properties of Continuous-Filament Ceramic Composites. *Science, 253*(5024), 1104-1109. doi:10.1126/science.253.5024.1104

Caddick, S. (1995). Microwave Assisted Organic Reactions. *Tetrahedron, 51*(38), 10403-10432. doi:10.1016/0040-4020(95)00662-r

Choy, K. L. (2003). Chemical vapour deposition of coatings. *Progress in Materials Science, 48*(2), 57-170. doi:http://dx.doi.org/10.1016/S0079-6425(01)00009-3

Clark, D. E., Folz, D. C., & West, J. K. (2000). Processing materials with microwave energy. *Materials Science and Engineering: A, 287*(2), 153-158. doi:http://dx.doi.org/10.1016/S0921-5093(00)00768-1

Dahl, J. K., Buechler, K. J., Weimer, A. W., Lewandowski, A., & Bingham, C. (2004). Solar-thermal dissociation of methane in a fluid-wall aerosol flow reactor. *International Journal of Hydrogen Energy, 29*(7), 725-736. doi:http://dx.doi.org/10.1016/j.ijhydene.2003.08.009

Dahl, J. K., Tamburini, J., Weimer, A. W., Lewandowski, A., Pitts, R., & Bingham, C. (2001). Solar-Thermal Processing of Methane to Produce Hydrogen and Syngas. *Energy & Fuels, 15*(5), 1227-1232. doi:10.1021/ef0100606

Danafar, F., Fakhru'l-Razi, A., Salleh, M. A. M., & Biak, D. R. A. (2009). Fluidized bed catalytic chemical vapor deposition synthesis of carbon nanotubes—A review. *Chemical Engineering Journal, 155*(1–2), 37-48. doi:http://dx.doi.org/10.1016/j.cej.2009.07.052

Das, S., Mukhopadhyay, A. K., Datta, S., & Basu, D. (2009). Prospects of microwave processing: An overview. *Bulletin of Materials Science, 32*(1), 1-13. doi:10.1007/s12034-009-0001-4

Davies, J. (1990). *Conduction and induction heating* (Vol. 11): IET.

Dominguez, A., Fernandez, Y., Fidalgo, B., Pis, J. J., & Menendez, J. A. (2007). Biogas to syngas by microwave-assisted dry reforming in the presence of char. *Energy & Fuels, 21*(4), 2066-2071. doi:Doi 10.1021/Ef070101j

Dominguez, A., Menendez, J. A., Fernandez, Y., Pis, J. J., Nabais, J. M. V., Carrott, P. J. M., & Carrott, M. M. L. R. (2007). Conventional and microwave induced pyrolysis of coffee hulls for the production of a hydrogen rich fuel gas. *Journal of Analytical and Applied Pyrolysis, 79*(1-2), 128-135. doi:Doi 10.1016/J.Jaap.2006.08.003

Doucet, J., Laviolette, J.-P., Farag, S., & Chaouki, J. (2014). Distributed microwave pyrolysis of domestic waste. *Waste and Biomass Valorization, 5*(1), 1-10. doi:10.1007/s12649-013-9216-0

Dunker, A. M., Kumar, S., & Mulawa, P. A. (2006). Production of hydrogen by thermal decomposition of methane in a fluidized-bed reactor—Effects of catalyst, temperature, and residence time. *International Journal of Hydrogen Energy, 31*(4), 473-484. doi:http://dx.doi.org/10.1016/j.ijhydene.2005.04.023

Dunker, A. M., & Ortmann, J. P. (2006). Kinetic modeling of hydrogen production by thermal decomposition of methane. *International Journal of Hydrogen Energy, 31*(14), 1989-1998. doi:http://dx.doi.org/10.1016/j.ijhydene.2006.01.013

Farag, S., & Chaouki, J. (2015). A modified microwave thermo-gravimetric-analyzer for kinetic purposes. *Applied Thermal Engineering, 75*, 65-72. doi:http://dx.doi.org/10.1016/j.applthermaleng.2014.09.038

Farag, S., Fu, D., Jessop, P. G., & Chaouki, J. (2014). Detailed compositional analysis and structural investigation of a bio-oil from microwave pyrolysis of kraft lignin. *Journal of Analytical and Applied Pyrolysis, 109*(0), 249-257. doi:http://dx.doi.org/10.1016/j.jaap.2014.06.005

Farag, S., Kouisni, L., & Chaouki, J. (2014). Lumped approach in kinetic modeling of microwave pyrolysis of kraft lignin. *Energy & Fuels, 28*(2), 1406-1417. doi:10.1021/ef4023493

Farag, S., Sobhy, A., Akyel, C., Doucet, J., & Chaouki, J. (2012). Temperature profile prediction within selected materials heated by microwaves at 2.45GHz. *Applied Thermal Engineering, 36*, 360-369. doi:Doi 10.1016/J.Applthermaleng.2011.10.049

Gabriel, C., Gabriel, S., H. Grant, E., H. Grant, E., S. J. Halstead, B., & Michael P. Mingos, D. (1998). Dielectric parameters relevant to microwave dielectric heating. *Chemical Society Reviews, 27*(3), 213-224. doi:10.1039/A827213Z

Gaudernack, B., & Lynum, S. (1998). Hydrogen from natural gas without release of CO2 to the atmosphere. *International Journal of Hydrogen Energy, 23*(12), 1087-1093. doi:http://dx.doi.org/10.1016/S0360-3199(98)00004-4

Gómez-Barea, A., & Leckner, B. (2013). Estimation of gas composition and char conversion in a fluidized bed biomass gasifier. *Fuel, 107*, 419-431. doi:http://dx.doi.org/10.1016/j.fuel.2012.09.084

Gupta, M., & Wong, W. L. (2007). *Microwaves and metals*. Singapore: John Wiley & Sons.
Haimbaugh, R. E. (2001). *Practical induction heat treating*: ASM International.
Holmen, A., Olsvik, O., & Rokstad, O. A. (1995). Pyrolysis of natural gas: chemistry and process concepts. *Fuel Processing Technology, 42*(2–3), 249-267. doi:http://dx.doi.org/10.1016/0378-3820(94)00109-7
Hussain, Z., Khan, K. M., Basheer, N., & Hussain, K. (2011). Co-liquefaction of Makarwal coal and waste polystyrene by microwave–metal interaction pyrolysis in copper coil reactor. *Journal of Analytical and Applied Pyrolysis, 90*(1), 53-55. doi:http://dx.doi.org/10.1016/j.jaap.2010.10.002
Hussain, Z., Khan, K. M., & Hussain, K. (2010). Microwave–metal interaction pyrolysis of polystyrene. *Journal of Analytical and Applied Pyrolysis, 89*(1), 39-43. doi:http://dx.doi.org/10.1016/j.jaap.2010.05.003
Jones, A. C., & O'Brien, P. (2008). *CVD of compound semiconductors: Precursor synthesis, developmeny and applications*: John Wiley & Sons.
Jones, D. A., Lelyveld, T. P., Mavrofidis, S. D., Kingman, S. W., & Miles, N. J. (2002). Microwave heating applications in environmental engineering—a review. *Resources, Conservation and Recycling, 34*(2), 75-90. doi:http://dx.doi.org/10.1016/S0921-3449(01)00088-X
Khaghanikavkani, E., & Farid, M. M. (2013). Mathematical Modelling of Microwave Pyrolysis. *International Journal of Chemical Reactor Engineering, 11*. doi:10.1515/ijcre-2012-0060
Latifi, M., Berruti, F., & Briens, C. (2014). A novel fluidized and induction heated microreactor for catalyst testing. *Aiche Journal, 60*(9), 3107-3122.
Latifi, M., & Chaouki, J. (2015). A novel induction heating fluidized bed reactor: Its design and applications in high temperature screening tests with solid feedstocks and prediction of defluidization state. *Aiche Journal, 61*(5), 1507-1523. doi:10.1002/aic.14749
Lee, C. H., Luan, H. F., Bai, W. P., Lee, S. J., Jeon, T. S., Senzaki, Y., . . . Kwong, D. L. (2000, 10-13 Dec. 2000). *MOS characteristics of ultra thin rapid thermal CVD ZrO/sub 2/ and Zr silicate gate dielectrics.* Paper presented at the Electron Devices Meeting, 2000. IEDM '00. Technical Digest. International.
Liu, X., Sun, H., Chen, Y., Lau, R., & Yang, Y. (2008). Preparation of large particle MCM-41 and investigation on its fluidization behavior and application in single-walled carbon nanotube production in a fluidized-bed reactor. *Chemical Engineering Journal, 142*(3), 331-336. doi:http://dx.doi.org/10.1016/j.cej.2008.04.035
Menéndez, J. A., Arenillas, A., Fidalgo, B., Fernández, Y., Zubizarreta, L., Calvo, E. G., & Bermúdez, J. M. (2010). Microwave heating processes involving carbon materials. *Fuel Processing Technology, 91*(1), 1-8. doi:http://dx.doi.org/10.1016/j.fuproc.2009.08.021
Metaxas, A. C., & Meredith, R. J. (1983). *Industrial microwave heating*. London, UK: P. Peregrinus on behalf of the Institution of Electrical Engineers.
Motasemi, F., & Afzal, M. T. (2013). A review on the microwave-assisted pyrolysis technique. *Renewable & Sustainable Energy Reviews, 28*, 317-330. doi:10.1016/j.rser.2013.08.008
Muradov, N. (2001). Catalysis of methane decomposition over elemental carbon. *Catalysis Communications, 2*(3–4), 89-94. doi:http://dx.doi.org/10.1016/S1566-7367(01)00013-9
Muradov, N. (2001). Hydrogen via methane decomposition: an application for decarbonization of fossil fuels. *International Journal of Hydrogen Energy, 26*(11), 1165-1175. doi:http://dx.doi.org/10.1016/S0360-3199(01)00073-8
Muradov, N., Smith, F., & T-Raissi, A. (2005). Catalytic activity of carbons for methane decomposition reaction. *Catalysis Today, 102–103*(0), 225-233. doi:http://dx.doi.org/10.1016/j.cattod.2005.02.018

Muradov, N. Z. (1998). CO2-free production of hydrogen by catalytic pyrolysis of hydrocarbon fuel. *Energy & Fuels, 12*(1), 41-48. doi:10.1021/ef9701145

Mushtaq, F., Mat, R., & Ani, F. N. (2014). A review on microwave assisted pyrolysis of coal and biomass for fuel production. *Renewable and Sustainable Energy Reviews, 39*(0), 555-574. doi:http://dx.doi.org/10.1016/j.rser.2014.07.073

Naslain, R., & Langlais, F. (1986). CVD-processing of ceramic-ceramic composite materials. In R. Tressler, G. Messing, C. Pantano, & R. Newnham (Eds.), *Tailoring Multiphase and Composite Ceramics* (pp. 145-164): Springer US.

Oehr, C., & Suhr, H. (1988). Thin copper films by plasma CVD using copper-hexafluoro-acetylacetonate. *Applied Physics A, 45*(2), 151-154. doi:10.1007/BF02565202

Pert, E., Carmel, Y., Birnboim, A., Olorunyolemi, T., Gershon, D., Calame, J., . . . Wilson, O. C. (2001). Temperature measurements during microwave processing: The significance of thermocouple effects. *Journal of the American Ceramic Society, 84*(9), 1981-1986. doi:10.1111/j.1151-2916.2001.tb00946.x

Philippe, R., Serp, P., Kalck, P., Kihn, Y., Bordère, S., Plee, D., . . . Caussat, B. (2009). Kinetic study of carbon nanotubes synthesis by fluidized bed chemical vapor deposition. *Aiche Journal, 55*(2), 450-464. doi:10.1002/aic.11676

Roy, R., Agarwal, D., Chen, J. P., & Gedevanishvili, S. (1999). Full sintering of powdered-metal bodies in a microwave field. *Nature, 399*(6737), 668-670.

Rudnev, V., Loveless, D., Cook, R. L., & Black, M. (2002). *Handbook of induction heating*: CRC Press.

Russell, A. D., Antreou, E. I., Lam, S. S., Ludlow-Palafox, C., & Chase, H. A. (2012). Microwave-assisted pyrolysis of HDPE using an activated carbon bed. *RSC Advances, 2*(17), 6756-6760. doi:10.1039/C2RA20859H

Samih, S., & Chaouki, J. (2014). Development of a fluidized bed thermogravimetric analyzer. *Aiche Journal, 61*(1), 84-89. doi:10.1002/aic.14637

See, C. H., & Harris, A. T. (2008). CaCo3 supported Co-Fe catalysts for carbon nanotube synthesis in fluidized bed reactors. *Aiche Journal, 54*(3), 657-664. doi:10.1002/aic.11403

Serban, M., Lewis, M. A., Marshall, C. L., & Doctor, R. D. (2003). Hydrogen production by direct Contact pyrolysis of natural gas. *Energy & Fuels, 17*(3), 705-713. doi:10.1021/ef020271q

Shabanian, J., & Chaouki, J. (2015). Fluidization characteristics of a bubbling gas-solid fluidized bed at high temperature in the presence of interparticle forces. *Chem. Eng. J., Submitted for publication*.

Shah, N., Panjala, D., & Huffman, G. P. (2001). Hydrogen production by catalytic decomposition of methane. *Energy & Fuels, 15*(6), 1528-1534. doi:10.1021/ef0101964

Sobhy, A., & Chaouki, J. (2010). Microwave-assisted Biorefinery. *Cisap4: 4th International Conference on Safety & Environment in Process Industry, 19*, 25-29. doi:Doi 10.3303/Cet1019005

Steinberg, M. (1998). Production of hydrogen and methanol from natural gas with reduced CO2 emission. *International Journal of Hydrogen Energy, 23*(6), 419-425. doi:http://dx.doi.org/10.1016/S0360-3199(97)00092-X

Steinberg, M. (1999). Fossil fuel decarbonization technology for mitigating global warming. *International Journal of Hydrogen Energy, 24*(8), 771-777. doi:http://dx.doi.org/10.1016/S0360-3199(98)00128-1

Tai, H.-S., & Jou, C.-J. G. (1999). Application of granular activated carbon packed-bed reactor in microwave radiation field to treat phenol. *Chemosphere, 38*(11), 2667-2680. doi:http://dx.doi.org/10.1016/S0045-6535(98)00432-9

Thostenson, E. T., & Chou, T. W. (1999). Microwave processing: fundamentals and applications. *Composites Part a-Applied Science and Manufacturing, 30*(9), 1055-1071. doi:Doi 10.1016/S1359-835x(99)00020-2

Tinga, W. R., & Nelson, S. O. (1973). Dielectric properties of materials for microwave processing-tabulated. *J. Microwave Power, 8*(1), 23-66.

Undri, A., Frediani, M., Rosi, L., & Frediani, P. (2014). Reverse polymerization of waste polystyrene through microwave assisted pyrolysis. *Journal of Analytical and Applied Pyrolysis, 105*, 35-42. doi:http://dx.doi.org/10.1016/j.jaap.2013.10.001

Vahlas, C., Caussat, B., Serp, P., & Angelopoulos, G. N. (2006). Principles and applications of CVD powder technology. *Materials Science and Engineering: R: Reports, 53*(1–2), 1-72. doi:http://dx.doi.org/10.1016/j.mser.2006.05.001

Von Hippel, A. R. (1954). *Dielectric materials and applications ; papers by twenty-two contributors*. Cambridge New York: Technology Press of M.I.T. ; Wiley.

Wang, J., & Sun, X. (2012). Understanding and recent development of carbon coating on LiFePO4 cathode materials for lithium-ion batteries. *Energy & Environmental Science, 5*(1), 5163-5185. doi:10.1039/c1ee01263k

Warnecke, R. (2000). Gasification of biomass: comparison of fixed bed and fluidized bed gasifier. *Biomass and Bioenergy, 18*(6), 489-497. doi:http://dx.doi.org/10.1016/S0961-9534(00)00009-X

Weizhong, Q., Fei, W., Zhanwen, W., Tang, L., Hao, Y., Guohua, L., . . . Xiangyi, D. (2003). Production of carbon nanotubes in a packed bed and a fluidized bed. *Aiche Journal, 49*(3), 619-625. doi:10.1002/aic.690490308

Wiesbrock, F., Hoogenboom, R., & Schubert, U. S. (2004). Microwave-assisted polymer synthesis: State-of-the-art and future perspectives. *Macromolecular Rapid Communications, 25*(20), 1739-1764. doi:10.1002/marc.200400313

Xu, Y., & Yan, X.-T. (2010). Introduction to chemical vapour deposition. *Chemical Vapour Deposition: An Integrated Engineering Design for Advanced Materials*, 1-28.

Yen, Y.-w., Huang, M.-D., & Lin, F.-J. (2008). Synthesize carbon nanotubes by a novel method using chemical vapor deposition-fluidized bed reactor from solid-stated polymers. *Diamond and Related Materials, 17*(4–5), 567-570. doi:http://dx.doi.org/10.1016/j.diamond.2007.12.020

Zhang, M., Tang, J., Mujumdar, A. S., & Wang, S. (2006). Trends in microwave-related drying of fruits and vegetables. *Trends in Food Science & Technology, 17*(10), 524-534. doi:10.1016/j.tifs.2006.04.011

Zinn, S., & Semiatin, S. (1988). *Elements of induction heating: Design, control and applications*. Metals PArk, Ohio: ASM International.

CHAPTER 6 ARTICLE 2: EFFECT OF MICROWAVE HEATING ON THE PERFORMANCE OF CATALYTIC OXIDATION OF N-BUTANE IN A GAS-SOLID FLUIDIZED BED REACTOR

Sepehr Hamzehlouia, Jaber Shabanian, Mohammad Latifi and Jamal Chaouki[1]

[1]Department of Chemical Engineering, Polytechnique Montreal, c.p. 6079, Succ. Centre-ville, Montreal, Quebec, H3C 3A7, Canada

6.1 Abstract

Catalytic oxidation is widely acknowledged as the most promising technology for the conversion of Hydrocarbon Feedstocks to a variety of bulk industrial chemicals. The formation of undesired by-products through secondary gas-phase reactions has been underscored as the limiting step for this technology. In this study, microwave heating is proposed to challenge the evolution of undesired by-products based on the exclusive selective heating mechanism. This task is accomplished through a significantly higher solid (as microwave receptors) temperature compared to the gas phase temperature according to the principles of microwave irradiation approach. In order to highlight the influence of microwave heating on the overall performance of a gas-solid fluidized bed reactor, a simulation study was attempted for a model reactive system. Thus, catalytic oxidation of n-butane over the fluidized vanadium phosphorous oxide catalyst to produce maleic anhydride was selected as the model reaction. The bed hydrodynamics was described by a dynamic two-phase flow model while a kinetic model, adopted from the available literature, represented the reaction feature of the reactor. The original experimental data from a lab-scale microwave-heated fluidized bed reactor and the respective energy balance modeling were employed to describe the temperature distribution between bulk, solids, and gas segments of the simulated bed for the microwave heating scenario. The simulation study indicated that when competitive gas and solid phase reactions are occurring in a gas-solid fluidized bed reactor, the application of microwave selective heating approach can significantly enhance the overall performance of the reaction in comparison with the conventional heating, where solids, bulk, and bed temperatures are identical.

Consequently, the application of microwave heating has been proposed as a promising approach to promote catalytic selective oxidation of hydrocarbons.

6.2 Introduction

Selective oxidation of hydrocarbons is a distinguished method for the production of chemical intermediates to manufacture large-scale commodities and value-added chemicals with distinctive applications in agricultural and pharmaceutical industries (Hughes, Yi-Jun, Jenkins, & McMorn, 2005; R. Sheldon, 2012; R. A. Sheldon, 1991). Traditionally, high selectivity of desired products is strictly achieved at low conversion of the hydrocarbon reactants (A.K. Sinha, S. Seelan, S. Tsubota, & M. Haruta, 2004; Anil K. Sinha, Sindhu Seelan, Susumu Tsubota, & Masatake Haruta, 2004). Such compensation is associated with the evolution of secondary gas-phase reactions, which lead to the production of undesired by-products. Consequently, endeavours have been perceived to restrict the gas-phase secondary reactions to improve the overall yield of the reaction. Earlier, DuPont proposed a circulating fluidized bed reactor to perform selective oxidation of n-butane (n-C_4) over a vanadium phosphorous oxide (VPO) catalyst to produce maleic anhydride (MAN). In this process, the catalytic oxidation reaction and reduction of catalyst are accomplished in two separate reactors while catalyst particles circulate between them. This configuration restricts the secondary gas-phase reactions as the adsorbed oxygen on the surface of regenerated catalyst is merely available for the reaction in the oxidation reactor (Rashmi M. Contractor, 1999; R. M. Contractor et al., 1988). Moreover, development of new catalysts to simultaneously increase the conversion of reactants and selectivity of desired products has been demonstrated in the available literature (J. D. Chen & Sheldon, 1995; Grzybowska, Haber, & Janas, 1977; Hughes et al., 2005; Shimizu et al., 2002).

Implementing catalytic reactions with novel heating methods, namely microwave heating, provides new opportunities for chemical reactions, particularly, selective catalytic oxidation of hydrocarbons. Microwave heating denotes multiple exceptional advantages over conventional heating methods, namely uniform, selective and volumetric heating, instantaneous temperature control, high power density, reduced energy consumption, high reaction selectivity, less heat transfer limitations, process flexibility, and equipment portability (Dominguez et al., 2007; Doucet, Laviolette, Farag, & Chaouki, 2014; Sherif Farag & Chaouki, 2015; S. Farag, Sobhy, Akyel, Doucet, & Chaouki, 2012; Metaxas, 1988; Sobhy & Chaouki, 2010). The imperative feature of the

microwave heating process is highlighted as the distinctive temperature distribution scheme generated inside the heating zone. Prominently, while in conventional heating methods, an external source provides the heat, microwave heating mechanism is driven by the interaction of electromagnetic wave with the dielectric material within the reaction zone, i.e., solid particles, which leads to a higher solid surface temperature compared to the gas. Moreover, due to the insignificant dielectric properties of gases, there will be negligible interaction between the gas phase components and the alternating electromagnetic field. This exceptional mechanism provides an esteemed opportunity for catalytic reactions accordingly. Whereas a higher local temperature on the active sites of catalyst promotes selectivity and yield of catalytic reactions, a lower bulk temperature and negligible microwave interaction of the gaseous components restrict the prospect of the production of undesired gas-phased products. As a critical requisite for this approach, the solid particles (catalyst surface or support material) should project adequate microwave interaction to compensate for the heat generation.

The objective of this study is to explore the impact of heating approach on the overall performance of a gas-solid fluidized bed reactor designated for selective catalytic oxidation of a hydrocarbon. Consequently, an industrial-scale fluidized bed reactor for the catalytic oxidation of n-C_4 over the fluidized VPO catalyst to produce MAN was simulated in the present study. The simulation was performed for both conventional and microwave heating scenarios to study the effect of the heating mechanism on the overall performance of the reactor. Accordingly, the effect of the selective microwave heating mechanism, which supposedly develops a temperature gradient between the solid and gas phases, on the prospect of the reaction was investigated. Due to the restrictions on the measurement of the gas temperature in particular, a predictive model has been developed according to the experimental temperature data, acquired for the solids and bulk in a lab-scale microwave-heated fluidized bed reactor and a general energy balance on the reactor for the estimation of the gas phase temperature for the microwave heating scenario.

6.3 Methodology

Simulation of an industrial-scale catalytic gas-solid fluidized bed reactor was attempted to highlight the influence of the heating method (conventional vs. microwave) on the overall performance of the reactor. Consequently, production of MAN by the partial oxidation of n-C_4 over the VPO catalyst was selected as the reaction model. The simulation was accomplished by application of

pertinent hydrodynamic correlations/models for the dynamic two-phase flow modeling of a bubbling gas-solid fluidized bed reactor as well as a kinetic model to represent the selected reaction model. The hydrodynamic and kinetic models were entirely collected from the available literature.

Understanding the temperature distribution in a gas-solid fluidized bed reactor is critical to evaluate the prospective outcome of the designated reactions. Consequently, the effects of microwave selective heating on the solid surface and bulk temperature profiles were investigated in a lab-scale microwave heating-assisted fluidized bed reactor. Furthermore, a temperature model has been proposed to predict the axial distribution of the gas temperature in the designated heating zone based on the acquired experimental data and an energy balance. The temperature model was further adopted for application in the simulation of the industrial-scale fluidized bed reactor.

6.3.1 Hydrodynamic model

In a real gas-solid fluidized bed that is operating in the bubbling fluidization regime, gas and solids are distributed between the bubble and emulsion phases while the former is rich in gas and the latter is rich in solids (Cui, Mostoufi, & Chaouki, 2000). The dynamic evolutions of the bubble and emulsion phases in the bed can yield the bed voidage to alter between the extreme voidages, i.e., minimum fluidization voidage ε_{mf} and 1 (Li et al., 1996). Therefore, in the case of a catalytic reaction in a bubbling gas-solid fluidized bed reactor, the progress of the reaction in both bubble and emulsion phases must be taken into consideration. In this regard, since these hydrodynamic considerations are embedded into the dynamic two-phase flow modeling of a gas-solid fluidized bed, the hydrodynamics of the simulated fluidized bed reactor is represented by this approach. The general hypotheses associated with the adopted hydrodynamic model are listed as follows:

1) The fluidized bed reactor operates at steady-state condition.
2) The radial concentration gradients within the bed are assumed to be negligible in the mole balance equations.
3) The bubble diameter can change along the bed height.
4) There is a uniform temperature distribution throughout the bed. Hence, the physical properties of fluidizing gas and kinetic constants remain unvaried along the axis.
5) Hydrodynamic parameters measured and/or calculated based on the correlations, which are developed at ambient conditions, are valid under high temperature simulation conditions.

6) The temperature models and correlations developed for a lab-scale microwave heating fluidized bed reactor are extendable to the larger industrial-scale units.
7) The operating temperature is controlled by microwave power, and the generated heat from the oxidation reaction has a minimal impact on the temperature distribution within the reactor.
8) Owing to the negligible wall effects in an industrial-scale fluidized bed (Glicksman & McAndrews, 1985; Krishna, van Baten, & Ellenberger, 1998; Rüdisüli, Schildhauer, Biollaz, & van Ommen, 2012), it is rational to utilize the hydrodynamic correlations, which are developed based on the experimental data collected from the pilot-scale fluidized beds, in the present simulation study.
9) The industrial-scale fluidized bed reactor is equipped with a perforated distributor plate, which yields an initial bubble size identical to what could be obtained by the distributor plate adopted in Liu et al. (Liu, Zhang, Bi, Grace, & Zhu, 2010).

Table 1 reports the general mass balance equations as well as the mass transfer and pertinent hydrodynamic correlations required for solving the state equations. Since the size and physical properties of VPO catalyst are very similar to FCC particles, the physical properties of FCC powders (d_p=70 μm, ρ_p=1673 kg/m^3, ε_{mf}=0.45, U_{mf} at ambient conditions=0.003 m/s, U_c at ambient conditions=0.77 m/s) adopted by Cui *et al.* were applied for the development of local hydrodynamic correlations (Cui et al., 2000). The sample powders behave similarly to Geldart's group A powders at ambient conditions.

Table 6-1: General mass balance equations and mass transfer and hydrodynamic correlations

Mole balance for species i in the emulsion phase	$\frac{dC_{i,e}}{dz} = \frac{r_{i,e}\,(1-f_b)\,(1-\varepsilon_e)\rho_p + K_{be}\,f_b\,(C_{i,b}-C_{i,e})}{U_e\,(1-f_b)}$
Mole balance for species i in the bubble phase	$\frac{dC_{i,b}}{dz} = \frac{r_{i,b}\,(1-\varepsilon_b)\rho_p - K_{be}\,(C_{i,b}-C_{i,e})}{U_b}$
Mean concentration of species i	$C_i = \frac{U_b\,f_b}{U_g}\,C_{i,b} + \frac{U_e\,(1-f_b)}{U_g}\,C_{i,e}$
Bubble to emulsion gas interchange coefficient (K_{be}) (Kunii & Levenspiel, 1991)	$\frac{1}{K_{be}} = \frac{1}{K_{bc}} + \frac{1}{K_{ce}}$ $K_{bc} = 4.5\left(\frac{U_e}{d_b}\right) + 5.85\left(\frac{{D_{AB}}^{0.5}\,g^{0.25}}{{d_b}^{1.25}}\right)$ $K_{ce} = 6.77\left(\frac{0.71\sqrt{g\,d_b}\,D_{AB}\,\varepsilon_e}{{d_b}^3}\right)^{0.5}$
Time-averaged emulsion phase voidage (Cui et al., 2000)	$\varepsilon_e = \varepsilon_{mf} + 0.00061\exp\left(\frac{U_g - U_{mf}}{0.262}\right)$
Time-averaged bubble phase voidage (Cui et al., 2000)	$\varepsilon_b = 0.784 - 0.139\exp\left(-\frac{U_g - U_{mf}}{0.272}\right)$
Superficial gas velocity of emulsion phase (Kunii & Levenspiel, 1991)	$\left(\frac{U_e}{U_{mf}}\right)^{0.7} = \left(\frac{\varepsilon_e}{\varepsilon_{mf}}\right)^3\left(\frac{1-\varepsilon_{mf}}{1-\varepsilon_e}\right)$
Bubble size (Horio & Nonaka, 1987)	$\left(\frac{\sqrt{d_b}-\sqrt{d_{be}}}{\sqrt{d_{b0}}-\sqrt{d_{be}}}\right)^{1-\frac{\gamma_m}{\eta}}\left(\frac{\sqrt{d_b}+\sqrt{\delta'}}{\sqrt{d_{b0}}+\sqrt{\delta'}}\right)^{1+\frac{\gamma_m}{\eta}} = \exp\left(-0.3\,\frac{z}{D_c}\right)$ $d_{be} = \frac{D_c}{4}\left(-\gamma_m + \left({\gamma_m}^2 + \frac{4d_{bm}}{D_c}\right)^{0.5}\right)^2$

$$\delta' = \frac{D_c(\gamma_m+\eta)^2}{4}$$

$$\eta = (\frac{\gamma_m+4d_{bm}}{D_c})^{0.5}$$

$$d_{bm} = 2.59g^{-0.2}((U_g - U_e)A_c)^{0.4}$$

$$\gamma_m = 7.22\times10^{-3}\ \frac{(D_c/g)^{0.5}}{U_{mf}{}^{1.2}}$$

$$d_{b0} = 1.38g^{-0.2}(\frac{(U_g-U_e)A_c}{n_{or}})^{0.4}$$

By taking the last assumption into consideration, the initial bubble size can be calculated as follows:

$$d_{b0} = 1.38g^{-0.2}(\frac{(U_g-U_e)\frac{\pi}{4}0.29^2}{98})^{0.4}$$ (M. Liu et al., 2010)

Bubble rise velocity

$$U_b = \psi(U_g - U_{mf}) + 0.71\upsilon\sqrt{g\ d_b}$$

$$\upsilon = 3.2\ D_c{}^{1/3}$$

$$\psi = \begin{cases} 0.8 & z/D_c < 1.0 \\ 0.8\left(\frac{h}{D_c}\right)^{0.5} & 1.0 \le z/D_c \le 1.56 \\ 1.0 & z/D_c > 1.56 \end{cases}$$

Required correlations and information for calculation of D_{AB} were extracted from Treybal, Poling, and Yaws (Poling, Prausnitz, & O'Connell, 2001; Treybal, 1981; Yaws, 1999).

6.3.2 Kinetic model

As alluded to earlier, when a gas-solid fluidized bed reactor is heated by the microwave heating approach while fluidized particles constitute dielectric material, solid particles can experience significantly higher temperatures than the fluidizing gas. Accordingly, if the catalyst particles function as dielectric material in the bed, the microwave heating approach could ameliorate the reactor performance through (i) enhancing the progress of desired catalytic reactions that happen

on the active sites of catalyst and (ii) decelerating the undesired reactions that potentially happen in the gas phase. By contemplating these points, the sample reactive system must contain desired reaction(s) that happen(s) on the surface of the catalyst whereas the undesired ones may occur in the gas phase. Therefore, the catalytic partial oxidation of n-C_4 to MAN over VPO catalyst was selected to satisfy the aforementioned conditions. Centi *et al.* proposed the following reaction scheme for the partial oxidation of n-butane (Centi, Fornasari, & Trifiro, 1985):

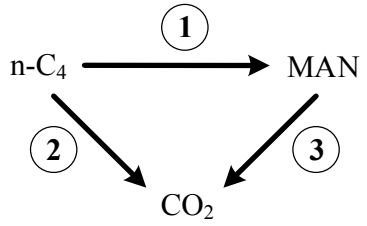

where n-C_4 is the main reactant and MAN is the target product. The reactions involved in this triangular network and the corresponding rate equations are inspired from the kinetic model proposed by Centi *et al.* and are summarized by the following equations (Centi et al., 1985):

$$n - C_4H_{10} + 3.5O_2 \rightarrow C_4H_{10}O_3 + 4H_2O \qquad r_1 = \frac{k_1 K_B C_B {C_O}^{\alpha}}{1 + K_B C_B} \tag{6.1}$$

$$n - C_4H_{10} + 6.5O_2 \rightarrow 4CO_2 + 5H_2O \qquad r_2 = k_2 {C_O}^{\beta} \tag{6.2}$$

$$C_4H_{10}O_3 + 3O_2 \rightarrow 4CO_2 + H_2O \qquad r_3 = k_3 C_{MAN} \left(\frac{{C_O}^{\alpha}}{{C_B}^{\delta}}\right) \tag{6.3}$$

where r_1 and r_2 are respectively the rates of MAN and CO_2 formation from n-C_4, r_3 is the rate of MAN decomposition to CO_2, k_1, k_2, and k_3 are reaction rate constants, and C_B, C_O, and C_{MAN} represent the concentrations of n-C_4, oxygen, and MAN, respectively. The provided reaction network assumes that the complete oxidations of n-C_4 and MAN were the only undesired reactions in the network and the production of carbon monoxide through the partial oxidation of these reactants was negligible. In order to provide additional flexibility to Centi's kinetic model to be

conveniently employed at operating temperatures different from those tested experimentally for kinetic modeling, the reaction rate constants are presented as follows:

$$k_i = k_{i0} \exp\left(-\frac{E_i}{R}\left(\frac{1}{T} - \frac{1}{T_0}\right)\right), \qquad i = 1, 2, 3 \tag{6.4}$$

where k_{i0} and E_i are the pre-exponential factor and activation energy for each reaction rate, R is the gas constant, T is the operating temperature, and T_0 is the reference temperature. The kinetic parameters are summarized in Table 6-2.

Table 6-2: Kinetic parameters

Parameter	Value (units)
k_{10}	3.357×10^{-7} ($mol^{(1-\alpha)}L^{\alpha}/(gr.s)$)
k_{20}	2.001×10^{-7} ($mol^{(1-\beta)}L^{\beta}/(gr.s)$)
k_{30}	4.400×10^{-7} ($mol^{(\delta-\gamma)}L^{(1-\delta+\gamma)}/(gr.s)$)
E_1	45167 (kJ/kmol)
E_2	110158 (kJ/kmol)
E_3	57429 (kJ/kmol)
K_B	2616 (L/mol)
α	0.2298 (-)
β	0.2298 (-)
γ	0.6345 (-)
δ	1.151 (-)
T_0	300 (K)

6.3.3 Temperature Distribution Model

The knowledge of temperature distributions of solids and gaseous components is essential to predict the conversion of the reactants and selectivity of the products in a gas-solid fluidized bed reactor. While materials are exposed to a microwave radiation, the extent of the interaction, exhibited by the heat generation in the molecular scale, is expressed by the dielectric properties. Permittivity is the resistance that is encountered in an electric field imposed on a medium, which further predicts the behavior of a dielectric material exposed to an alternating electric field, derived by the dielectric constant and the loss factor. Dielectric constant is the ability of the dielectric material to conserve electrical energy while the loss factor demonstrates the potential of the dielectric material to dissipate microwave energy in the context of heat. Furthermore, the loss factor to the dielectric constant ratio, referred as the loss tangent, signifies the amount of absorbed microwave energy converted to the thermal energy by the dielectric material. The presence of a temperature distribution in solids, bulk, and gas is associated with the selective heating mechanism of microwave heating. Due to their physical structure, most materials, particularly gaseous components, do not project satisfactory microwave interaction according to the insignificant dielectric properties (Metaxas, 1988). Consequently, microwave receptors in the form of solid particles with exceptional dielectric properties, are deployed as bed material to mitigate the heat generation inside a gas-solid fluidized bed reactor.

The temperature distribution of the solid particles and the bed bulk can be obtained with the assistance of radiometry and thermometry methods, respectively. However, the discrete measurement of gas temperature within the reactor is exceptionally complicated due to the physical properties of the gaseous components. Consequently, in this study, the gas temperature distribution is assessed by driving an energy balance on the fluidized bed reactor together with the application of experimental data attained by the solids and bulk temperature profile measurements in a lab-scale microwave heating-assisted fluidized bed reactor.

6.3.3.1 Solid Particles and Bulk Temperature Measurements

In 2017, Hamzehlouia *et al.* performed carbon coating of silica sand particles with an induction heating-assisted fluidized bed chemical vapor deposition (FBCVD) process (Hamzehlouia, Latifi,

& Chaouki, 2017; Latifi & Chaouki, 2015). The developed carbon-coated sand (C-SiO_2) particles projected substantial dielectric properties and microwave heating characteristics and, hence, were further recommended for application as microwave receptor/catalyst support in catalytic gas-solid fluidized bed reactions. In the present study, C-SiO_2 particles (ρ_p=2650 kg/m^3, d_p= 212-250 μm, carbon composition = 0.25 wt% and coating thickness = 72±7 nm) were employed as microwave receptors to perform solids and bulk temperature measurements in a lab-scaled microwave heating-assisted fluidized bed reactor. Due to the enormous energy requirement of the carbon precursor decomposition process, the reaction was performed at 900^{o}C to achieve a satisfactory carbon coating layer. It should be noted that during the FBCVD process, agglomeration/defluidization incidents with smaller size SiO_2 particles due to a discernible increase in the level of interparticle forces at elevated operating temperatures were observed. Consequently, SiO_2 with a size range of 212-250 μm particles, which belongs to Geldart group B powders (refer to the fluidization behavior at ambient conditions), were employed to bypass the challenge.

Experimental trials were carried out in a transparent fused quartz tube with a 20-cm height and 2.24-cm ID. The selection of the reactor material was associated with the negligible dielectric properties of quartz, minimizing the microwave heating effect from the reactor body. The reactor was further enclosed in a copper/bras tubular electromagnetic shield to restrict microwave leakage to the operating environment and comply with the safety regulations. The receptors were loaded and unloaded to the reactor throughout a removable copper compression cap at the top section of the reactor. Nitrogen (99.99% purity, Canadian Air Liquid) was employed as the fluidizing gas and was introduced to the reactor through a quartz fritted disk distributor with an average pore size of 15 – 40 μm. A single–mode 2.5 KW and 2.45 GHz frequency water-cooled Genesys system microwave generator was deployed to provide the compulsory heating power. The generated microwave was transferred from the magnetron to the cavity using triangular bras waveguides. The microwave heating apparatus schematic diagram is presented in Figure 6-1.

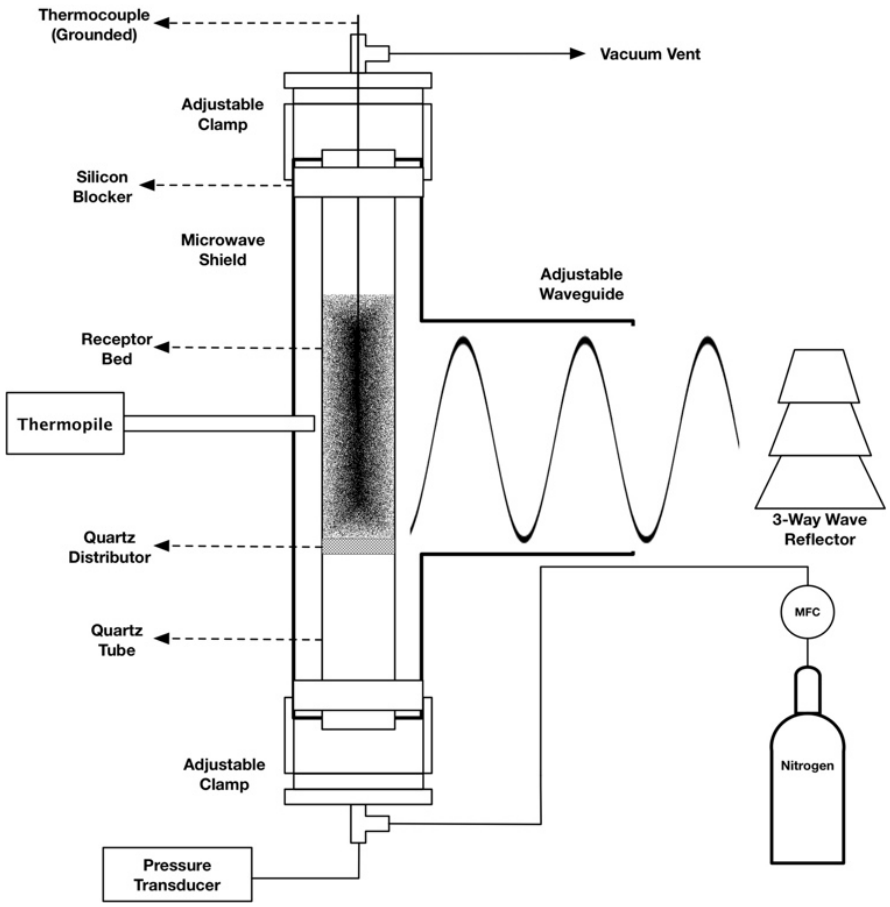

Figure 6-1: Schematic diagram of the microwave heating-assisted fluidized bed apparatus

For each experiment, 30 gr of the receptor was loaded into the reactor to yield a fixed bed height of approximately 6 cm. Afterwards, the bed was fluidized at the ambient temperature with nitrogen at superficial gas velocity of 10 cm/s maintained by a Bronkhorst F-201CV mass flow controller. In order to sustain bubbling fluidization regime, the superficial velocity of the fluidizing gas was persistently adjusted based on the transitorily bulk temperature value by the mass flow controller. Thereafter, the designated particle surface temperature was instructed to the microwave power generator with a computer connection through a Labview software interface. Subsequently, the microwave controller adjusted the dissipated power based on the solid temperature readings provided by a thermopile, a radiometry light-capturing temperature measurement device.

The concept of thermopile temperature measurement is based on the radiometry from the thermal irradiation emissions of solid components exposed to a heating resource. Thermopile converts the radiation signals by a light-capturing technique to an alternating voltage based on the thermoelectric effect. The voltage is further calibrated to correlate a temperature reading for the

solid surface measurement based on the captured signals. The thermopile assumes gaseous components and quartz material as transparent mediums and is only capable to acquire radiation signals from the receptor particles surface. Consequently, the thermopile temperature measurement method was employed for measuring the temperature of the solid particles surface, referred as the solid phase. Furthermore, a K type thermocouple located inside the heating bed was adopted to measure the temperature of the bulk, a contributive temperature of gas and solids simultaneously. The thermocouple was electrically grounded to eliminate the risk of thermocouple effect due to the interaction with the electromagnetic field (Pert et al., 2001). The axial bulk temperature profile was subsequently measured with the assistance of the thermocouple. For each experiment, whilst the reactor reached the thermal equilibrium state, the bed temperature was recorded prior to reaching thermal equilibrium to determine the bed temperature profile.

Multiple experiments were attempted at various superficial velocities (3.4 cm/s, 6.7 cm/s and 10 cm/s) and alternating solid particle surface temperatures (500, 600 and 700^{o}C) to establish the effect of the operating parameters on the temperature distributions of the solids and bulk in the microwave heated fluidized bed reactor. Furthermore, the temperature of the gas at the entrance of the reactor and at the wall were continuously monitored and recorded using K type thermocouples.

Table 3 summarizes the dielectric properties of materials and components adopted in the present study. It has been highlighted that the dielectric properties are significantly subjugated to the operating frequency and temperature (Tinga & Nelson, 1973). According to the reported dielectric properties value, the silica sand substrate particles and quartz reactor surface would not participate in the microwave heating mechanism due to the lack of significant dielectric properties. Moreover, the fluidizing gas in the system, i.e., nitrogen, would project negligible microwave interaction due to the unsatisfactory dielectric properties, similar to any other gaseous component. Consequently, the carbon coating layer deposited on the silica sand substrates has been regarded as the individual dielectric component, which demonstrates intriguing interaction with microwave in order to provide heat for the process.

Table 6-3: Dielectric properties of the employed material at ambient temperature and 2.45 GHz frequency

Material	Dielectric Constant (ε')	Loss Factor (ε'')	$tan\delta$
Silica Sand	3.066 (Ma et al., 1997)	0.215 (Ma et al., 1997)	0.070 (Ma et al., 1997)
Carbon	7 (Vos, Mosman, Zhang, Poels, & Bliek, 2003)	2 (Vos et al., 2003)	0.285
C – SiO_2	13.7*	6*	0.437
Nitrogen	1.00058 (Uhlig & Keyes, 1933)	-	-
Fused Quartz	4.0 (Gupta & Wong, 2007)	0.001(Gupta & Wong, 2007)	0.00025

* Based on measurements reported in this study.

Figure 6-2 represents the temperature profile of the solid surfaces and bulk at a constant superficial gas velocity of 6.7 cm/s and operating temperatures of 500, 600, and 700^{o}C. Due to the high mixing quality and the automatic power control, the temperature of the solid surfaces was assumed stationary through each individual experimental operation while the particle sizes (212-250 μm) were evidently below the microwave penetration depth of 26 mm at 2.45 MHz frequency. Furthermore, the bulk temperature was referred to as the contributive temperature of the emulsion phase and the bubble phase within the heating zone of the fluidized bed reactor.

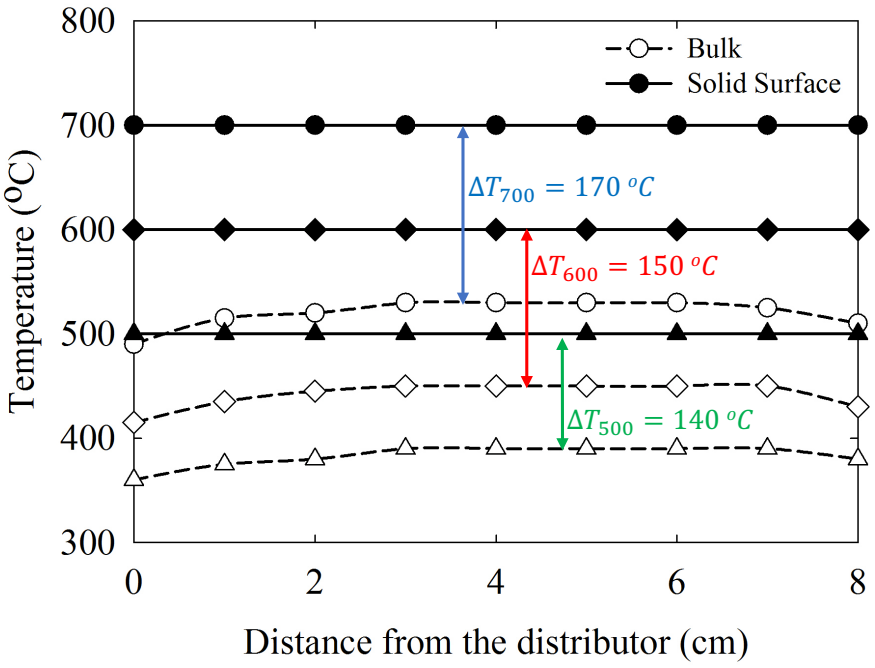

Figure 6-2: Effect of the operating temperature on the solids and bulk temperature in the C-SiO_2 receptor bed at U_g= 6.7 cm/s

Figure 6-2 shows that the bulk temperature right above the distributor plate is discernibly influenced by the low gas temperature at the entrance of the reactor but rises and gradually stabilizes upon further intrusion to the bed due to the presence of hot solids within the bed. The bulk temperature drops slightly at the top of the bed due to the lack of the receptor particles and the dominance of the lower gas temperature. The figure also demonstrates that the difference between the solid surface temperature and the bulk temperature significantly expanded upon increasing the operating temperature. The temperature gradient between the solids and bulk was observed as 140, 150, and 170°C at solid surface temperatures of 500, 600, and 700°C, respectively. The observation can be attributed to the negligible dielectric properties and relatively low residence time of the fluidizing gas, which prevents it from approaching the solid surface temperature. Furthermore, the bulk temperature gradient alon the axes was solely 15°C for all solid surface temperatures of 500, 600, and 700°C. The relatively minor bulk temperature gradient along the axis further verifies the appropriate quality of solids mixing within the bed.

The effect of the superficial gas velocity on the particle surface and bulk temperature distribution within the fluidized bed was additionally investigated. The experiments were conducted at three different superficial gas velocities of 3.4, 6.7 and 10 cm/s at a fixed operating temperature of 700°C. Figure 6-3 illustrates the effect of the gas velocity on the temperature distribution within the bed. The figure demonstrates that the temperature gradient between the solid surface and the bulk escalates by increasing the superficial gas velocity. Moreover, through scrutinizing Figure 6-2 and Figure 6-3, one can infer that the effect of the solid surface temperature on the temperature gradient between solids and bulk is more dominant in comparison with the superficial gas velocity.

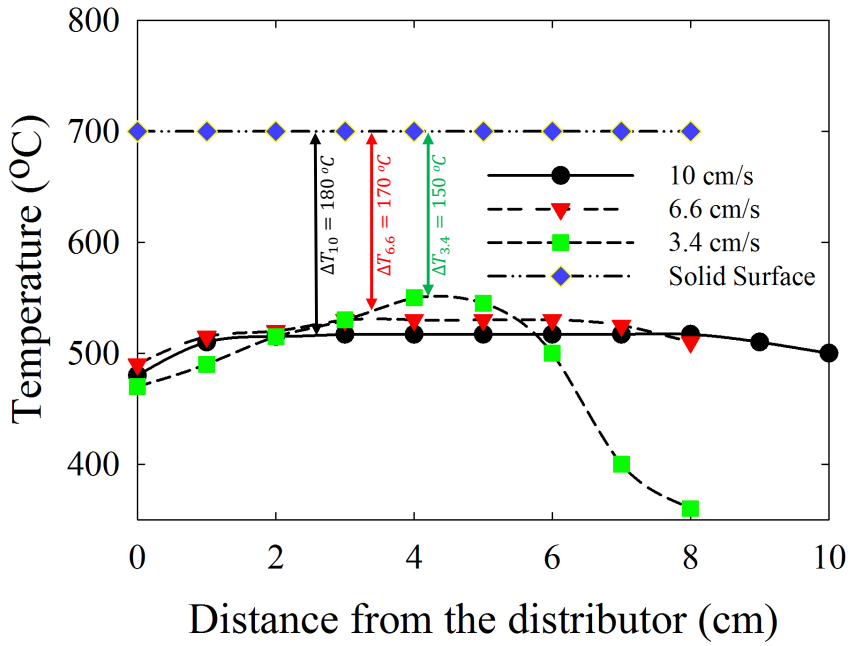

Figure 6-3: Effect of superficial gas velocity on the solids and bulk temperature distribution in the C-SiO_2 receptor bed at solid surface temperature of 700°C

The evident temperature gradient reported in Figure 6-3 is associated with the negligible dielectric properties and low residence time of the fluidizing gas compared to the solid particles, while the effect enhances by introducing a higher volume of gas by elevating the superficial gas velocity. Moreover, the convective heat transfer in the system is marginally enhanced by increasing the fluidization velocity from 3.4 cm/s to 10 cm/s, which manipulated the convective heat transfer coefficient according to the available literature (Kim, Ahn, Kim, & Hyun Lee, 2003). Furthermore, the apparent decline in the bulk temperature at superficial gas velocity of 3.4 cm/s and at axial levels higher than 6 cm is associated with the lower bed expansion owing to the operation close to

the minimum fluidization velocity. Due to the low fluidization velocity, the bed expansion is particularly lower and, consequently, there is a lack of microwave receptor particles at the axial levels above 6 cm. This phenomenon is remedied by increasing the superficial gas velocity.

6.3.3.2 Development of the Temperature Distribution Model

Due to the restrictions associated with the direct gas temperature measurement in the lab-scale microwave heating-assisted fluidized bed reactor, a model was developed, employing the experimental temperature data and an energy balance to estimate the corresponding values. Accordingly, the energy balance equation was developed for a discreet element of the bed along the axix with the following assumptions:

1) The temperature distribution through the bed exclusively evolves along the Z direction. All radial and angular variations of the energy transfer terms and temperature gradient have been subsequently neglected due to small dimensions of the adopted reactor.
2) The reactor operated in steady state condition. Hence, the time dependency of the variables is neglected, and all time dependent terms of the energy balance equation have been disregarded.
3) The incoming energy terms exposed to the designated element have been considered as energy transfer due to convective movement of the fluidizing gas (all shown with the subscript *g*), energy transfer due to convective movement of the particles (all shown with the subscript *p*), and energy transfer due to the microwave heating (shown with the subscript *mw*).
4) The outgoing energy terms from the designated element have been considered as energy transfer due to convective movement of the fluidizing gas and, energy transfer due to convective movement of the particles, heat loss from the wall for gas (all shown with the subscript *Lg*), and heat loss from the wall for particles (all shown with the subscript *Lp*).
5) All other forms of energy generation and consumption, namely, pressure and viscous terms, have been thoroughly neglected.
6) Due to the uniform distribution of the gas and solid temperature along the bed, the properties of gas and the bed particles, namely, density, viscosity, specific heat capacity, superficial gas velocity and bed voidage have been assumed stationary across the heating zone.

7) Due to the insufficient dielectric properties, the interaction between the gaseous components and the microwave has been thoroughly neglected. Consequently, the heat generated within the receptor particles is the only source of energy transition along the bed. The heat of reaction was neglected due to the absence of any reaction in the reactor.
8) The effect of heat transfer associated with radiation has been neglected since the model was developed for temperatures below 700^{o}C.

Since the temperature distributions of the fluidizing gas and solids were merely evolving along Z direction, an element of the bed with the length of ΔZ has been selected. Implementing the energy balance on the selected control volume gives:

$$Q_g\big|_z + Q_p\big|_z + Q_{mw} - Q_g\big|_{z+\Delta z} - Q_p\big|_{z+\Delta z} - Q_{Lg} - Q_{Lp} = 0 \tag{6.5}$$

whereas each equation term is expressed discreetly in Table 6-4. Replacing the terms with corresponding expressions and rearranging gives:

$$\frac{dT_g}{dz} + \frac{\rho_p U_p c_{pp}}{(\rho_g U_g)_{in} c_{pg}} \frac{dT_p}{dz} = \frac{(1-\varepsilon)\rho_p}{(\rho_g U_g)_{in} c_{pg}} q_{mw} - \frac{4\varepsilon h_{gw}}{D(\rho_g U_g)_{in} c_{pg}} (T_g - T_w) - \frac{4(1-\varepsilon) h_{pw}}{D(\rho_g U_g)_{in} c_{pg}} (T_p - T_w) \tag{6.6}$$

It is underlined that although the superficial velocity and density of the fluidizing gas transform with temperature fluctuations, the aggregate mass flow of the gas is constant along the entire bed according to the conservation of mass law. Thus, $\rho_g U_g$ is constant throughout the bed and is equal to the designated value at the entrance of the imaginary control volume (marked by the subscript *in*).

Table 6-4: The definition and expressions of energy balance terms

Term	Description	Mathematical Expression
Q_g	Heat transfer inside the gas phase	$\pi\frac{D^2}{4}\rho_g U_g c_{p_g} T_g$
Q_p	Heat transfer inside the solid phase	$\pi\frac{D^2}{4}\rho_p U_p c_{p_p} T_p$
Q_{Lg}	Convective heat transfer by the gas phase	$(\pi D\Delta z)\varepsilon h_{gw}(T_g - T_w)$
Q_{Lp}	Convective heat transfer by the solid phase	$(\pi D\Delta z)(1-\varepsilon)h_{pw}(T_p - T_w)$
Q_{mw}	Microwave heat transfer	$q_{mw}\left(\pi\frac{D^2}{4}\Delta z\right)(1-\varepsilon)\rho_p$

Moreover, the dependence of the heat capacity of the components on the operating temperature is neglected in Eq. (6.1). Since the model is developed for a bubbling fluidize bed, the temperature gradient of solids throughout the bed has been neglected due to the high quality of the solids mixing within the bed. Furthermore, the net superficial velocity of the solids particles is punctually negligible. Further simplification and rearranging for T_g and integration gives:

$$\frac{1}{a}\ln\frac{T_g + (\frac{b}{a} - T_w)}{T_{g0} + (\frac{b}{a} - T_w)} = z - z_0 \tag{6.7}$$

Where;

$$a = -\frac{4\varepsilon h_{gw}}{D\left(\rho_g U_g\right)_{in} c_{pg}} \tag{6.8}$$

$$b = \frac{\left[\rho_p q_{mw} - \frac{4h_{pw}(T_p - T_w)}{D}\right](1-\varepsilon)}{\left(\rho_g U_g\right)_{in} c_{pg}} \tag{6.9}$$

In order to resolve Eq. (6.7) to estimate the gas temperature distribution according to the length of the bed, the knowledge of the gas and solid convective heat transfer coefficients, h_{gw} and h_{pw}, is essential. In general, the overall time–averaged bed–surface heat transfer coefficient can be considered as the summation of particulate heat transfer and gas heat transfer coefficients in the absence of radiation heat transfer and is expressed as (Knowlton, 1999):

$$h = h_{pw} + h_{gw} \tag{6.10}$$

The solid particles in the fluidized bed project significantly higher specific heat capacity compared to the gas (volumetric basis). In addition, since the solids are continuously circulating within the fluidized bed, they are majorly accountable for the heat transfer throughout the bed. The recommendation is to use Zabrodskiĭ correlation for h_{pw} (max) for Group B powders, whereas (Zabrodskiĭ, 1966):

$$h_{pw}(max) = 35.8 \frac{{k_g}^{0.6} {\rho_p}^{0.2}}{{d_p}^{0.36}} \tag{6.11}$$

Unfortunately, the lack of gas convective heat transfer coefficient correlations has been evidenced in the literature. However, in general, the total heat transfer coefficient for a bubbling gas-solid fluidized bed reactor is approximately estimated as 450 W/m^{2}K, thus (J. C. Chen, Grace, & Golriz, 2005). Thus, substituting for h and h_{pw} in Eq. (6.10), the value for h_{gw}will be calculated accordingly.

Table 6-5 shows a summary of the physical and hydrodynamic properties of the bed and fluidizing material required to estimate the gas temperature distribution based on the associated temperature measurements.

Table 6-5: Physical and hydrodynamic properties of the solid and gas phase material for the temperature distribution calculations.

Parameter	Value (Unit)
ID	0.0224 (m)
H_0	0.08 (m)
P	101.325 (kPa)
C-SiO_2 Receptor (Bed Particles)	
d_p	230 (μm)
ρ_p	2650 (kg/m^3)
c_{p_p}	705 (J/kgK)
ε	0.44
Nitrogen (Fluidizing Gas)	
ρ_g	1.2 (kg/m^3)
c_{p_g}	1041 (J/kgK)
U_g	0.034 0.067 0.1 (m/s)
T_w	568.15 563.15 558.15 (K)
T_{g0}	453.15 427.15 416.15 (K)
K_g	0.024 (W/mK)

Owing to the high quality of solids mixing in the bubbling fluidization regime, which was justified by the minor temperature gradient along the bed, the value of h_{pw} was anticipated equivalent to the maximum particulate heat transfer coefficient limit, h_{pw} (max). The microwave heating contribution, q_{mw} is expressed as the total microwave absorbed per unit mass of the receptor particles during the temperature measurements, which was measured as 4870 J/kg using the real-time power measurement system. Consequently, the gas temperature distribution alongside the

receptor bed at the particle temperature of 700°C and superficial gas velocities of 3.4, 6.7 and 10 cm/s has been predicted, where the results are demonstrated in Figure 6-4. It revealed that increasing the superficial gas velocity decreases the gas temperature due to the reduction of the residence time of the fluidizing gas within the reactor and negligible dielectric properties.

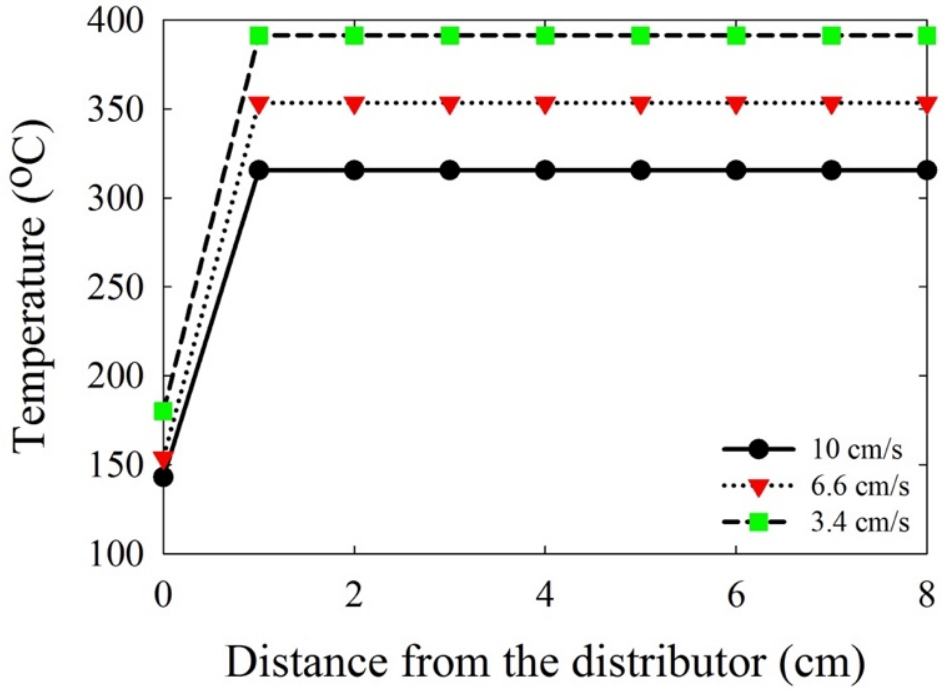

Figure 6-4: Effect of superficial gas velocity on the estimated gas temperature distribution in the C-SiO_2 receptor bed at 700°C operating temperature

By the application of the experimental data obtained through the bulk and solids temperature measurements together with the gas temperature estimation, the temperature distribution of solids, bulk, and fluidizing gas were investigated at particle temperature of 700°C and superficial gas velocities of 3.4, 6.7 and 10 cm/s. Figure 6-5 represents the corresponding experimental and model results at the superficial gas velocity of 10 cm/s as an instance of the investigation. It can be inferred that by increasing the superficial gas velocity at a fixed solid surface temperature, the gradient between solid surface and bulk temperatures and gas and bulk temperatures significantly enhances. The outcome is justified by increasing the concentration and decreasing the residence time of the fluidizing gas within the reactor.

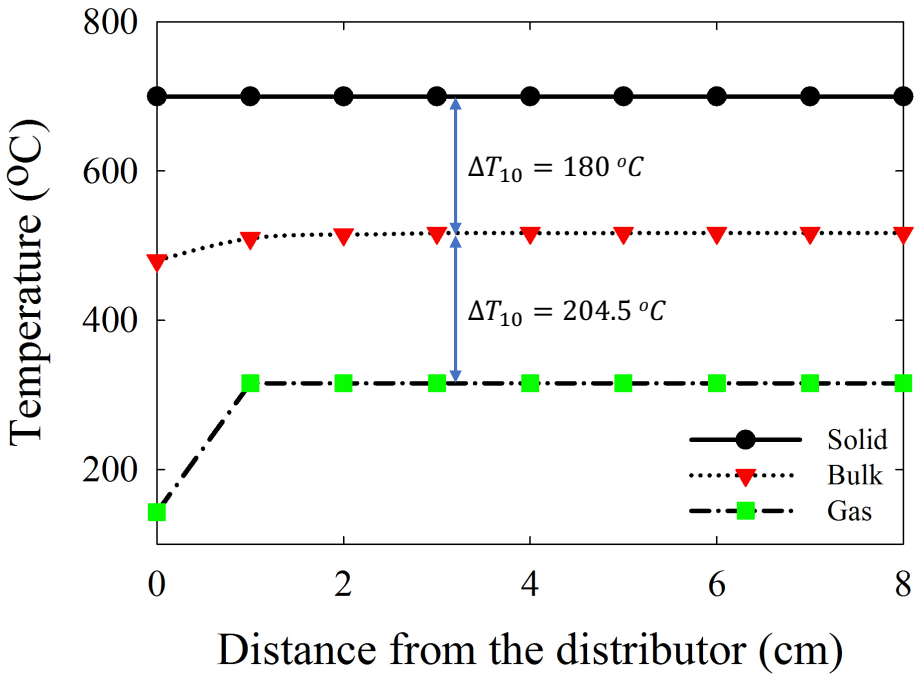

Figure 6-5: Temperature distribution of the solids, bulk and gas in the C-SiO_2 receptor bed at 700°C operating temperature and $u_g = 10\,\frac{cm}{s}$

Ultimately, contemplating the experimental data obtained by the temperature measurement and with the support of the developed model, two correlations have been proposed by means of the least squares method. They can be adopted to estimate the bulk and gas temperatures according to the gas and particle physical properties and the hydrodynamic characteristics of the bed, given as:

$$T_b = T_p - 126T_p^{0.04/\tau_s} \tag{6.12}$$

$$T_b = 0.54(1-\varepsilon)T_s \frac{\rho_p C_{p_p}}{\varepsilon\rho_g C_{p_g} + (1-\varepsilon)\rho_p C_{p_p}} + 834\varepsilon T_g \frac{\rho_g C_{p_g}}{\varepsilon\rho_g C_{p_g} + (1-\varepsilon)\rho_p C_{p_p}} \tag{6.13}$$

Figure 6-6 is a pictorial representation of the comparative predictability performance of Eq. (6.12) and (6.13) versus the experimental data of the bulk temperature. The developed correlations are further employed to estimate the gas temperature through the kinetic investigations of the present study in an industrial-scale fluidized bed reactor. The average error of Eq. (6.12) and (6.13) are 2.1% and 0.2%, respectively.

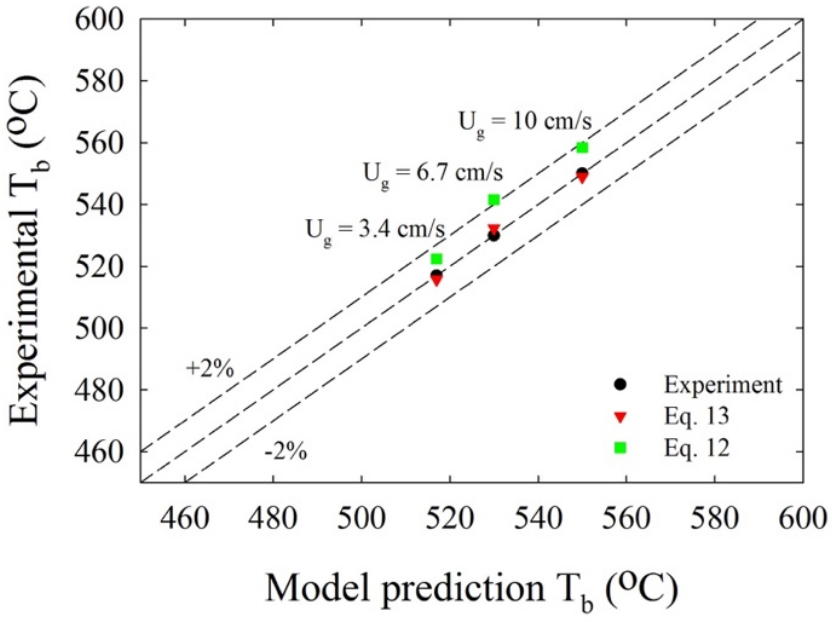

Figure 6-6: Comparative demonstration of the experimental values and the estimations for the bulk temperature by Eq. 6.12 and 6.13 at superficial gas velocities of 3.4, 6.7 and 10 cm/s

6.4 Reactor Simulation Results and Discussion

It is worth noting that the application of microwave heating in a catalytic gas-solid fluidized bed reactor, where particles contain dielectric material, would not only influence the reactor performance through the reported thermal effect, but also impact the reaction rate at the active of the catalyst particles. It has been reported that the pre-exponential constant value increases for the reactions which are influenced by the microwave heating mechanism (Sherif Farag & 2015; Temur Ergan & Bayramoğlu, 2011; Yadav & Borkar, 2006). The changes are associated with the agitation of the molecules exposed to microwave radiation, which increases the chance molecular-scale collision, whereas the values of pre-exponential factor are associated with the collision frequency, which utterly increase under a microwave heating mechanism. Therefore, in order to highlight the effect of microwave heating on the performance of a catalytic gas-solid fluidized bed reactor in comparison with the conventional heating, the fluidized bed reactor simulation was attempted for three cases: (i) conventional heating, where solids, bulk, and gas temperatures are identical; (ii) microwave heating, where solids, bulk, and gas temperatures are

different from each other and can be defined with the assistance of the developed correlations in section (2.3.2); the reaction rate constant of catalytic reaction, i.e., formation of MAN from n-C_4, is considered to be identical to the first scenario. Hence, the thermal effect of microwave heating is solely considered in this case; (iii) the fluidized bed reactor is influenced by both thermal and kinetic effects of microwave heating. For the last simulation scenario, it is postulated that the reaction rate constant of formation of MAN from n-C_4 increases tenfold upon the application of microwave heating, i.e., $k_{1,mw}$=$10k_{1,conv}$. Summary of specifications and operating conditions exploited for the simulation study are provided in Table 6-6. Also,

Table 6-7 reports the overall reaction rates of all species that are involved in the reaction network.

Table 6-6: Operating conditions for the simulation

Parameter	Value (unit)
D_c	2 (m)
H	6 (m)
d_p	70 (μm)
ρ_p	1673 (kg/m^3)
ε_{mf} (at ambient conditions)	0.45 (-)
U_{mf} (at ambient conditions)	0.003 (m/s)
T	350 (^{o}C)
P	101.325 (kPa)
U_g	0.1 – 0.6 (m/s)
y_{B0}	5 (% v/v)

Table 6-7: Overall reaction rates

Species i	r_i
n-C_4	$-r_1 - r_2$
O_2	$-3.5r_1 - 6.5r_2 - 3r_3$
MAN	$r_1 - r_3$
CO_2	$4r_2 + 4r_3$
H_2O	$4r_1 + 5r_2 + r_3$

The solids surface, bulk, and gas temperature distributions were evaluated with the assistance of the developed correlations, i.e., Eq. (6.12) and (6.13). The effect of superficial gas velocity on the evolutions of solids surface, bed bulk, and fluidizing gas temperatures is demonstrated in Figure 6-7. While a uniform temperature distribution was signified for the reaction system under conventional heating method, a considerable temperature gradient was present between the solids, bulk, and gas upon exposure to a microwave irradiation. Figure 6-7 shows that temperature gradients between solids and bulk as well as bulk and gas increased by increasing the superficial gas velocity, which are comparable to the experimental data reported in section (6.3.3).

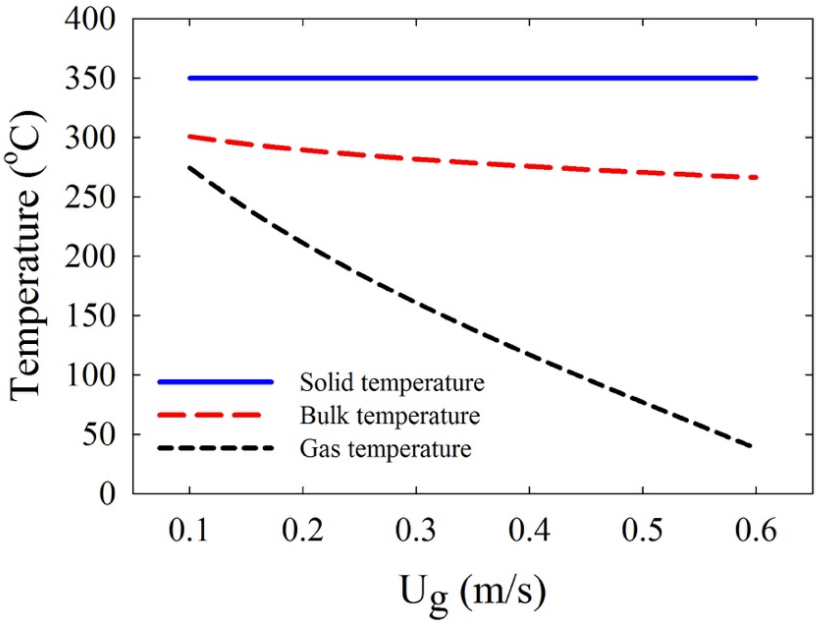

Figure 6-7: The effect of superficial gas velocity on the temperature distribution of solids, bulk, and gas for the microwave heating scenario

The simulation results for the explored scenarios are compared in terms of the conversion of n-C_4, $X = (C_{B0} - C_B)/C_{B0}$, the selectivity of MAN, $S = C_{MAN}/(C_{B0} - C_B)$, and the yield of MAN produced, $Y = C_{MAN}/C_{B0}$, where C_{B0} is the concentration of n-C_4 fed to the reactor. Figure 6-8 illustrates the evolutions of these parameters for the simulated scenarios over a wide range of superficial gas velocities, 0.1 – 0.6 m/s, in the bubbling fluidization regime. It shows that X decreases with U_g in all cases. This observation can be mainly attributed to less residence time of the reactants at higher superficial gas velocities in the reactor. Moreover, since emulsion phase fraction is discernibly high in a gas-solid fluidized bed at low superficial gas velocities and the emulsion phase is rich in solids/catalysts, the reactions can progress faster under these conditions and, hence, a higher conversion can be achieved. However, since the fluidizing gas is more prone to pass through the bed in the bubble phase, which is less concentrated in catalysts, upon increasing U_g, a lower reaction rate can be experienced, which yields a decrease in X. Contrary to the drift that was observed for X vs. U_g, Figure 6-8 shows that the selectivity of MAN increases with U_g for all scenarios. This drift can be explained by the kinetics of MAN oxidation (Eq. (6.3)). According to Eq. (6.3), the rate of oxidation of MAN is inversely proportional to C_B. Since the conversion of

n-C_4 decreases with U_g, a higher C_B can be attained at higher U_g and, hence, the rate of oxidation of MAN decelerates. Consequently, the selectivity of MAN augments with U_g.

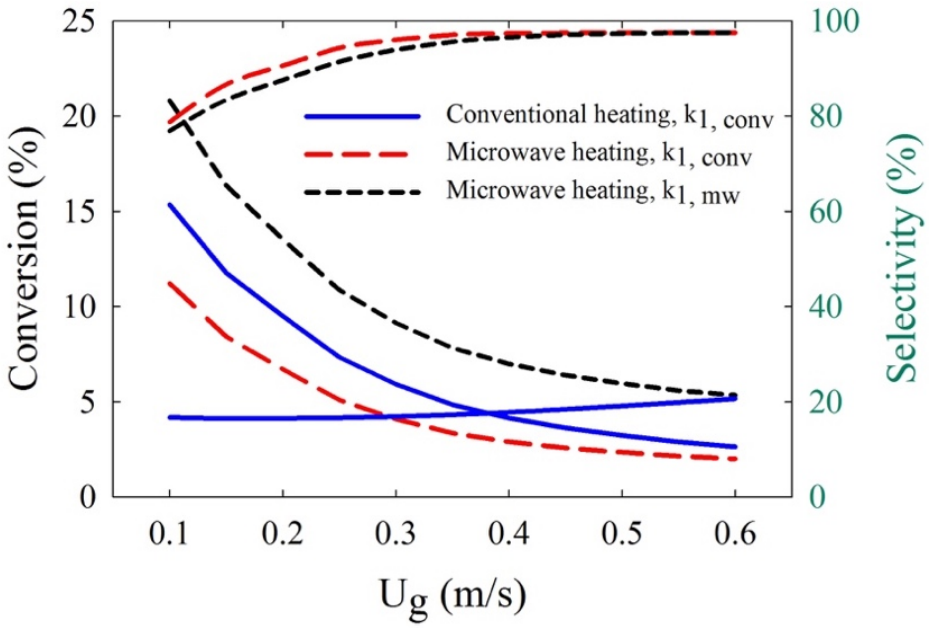

Figure 6-8: Prediction of performance of the fluidized bed reactor for all three scenarios at different superficial gas velocities.

Microwave heating mechanism exceptionally improves the selectivity of MAN, whereas the selectivity value escalates from a maximum of 20% in the case of the conventional heating to a substantial maximum of 97%. Meanwhile, the conversion of n-C_4 under microwave heating (2nd scenario) originally declines for the microwave heating scenario to a maximum of 12%, below the maximum value of 15% reported for the conventional heating mechanism. The decline is associated with the restriction of the reaction expressed by Eqs. (6.2) and (6.3) due to minimizing the gas phase reactions. However, when the effect of the microwave heating on the pre-exponential factor is acknowledged, the n-C_4 conversion exceeds the conventional heating range to a maximum of approximately 20%. Furthermore, comparing the performance of the reactor based on the yield of MAN produced reveals a typical increase of 275% and 750% for the second and third scenarios, respectively, in comparison with the conventional heating (first) scenario over the range of simulated gas velocities. This difference can be directly attributed to the thermal and simultaneous thermal and kinetic effects of the microwave heating approach on the

performance of a catalytic oxidation fluidized bed reactor. Accordingly, the difference proves the promising capability of microwave heating in ameliorating the progress of selective catalytic oxidation reactions toward the production of desired products.

Ultimately, the distribution of conversion of n-C_4 and selectivity of MAN for conventional and microwave heating mechanisms have been investigated and demonstrated in Figure 6-9. In general, when a fluidized bed reactor is heated through the conventional heating approach, the conversion of reactants and selectivity of desired products are inversely correlated, e.g., a higher selectivity of desired products is achieved at a lower conversion of the reactants. Although a similar observation was exhibited for the case of conventional heating in the simulation results, the application of the microwave heating approach significantly enhanced the selectivity of MAN production for the identical conversion range. Nonetheless, when considering the effect of the microwave heating on the pre-exponential factor, the concluded n-C_4 conversion values exceeded the conventional heating results. Thus, it can be underlined that if the application of microwave heating is coupled with a high-performance catalyst or development of novel processes to enhance the conversion of n-C_4, the reactor performance range will shift toward the superior range, i.e., conversion and selectivity are simultaneously at or close to 100%. The achievement of this goal will be particularly significant for the industrial sector.

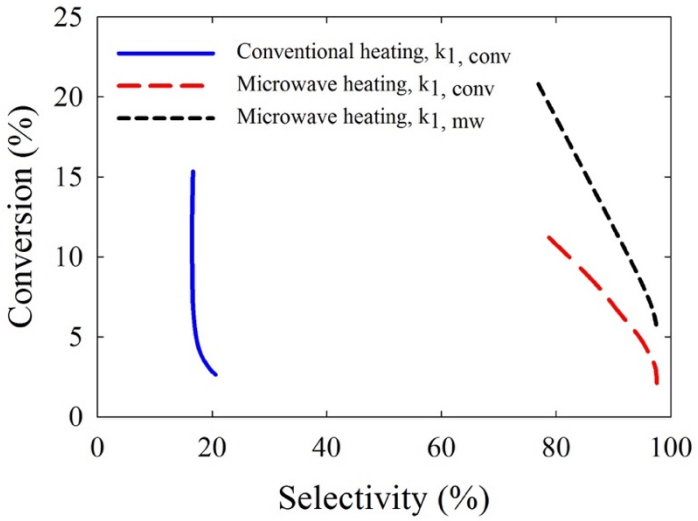

Figure 6-9: The distribution of n-C_4 conversion and MAN selectivity for conventional and microwave heating mechanisms in the range of superficial gas velocities 0.1 – 0.6 m/s

6.5 Conclusion

In this study, the effect of conventional and microwave heating mechanisms on the performance of the selective oxidation of n-butane over the fluidized vanadium phosphorous oxide catalyst to produce maleic anhydride, in an industrial-scale fluidized bed reactor was simulated. The reaction was proposed as a model for selective oxidation of hydrocarbons in general. The simulation study intended to shed light on the effectiveness of applying microwave heating approach in decreasing the formation of secondary gas-phase side products and their destructive effect on the selectivity of desired products as the major productivity issue of the selective oxidation reactions. However, based on the exclusive microwave heating mechanism, the dielectric components, the catalyst or the support material, project superior interaction compared to the gaseous components. The established temperature gradient between the solid and gas phase restricts the prosper of the secondary gas-phase reactions, correspondingly. Due to the inability of direct gas temperature measurement, correlations were proposed, with the assistance of solid and bulk temperature measurements in a lab-scale microwave-heated fluidized bed reactor and a general energy balance. The correlations were adopted to describe the solids surface, bulk, and gas temperature distributions in the simulated bed for the microwave heating scenario. The simulation results showed a significant increase for the selectivity of MAN in a wide range of superficial gas velocities in the bubbling fluidization regime when the bed was simulated under the microwave heating condition. Moreover, it was established that the conversion of n-C_4 was superior during the microwave heating-assisted reaction in case the effect of the heating mechanism on the kinetic parameters, namely, pre-exponential factor, was contemplated. Consequently, it was proposed that by optimizing the performance of the catalyst or developing novel processes, the microwave heating mechanism can enhance the productivity of the selective oxidation reactions to a conversion and selectivity simultaneously, which is substantial for the industrial applications. Finally, deliberating the distinctive thermal behavior of the catalytic and gas-phase reactions, microwave heating mechanism can be adopted to identify the mechanism of the catalytic gas-solid reactions by distinguishing between the solid-phase and gas-phase reactions in the reaction system.

6.6 Nomenclature

6.6.1 Acronyms

FBCVD	Fluidized bed chemical vapour deposition
MAN	Maleic anhydride
n-C_4	Normal butane
PEA	Poly ethyl acrylate
VPO	Vanadium phosphorus oxide
wt%	Total weight percentage

6.6.2 Symbols

A_c	Bed cross-sectional area (m^2)
Ar	Archimedes number
c_{p_g}	Gas specific heat capacity (J/kgK)
c_{p_p}	Particles specific heat capacity (J/kgK)
C_B	Concentration of n-butane (mol/L)
C_{B0}	Concentration of n-butane fed (mol/L)
C_i	Mean concentration of species i (mol/L)
$C_{i,b}$	Concentration of species i in the bubble phase (mol/L)
$C_{i,e}$	Concentration of species i in the emulsion phase (mol/L)
C_{MAN}	Concentration of MAN (mol/L)
C_O	Concentration of oxygen (mol/L)

d_b	Bubble size (m)
d_{be}	Equilibrium bubble size (m)
d_{bm}	Maximum bubble size from total coalescence of bubbles (m)
d_{b0}	Maximum bubble size from total coalescence of bubbles (m)
d_p	Particle diameter (μm)
D_{AB}	Gas diffusion coefficient (m^2/s)
D_c	Reactor diameter (m)
E_1	Activation energy for MAN formation (kJ/kmol)
E_2	Activation energy for CO_2 formation (kJ/kmol)
E_3	Activation energy for MAN decomposition (kJ/kmol)
f_b	Bubble phase fraction (-)
g	Gravity acceleration (m/s^2)
h_{gw}	Gas heat transfer coefficient (W/m^2K)
h_{pw}	Particulate heat transfer coefficient (W/m^2K)
ΔH	Enthalpy of reaction (kJ/mol)
H	Reactor height (m)
h_r	Radiation heat transfer coefficient (W/m^2K)
ID	Inside diameter (cm)
k_1	Rate constant for MAN formation ($mol^{(1-\alpha)}\ L^{\alpha}/(g.s)$)

$k_{1,mw}$	Microwave reaction rate constant for MAN formation (mol$^{(1-\alpha)}$ L$^{\alpha}$/(g.s))
$k_{1,conv}$	Conventional reaction rate constant for MAN formation = k_1 (mol$^{(1-\alpha)}$ L$^{\alpha}$/(g.s))
k_2	Rate constant for CO_2 formation (mol$^{(1-\beta)}$ L$^{\beta}$/(g.s))
k_3	Rate constant for MAN decomposition (mol$^{(\delta-\gamma)}$ L$^{(1-\delta+\gamma)}$/(g.s))
k_{10}	Pre-exponential factor for MAN formation (mol$^{(1-\alpha)}$ L$^{\alpha}$/(g.s))
k_{20}	Pre-exponential factor for CO_2 formation (mol$^{(1-\beta)}$ L$^{\beta}$/(g.s))
k_{30}	Pre-exponential factor for MAN decomposition (mol$^{(\delta-\gamma)}$ L$^{(1-\delta+\gamma)}$/(g.s))
K_{be}	Bubble to emulsion gas interchange coefficient (1/s)
K_{bc}	Bubble to cloud gas interchange coefficient (1/s)
K_{ce}	Cloud to emulsion gas interchange coefficient (1/s)
k_g	Gas thermal conductivity (W/mK)
Nu_{pw}	Particulate Nusselt number
P	Pressure (kPa)
q_{mw}	Microwave energy absorbed per unit mass of the receptor (J/kg)
Q_g	Heat transfer inside the gas phase (J)
Q_p	Heat transfer inside the solid phase (J)
Q_{Lg}	Convective heat transfer by the gas phase (J)
Q_{Lp}	Convective heat transfer by the solid phase (J)
Q_{mw}	Microwave heat transfer (J)

r_1	Rate of MAN formation (mol/(g.s))
r_2	Rate of CO_2 formation (mol/(g.s))
r_3	Rate of MAN decomposition (mol/(g.s))
$r_{i,b}$	Overall reaction rate of species i in the bubble phase (mol/(g.s))
$r_{i,e}$	Overall reaction rate of species i in the emulsion phase (mol/(g.s))
R	Gas constant, 8.3144598 (kJ/(kmol.K))
S	Selectivity of MAN, number of moles of MAN produced per moles of n-C_4 converted (-)
T	Operating temperature (^{o}C, K)
T_0	Reference temperature (K)
ΔT	Temperature gradient (^{o}C)
T_{g0}	Gas temperature under the distributor (K)
T_b	Bulk temperature (K)
T_g	Gas temperature (K)
T_p	Particle surface temperature (K)
T_w	Reactor wall temperature (K)
U_b	Bubble rise velocity (m/s)
U_c	Transition velocity from bubbling to turbulent fluidization regime (m/s)
U_e	Superficial gas velocity of emulsion phase (m/s)

U_g	Superficial gas velocity (m/s)
U_{mf}	Minimum fluidization velocity (m/s)
U_p	Particle movement velocity (m/s)
X	Conversion of n-C_4, number of moles of n-C_4 converted per moles of n-C_4 fed (-)
y_{B0}	Feed n-C_4 concentration (% v/v)
Y	Yield of MAN, number of moles of MAN produced per moles of n-C_4 fed (-)
z	Distance above the distributor plate (m)
Δz	Height difference (m)

6.6.3 Greek Letters

$\alpha, \beta, \gamma, \delta$	exponents in Centi *et al.* (Centi et al., 1985) rate expressions (-)
γ_m	Parameter in calculation of d_b (-)
δ'	Parameter in calculation of d_b (m)
ε	Bed voidage (-)
ε^*	Complex permittivity (-)
ε'	Dielectric constant (-)
ε''	Loss factor (-)
ε_{mf}	Minimum fluidization voidage (-)
η	Parameter in calculation of d_b (-)
ρ_g	As density (kg/m^3)

ρ_p	Particle density (kg/m^3)
τ_s	Space velocity (s)
υ	Parameter in calculation of U_b (m)
ψ	Parameter in calculation of U_b (-)
$tan\delta$	Loss tangent (-)

6.7 Acknowledgments

The authors are grateful to the Natural Sciences and Research Council of Canada (NSERC) through discovery grant and NSERC/Total chair for financial support of the project. The authors acknowledge Mr. Sami Chaouki for his invaluable cooperation during the experiments through the undergraduate internship program. The authors further acknowledge the instrumental endeavors of Mr. Daniel Pilon for developing the experimental setup.

6.8 References

Centi, G., Fornasari, G., & Trifiro, F. (1985). n-Butane oxidation to maleic anhydride on vanadium-phosphorus oxides: kinetic analysis with a tubular flow stacked-pellet reactor. *Industrial & Engineering Chemistry Product Research and Development, 24*(1), 32-37. doi: 10.1021/i300017a007

Chen, J. C., Grace, J. R., & Golriz, M. R. (2005). Heat transfer in fluidized beds: design methods. *Powder Technology, 150*(2), 123-132. doi: http://dx.doi.org/10.1016/j.powtec.2004.11.035

Chen, J. D., & Sheldon, R. A. (1995). Selective Oxidation of Hydrocarbons with O2 over Chromium Aluminophosphate-5 Molecular-Sieve. *Journal of Catalysis, 153*(1), 1-8. doi: http://dx.doi.org/10.1006/jcat.1995.1101

Contractor, R. M. (1999). Dupont's CFB technology for maleic anhydride. *Chemical Engineering Science, 54*(22), 5627-5632. doi: http://dx.doi.org/10.1016/S0009-2509(99)00295-X

Contractor, R. M., Bergna, H. E., Horowitz, H. S., Blackstone, C. M., Chowdhry, U., & Sleight, A. W. (1988). Butane Oxidation to Maleic Anhydride in A Recirculating Solids Reactor. *Studies in Surface Science and Catalysis, 38*, 645-654. doi: http://dx.doi.org/10.1016/S0167-2991(09)60694-7

Cui, H., Mostoufi, N., & Chaouki, J. (2000). Characterization of dynamic gas-solid distribution in fluidized beds. *Chemical Engineering Journal, 79*(2), 133-143. doi: Doi: 10.1016/s1385-8947(00)00178-9

Dominguez, A., Menendez, J. A., Fernandez, Y., Pis, J. J., Nabais, J. M. V., Carrott, P. J. M., & Carrott, M. M. L. R. (2007). Conventional and microwave induced pyrolysis of coffee hulls for the production of a hydrogen rich fuel gas. *Journal of Analytical and Applied Pyrolysis, 79*(1-2), 128-135. doi: Doi 10.1016/J.Jaap.2006.08.003

Doucet, J., Laviolette, J.-P., Farag, S., & Chaouki, J. (2014). Distributed microwave pyrolysis of domestic waste. *Waste and Biomass Valorization, 5*(1), 1-10. doi: 10.1007/s12649-013-9216-0

Farag, S., & Chaouki, J. (2015). A modified microwave thermo-gravimetric-analyzer for kinetic purposes. *Applied Thermal Engineering, 75*, 65-72. doi: http://dx.doi.org/10.1016/j.applthermaleng.2014.09.038

Farag, S., Sobhy, A., Akyel, C., Doucet, J., & Chaouki, J. (2012). Temperature profile prediction within selected materials heated by microwaves at 2.45GHz. *Applied Thermal Engineering, 36*, 360-369. doi: Doi 10.1016/J.Applthermaleng.2011.10.049

Glicksman, L. R., & McAndrews, G. (1985). The effect of bed width on the hydrodynamics of large particle fluidized beds. *Powder Technology, 42*(2), 159-167. doi: http://dx.doi.org/10.1016/0032-5910(85)80049-8

Grzybowska, B., Haber, J., & Janas, J. (1977). Interaction of allyl iodide with molybdate catalysts for the selective oxidation of hydrocarbons. *Journal of Catalysis, 49*(2), 150-163. doi: http://dx.doi.org/10.1016/0021-9517(77)90251-2

Gupta, M., & Wong, W. L. (2007). *Microwaves and metals*. Singapore: John Wiley & Sons.

Hamzehlouia, S., Latifi, M., & Chaouki, J. (2017). Development of a Novel Silica-Based Microwave Receptor for High Temperature Processes. *Pending submission*.

Horio, M., & Nonaka, A. (1987). A generalized bubble diameter correlation for gas-solid fluidized beds. *AIChE Journal, 33*(11), 1865-1872. doi: 10.1002/aic.690331113

Hughes, M. D., Yi-Jun, X., Jenkins, P., & McMorn, P. (2005). Tunable gold catalysts for selective hydrocarbon oxidation under mild conditions. *Nature, 437*(7062), 1132.

Kim, S. W., Ahn, J. Y., Kim, S. D., & Hyun Lee, D. (2003). Heat transfer and bubble characteristics in a fluidized bed with immersed horizontal tube bundle. *International Journal of Heat and Mass Transfer, 46*(3), 399-409. doi: https://doi.org/10.1016/S0017-9310(02)00296-X

Knowlton, T. M. (1999). Pressure and Temperature Effects in Fluid-Particle Systems. In W. C. Yang (Ed.), *Fluidization, Solid Handling and Processing: Industrial Applications* (pp. 111-152). New Jersey: Noyes.

Krishna, R., van Baten, J. M., & Ellenberger, J. (1998). Scale effects in fluidized multiphase reactors. *Powder Technology, 100*(2–3), 137-146. doi: http://dx.doi.org/10.1016/S0032-5910(98)00134-X

Kunii, D., & Levenspiel, O. (1991). *Fluidization Engineering*. Boston: Butterworth-Heinemann.

Latifi, M., & Chaouki, J. (2015). A novel induction heating fluidized bed reactor: Its design and applications in high temperature screening tests with solid feedstocks and prediction of defluidization state. *Aiche Journal, 61*(5), 1507-1523. doi: 10.1002/aic.14749

Li, J., Wen, L., Qian, G., Cui, H., Kwauk, M., Schouten, J. C., & Van den Bleek, C. M. (1996). Structure heterogeneity, regime multiplicity and nonlinear behavior in particle-fluid systems. *Chemical Engineering Science, 51*(11), 2693-2698. doi: Doi: 10.1016/0009-2509(96)00138-8

Liu, M., Zhang, Y., Bi, H., Grace, J. R., & Zhu, Y. (2010). Non-intrusive determination of bubble size in a gas–solid fluidized bed: An evaluation. *Chemical Engineering Science, 65*(11), 3485-3493. doi: http://dx.doi.org/10.1016/j.ces.2010.02.049

Ma, J., Fang, M., Li, P., Zhu, B., Lu, X., & Lau, N. T. (1997). Microwave-assisted catalytic combustion of diesel soot. *Applied Catalysis A: General, 159*(1), 211-228. doi: http://dx.doi.org/10.1016/S0926-860X(97)00043-4

Metaxas, A. C. (1988). *Industrial Microwave Heating Power and Energy* (pp. 1 online resource (376 p.)).

Pert, E., Carmel, Y., Birnboim, A., Olorunyolemi, T., Gershon, D., Calame, J., . . . Wilson, O. C. (2001). Temperature measurements during microwave processing: The significance of thermocouple effects. *Journal of the American Ceramic Society, 84*(9), 1981-1986. doi: 10.1111/j.1151-2916.2001.tb00946.x

Poling, B. E., Prausnitz, J. M., & O'Connell, J. P. (2001). *The properties of gases and liquids* (Vol. 5): Mcgraw-hill New York.

Rüdisüli, M., Schildhauer, T. J., Biollaz, S. M. A., & van Ommen, J. R. (2012). Scale-up of bubbling fluidized bed reactors — A review. *Powder Technology, 217*(0), 21-38. doi: 10.1016/j.powtec.2011.10.004

Sheldon, R. (2012). *Metal-catalyzed oxidations of organic compounds: mechanistic principles and synthetic methodology including biochemical processes*: Elsevier.

Sheldon, R. A. (1991). Heterogeneous Catalytic Oxidation and Fine Chemicals. *Studies in Surface Science and Catalysis, 59*, 33-54. doi: http://dx.doi.org/10.1016/S0167-2991(08)61106-4

Shimizu, K.-I., Kaneko, T., Fujishima, T., Kodama, T., Yoshida, H., & Kitayama, Y. (2002). Selective oxidation of liquid hydrocarbons over photoirradiated TiO2 pillared clays. *Applied Catalysis A: General, 225*(1), 185-191. doi: http://dx.doi.org/10.1016/S0926-860X(01)00863-8

Sinha, A. K., Seelan, S., Tsubota, S., & Haruta, M. (2004). Catalysis by Gold Nanoparticles: Epoxidation of Propene. *Topics in Catalysis, 29*(3), 95-102. doi: 10.1023/b:toca.0000029791.69935.53

Sinha, A. K., Seelan, S., Tsubota, S., & Haruta, M. (2004). A Three-Dimensional Mesoporous Titanosilicate Support for Gold Nanoparticles: Vapor-Phase Epoxidation of Propene with High Conversion. *Angewandte Chemie International Edition, 43*(12), 1546-1548. doi: 10.1002/anie.200352900

Sobhy, A., & Chaouki, J. (2010). Microwave-assisted Biorefinery. *Cisap4: 4th International Conference on Safety & Environment in Process Industry, 19*, 25-29. doi: Doi 10.3303/Cet1019005

Temur Ergan, B., & Bayramoğlu, M. (2011). Kinetic Approach for Investigating the "Microwave Effect": Decomposition of Aqueous Potassium Persulfate. *Industrial & Engineering Chemistry Research, 50*(11), 6629-6637. doi: 10.1021/ie200095y

Tinga, W. R., & Nelson, S. O. (1973). Dielectric properties of materials for microwave processing-tabulated. *J. Microwave Power, 8*(1), 23-66.

Treybal, R. E. (1981). *Mass-Transfer Operations* (Third Edition ed.). London: McGraw-Hill Book Company.

Uhlig, H. H., & Keyes, F. G. (1933). The Dependence of the Dielectric Constants of Gases on Temperature and Density. *The Journal of Chemical Physics, 1*(2), 155-159.

Vos, B., Mosman, J., Zhang, Y., Poels, E., & Bliek, A. (2003). Impregnated carbon as a susceptor material for low loss oxides in dielectric heating. *Journal of Materials Science, 38*(1), 173-182. doi: 10.1023/a:1021138505264

Yadav, G. D., & Borkar, I. V. (2006). Kinetic modeling of microwave-assisted chemoenzymatic epoxidation of styrene. *Aiche Journal, 52*(3), 1235-1247. doi: 10.1002/aic.10700

Yaws, C. L. (1999). *Chemical properties handbook*: McGraw-Hill.
Zabrodskiĭ, S. S. (1966). *Hydrodynamics and heat transfer in fluidized beds*: Massachusetts Institute of Technology.

CHAPTER 7 ARTICLE 3: MICROWAVE HEATING-ASSISTED CATALYTIC DRY REFORMING OF METHANE

Sepehr Hamzehlouia, Shaffiq Jaffer[1] and Jamal Chaouki[2]

[1]Total American Services, Inc., 82 South St., Hopkinton, MA, 01748

[2]Department of Chemical Engineering, Polytechnique Montreal, c.p. 6079, Succ. Centre-ville, Montreal, Quebec, H3C 3A7, Canada

7.1 Abstract

Natural gas has been regarded as a revolutionary resource for energy and chemical production applications. Whereas the conversion of methane--the dominant constituent of natural gas--to syngas projects exceptional economic benefits by facilitating the transportation process and evolution of value-added products, the secondary gas-phase reactions within the conversion mechanism reduce the quality of the syngas components by generating undesired gas-phase by-products. Although the effects of the catalyst optimization and structure on the syngas selectivity have been thoroughly studied in the available literature, the lack of studies concentrating on the role of the heating method is critically evident. The development of the affordable and sustainable renewable energies, namely, wind and solar power, due to the environmental concerns associated with the application of conventional fossil fuels and the inevitable depletion of the available reserves, has exhibited novel opportunities for chemical reactions. However, the advent of economically feasible and accessible electricity provides an esteemed opportunity to deploy electrical heating methods, namely, induction heating, microwave heating and ultrasound heating, for chemical processing applications. In this study, the effect of the microwave heating selective mechanism on a crucial gas-solid catalytic reaction, dry reforming of methane, was investigated. Subsequently, a significant temperature gradient between the solids surface, bulk and fluidizing gas was revealed, which predominantly affected the reaction mechanism. Furthermore, microwave heating mechanism projected exceptional characteristics to promote catalytic reaction, by maintaining a high conversion of the reactants, CH_4 and CO_2, and restricting the undesired gas-phase side reactions by developing high selectivity for the products, H_2 and CO, simultaneously.

7.2 Introduction

Natural gas has been highlighted as the fastest-growing energy resource, while conventional reserves, oil and coal, are suffering from a declining transition period. Such a prospect is explicitly associated with the intensification in US shale gas and liquefied natural gas (LNG) production rates, strict environmental policies reinstated by the governments and the significant elevation of demands from emerging economies with China, India and the Middle East leading the market shares(BP, 2016). Early predictions have underlined natural gas to surpass coal as the second dominant energy vector, and further reach the petroleum supremacy level in the short-term energy outlook (Birol & Argiri, 1999; BP, 2016; IEA, 2016). Natural gas is majorly confined in hydrate form allocated in remote regions and deep ocean environments. Hence, the majority of the reserves are barely accessible(Sloan, 2003). Natural Gas is structurally dominated by methane as the key ingredient and minor proportions of ethane, propane, butane, pentane and acid gasses (Lee, 1996). Presently, methane has been an indispensable component of various industrial applications, including energy supply for power plants and electricity generation, automotive fuels, syngas production, and production of various value-added chemicals, including hydrogen cyanide, chloromethane and carbon disulfide (Edwards, Mahieu, Griesemann, Larivé, & Rickeard, 2004; Eriksson et al., 2006; Folkins, Miller, & Hennig, 1950; Hickman & Schmidt, 1993; Koberstein, 1973; Murray, Tsai, & Barnett, 1999; Podkolzin, Stangland, Jones, Peringer, & Lercher, 2007).

Reflecting the critical accessibility issues associated with the discovered reserves and the general complexity convoying the transportation of gaseous components, the conversion of methane resources to value-added chemicals have been promptly perused (C. A. Jones, Leonard, & Sofranko, 1987). The conversion of methane aims to address the transportation deficiencies while economically justifies the processing for the energy sector (Rostrup-Nielsen, 1994). Meanwhile, conversion of methane into syngas has aroused prominent interest to preserve a carbon-neutral energy cycle on the future industrial outlook. However, the major methane to syngas conversion processes, namely, steam reforming, dry reforming and partial oxidation, undergo a severe lack of productivity due to the complex thermodynamic equilibria (Christian Enger, Lødeng, & Holmen, 2008; Ostrowski, Giroir-Fendler, Mirodatos, & Mleczko, 1998). Whereas secondary gas-phase reactions, namely, thermal degradation of methane, water-gas shift reaction and carbon monoxide disproportionation, decrease the selectivity of the desired syngas components, H_2 and CO,

enhanced endeavours to develop an economically feasible catalyst to restrict the secondary gas-phase reactions have utterly failed (Christian Enger et al., 2008; Hu & Ruckenstein, 2004; Usman, Wan Daud, & Abbas, 2015; Vernon, Green, Cheetham, & Ashcroft, 1990). While most studies concentrate on improving the performance of the catalysts, the scarcity of the investigations demonstrating the effect of the heating methods on the performance of the reactions is evidently substantiated in the available literature.

The environmental concerns associated with the combustion and processing of petroleum-based resources, namely, sulfur dioxide, nitrogen oxides, carbon monoxide, carbon dioxide and particulate matter, have urged the governments to mandate strict policies to control the emission crisis (IEA, 2016), while the irrepressible depletion of available dominant energy reserves, oil, and coal, has inspired the energy sector to pursue an alternative roadmap for the global demand outlook (Shafiee & Topal, 2009). It has been estimated that the global energy demands would increase at an average rate of 1.1% per annum, from 500 quadrillion Btu in 2006 to 701.6 quadrillion Btu in 2030 (Shafiee & Topal, 2008). Consequently, the global energy sector is urged to investigate sustainable, innovative and alternative resources to satisfy the global energy market demands. Hence, renewable energy resources have been acknowledged as noteworthy possibilities to maintain the ever-growing energy market while complying with strict environmental regulations to persevere the planet from further irretrievable destruction (Turner, 1999). The application of renewable energy resources in transportation, electricity and power generation, and industrial processes has been highly regarded as the coherent alternative to economically unfeasible carbon dioxide sequestration endeavours (Pimentel & Patzek, 2008). Recent developments and breakthroughs in the production and harvesting methods, depletion and exhaustion of the fossil fuel reserves, mass production processes and diverse feedstock have developed renewable energy criteria from economically unfeasible to highly affordable and accessible resources (Timmons, Harris, & Roach, 2014). Moreover, a significant production, maintenance and distribution cost decline trend for solar- and wind-based electricity has been evidenced during the last three decades (Saidur, Islam, Rahim, & Solangi, 2010; Solangi, Islam, Saidur, Rahim, & Fayaz, 2011; Timilsina, Kurdgelashvili, & Narbel, 2012; Wiser et al.). Consequently, the convenience of affordable renewable electricity which projects substantially lower carbon footprint and CO_2 emission during the production, distribution and application stages provides a unique potential to preform chemical

reactions via electromagnetic processing methods, namely, induction heating, ultrasound heating and microwave heating, correspondingly.

Adopting gas-solid catalytic reactions with innovative heating methods, namely, microwave heating, stipulates an esteemed opportunity to optimize the performance of the catalysts according to the process characteristics. Microwave heating offers multiple established advantages over conventional heating methods, namely, selective and uniform heating, instantaneous temperature control, reduced energy consumption and process diversity (Farag, Sobhy, Akyel, Doucet, & Chaouki, 2012; Gupta & Wong, 2007; Metaxas & Meredith, 1983). Whereas the application of microwave heating has been extended to waste and biomass conversion, polymer synthesis, drying and moisture removal, ceramics sintering and environmental activities (Antti & Perre, 1999; Doucet, Laviolette, Farag, & Chaouki, 2014; D. A. Jones, Lelyveld, Mavrofidis, Kingman, & Miles, 2002; Mushtaq, Mat, & Ani, 2014; Roy, Agarwal, Chen, & Gedevanishvili, 1999; Sobhy & Chaouki, 2010; Wiesbrock, Hoogenboom, & Schubert, 2004). The selective heating mechanism of microwave irradiation provides an exceptional opportunity for gas-solid catalytic reactions. Microwave heating is the consequence of the exposure of a dielectric material to a high frequency electromagnetic field. Thus, the heat source is enclosed within the dielectric material structure, contrasting the conventional heating mechanism(Metaxas & Meredith, 1983). Consequently, due to insignificant dielectric properties most common material, namely, gaseous components, fail to interact with microwave irradiation. Hence, in a gas-solid reaction, in case the catalyst active sites or the support project significant dielectric properties, a temperature gradient arises within the gas and solid phase. Accordingly, while the active site is incorporated into a higher local temperature, the gas phase in exposed to a considerably lower temperature values. Subsequently, such temperature gradient establishes the prospect to promote catalytic reactions while restricting the secondary gas-phase reactions from the kinetics perspective.

Therefore, in the present study, the effect of the microwave selective heating mechanism on the productivity of gas-solid catalytic conversion of methane to syngas has been investigated. Dry reforming of methane (DRM) was substantiated as the reaction model due to the importance of the development of the reaction to the commercial sector. Catalytic dry (CO_2) reforming, the conversion of hydrocarbons to synthetic gas in the presence of carbon dioxide, of methane has been extensively investigated in the available literature due to the environmental benefits and the process flexibility (M. C. J. Bradford & Vannice, 1999; Pakhare & Spivey, 2014; Usman et al., 2015).

However, the industrial application of dry reforming has been stalled due to the scarcity of an effective and economical catalyst and high energy requirements (Puskas, 1995). Moreover, due to the multiple thermodynamic equilibria, evolution of the undesired gas-phase, secondary reactions have been promptly inevitable (Nikoo & Amin, 2011). Accordingly, a single-mode lab-scale microwave heating-assisted fluidized bed reactor was developed to study the effect of microwave irradiation on the prospect of the DRM catalytic reaction. Hence, the effect of the microwave heating mechanism within a temperature range of 650^{o}C to 900^{o}C on the conversion of the reactants, CH_4 and CO_2, selectivity of the products, H_2 and CO and activity of the catalyst was comprehensively investigated.

7.3 Experiments

7.3.1 Materials

Carbon-coated silica sand particles (C-SiO_2, ρ_p=2650 kg/m^3, d_p= 212-250 µm) developed by the induction heating-assisted FBCVD of methane were selected as the microwave receptor/catalyst promoter components. Moreover, HiFUEL® R110 nickel-based and alumina-supported steam reforming catalyst (15.9 – 20.0 wt% Ni, Alfa Aesar) was selected to stipulate the compulsory active-sites for the reaction. The catalyst particles were supplied in 4-hole quadralobe pellets which were further grinded and transformed to 212 – 250 µm Geldart group B powder. Subsequently, methane (99.92% purity, Canadian Air Liquid) and carbon dioxide (99.92% purity, Canadian Air Liquid) were deployed to perform the dry reforming reactions. In addition, nitrogen (99.99% purity, Canadian Air Liquid) was employed for pre-reaction bed fluidization and the reference component for gas chromatographic analysis. Furthermore, hydrogen (5% plus 94.99 nitrogen balance, Canadian Air Liquid) was retained for catalyst activation and regeneration purposes.

7.3.2 Dry Reforming of Methane (DRM)

In 2017, Hamzehlouia *et al.* developed an induction heating-assisted FBCVD process to produce carbon-coated silica sand particles with 0.25 wt% carbon composition and 72±7 nm coating layer thickness (Hamzehlouia, Latifi, & Chaouki, 2017; Latifi & Chaouki, 2015). Following exceptional dielectric properties and acclaimed interaction with microwave radiation, the developed C-SiO_2 particles were further recommended for simultaneous application as a microwave receptor/catalyst

promoter for the catalytic gas-solid reactions, respectively. Consequently, C-SiO_2 particles were selected as the bed material for the present microwave heating study. Furthermore, HiFUEL R110 catalyst, a nickel-based catalyst specifically designed for reforming reactions, was employed to enhance the reaction mechanism. Initially, the HIFUEL R110 catalyst particles were transformed from 4-hole quadralobe pellets to 212-250 μm Geldart's group B powder to enhance the uniformity of the bed and restrict the destructive segregation effects. The catalyst particles were further regenerated in the induction heating-assisted fluidized bed reactor to optimize the catalytic activity of the powders. The catalyst regeneration process was performed at 800^oC under an atmosphere of 5% H_2 balanced by inert nitrogen for a period of 6 hours. The heating rate of the regeneration process was adjusted to 10^oC/min while the superficial velocity of the active gas was adjusted in the range of 0.1 m/s to 0.034 m/s according to the process temperature. The superficial gas velocity was maintained by a Bronkhorst F-201CV mass flow controller in order to sustain a bubbling fluidization regime in the reactor. The temperature of the bed was continuously monitored with a K type thermocouple while the superficial velocity of the gas was adjusted accordingly. The regenerated catalyst particles were further cooled down under an atmosphere of 5% H_2 balanced by nitrogen to diminish contamination and oxidation threats to the powder. The regenerated catalyst particles were subsequently transferred to tight-sealed containers and stocked in a desiccator unit to prevent humidity and contamination hazards accordingly.

The dry reforming of methane (DRM) reactions were attained in a microwave heating-assisted lab-scale fluidized bed reactor. The experiments were performed in a 2.54-cm ID and 20-cm long fused quartz tube. The reactor material was selected due to the insignificant dielectric properties of quartz, which restrict any prospective microwave-heating effects, accordingly. A quartz-fritted disk distributor plate with an average pore size of 15 – 40 micrometers was attached to the reactor tube to provide a uniform distribution of the gas and further support to the bed material. The quartz tube was enclosed by copper/bras alloy electromagnetic shield tube to inhibit microwave radiation exposure and comply with the safety regulations. The quartz reactor was further mounted to the electromagnetic shield tube with the assistance of silicon high temperature seals enclosed by removable copper compression caps on the top and the bottom of the tube. To develop a microwave heating power, a 2.5 kW and 2.45 GHz frequency Genesys system magnetron with an internal water cooling mechanism was commissioned. The microwave irradiation was transferred from the magnetron to the cavity with the assistance of rectangular bras waveguides.

A mixture of 12 gr of the HiFUEL R110 and 28 gr of the C-SiO_2 receptor/promoter was prepared and loaded to the reactor as the bed material composition. The presence of the C-SiO_2 particles are essential to mitigate for the microwave-assisted uniform heat generation inside the bed and enhancement of the activity of the catalytic particles. Afterwards, the catalyst bed was fluidized at the ambient temperature with inert nitrogen at 0.1 m/s superficial gas velocity maintained by a Bronkhorst F-201CV mass flow controller. Due to the complications associated with temperature measurements inside an electromagnetic field deploying thermometric methods, a thermopile, a radiometry light-capturing radiation measurement device, was designed and engaged to the reactor (Pert et al., 2001). In order to preserve the bubbling fluidization regime, the superficial gas velocity was promptly regulated according to the thermopile temperature measurements, correspondingly. It should be noted that the thermopile measurements are based on the irradiation of the dielectric solid surfaces while exposed to the high frequency electromagnetic wave exclusively and disregards the gaseous components and the non-dielectric quartz tube. The thermopile further converts the radiation extensity signals acquired by light-capturing mechanism to an alternating voltage between 0 to 10 V according to the thermoelectric effect. The response voltage was subsequently calibrated according to the representing temperature. The operating temperature was introduced through a LabView software interface. Afterwards, a PID controller adjusted the dissipated power according to the temperature readings stipulated by the thermopile measurements.

The dielectric material, while exposed to a high frequency electromagnetic field, absorb and reflect a ration of the transmitted wave proportional to their dielectric properties, dielectric constant (ε') and loss factor (ε''). Subsequently, a three-way wave reflected was attached to the wave guide to prevent the reflected traveling microwave emissions from approaching and destroying the magnetron. The 3-way reflector was further air-cooled to preclude overheating threats. Thus, in order to maximize the microwave heating efficiency, the amount of the incident power absorbed by the bed material should be amplified while simultaneously diminishing the reflected power portion. Consequently, a power measurement mechanism was designed to monitor the incident and the reflected microwave power simultaneously. Hence, the incident to the reflected power was adjusted deploying a set of screws incorporated into the waveguide prior to the cavity to further optimize the microwave heating mechanism.

Once the system approached the designated reaction temperature and following a period of stabilization to maintain a uniform operating condition throughout the reactor, the gas flow was

switched from the fluidizing gas, nitrogen, to a mixture of the DRM reactant gaseous components, CH_4 and CO_2. The superficial velocity and the equilibrium ratio of the reactants were maintained employing two Bronkhorst F-201CV mass flow controller. Ultimately, the gaseous products departing the reactor were analyzed with the assistance of a Varian CP-4900 micro gas chromatographer (GC) to detect the volumetric fraction of each component. A stationary flow of inert nitrogen was purged to the micro GC as a reference gas for further conversion and selectivity measurements using a flow meter. Due to the enhanced coke production associated with the DRM reactions over the nickel-based catalyst, the reactor and pipelines were thoroughly dismantled and evacuated prior to every experiment, accordingly. Figure 7-1 exhibits a pictorial presentation of the microwave heating apparatus.

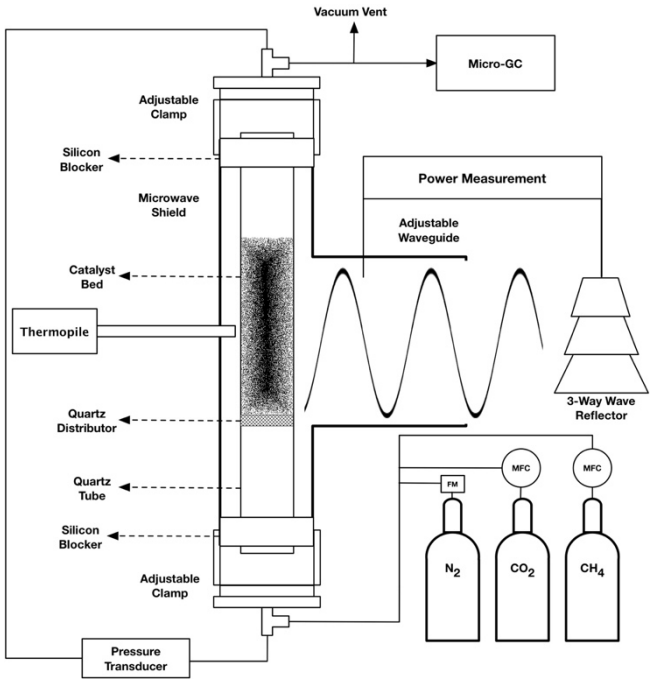

Figure 7-1: Schematic demonstration of the microwave heating apparatus

7.4 Results and discussion

In general, while the dielectric materials are exposed to a high frequency electromagnetic field, the internal energy of these components is rehabilitated. The phenomenon arises as a consequence of the reorientation of the charged particles or the interfacial charge distribution of the molecular dipoles which is further demonstrated by the heat generation. In fact, the behaviour of material exposed to electromagnetic irradiation can be predicted by their dielectric properties. Complex

permittivity (ε^*), resistance of material exhibited while exposed to a high frequency electromagnetic field, expresses the ability of components to generate heat while affected by irradiation. Hence, the real portion, *dialectic constant*, is referred as the ability of a dielectric material to absorb the electromagnetic energy, whereas the imaginary portion, *loss factor*, exhibits the potential of that dielectric material to dissipate the absorbed electromagnetic energy in the form of thermal energy, accordingly. Furthermore, the ratio of loss factor over the dielectric constant, highlighted as the *loss tangent*, demonstrated the efficiency of the dielectric material to discharge the absorbed electromagnetic energy into thermal energy.

The dielectric properties of the material are significantly manipulated by the frequency, temperature and humidity of the exposed operating conditions (Metaxas & Meredith, 1983). Table 7-1 has summarized the dielectric properties of multiple material deployed in the present study. It should be noted that due to the chemical properties and physical structure, most material reflects insignificant interaction while exposed to an electromagnetic field, namely, microwave irradiation. In general, gaseous components project extremely low dielectric properties restricting them from any interaction while exposed to microwaves. In the present study, the inert fluidizing gas (nitrogen), the reactant gaseous components (CH_4 and CO_2), the reactor structure (fused quartz), and the HiFUEL R110 project insignificant dielectric properties and are either transparent or reflect the microwave irradiation, respectively. Thus, only the C-SiO_2 particles are subject to the microwave interaction and mitigate for the heat generation throughout the system, exclusively.

Table 7-1: The summary of the dielectric properties of the employed material at ambient temperature and 2.45 GHz frequency

Material	Dielectric Constant (ε')	Loss Factor (ε'')	tanδ
Silica Sand	3.066 (Ma et al., 1997)	0.215 (Ma et al., 1997)	0.070 (Ma et al., 1997)
Carbon	7 (Vos et al., 2003)	2 (Vos et al., 2003)	0.285
C – SiO_2	13.7*	6*	0.437
Nitrogen	1.00058 (Uhlig & Keyes, 1933)	-	-
Fused Quartz	4.0 (Gupta & Wong, 2007)	0.001(Gupta & Wong, 2007)	0.00025

* Based on measurements reported in this study.

The general mechanism of the DRM reaction has been expressed as:

$$CH_4 + CO_2 \rightarrow 2CO + 2H_2 \qquad \Delta H^0_{298} = +247 \text{ kJ mol}^{-1} \qquad (7.1)$$

$$\Delta G^o = 61770 - 67.32T$$

The dry reforming process in principle is intensely endothermic, thus obliging enormously high temperatures to attain high conversion of reactants to the dominant products, H_2 and CO, based on the thermodynamic equilibria (Brungs, York, Claridge, Márquez-Alvarez, & Green, 2000; Wang, Lu, & Millar, 1996). However, due to the presence of multiple thermodynamic equilibria, the reaction mechanism is significantly diverse, which concludes various side reactions depending on the operating conditions, namely, reversed water-gas shift reaction (RWGS) and carbon monoxide disproportionation, expressed as:

$$CO_2 + H_2 \leftrightarrow CO + H_2O \qquad \Delta H^0_{298} = 41.2 \text{ kJ mol}^{-1} \qquad (7.2)$$

$$\Delta G^o = -8545 - 7.84T$$

$$2CO \leftrightarrow C + CO_2 \qquad \Delta H^0_{298} = -172.4 \text{ kJ mol}^{-1} \qquad (7.3)$$

$$\Delta G^{o} = -39810 + 40.87T$$

The diverse mechanism of the DRM reactions leads to the production of multiple undesired gas-phase by-products which significantly affect the product stream quality by deteriorating the selectivity of the desired syngas, H_2 and CO, components. Furthermore, secondary gas-phase reactions such as carbon monoxide disproportionation severely enhance one of the major DRM inadequacies: the production of coke. In general, the production of coke in excess interferes with the activity of the reaction catalyst by inhibiting the active sites, accordingly. Table 7-2 has summarized a comprehensive summary of the DRM reaction system mechanism. In 2013, Pakhare *et al.* investigated the effect of temperature on the thermodynamic behaviour of DRM (Pakhare, Shaw, Haynes, Shekhawat, & Spivey, 2013). It was concluded that the highest conversion of CO_2 and CH_4 and selectivity of CO and H_2, while restricting the production of undesired secondary components, was established in the operating temperature range of 650^{o}C to 1000^{o}C. Thus, a temperature range of 650^{o}C to 900^{o}C was selected to optimize the reaction thermodynamics and maintain the structural restriction of the reactor respectively. It should be noted that the term "operating temperature" is associated with the temperature of the solid particles measured by the thermopile. Due to the chemical properties and physical structure of gaseous components, temperature measurement through radiometry method was not conceivable. Furthermore, due to the insignificant dielectric properties of gases in general, the microwave heating effects of such material are extremely restricted. Consequently, based on the principles of microwave heating, a substantial temperature gradient endures concerning the solid phase and the gas phase while exposed to microwave irradiation. In 2017, Hamzehlouia *et al.* investigated the effect of microwave heating on the temperature distribution of the gas phase and the solid phase with the assistance of a general two-phase model in a fluidized bed reactor (Hamzehlouia, Shabanian, Latifi, & Chaouki, 2017). It was established that a significant temperature gradient exists amongst the solid and gas phases, which is predominantly affected by the superficial gas velocity and the temperature of the solid particles. The aforementioned temperature gradient was a product of the insignificant dielectric properties of gaseous components, which project inadequate microwave interaction. Subsequently, mathematical correlations were developed to predict the temperature distribution of the bulk, the contributive proportion of the solid and gas phase on the reaction bed, and the gas

phase according to the superficial gas velocity and the physical properties of the bed constituents. The predictive correlations were expressed as (Hamzehlouia, Shabanian, et al., 2017):

$$T_b = T_p\text{-}125.9T_p^{0.04/\tau_s} \tag{7.4}$$

$$T_b = 0.54(1\text{-}\varepsilon)T_p \frac{\rho_p C_{p_p}}{\varepsilon\rho_g C_{p_g} + (1\text{-}\varepsilon)\rho_p C_{p_p}} + 834\varepsilon T_g \frac{\rho_g C_{p_g}}{\varepsilon\rho_g C_{p_g} + (1\text{-}\varepsilon)\rho_p C_{p_p}} \tag{7.5}$$

where T_b, T_p and T_g represent the bulk, solid surface and gas temperatures respectively. Figure 7-2 demonstrates the distribution of the bulk, gas and solid temperature distributions according to the DRM operating conditions. The results exhibited a significant temperature gradient between the solid and gas phase at all DRM operating conditions. It has been concluded that while the solid surface of the active sites was maintained at high temperatures, the associated gas phase components were predominantly exposed to extremely lower temperatures simultaneously, due to inadequate microwave interaction.

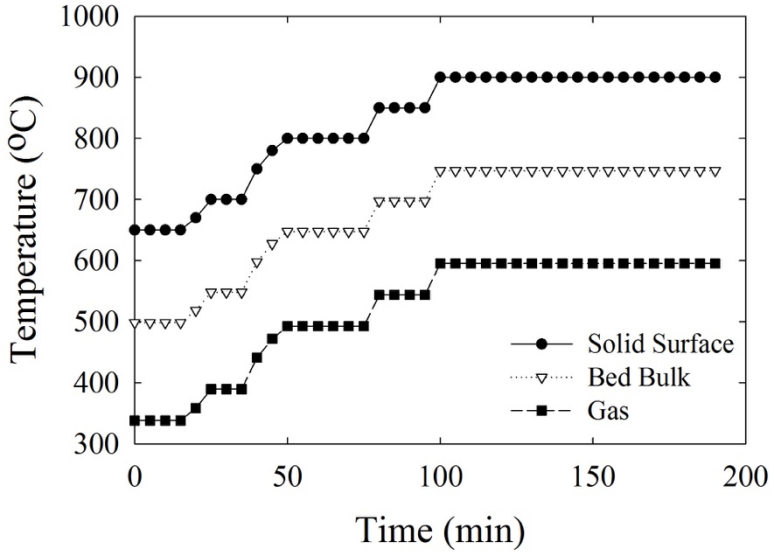

Figure 7-2: The distribution of the solid, bulk and gas temperatures according to the DRM operating conditions in a microwave-assisted fluidized bed reactor.

Meanwhile, the dry reforming of methane reactions were performed at an equivalent ratio of unity (CO_2/CH_4=1:1) in order to investigate the effect of microwave heating on the conversion of the reactants and the selectivity of the desired products exclusively. Conversely, to address the carbon deposition deficiency, thermodynamic investigations have suggested the application of high CO_2/CH_4 ratio, significantly exceeding unity, at high temperatures (~1000 K) (Gadalla & Bower, 1988; Reitmeier, Atwood, Bennett, & Baugh, 1948; White, Roszkowski, & Stanbridge, 1975). However, low CO_2/CH_4 (near unity) ratio at low operating temperatures is commonly favoured by the commercial sector (M. C. J. Bradford & Vannice, 1999; Hu & Ruckenstein, 2004). Such requirements necessitate the application of a reforming catalyst which incorporates the kinetics of the carbon formation and the deposition, whereas the thermodynamics of such deposition is favorable by the reaction mechanism.

Table 7-2: Complete reaction mechanism pathways for dry reforming of methane (Nikoo & Amin, 2011)

Reaction #	Reaction	ΔH_{298}(kJ/mol)
1	$CH_4 + CO \leftrightarrow CO + 2H_2$	247
2	$CO_2 + H_2 \leftrightarrow CO + H_2O$	41
3	$2CH_4 + CO_2 \leftrightarrow C_2H_6 + CO + H_2O$	106
4	$2CH_4 + 2CO_2 \leftrightarrow C_2H_4 + 2CO + 2H_2O$	284
5	$C_2H_6 \leftrightarrow CH_4 + H_2$	136
6	$CO + 2H_2 \leftrightarrow CH_3OH$	-90.6
7	$CO_2 + 3H_3 \leftrightarrow CH_3OH + H_2O$	-49.1
8	$CH_4 \rightarrow C + 2H_2$	74.9
9	$2CO \rightarrow C + CO_2$	-172.4
10	$CO_2 + 2H_2 \leftrightarrow C + 2H_2O$	-90
11	$H_2 + CO \leftrightarrow H_2O + C$	-131.3
12	$CH_3OCH_3 + CO_2 \leftrightarrow 3CO + 3H_2$	248.4
13	$3H_2O + CH_3OCH_3 \leftrightarrow 2CO_2 + 2H_2$	136
14	$CH_3OCH_3 + H_2O \leftrightarrow 2CO + 4H_2$	204.8
15	$2CH_3OH \leftrightarrow CH_3OCH_3 + H_2O$	-37
16	$CO_2 + 4H_2 \leftrightarrow CH_4 + 2H_2O$	-165
17	$CO + 3H_2 \leftrightarrow CH_4 + H_2O$	-206.2

The application of transition metal catalysts, namely, nickel (Ni) and cobalt (CO), has been thoroughly studied in the available literature, while nickel-based catalysts have been particularly adopted due to the established extraordinary reactivity with methane reactants (Avetisov et al., 2010; Budiman, Song, Chang, Shin, & Choi, 2012; Lavoie, 2014; Usman et al., 2015). From an economical perspective, the application of transition metals for DRM catalytic reaction is

extremely profitable. However, thermodynamic investigations have disclosed the vulnerability of these types of metal catalysts to carbon deposition which consequently leads to deactivation of the active sites (Gadalla & Bower, 1988), whereas two substantial parameters to inhibit carbon deposition on the catalyst surface have been highlighted as surface structure and acidity (Hu & Ruckenstein, 2002). Furthermore, the effect of the catalyst support on the activity of the catalyst and carbon deposition issue has been underlined (Usman et al., 2015). In 2006, Hou *et al.* investigated the application of transition metal catalysts, alumina-supported Ni and CO, which established a higher activity (Hou, Chen, Fang, Zheng, & Yashima, 2006). Consequently, HiFUEL R110 nickel based and alumina supported catalyst was selected for performing the microwave-assisted DRM reactions.

The fundamental application of the DRM process is the conversion of methane into valuable syngas products, a mixture of H_2 and CO. Thus, maximizing the selectivity of syngas components is essential for the commercial sector, accordingly. Consequently, in order to accomplish the optimal productivity, the production of undesired gas-phase reactions should be promptly restricted while the maximal selectivity of the syngas components is maintained. Thus, the dry reforming of methane was performed in an operating temperature range of 650^{o}C to 900^{o}C. Figure 7-3 demonstrates the conversion of the reactants, CH_4 and CO_2, and the selectivity of the desired products, H_2 and CO, according to the operating temperatures. It was concluded that the conversion of both reactants, methane and carbon dioxide, increased by escalating the operating temperature, which is in compliance with the endothermic characteristics of the reaction and the prior studies reported in the literature (Jablonski, Schmidhalter, De Miguel, Scelza, & Castro, 2005; Khalesi, Arandiyan, & Parvari, 2008; Nikoo & Amin, 2011; Pakhare et al., 2013). However, the conversion of CH_4 slightly exceeds the equivalent conversion of CO_2, which is associated with the methane decomposition reaction (reaction 8 of table 2). It has been established that at CO_2/CH_4 ratios of 0.5 to 1, since CO_2 is not capable to convert the methane completely and acts as the restricting reaction, it facilitates the conversion of methane into hydrogen and carbon through the decomposition reaction (Nikoo & Amin, 2011). Furthermore, the conversion of the reactants was in compliance with the study performed by Fidalgo *et al.* in a fixed bed microwave-heated reactor deploying carbonaceous catalysts (Fidalgo, Domínguez, Pis, & Menéndez, 2008).

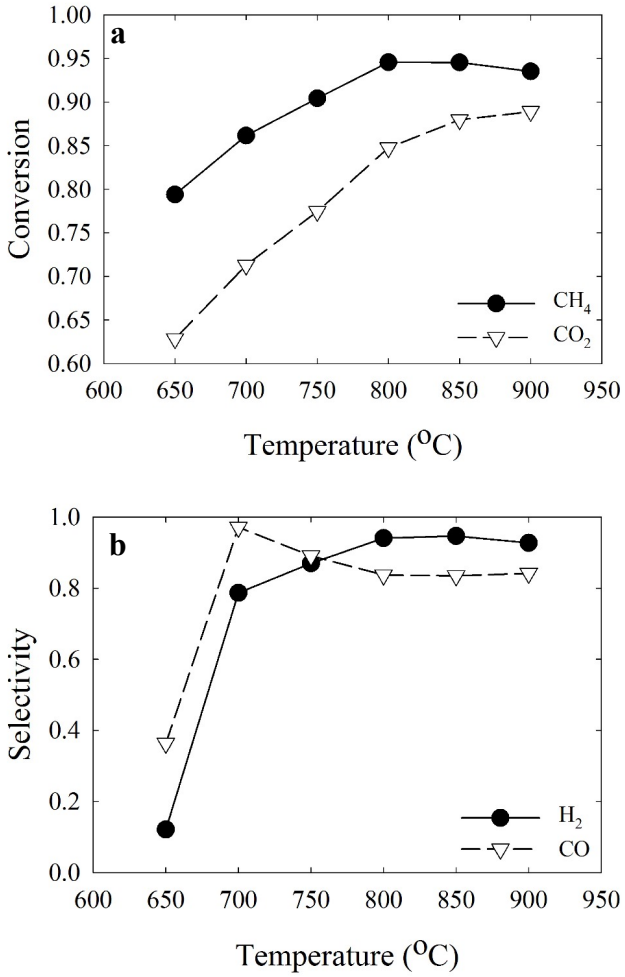

Figure 7-3: a) Conversion of the reactants (CH_4 and CO_2) and b) selectivity of the products (H_2 and CO) at the operating temperature range of 650°C to 900°C.

The selectivity of H_2 enhances by increasing the operating temperature in general, however, faces a minor decline in temperature around 900°C. It has been demonstrated that at CO_2/CH_4 ratios of close to unity, an excessive amount of H_2 is generated through the decomposition of methane. However, at higher operating temperatures, the H_2 selectivity is affected by the dominance of the reverse water-gas shift reaction (RWGS), which leans towards the production of CO and H_2O (Istadi, Amin, & Aishah, 2005; Tsai & Wang, 2008). On the other hand, the deactivation of the catalyst is enhanced at higher temperatures due to the excessive production of carbon at lower CO_2/CH_4 ratios which affects the production of H_2 accordingly (Barrai, Jackson, Whitmore, & Castaldi, 2007). On the contrary, the CO selectivity initially escalates to the maximal value close to 1 at temperatures around 700°C, however, it exhibits a decline before recuperating at higher temperatures. Primarily, due to the presence of carbon coating on the receptor particles, the reverse

CO disproportionation reaction is uncontested. However, by increasing the temperature, CO_2 converts to the restricting reactant at CO_2/CH_4 close to unity, which demonstrates a decline in the CO production. However, due to the endothermic thermal property of the CO production reactions, the selectivity is slightly enhanced by increasing the operating temperature of the reaction. Moreover, due to the initiation of the methane decomposition reaction at temperatures close to 700^{o}C, CO production is affected by the gradual deactivation of the catalyst active sights associated with the coking phenomenon (Barrai et al., 2007; Michael C. J. Bradford & Vannice, 1996; Nikoo & Amin, 2011). In general, the selectivity of H_2 and CO is both higher than the thermodynamically predicted equilibrium values and available studies in the literature. The enhanced selectivity of the syngas components is associated with the exceptional heating mechanism of the microwave. The microwave selective heating promptly restricts the secondary gas-phase reactions due to the temperature gradient between the gas and solid phase and maintains a higher selectivity of the desired products.

Subsequently, in order to thoroughly clarify the effect of the microwave selective heating on the conversion of the reactants and selectivity of the desired products, Figure 7-4 demonstrates the cumulative results for the TDM reaction at 800^{o}C to 900^{o}C operating temperatures. The results have established that an optimal conversion of the reactants and selectivity of the products have been achieved simultaneously which is justified by the microwave selective heating mechanism. The results significantly exceeded equivalent conversion and selectivity values reported in the associated conventional heating studies in the literature, which is generally a compromise between the respective values (Usman et al., 2015). Hao *et al.* reported 63% and 69% conversion of methane and carbon dioxide, respectively, at 800^{o}C operating temperature for 10 gr of alumina-supported nickel catalyst in a fluidized bed conventional heated reactor (Hao, Zhu, Jiang, Hou, & Li, 2009), although an enhanced activity of the catalyst was reported by altering the preparation technique. Furthermore, Effendi *et al.* reported 63% and 69% conversion of methane and carbon dioxide, respectively at 750^{o}C operating temperature for 4.5 gr loading of a silica supported nickel catalyst in a fluidized bed conventional heated reactor. The conversion values declined while operating in a fixed bed reactor, accordingly (Effendi, Hellgardt, Zhang, & Yoshida, 2003). Moreover, Rahemi *et al.* stated 80% and 81% conversion of CH_4 and CO_2 respectively for 10 gr loading of an alumina- and zirconia oxide-supported nickel catalyst at 850^{o}C operating condition in a fluidized bed reactor (Rahemi, Haghighi, Babaluo, Jafari, & Estifaee, 2013). The effect of the catalyst preparation

method on the conversion of the reactants was further investigated. The superior conversion of the reactants in a microwave-assisted reactor is in compliance with the relevant investigations in the available literature which further verify the advantage of the MW heating mechanism (Domínguez, Fidalgo, Fernández, Pis, & Menéndez, 2007; Fidalgo et al., 2008; Menéndez, Domínguez, Fernández, & Pis, 2007). In general, in order to achieve high selectivity of the syngas components in a conventional heating reactor, the reactions are opted at lower reaction conversions to compromise for the production of the undesired gas-phase by-products, whereas in microwave-assisted DRM reaction, the production of the undesired gas-phase components is significantly restricted according to the exclusive heating mechanism of the microwave irradiation.

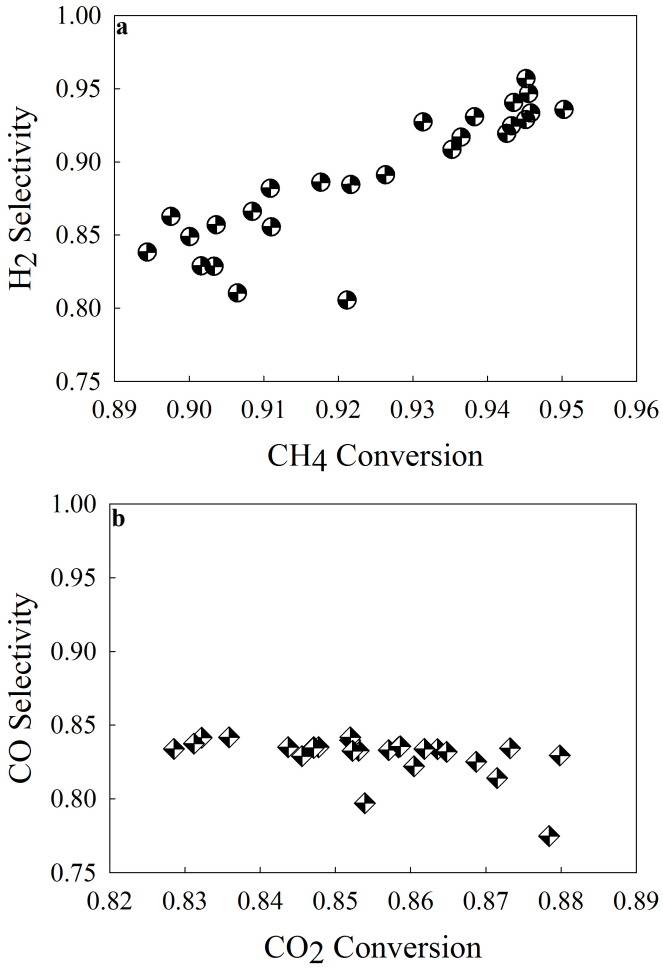

Figure 7-4: a) Selectivity of H_2 based on the conversion of CH_4 and b) Selectivity of CO based on the conversion of CO_2 at the operating temperature range of 800^{o}C to 900^{o}C

Ultimately, the effect of the microwave heating mechanism on the HiFUEL R110 catalyst deactivation has been investigated and demonstrated in Figure 7-5. It has been concluded that at high temperature ranges of 800^{o}C to 900^{o}C, the effect of catalyst deactivation is exceptionally enhanced. The results are associated with the dominance of the methane thermal degradation at high operating temperatures close to 900^{o}C (Dunker, Kumar, & Mulawa, 2006). Consequently, due to the enhanced kinetics of the methane decomposition reaction, CO_2 develops as the limiting reactant, and the kinetics of the carbon dioxide carbon gasification reaction (reversed CO disproportionation) fails to contest with the former, leading to an excess amount of carbon production. The enhanced production of the carbon mechanism further leads to the deactivation of the nickel-based catalyst by covering the active sites and preventing the adsorption of the reactants in the catalyst surface (Barrai et al., 2007). Subsequently, the catalyst was completely deactivated after 195 minutes of application at the CO_2/CH_4 ratio of unity and operating temperature range of 800^{o}C to 900^{o}C. Following the completion of the reaction, 8 gr of coke was recovered from the associated tubing.

It is noteworthy to acknowledge that since the effect of the microwave heating mechanism is exclusively observed on the performance of reactions on the catalyst active sites, the method is further recommended to distinguish between catalytic and gas-phase reaction. Consequently, the mechanism of the catalytic gas-solid reactions can be thoroughly defined by microwave heating-assisted investigation.

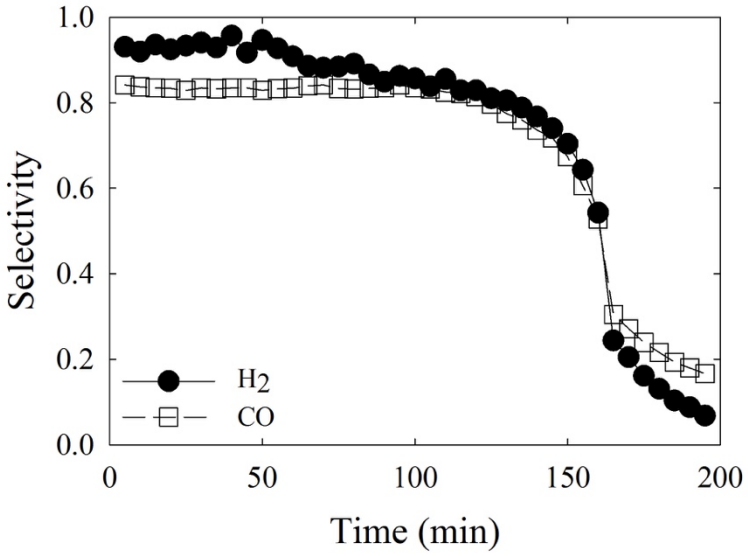

Figure 7-5: HiFUEL R110 catalyst deactivation as a function of time at 800°C to 900°C operating temperature range and CO_2/CH_4=1:1

7.5 Conclusion

In this study, microwave heating-assisted catalytic dry reforming of methane (DRM) was developed. Moreover, the temperature distribution of the solid particles, bulk and fluidizing gas, with the assistance of the experimental data obtained by the radiometry method and the associated correlations were studied. Hence, a significant temperature gradient between the solid particles, bed bulk and the gaseous components was observed where the results are associated with the microwave heating principles. Furthermore, the effect of the microwave heating mechanism on the conversion of the reactants, methane and carbon dioxide, selectivity of the desired products, hydrogen and carbon monoxide and the catalyst activity in a temperature range of 650°C to 900°C was thoroughly investigated. It was established that the microwave heating mechanism significantly enhances the conversion of the reactants while increasing the operating temperature. In addition, microwave heating maintained a high selectivity of both H_2 and CO at the operating temperature as low as 700°C which is a consequence of restricting the secondary gas-phase reactions, namely, water gas shift reaction (WGS) and CO disproportionation, while the catalyst remained active. It should be underscored that the microwave heating catalytic reactions concluded extremely high values for the conversion of the reactants and the selectivity of the products

simultaneously, which is in contradiction with the reported conventional heating mechanisms, while the values are exceptionally superior. Furthermore, due to the enhanced methane decomposition and lower kinetics of the CO_2 reactions, the excess carbonaceous material generated eventually blocked the active sites in the surface of the catalyst. Ultimately, microwave heating was proposed as an exceptional method to promote gas-solid endothermic catalytic reaction while simultaneously restricting the undesired secondary gas-phase by-products.

7.6 Acknowledgments

The authors are grateful to the Natural Sciences and Research Council of Canada (NSERC) through discovery grant and NSERC/Total chair for financial support of the project. The authors acknowledge Ms. Abidah Bachoo and Ms. Aya Kanso for their invaluable cooperation during the experiments through the undergraduate internship program. The authors further acknowledge the instrumental endeavors of Mr. Daniel Pilon for developing the experimental setup.

7.7 Nomenclature

7.7.1 Acronyms

DRM	Dry Reforming of Methane
FBCVD	Fluidized bed chemical vapour deposition
GC	Gas chromatographer
RWGS	Reverse water-gas shift reaction
WGS	Water-gas shift reaction
wt%	Total weight percentage

7.7.2 Symbols

c_{p_g}	Gas specific heat capacity (J/kgK)
c_{p_p}	Particles specific heat capacity (J/kgK)
ΔH	Enthalpy of reaction (kJ/mol)
ID	Inside diameter (cm)
OD	Outside diameter (cm)
T_b	Bulk temperature (K)
T_g	Gas temperature (K)
T_p	Particle surface temperature (K)

7.7.3 Greek Letters

ρ_g	As density (kg/m^3)
ρ_p	Particle density (kg/m^3)
ε	Bed voidage (-)
ε^*	Complex permittivity (-)
ε'	Dielectric constant (-)
ε''	Loss factor (-)
$\tan\delta$	Loss tangent (-)
τ_s	Space velocity (s)

7.8 References

Antti, A. L., & Perre, P. (1999). A microwave applicator for on line wood drying: Temperature and moisture distribution in wood. *Wood Science and Technology, 33*(2), 123-138.

Avetisov, A. K., Rostrup-Nielsen, J. R., Kuchaev, V. L., Bak Hansen, J. H., Zyskin, A. G., & Shapatina, E. N. (2010). Steady-state kinetics and mechanism of methane reforming with steam and carbon dioxide over Ni catalyst. *Journal of Molecular Catalysis A: Chemical, 315*(2), 155-162. doi: http://dx.doi.org/10.1016/j.molcata.2009.06.013

Barrai, F., Jackson, T., Whitmore, N., & Castaldi, M. J. (2007). The role of carbon deposition on precious metal catalyst activity during dry reforming of biogas. *Catalysis Today, 129*(3–4), 391-396. doi: http://dx.doi.org/10.1016/j.cattod.2007.07.024

Birol, F., & Argiri, M. (1999). World energy prospects to 2020. *Energy, 24*(11), 905-918.

BP. (2016). BP Energy Outlook 2016 Edition. London, UK: BP.

Bradford, M. C. J., & Vannice, M. A. (1996). Catalytic reforming of methane with carbon dioxide over nickel catalysts I. Catalyst characterization and activity. *Applied Catalysis A: General, 142*(1), 73-96. doi: http://dx.doi.org/10.1016/0926-860X(96)00065-8

Bradford, M. C. J., & Vannice, M. A. (1999). CO2 Reforming of CH4. *Catalysis Reviews, 41*(1), 1-42. doi: 10.1081/cr-100101948

Brungs, A. J., York, A. P. E., Claridge, J. B., Márquez-Alvarez, C., & Green, M. L. H. (2000). Dry reforming of methane to synthesis gas over supported molybdenum carbide catalysts. *Catalysis Letters, 70*(3), 117-122. doi: 10.1023/a:1018829116093

Budiman, A. W., Song, S.-H., Chang, T.-S., Shin, C.-H., & Choi, M.-J. (2012). Dry Reforming of Methane Over Cobalt Catalysts: A Literature Review of Catalyst Development. *Catalysis Surveys from Asia, 16*(4), 183-197. doi: 10.1007/s10563-012-9143-2

Christian Enger, B., Lødeng, R., & Holmen, A. (2008). A review of catalytic partial oxidation of methane to synthesis gas with emphasis on reaction mechanisms over transition metal catalysts. *Applied Catalysis A: General, 346*(1–2), 1-27. doi: http://dx.doi.org/10.1016/j.apcata.2008.05.018

Domínguez, A., Fidalgo, B., Fernández, Y., Pis, J. J., & Menéndez, J. A. (2007). Microwave-assisted catalytic decomposition of methane over activated carbon for CO2-free hydrogen production. *International Journal of Hydrogen Energy, 32*(18), 4792-4799. doi: http://dx.doi.org/10.1016/j.ijhydene.2007.07.041

Doucet, J., Laviolette, J.-P., Farag, S., & Chaouki, J. (2014). Distributed microwave pyrolysis of domestic waste. *Waste and Biomass Valorization, 5*(1), 1-10. doi: 10.1007/s12649-013-9216-0

Dunker, A. M., Kumar, S., & Mulawa, P. A. (2006). Production of hydrogen by thermal decomposition of methane in a fluidized-bed reactor—Effects of catalyst, temperature, and residence time. *International Journal of Hydrogen Energy, 31*(4), 473-484. doi: http://dx.doi.org/10.1016/j.ijhydene.2005.04.023

Edwards, R., Mahieu, V., Griesemann, J.-C., Larivé, J.-F., & Rickeard, D. J. (2004). Well-to-wheels analysis of future automotive fuels and powertrains in the European context: SAE Technical Paper.

Effendi, A., Hellgardt, K., Zhang, Z. G., & Yoshida, T. (2003). Characterisation of carbon deposits on Ni/SiO2 in the reforming of CH4–CO2 using fixed- and fluidised-bed reactors. *Catalysis Communications, 4*(4), 203-207. doi: http://dx.doi.org/10.1016/S1566-7367(03)00034-7

Eriksson, S., Wolf, M., Schneider, A., Mantzaras, J., Raimondi, F., Boutonnet, M., & Järås, S. (2006). Fuel-rich catalytic combustion of methane in zero emissions power generation processes. *Catalysis Today, 117*(4), 447-453.

Farag, S., Sobhy, A., Akyel, C., Doucet, J., & Chaouki, J. (2012). Temperature profile prediction within selected materials heated by microwaves at 2.45GHz. *Applied Thermal Engineering, 36*, 360-369. doi: Doi 10.1016/J.Applthermaleng.2011.10.049

Fidalgo, B., Domínguez, A., Pis, J. J., & Menéndez, J. A. (2008). Microwave-assisted dry reforming of methane. *International Journal of Hydrogen Energy, 33*(16), 4337-4344. doi: http://dx.doi.org/10.1016/j.ijhydene.2008.05.056

Folkins, H. O., Miller, E., & Hennig, H. (1950). Carbon Disulfide from Natural Gas and Sulfur. Reaction of Methane and Sulfur over a Silica Gel Catalyst. *Industrial & Engineering Chemistry, 42*(11), 2202-2207.

Gadalla, A. M., & Bower, B. (1988). The role of catalyst support on the activity of nickel for reforming methane with CO2. *Chemical Engineering Science, 43*(11), 3049-3062. doi: http://dx.doi.org/10.1016/0009-2509(88)80058-7

Gupta, M., & Wong, W. L. (2007). *Microwaves and metals*. Singapore: John Wiley & Sons.

Hamzehlouia, S., Latifi, M., & Chaouki, J. (2017). Development of a Novel Silica-Based Microwave Receptor for High Temperature Processes. *Pending submission*.

Hamzehlouia, S., Shabanian, J., Latifi, M., & Chaouki, J. (2017). Effect of Microwave Heating on the Performance of Catalytic Oxidation of n-Butane in a Gas-Solid Fluidized Bed Reactor. *Under preparation*.

Hao, Z., Zhu, Q., Jiang, Z., Hou, B., & Li, H. (2009). Characterization of aerogel Ni/Al2O3 catalysts and investigation on their stability for CH4-CO2 reforming in a fluidized bed. *Fuel Processing Technology, 90*(1), 113-121. doi: http://dx.doi.org/10.1016/j.fuproc.2008.08.004

Hickman, D. A., & Schmidt, L. D. (1993). Production of syngas by direct catalytic oxidation of methane. *Science-new york then washington-, 259*, 343-343.

Hou, Z., Chen, P., Fang, H., Zheng, X., & Yashima, T. (2006). Production of synthesis gas via methane reforming with CO on noble metals and small amount of noble-(Rh-) promoted Ni catalysts. *International Journal of Hydrogen Energy, 31*(5), 555-561. doi: http://dx.doi.org/10.1016/j.ijhydene.2005.06.010

Hu, Y. H., & Ruckenstein, E. (2002). Binary MgO-Based Solid Solution Catalysts for Methane Conversion to Syngas. *Catalysis Reviews, 44*(3), 423-453. doi: 10.1081/cr-120005742

Hu, Y. H., & Ruckenstein, E. (2004). Catalytic Conversion of Methane to Synthesis Gas by Partial Oxidation and CO2 Reforming *Advances in Catalysis* (Vol. Volume 48, pp. 297-345): Academic Press.

IEA. (2016). *Energy and Air Pollution*. Paris, France: Inetrational Energy Agency.

Istadi, I., Amin, N. A. S., & Aishah, N. (2005). Co-generation of C2 hydrocarbons and synthesis gases from methane and carbon dioxide: a thermodynamic analysis. *J. Nat. Gas Chem, 14*, 140-150.

Jablonski, E. L., Schmidhalter, I., De Miguel, S. R., Scelza, O. A., & Castro, A. A. (2005). *Dry reforming of methane on Pt/Al2O3–alkaline metal catalysts.* Paper presented at the 2nd mercosur congress on chemical engineering, Rio de.

Jones, C. A., Leonard, J. J., & Sofranko, J. A. (1987). Fuels for the future: remote gas conversion. *Energy & Fuels, 1*(1), 12-16. doi: 10.1021/ef00001a002

Jones, D. A., Lelyveld, T. P., Mavrofidis, S. D., Kingman, S. W., & Miles, N. J. (2002). Microwave heating applications in enviromnental engineering - a review. *Resources Conservation and Recycling, 34*(2), 75-90. doi: 10.1016/s0921-3449(01)00088-x

Khalesi, A., Arandiyan, H. R., & Parvari, M. (2008). Effects of Lanthanum Substitution by Strontium and Calcium in La-Ni-Al Perovskite Oxides in Dry Reforming of Methane. *Chinese Journal of Catalysis, 29*(10), 960-968. doi: http://dx.doi.org/10.1016/S1872-2067(08)60079-0

Koberstein, E. (1973). Model Reactor Studies of the Hydrogen Cyanide Synthesis from Methane and Ammonia. *Industrial & Engineering Chemistry Process Design and Development, 12*(4), 444-448. doi: 10.1021/i260048a010

Latifi, M., & Chaouki, J. (2015). A novel induction heating fluidized bed reactor: Its design and applications in high temperature screening tests with solid feedstocks and prediction of defluidization state. *Aiche Journal, 61*(5), 1507-1523. doi: 10.1002/aic.14749

Lavoie, J.-M. (2014). Review on dry reforming of methane, a potentially more environmentally-friendly approach to the increasing natural gas exploitation. *Frontiers in Chemistry, 2*, 81. doi: 10.3389/fchem.2014.00081

Lee, S. (1996). *Methane and its Derivatives* (Vol. 70): CRC Press.

Ma, J., Fang, M., Li, P., Zhu, B., Lu, X., & Lau, N. T. (1997). Microwave-assisted catalytic combustion of diesel soot. *Applied Catalysis A: General, 159*(1), 211-228. doi: http://dx.doi.org/10.1016/S0926-860X(97)00043-4

Menéndez, J. A., Domínguez, A., Fernández, Y., & Pis, J. J. (2007). Evidence of Self-Gasification during the Microwave-Induced Pyrolysis of Coffee Hulls. *Energy & Fuels, 21*(1), 373-378. doi: 10.1021/ef060331i

Metaxas, A. C., & Meredith, R. J. (1983). *Industrial microwave heating*. London, UK: P. Peregrinus on behalf of the Institution of Electrical Engineers.

Murray, E. P., Tsai, T., & Barnett, S. A. (1999). A direct-methane fuel cell with a ceria-based anode. *Nature, 400*(6745), 649-651.

Mushtaq, F., Mat, R., & Ani, F. N. (2014). A review on microwave assisted pyrolysis of coal and biomass for fuel production. *Renewable and Sustainable Energy Reviews, 39*(0), 555-574. doi: http://dx.doi.org/10.1016/j.rser.2014.07.073

Nikoo, M. K., & Amin, N. A. S. (2011). Thermodynamic analysis of carbon dioxide reforming of methane in view of solid carbon formation. *Fuel Processing Technology, 92*(3), 678-691. doi: http://dx.doi.org/10.1016/j.fuproc.2010.11.027

Ostrowski, T., Giroir-Fendler, A., Mirodatos, C., & Mleczko, L. (1998). Comparative study of the catalytic partial oxidation of methane to synthesis gas in fixed-bed and fluidized-bed membrane reactors: Part I: A modeling approach. *Catalysis Today, 40*(2), 181-190.

Pakhare, D., Shaw, C., Haynes, D., Shekhawat, D., & Spivey, J. (2013). Effect of reaction temperature on activity of Pt- and Ru-substituted lanthanum zirconate pyrochlores (La2Zr2O7) for dry (CO2) reforming of methane (DRM). *Journal of CO2 Utilization, 1*, 37-42. doi: http://dx.doi.org/10.1016/j.jcou.2013.04.001

Pakhare, D., & Spivey, J. (2014). A review of dry (CO2) reforming of methane over noble metal catalysts. *Chemical Society Reviews, 43*(22), 7813-7837. doi: 10.1039/c3cs60395d

Pert, E., Carmel, Y., Birnboim, A., Olorunyolemi, T., Gershon, D., Calame, J., . . . Wilson, O. C. (2001). Temperature measurements during microwave processing: The significance of thermocouple effects. *Journal of the American Ceramic Society, 84*(9), 1981-1986. doi: 10.1111/j.1151-2916.2001.tb00946.x

Pimentel, D., & Patzek, T. W. (2008). Biofuels, solar and wind as renewable energy systems. *Benefits and risks. New York: Springer*.

Podkolzin, S. G., Stangland, E. E., Jones, M. E., Peringer, E., & Lercher, J. A. (2007). Methyl chloride production from methane over lanthanum-based catalysts. *Journal of the American Chemical Society, 129*(9), 2569-2576.

Puskas, I. (1995). Natural gas to syncrude: Making the process pay off. *CHEMTECH, 25*(12).

Reitmeier, R. E., Atwood, K., Bennett, H. A., & Baugh, H. M. (1948). Production of Synthesis Gas by Reacting Light Hydrocarbons Wit Steam and Carbon Dioxide. *Ind. Eng. Chem., 40*, 620-626.

Rostrup-Nielsen, J. R. (1994). Catalysis and large-scale conversion of natural gas. *Catalysis Today, 21*(2), 257-267. doi: http://dx.doi.org/10.1016/0920-5861(94)80147-9

Roy, R., Agarwal, D., Chen, J. P., & Gedevanishvili, S. (1999). Full sintering of powdered-metal bodies in a microwave field. *Nature, 399*(6737), 668-670.

Saidur, R., Islam, M. R., Rahim, N. A., & Solangi, K. H. (2010). A review on global wind energy policy. *Renewable and Sustainable Energy Reviews, 14*(7), 1744-1762. doi: http://dx.doi.org/10.1016/j.rser.2010.03.007

Shafiee, S., & Topal, E. (2008). An econometrics view of worldwide fossil fuel consumption and the role of US. *Energy Policy, 36*(2), 775-786. doi: http://dx.doi.org/10.1016/j.enpol.2007.11.002

Shafiee, S., & Topal, E. (2009). When will fossil fuel reserves be diminished? *Energy Policy, 37*(1), 181-189. doi: http://dx.doi.org/10.1016/j.enpol.2008.08.016

Sloan, E. D. (2003). Fundamental principles and applications of natural gas hydrates. *Nature, 426*(6964), 353-363.

Sobhy, A., & Chaouki, J. (2010). Microwave-assisted Biorefinery. *Cisap4: 4th International Conference on Safety & Environment in Process Industry, 19*, 25-29. doi: Doi 10.3303/Cet1019005

Solangi, K. H., Islam, M. R., Saidur, R., Rahim, N. A., & Fayaz, H. (2011). A review on global solar energy policy. *Renewable and Sustainable Energy Reviews, 15*(4), 2149-2163. doi: http://dx.doi.org/10.1016/j.rser.2011.01.007

Timilsina, G. R., Kurdgelashvili, L., & Narbel, P. A. (2012). Solar energy: Markets, economics and policies. *Renewable and Sustainable Energy Reviews, 16*(1), 449-465. doi: http://dx.doi.org/10.1016/j.rser.2011.08.009

Timmons, D., Harris, J. M., & Roach, B. (2014). The economics of renewable energy. *Global Development And Environment Institute, Tufts University*, 52.

Tsai, H. L., & Wang, C. S. (2008). Thermodynamic equilibrium prediction for natural gas dry reforming in thermal plasma reformer. *Journal of the Chinese Institute of Engineers, 31*(5), 891-896.

Turner, J. A. (1999). A Realizable Renewable Energy Future. *Science, 285*(5428), 687-689. doi: 10.1126/science.285.5428.687

Uhlig, H. H., & Keyes, F. G. (1933). The Dependence of the Dielectric Constants of Gases on Temperature and Density. *The Journal of Chemical Physics, 1*(2), 155-159.

Usman, M., Wan Daud, W. M. A., & Abbas, H. F. (2015). Dry reforming of methane: Influence of process parameters—A review. *Renewable and Sustainable Energy Reviews, 45*, 710-744. doi: http://dx.doi.org/10.1016/j.rser.2015.02.026

Vernon, P. D. F., Green, M. L. H., Cheetham, A. K., & Ashcroft, A. T. (1990). Partial oxidation of methane to synthesis gas. *Catalysis Letters, 6*(2), 181-186.

Vos, B., Mosman, J., Zhang, Y., Poels, E., & Bliek, A. (2003). Impregnated carbon as a susceptor material for low loss oxides in dielectric heating. *Journal of Materials Science, 38*(1), 173-182. doi: 10.1023/a:1021138505264

Wang, S., Lu, G. Q., & Millar, G. J. (1996). Carbon Dioxide Reforming of Methane To Produce Synthesis Gas over Metal-Supported Catalysts: State of the Art. *Energy & Fuels, 10*(4), 896-904. doi: 10.1021/ef950227t

White, G. A., Roszkowski, T. R., & Stanbridge, D. W. (1975). Predict carbon formation.[Synthesis gas and SNG operations]. *Hydrocarbon Process.;(United States), 54*(7).

Wiesbrock, F., Hoogenboom, R., & Schubert, U. S. (2004). Microwave-assisted polymer synthesis: State-of-the-art and future perspectives. *Macromolecular Rapid Communications, 25*(20), 1739-1764. doi: 10.1002/marc.200400313

Wiser, R., Bolinger, M., Barbose, G., Darghouth, N., Hoen, B., Mills, A., . . . Widiss, R. 2015 Wind Technologies Market Report. *Energy Efficiency and Renewable Energy*.

CHAPTER 8 GENERAL DISCUSSION

Methane conversion reactions are an integral part of the chemical production and energy sector. Whereas, such reactions extensively facilitate the transportation and the handling of the methane-deviated products. However, due to the diverse thermodynamic equilibria, evolution of undesired by-products via the secondary gas-phase reactions profoundly affects the selectivity of the syngas components and the general performance of the reactions, accordingly. Meanwhile, various endeavours concentrated on the catalyst systems performance and structure optimizations have fail to fulfill the technical and economical requirements of the industrial applications. While multiple studies associated with the role of the particle have been presented in the available literature, however, the lack of investigations regarding the effect of the heating method on the performance of the reactions is evident. Meanwhile, development of sustainable and environmental friendly renewable energies, namely, solar and wind power, has provided the opportunity to produce affordable and widespread renewable electricity. Hence, the production of the renewable electricity justifies the application of the electrical heating methods, namely, induction heating, microwave heating and sonication, for the chemical reactions, correspondingly. Consequently, the exclusive microwave selective heating mechanism, provides an esteemed opportunity to optimize the performance of the gas-solid catalytic reactions, namely, catalytic conversion of methane to syngas. Whereas, while the active site of the dielectric catalyst system promotes the catalytic reactions at a higher temperature, the secondary gas-phase reactions are promptly restricted due to the significantly lower temperature of the gas phase. The temperature gradient between the solid and gas phases is associated with the incompetency of the gaseous material to project significant microwave interaction due to the insignificant dielectric properties. The present study, has deployed the exclusive microwave selecting mechanism for the catalytic dry reforming of methane, as an innovative method to optimize the performance of the reaction towards high conversion of the reactants, CO_2 and CH_4, and high selectivity of the products, CO and H_2, simultaneously.

In the first part of this work, a novel microwave receptor was developed by carbon coating of silica sand particles through fluidized bed chemical vapor deposition (FDCVD) in an induction heating stainless steel reactor. Silica sand (SiO_2) particles as the substrate and methane (CH_4) as carbon precursor were employed for successful coating of the base material. The required carbon was produced through thermal degradation of methane (TDM) in the absence of any catalyst. The

reaction was implemented at 800, 900 and 1000^{o}C temperatures and 60-,120- and 240-minute reaction times to study the effect of operating conditions on the quality and composition of the coated layer. TGA results exposed the carbon content of the coating layer for coated samples produced under a wide range of reaction temperatures and durations. Moreover, TGA results investigated the thermal resistivity of the receptor particles under air and verified the upper threshold of 600^{o}C. Furthermore, combustion infrared carbon detection (LECO) tests further substantiated the effect of reaction temperature and time on the carbon composition of the samples, whose outcome was in compliance with the TGA results. It was concluded that increasing both reaction temperature and time significantly affects the deposition of carbon on the silica sand particles, although temperature dominated the coating mechanism, from 0.1% for the base sand material to 2.8% for 1000^{o}C and 240 minutes operating conditions. The morphological study of the samples with microscopic analysis methods disclosed valuable information regarding the dependence of reaction time and temperature on the coating layer uniformity and thickness. The SEM imaging helped infer the TDM temperature and time impacts on the uniformity of the coated surface. The combination of FIB milling with SEM imaging denoted the effect of CVD operational conditions on the coating layer thickness and quantified carbon deposition on the receptor samples. Eventually, XPS and EDX results provided a discrete analysis of the coating surface composition, revealing the ratio of carbon content to the core sand structural elements, thus quantifying the coating homogeneity of the deposition layer. Furthermore, the microwave performance of the carbon-coated sand receptors was investigated in a single-mode microwave apparatus. The heat generation mechanism of each sample was studied by microwave exposure from room temperature of 25^{o}C to a designated 500^{o}C temperature, while monitoring the temperature profile. Initially, samples with low TDM temperature and time failed to fulfill the minimum heating rate requirements to reach the designated temperature value. However, samples produced under higher reaction temperatures and times succeeded the microwave heating performance test in a matter of seconds, confirming the effect of FBCVD operating conditions on the dielectric properties of the receptor particles. Furthermore, the effect of microwave power on the heating performance of samples coated at extended 240minute period was investigated at 0.1-, 0.2- and 0.3- amp microwave power cycles. Moreover, the operational durability of the particles to surficial erosion and attrition was investigated by exposing the samples to repeated cycles of experimental conditions and evaluating the results. The durability tests revealed the significant resistance of the

samples to operating conditions, thus validating the use of the receptor particles for multiple applications. Ultimately, the microwave performance of various graphite and sand mixtures at different microwave power values were observed to compare the results with the behaviour of the novel receptors. It was highlighted that while mixtures with low graphite to sand composition failed to fulfill the heating tests, samples with higher graphite compositions (90%) showed a similar performance as our higher-grade coated receptors. Considering the maximum 2.8% carbon content of the coated receptors, the results emphasized the substantial effect of the carbon layer uniformity on the carbon content. Ultimately, the effect of deposited carbon composition and output power on the microwave heating rate was investigated for the novel receptors. It was strongly recommended to engage the developed silica based carbon coated microwave receptors simultaneously as a catalyst support or promoter to optimize gas-solid reactions based on the established characteristics of the particles.

In the second part of this work, the effect of the conventional and microwave heating mechanisms on the performance of the selective oxidation of n-butane over the fluidized vanadium phosphorous oxide catalyst to produce maleic anhydride, in an industrial-scale fluidized bed reactor was simulated. The reaction was proposed as a model for selective oxidation of hydrocarbons in general. The simulation study intended to address the formation of the secondary gas-phase side products and their destructive effect on the selectivity of the desired products as the major productivity issue of the selective oxidation reactions, accordingly. Whereas, based on the exclusive microwave heating mechanism, the dielectric components, catalyst or the support material, project significantly higher temperature compared to the gaseous components, which the established temperature gradient between the solid and gas phase restricts the prosper of the secondary gas-phase reactions correspondingly. Due to the complexity of the direct gas temperature measurement, correlations were proposed, with the assistance of solid and bulk temperature measurements in a lab-scale microwave heated fluidized bed reactor and a general energy balance. The correlations were employed to study the effect of the heating mechanism on the conversion of n-C_4 and the selectivity of MAN in the simulation study. The simulation results exhibited a significantly higher selectivity of MAN for microwave heating reaction at multiple superficial gas velocities. Moreover, it was established that the conversion of n-C_4 was superior during the microwave heating-assisted reaction in case the effect of the heating mechanism on the kinetic parameters, namely, pre-exponential factor, was contemplated. Consequently, it was

proposed that by optimizing the performance of the catalyst, microwave heating mechanism can enhance the productivity of the selective oxidation reactions to a conversion and selectivity simultaneously which is substantial for the industrial applications. Finally, deliberating the distinctive thermal behavior of the catalytic and gas-phase reactions, microwave heating mechanism was recommended to identify the mechanism of the catalytic gas-solid reactions, by distinguishing the solid phase and gas phase reactions, accordingly.

Finally, in the third part of this work, microwave heating-assisted catalytic dry reforming of methane (DRM) was developed. Moreover, the temperature distribution of the solid particles, bulk and fluidizing gas, with the assistance of the experimental data obtained by the radiometry method and the associated correlations were studied. Hence, a significant temperature gradient between the solid particles, bed bulk and the gaseous components were observed were the results are associated with the microwave heating mechanism principles. Furthermore, the effect of the microwave heating mechanism on the conversion of the reactants, methane and carbon dioxide, selectivity of the desired products, hydrogen and carbon monoxide and the catalyst activity in a temperature range of 650^{o}C to 900^{o}C was thoroughly investigated. It was established that microwave heating mechanism enhances the conversion of the reactants significantly while increasing the operating temperature. In addition, microwave heating maintained a high selectivity of both H_2 and CO at the operating temperature as low as 700^{o}C which is a consequence of restricting the secondary gas-phase reactions, namely, water gas shift reaction (WGS) and CO disproportionation, while the catalyst remained active. It should be underlined that the microwave heating catalytic reactions concluded extremely high values for the conversion of the reactants and the selectivity of the products simultaneously, which is in contrast with the reported conventional heating mechanisms, while the values are exceptionally superior. Furthermore, due to the enhanced methane decomposition and lower kinetics of the CO_2 reactions the excess carbonaceous material generated eventually blocked the active sites in the surface of the catalyst. Ultimately, microwave heating was proposed as an exceptional method to promote gas-solid endothermic catalytic reaction while simultaneously restricting the undesired secondary gas-phase by-products.

CHAPTER 9 CONCLUSION AND RECOMMENDATIONS

The main objective of this thesis was to optimize gas-solid catalytic reactions with the application of the microwave exclusive heating mechanism. Consequently, dry reforming of methane was selected and the effect of microwave radiation on the performance of the reaction was investigated.

Thus, in the first part of this study, a microwave receptor was developed by fluidized bed chemical vapor deposition (FBCVD) of carbon using methane over silica sand substrate material in an induction heating setup. The effect of the operating conditions, namely temperature (800, 900 and 1000 ^{o}C) and reaction time (60, 120 and 240 minutes), on the properties of the coating layer was attained. The composition, thickness and morphology of the developed carbo-coating layer for multiple operating conditions were further investigated, accordingly. Ultimately, the performance of the developed carbon-coated silica sand particles (C-SiO_2) in a lab-scale microwave heating-assisted fluidized bed reactor was thoroughly evaluated. It was demonstrated that the C-SiO_2 particles exhibited exceptional microwave intractability according to significant dielectric properties of the material. The developed C-SiO_2 particles were further recommended for application as microwave receptor and catalyst support/promoter in gas-solid catalytic reactions.

In the second part of this study, the effect of microwave heating mechanism on a gas-solid selective oxidation reaction was investigated by simulation of n-C4 conversion to MAN on the VOP catalyst in an industrial-scale fluidized bed reactor. It was exhibited that based on the dielectric properties of components a temperature gradient endures between the gas and the solid phases accordingly. Due to the inability for direct measurement of the gas temperature profile, the solid surface and bulk temperature profiles were demonstrated with the assistance of radiometry and thermometry methods in a lab-sale microwave heated fluidized bed reactor. Hence, the effect of operating conditions, temperature and superficial gas velocity, were investigated on the associated temperature profiles. Furthermore, correlations were proposed to estimate the gas temperature profile with the bed employing experimental data and an energy balance. The temperature profile of solids, bulk and gas were further deployed to compare (conventional vs microwave heating) the conversion of n-C4 and selectivity of MAN in the simulation study. The results revealed microwave heating superior in terms of the reaction productivity.

In the third and final part of this theses, dry reforming of methane in a lab-scale microwave heating-assisted fluidized bed reactor was performed to study the effect of the heating mechanism on the

evolution of the products. Whereas, the effect of the operating temperature on the conversion of the reactants and the selectivity of the desired products, H_2 and CO was thoroughly investigated. It was concluded that microwave heating promoted catalytic reactions while restricting the secondary undesired gas-phase reactions. The results were associated with high conversion of the reactants, CO_2 and CH_4 and high selectivity of the desire products, H_2 and CO, simultaneously.

Base on the discussions, the following recommendations for future research has been proposed:

1) To study the effect of the substrate material and the carbon precursor on the performance of the developed receptors;
2) To study the effect of microwave heating on the kinetic parameters of the reaction, namely, pre-exponential factor (k_0) and the activation energy (E);
3) To study the effect of the microwave frequency on the performance of the reactions;
4) To develop catalyst systems, using C-SiO_2 particles as the support material;
5) To compare the kinetics of the reactions in a microwave-heated reactor with a conventional heating reactor, experimentally;
6) To extend the application of microwave heating and study the corresponding effect on other methane conversion methods, namely, partial oxidation and dry reforming; and
7) To study the mechanism of the gas-solid catalytic reactions with the assistance of the microwave selective heating mechanism.

BIBLIOGRAPHY

Aasberg-Petersen, K., Bak Hansen, J. H., Christensen, T. S., Dybkjaer, I., Christensen, P. S., Stub Nielsen, C., . . . Rostrup-Nielsen, J. R. (2001). Technologies for large-scale gas conversion. *Applied Catalysis A: General, 221*(1–2), 379-387. doi:http://dx.doi.org/10.1016/S0926-860X(01)00811-0

Altman, J. L. (1964). *Microwave circuits*: Van Nostrand Reinhold.

Antti, A. L., & Perre, P. (1999). A microwave applicator for on line wood drying: Temperature and moisture distribution in wood. *Wood Science and Technology, 33*(2), 123-138.

Archer, N. J. (1979). Chemical vapour deposition. *Physics in Technology, 10*(4), 152.

Ashcroft, A. T., Cheetham, A. K., & Green, M. (1991). Partial oxidation of methane to synthesis gas using carbon dioxide. *Nature, 352*(6332), 225-226.

Ashcroft, A. T., Cheetham, A. K., Green, M. L. H., & Vernon, P. D. F. (1991). Partial oxidation of methane to synthesis gas using carbon dioxide. *Nature, 352*(6332), 225-226.

Avetisov, A. K., Rostrup-Nielsen, J. R., Kuchaev, V. L., Bak Hansen, J. H., Zyskin, A. G., & Shapatina, E. N. (2010). Steady-state kinetics and mechanism of methane reforming with steam and carbon dioxide over Ni catalyst. *Journal of Molecular Catalysis A: Chemical, 315*(2), 155-162. doi:http://dx.doi.org/10.1016/j.molcata.2009.06.013

Ballarini, A. D., de Miguel, S. R., Jablonski, E. L., Scelza, O. A., & Castro, A. A. (2005). Reforming of CH4 with CO2 on Pt-supported catalysts: Effect of the support on the catalytic behaviour. *Catalysis Today, 107–108*, 481-486. doi:http://dx.doi.org/10.1016/j.cattod.2005.07.058

Barrai, F., Jackson, T., Whitmore, N., & Castaldi, M. J. (2007). The role of carbon deposition on precious metal catalyst activity during dry reforming of biogas. *Catalysis Today, 129*(3–4), 391-396. doi:http://dx.doi.org/10.1016/j.cattod.2007.07.024

Bartholomew, C. H. (1982). Carbon Deposition in Steam Reforming and Methanation. *Catalysis Reviews, 24*(1), 67-112. doi:10.1080/03602458208079650

Beiter, P., & Tian, T. (2016). *2015 Renewable Energy Data Book*. Retrieved from

Bengtsson, N. E., & Risman, P. D. (1971). Dielectric properties of foods at 3 GHz as determined by cavity perturbation technique. *J. Microwave Power, 6*(2).

Besmann, T. M., Seldon, B. W., Lowden, R. A., & Stinton, D. P. (1991). Vapor-Phase Fabrication and Properties of Continuous-Filament Ceramic Composites. *Science, 253*(5024), 1104-1109. doi:10.1126/science.253.5024.1104

Birol, F., & Argiri, M. (1999). World energy prospects to 2020. *Energy, 24*(11), 905-918.

Bleaney, B. I., & Bleaney, B. (1965). *Electricity and magnetism* (Vol. 236): Clarendon Press Oxford.

BP. (2011). *BP Statistical Review of World Energy 2011*. Retrieved from London, UK:

BP. (2016a). *BP Energy Outlook 2016 Edition*. Retrieved from London, UK:

BP. (2016b). *BP Statistical Review of World Energy 2016*. Retrieved from London, UK:

Bradford, M. C. J., & Vannice, M. A. (1996). Catalytic reforming of methane with carbon dioxide over nickel catalysts I. Catalyst characterization and activity. *Applied Catalysis A: General, 142*(1), 73-96. doi:http://dx.doi.org/10.1016/0926-860X(96)00065-8

Bradford, M. C. J., & Vannice, M. A. (1999). CO2 Reforming of CH4. *Catalysis Reviews, 41*(1), 1-42. doi:10.1081/cr-100101948

Brungs, A. J., York, A. P. E., Claridge, J. B., Márquez-Alvarez, C., & Green, M. L. H. (2000). Dry reforming of methane to synthesis gas over supported molybdenum carbide catalysts. *Catalysis Letters, 70*(3), 117-122. doi:10.1023/a:1018829116093

Budiman, A. W., Song, S.-H., Chang, T.-S., Shin, C.-H., & Choi, M.-J. (2012). Dry Reforming of Methane Over Cobalt Catalysts: A Literature Review of Catalyst Development. *Catalysis Surveys from Asia, 16*(4), 183-197. doi:10.1007/s10563-012-9143-2

Caddick, S. (1995). Microwave Assisted Organic Reactions. *Tetrahedron, 51*(38), 10403-10432. doi:10.1016/0040-4020(95)00662-r

Campañone, L. A., & Zaritzky, N. E. (2005). Mathematical analysis of microwave heating process. *Journal of Food Engineering, 69*(3), 359-368. doi:http://dx.doi.org/10.1016/j.jfoodeng.2004.08.027

Carrasco, J. M., Franquelo, L. G., Bialasiewicz, J. T., Galvan, E., PortilloGuisado, R. C., Prats, M. A. M., . . . Moreno-Alfonso, N. (2006). Power-Electronic Systems for the Grid Integration of Renewable Energy Sources: A Survey. *IEEE Transactions on Industrial Electronics, 53*(4), 1002-1016. doi:10.1109/tie.2006.878356

Centi, G., Fornasari, G., & Trifiro, F. (1985). n-Butane oxidation to maleic anhydride on vanadium-phosphorus oxides: kinetic analysis with a tubular flow stacked-pellet reactor. *Industrial & Engineering Chemistry Product Research and Development, 24*(1), 32-37. doi:10.1021/i300017a007

Chen, J. C., Grace, J. R., & Golriz, M. R. (2005). Heat transfer in fluidized beds: design methods. *Powder Technology, 150*(2), 123-132. doi:http://dx.doi.org/10.1016/j.powtec.2004.11.035

Chen, J. D., & Sheldon, R. A. (1995). Selective Oxidation of Hydrocarbons with O2 over Chromium Aluminophosphate-5 Molecular-Sieve. *Journal of Catalysis, 153*(1), 1-8. doi:http://dx.doi.org/10.1006/jcat.1995.1101

Chen, X., Honda, K., & Zhang, Z.-G. (2005). CO2CH4 reforming over NiO/γ-Al2O3 in fixed/fluidized-bed multi-switching mode. *Applied Catalysis A: General, 279*(1–2), 263-271. doi:http://doi.org/10.1016/j.apcata.2004.10.041

Chen, Y.-G., Tomishige, K., & Fujimoto, K. (1997). Formation and characteristic properties of carbonaceous species on nickel-magnesia solid solution catalysts during CH4CO2 reforming reaction. *Applied Catalysis A: General, 161*(1), L11-L17. doi:http://dx.doi.org/10.1016/S0926-860X(97)00106-3

Choudhary, V. R., Rajput, A. M., & Prabhakar, B. (1995). Energy efficient methane-to-syngas conversion with low H2/CO ratio by simultaneous catalytic reactions of methane with carbon dioxide and oxygen. *Catalysis Letters, 32*(3), 391-396. doi:10.1007/bf00813234

Choy, K. L. (2003). Chemical vapour deposition of coatings. *Progress in Materials Science, 48*(2), 57-170. doi:http://dx.doi.org/10.1016/S0079-6425(01)00009-3

Christian Enger, B., Lødeng, R., & Holmen, A. (2008). A review of catalytic partial oxidation of methane to synthesis gas with emphasis on reaction mechanisms over transition metal catalysts. *Applied Catalysis A: General, 346*(1–2), 1-27. doi:http://dx.doi.org/10.1016/j.apcata.2008.05.018

Chubb, T. A. (1980). Characteristics of CO2-CH4 reforming-methanation cycle relevant to the solchem thermochemical power system. *Solar Energy, 24*(4), 341-345. doi:http://dx.doi.org/10.1016/0038-092X(80)90295-9

Ciacci, T., Galgano, A., & Di Blasi, C. (2010). Numerical simulation of the electromagnetic field and the heat and mass transfer processes during microwave-induced pyrolysis of a wood block. *Chemical Engineering Science, 65*(14), 4117-4133. doi:http://dx.doi.org/10.1016/j.ces.2010.04.039

Clark, D. E., Folz, D. C., & West, J. K. (2000). Processing materials with microwave energy. *Materials Science and Engineering: A, 287*(2), 153-158. doi:http://dx.doi.org/10.1016/S0921-5093(00)00768-1

Contractor, R. M. (1999). Dupont's CFB technology for maleic anhydride. *Chemical Engineering Science, 54*(22), 5627-5632. doi:http://dx.doi.org/10.1016/S0009-2509(99)00295-X

Contractor, R. M., Bergna, H. E., Horowitz, H. S., Blackstone, C. M., Chowdhry, U., & Sleight, A. W. (1988). Butane Oxidation to Maleic Anhydride in A Recirculating Solids Reactor. *Studies in Surface Science and Catalysis, 38*, 645-654. doi:http://dx.doi.org/10.1016/S0167-2991(09)60694-7

Couderc, D., Giroux, M., & Bosisio, R. G. (1973). Dynamic High-Temperature Microwave Complex Permittivity Measurements on Samples Heated via Microwave Absorption. *J. Microwave Power, 8*, 69.

Crisafulli, C., Scirè, S., Minicò, S., & Solarino, L. (2002). Ni–Ru bimetallic catalysts for the CO2 reforming of methane. *Applied Catalysis A: General, 225*(1–2), 1-9. doi:http://doi.org/10.1016/S0926-860X(01)00585-3

Cui, H., Mostoufi, N., & Chaouki, J. (2000). Characterization of dynamic gas-solid distribution in fluidized beds. *Chemical Engineering Journal, 79*(2), 133-143. doi:Doi: 10.1016/s1385-8947(00)00178-9

Dahl, J. K., Buechler, K. J., Weimer, A. W., Lewandowski, A., & Bingham, C. (2004). Solar-thermal dissociation of methane in a fluid-wall aerosol flow reactor. *International Journal of Hydrogen Energy, 29*(7), 725-736. doi:http://dx.doi.org/10.1016/j.ijhydene.2003.08.009

Dahl, J. K., Tamburini, J., Weimer, A. W., Lewandowski, A., Pitts, R., & Bingham, C. (2001). Solar-Thermal Processing of Methane to Produce Hydrogen and Syngas. *Energy & Fuels, 15*(5), 1227-1232. doi:10.1021/ef0100606

Danafar, F., Fakhru'l-Razi, A., Salleh, M. A. M., & Biak, D. R. A. (2009). Fluidized bed catalytic chemical vapor deposition synthesis of carbon nanotubes—A review. *Chemical Engineering Journal, 155*(1–2), 37-48. doi:http://dx.doi.org/10.1016/j.cej.2009.07.052

Daniel, V. V. (1967). *Dielectric relaxation* (Vol. 967): Academic Press London.

Das, S., Mukhopadhyay, A. K., Datta, S., & Basu, D. (2009). Prospects of microwave processing: An overview. *Bulletin of Materials Science, 32*(1), 1-13. doi:10.1007/s12034-009-0001-4

Davies, J. (1990). *Conduction and induction heating* (Vol. 11): IET.

Debye, P. J. W. (1929). *Polar molecules* (Vol. 172): Dover New York.

Dibbern, H. C., Olesen, P., Rostrup-Nielsen, J. R., Tottrup, P. B., & Udengaard, N. R. (1986). Make low H/sub 2//CO syngas using sulfur passivated reforming. *Hydrocarbon Process.;(United States), 65*(1).

Dicke, R. H., Montgomery, C. G., & Purcell, E. M. Principles of microwave circuits, 1948: McGraw-Hill.

Djinović, P., Osojnik Črnivec, I. G., Erjavec, B., & Pintar, A. (2012). Influence of active metal loading and oxygen mobility on coke-free dry reforming of Ni–Co bimetallic catalysts. *Applied Catalysis B: Environmental, 125*, 259-270. doi:http://doi.org/10.1016/j.apcatb.2012.05.049

Dominguez, A., Fernandez, Y., Fidalgo, B., Pis, J. J., & Menendez, J. A. (2007). Biogas to syngas by microwave-assisted dry reforming in the presence of char. *Energy & Fuels, 21*(4), 2066-2071. doi:Doi 10.1021/Ef070101j

Domínguez, A., Fidalgo, B., Fernández, Y., Pis, J. J., & Menéndez, J. A. (2007). Microwave-assisted catalytic decomposition of methane over activated carbon for CO2-free hydrogen

production. *International Journal of Hydrogen Energy, 32*(18), 4792-4799. doi:http://dx.doi.org/10.1016/j.ijhydene.2007.07.041

Dominguez, A., Menendez, J. A., Fernandez, Y., Pis, J. J., Nabais, J. M. V., Carrott, P. J. M., & Carrott, M. M. L. R. (2007). Conventional and microwave induced pyrolysis of coffee hulls for the production of a hydrogen rich fuel gas. *Journal of Analytical and Applied Pyrolysis, 79*(1-2), 128-135. doi:Doi 10.1016/J.Jaap.2006.08.003

Doucet, J., Laviolette, J.-P., Farag, S., & Chaouki, J. (2014). Distributed microwave pyrolysis of domestic waste. *Waste and Biomass Valorization, 5*(1), 1-10. doi:10.1007/s12649-013-9216-0

Dry, M. E. (2002). The Fischer–Tropsch process: 1950–2000. *Catalysis Today, 71*(3–4), 227-241. doi:http://dx.doi.org/10.1016/S0920-5861(01)00453-9

Dunker, A. M., Kumar, S., & Mulawa, P. A. (2006). Production of hydrogen by thermal decomposition of methane in a fluidized-bed reactor—Effects of catalyst, temperature, and residence time. *International Journal of Hydrogen Energy, 31*(4), 473-484. doi:http://dx.doi.org/10.1016/j.ijhydene.2005.04.023

Dunker, A. M., & Ortmann, J. P. (2006). Kinetic modeling of hydrogen production by thermal decomposition of methane. *International Journal of Hydrogen Energy, 31*(14), 1989-1998. doi:http://dx.doi.org/10.1016/j.ijhydene.2006.01.013

Dunn, D. A. (1967). Slow wave couplers for microwave dielectric heating systems.

Dyrssen, D., Turner, D., Paul, J., & Pradier, C. (1994). Carbon Dioxide Chemistry: Environmental Issues: Athenaeum Press, Cambridge.

Edwards, J. H., & Maitra, A. M. (1995). The chemistry of methane reforming with carbon dioxide and its current and potential applications. *Fuel Processing Technology, 42*(2), 269-289. doi:http://dx.doi.org/10.1016/0378-3820(94)00105-3

Edwards, R., Mahieu, V., Griesemann, J.-C., Larivé, J.-F., & Rickeard, D. J. (2004). *Well-to-wheels analysis of future automotive fuels and powertrains in the European context* (0148-7191). Retrieved from

Effendi, A., Hellgardt, K., Zhang, Z. G., & Yoshida, T. (2003). Characterisation of carbon deposits on Ni/SiO2 in the reforming of CH4–CO2 using fixed- and fluidised-bed reactors. *Catalysis Communications, 4*(4), 203-207. doi:http://dx.doi.org/10.1016/S1566-7367(03)00034-7

EPA. (2015). Overview of Greenhouse Gases. Retrieved from https://www.epa.gov/ghgemissions/overview-greenhouse-gases

Eriksson, S., Wolf, M., Schneider, A., Mantzaras, J., Raimondi, F., Boutonnet, M., & Järås, S. (2006). Fuel-rich catalytic combustion of methane in zero emissions power generation processes. *Catalysis Today, 117*(4), 447-453.

Farag, S., & Chaouki, J. (2015). A modified microwave thermo-gravimetric-analyzer for kinetic purposes. *Applied Thermal Engineering, 75*, 65-72. doi:http://dx.doi.org/10.1016/j.applthermaleng.2014.09.038

Farag, S., Fu, D., Jessop, P. G., & Chaouki, J. (2014). Detailed compositional analysis and structural investigation of a bio-oil from microwave pyrolysis of kraft lignin. *Journal of Analytical and Applied Pyrolysis, 109*(0), 249-257. doi:http://dx.doi.org/10.1016/j.jaap.2014.06.005

Farag, S., Kouisni, L., & Chaouki, J. (2014). Lumped approach in kinetic modeling of microwave pyrolysis of kraft lignin. *Energy & Fuels, 28*(2), 1406-1417. doi:10.1021/ef4023493

Farag, S., Sobhy, A., Akyel, C., Doucet, J., & Chaouki, J. (2012). Temperature profile prediction within selected materials heated by microwaves at 2.45GHz. *Applied Thermal Engineering, 36*, 360-369. doi:Doi 10.1016/J.Applthermaleng.2011.10.049

Fidalgo, B., Domínguez, A., Pis, J. J., & Menéndez, J. A. (2008). Microwave-assisted dry reforming of methane. *International Journal of Hydrogen Energy, 33*(16), 4337-4344. doi:http://dx.doi.org/10.1016/j.ijhydene.2008.05.056

Fisher, F., & Tropsch, H. (1928). Conversion of methane into hydrogen and carbon monoxide. *Brennst.-Chem., 9*.

Folkins, H. O., Miller, E., & Hennig, H. (1950). Carbon Disulfide from Natural Gas and Sulfur. Reaction of Methane and Sulfur over a Silica Gel Catalyst. *Industrial & Engineering Chemistry, 42*(11), 2202-2207.

Fraenkel, D., Levitan, R., & Levy, M. (1986). A solar thermochemical pipe based on the CO2-CH4 (1:1) system. *International Journal of Hydrogen Energy, 11*(4), 267-277. doi:http://dx.doi.org/10.1016/0360-3199(86)90187-4

Francis, G. (1960). *Ionization phenomena in gases*: Butterworths Scientific Publications London.

Fröhlich, H. (1958). Theory of dielectrics. *Clarendon, Oxford*.

Gabriel, C., Gabriel, S., H. Grant, E., H. Grant, E., S. J. Halstead, B., & Michael P. Mingos, D. (1998). Dielectric parameters relevant to microwave dielectric heating. *Chemical Society Reviews, 27*(3), 213-224. doi:10.1039/A827213Z

Gadalla, A. M., & Bower, B. (1988). The role of catalyst support on the activity of nickel for reforming methane with CO2. *Chemical Engineering Science, 43*(11), 3049-3062. doi:http://dx.doi.org/10.1016/0009-2509(88)80058-7

Gadde, S., Wu, J., Gulati, A., McQuiggan, G., Koestlin, B., & Prade, B. (2006). *Syngas capable combustion systems development for advanced gas turbines.* Paper presented at the ASME Turbo Expo 2006: Power for Land, Sea, and Air.

Gallego, G. S., Batiot-Dupeyrat, C., Barrault, J., Florez, E., & Mondragón, F. (2008). Dry reforming of methane over LaNi1−yByO3±δ (B = Mg, Co) perovskites used as catalyst precursor. *Applied Catalysis A: General, 334*(1–2), 251-258. doi:http://dx.doi.org/10.1016/j.apcata.2007.10.010

Gallego, G. S., Mondragón, F., Barrault, J., Tatibouët, J.-M., & Batiot-Dupeyrat, C. (2006). CO2 reforming of CH4 over La–Ni based perovskite precursors. *Applied Catalysis A: General, 311*, 164-171. doi:http://dx.doi.org/10.1016/j.apcata.2006.06.024

García-Diéguez, M., Finocchio, E., Larrubia, M. Á., Alemany, L. J., & Busca, G. (2010). Characterization of alumina-supported Pt, Ni and PtNi alloy catalysts for the dry reforming of methane. *Journal of Catalysis, 274*(1), 11-20. doi:http://doi.org/10.1016/j.jcat.2010.05.020

García-Diéguez, M., Pieta, I. S., Herrera, M. C., Larrubia, M. A., Malpartida, I., & Alemany, L. J. (2010). Transient study of the dry reforming of methane over Pt supported on different γ-Al2O3. *Catalysis Today, 149*(3–4), 380-387. doi:http://dx.doi.org/10.1016/j.cattod.2009.07.099

Gaudernack, B., & Lynum, S. (1998). Hydrogen from natural gas without release of CO2 to the atmosphere. *International Journal of Hydrogen Energy, 23*(12), 1087-1093. doi:http://dx.doi.org/10.1016/S0360-3199(98)00004-4

Glicksman, L. R., & McAndrews, G. (1985). The effect of bed width on the hydrodynamics of large particle fluidized beds. *Powder Technology, 42*(2), 159-167. doi:http://dx.doi.org/10.1016/0032-5910(85)80049-8

Gómez-Barea, A., & Leckner, B. (2013). Estimation of gas composition and char conversion in a fluidized bed biomass gasifier. *Fuel, 107*, 419-431. doi:http://dx.doi.org/10.1016/j.fuel.2012.09.084

Grzybowska, B., Haber, J., & Janas, J. (1977). Interaction of allyl iodide with molybdate catalysts for the selective oxidation of hydrocarbons. *Journal of Catalysis, 49*(2), 150-163. doi:http://dx.doi.org/10.1016/0021-9517(77)90251-2

Guo, J., Lou, H., Zhao, H., Chai, D., & Zheng, X. (2004). Dry reforming of methane over nickel catalysts supported on magnesium aluminate spinels. *Applied Catalysis A: General, 273*(1–2), 75-82. doi:http://dx.doi.org/10.1016/j.apcata.2004.06.014

Gupta, M., & Wong, W. L. (2007). *Microwaves and metals*. Singapore: John Wiley & Sons.

Haimbaugh, R. E. (2001). *Practical induction heat treating*: ASM International.

Hamzehlouia, S., Latifi, M., & Chaouki, J. (2017). Development of a Novel Silica-Based Microwave Receptor for High Temperature Processes. *Pending submission*.

Hamzehlouia, S., Shabanian, J., Latifi, M., & Chaouki, J. (2017). Effect of Microwave Heating on the Performance of Catalytic Oxidation of n-Butane in a Gas-Solid Fluidized Bed Reactor. *Under preparation*.

Hao, Z., Zhu, Q., Jiang, Z., Hou, B., & Li, H. (2009). Characterization of aerogel Ni/Al2O3 catalysts and investigation on their stability for CH4-CO2 reforming in a fluidized bed. *Fuel Processing Technology, 90*(1), 113-121. doi:http://dx.doi.org/10.1016/j.fuproc.2008.08.004

Harvey, A. F., & Harvey, A. F. (1963). *Microwave engineering* (Vol. 50): Academic Press London and New York.

Hasted, J. B. (1972). Water: A Comprehensive Treatise. *The Physics and Physical Chemistry of Water, 1*, 255-305.

Hasted, J. B. (1973). *Aqueous dielectrics* (Vol. 17): Chapman and Hall London.

Heenan, N. I. (1968). Travelling Wave Dryers. *Microwave Power Engineering, 2*, 126-144.

Hickman, D. A., & Schmidt, L. D. (1993). Production of syngas by direct catalytic oxidation of methane. *Science-new york then washington-, 259*, 343-343.

Hill, N. E., Vaughan, W. E., Price, A. H., & Davies, M. (1969). *Dielectric properties and molecular behaviour* (Vol. 53): Van Nostrand Reinhold London.

Hoel, M., & Kverndokk, S. (1996). Depletion of fossil fuels and the impacts of global warming. *Resource and Energy Economics, 18*(2), 115-136. doi:http://dx.doi.org/10.1016/0928-7655(96)00005-X

Holmen, A., Olsvik, O., & Rokstad, O. A. (1995). Pyrolysis of natural gas: chemistry and process concepts. *Fuel Processing Technology, 42*(2–3), 249-267. doi:http://dx.doi.org/10.1016/0378-3820(94)00109-7

Horio, M., & Nonaka, A. (1987). A generalized bubble diameter correlation for gas-solid fluidized beds. *AIChE Journal, 33*(11), 1865-1872. doi:10.1002/aic.690331113

Horiuchi, T., Sakuma, K., Fukui, T., Kubo, Y., Osaki, T., & Mori, T. (1996). Suppression of carbon deposition in the CO2-reforming of CH4 by adding basic metal oxides to a Ni/Al2O3 catalyst. *Applied Catalysis A: General, 144*(1), 111-120. doi:http://dx.doi.org/10.1016/0926-860X(96)00100-7

Hou, Z., Chen, P., Fang, H., Zheng, X., & Yashima, T. (2006). Production of synthesis gas via methane reforming with CO on noble metals and small amount of noble-(Rh-) promoted Ni catalysts. *International Journal of Hydrogen Energy, 31*(5), 555-561. doi:http://dx.doi.org/10.1016/j.ijhydene.2005.06.010

Hu, Y. H., & Ruckenstein, E. (2002). Binary MgO-Based Solid Solution Catalysts for Methane Conversion to Syngas. *Catalysis Reviews, 44*(3), 423-453. doi:10.1081/cr-120005742

Hu, Y. H., & Ruckenstein, E. (2004). Catalytic Conversion of Methane to Synthesis Gas by Partial Oxidation and CO2 Reforming *Advances in Catalysis* (Vol. Volume 48, pp. 297-345): Academic Press.

Huangt, H. F. (1976). Temperature Control in a Microwawe Resonant Cavity System for lapìd Heating of Nylon Monofilament. *Journal of Microwave Power, 11*(4), 5.4.

Hughes, M. D., Yi-Jun, X., Jenkins, P., & McMorn, P. (2005). Tunable gold catalysts for selective hydrocarbon oxidation under mild conditions. *Nature, 437*(7062), 1132.

Hussain, Z., Khan, K. M., Basheer, N., & Hussain, K. (2011). Co-liquefaction of Makarwal coal and waste polystyrene by microwave–metal interaction pyrolysis in copper coil reactor. *Journal of Analytical and Applied Pyrolysis, 90*(1), 53-55. doi:http://dx.doi.org/10.1016/j.jaap.2010.10.002

Hussain, Z., Khan, K. M., & Hussain, K. (2010). Microwave–metal interaction pyrolysis of polystyrene. *Journal of Analytical and Applied Pyrolysis, 89*(1), 39-43. doi:http://dx.doi.org/10.1016/j.jaap.2010.05.003

IEA. (2016). *Energy and Air Pollution*. Paris, France: Inetrational Energy Agency.

Inui, T., & Spivey, J. J. (2002). *Reforming of CH4 by CO2, O2 and/or H2O* (Vol. 16): The Royal Society of Chemistry: London.

Ishii, T. K. (1974). Theoretical Basis for Decision to Microwave Approach for Industrial Processing. *JMPEE, 9*(4), 355-360.

Iskander, M. F. S., & Stuchly, S. S. (1972). A time domain technique for measurement of the dielectric properties of biological substances. *IEEE J. IM-21, 4*(425).

Istadi, I., Amin, N. A. S., & Aishah, N. (2005). Co-generation of C2 hydrocarbons and synthesis gases from methane and carbon dioxide: a thermodynamic analysis. *J. Nat. Gas Chem, 14*, 140-150.

Jablonski, E. L., Schmidhalter, I., De Miguel, S. R., Scelza, O. A., & Castro, A. A. (2005). *Dry reforming of methane on Pt/Al2O3–alkaline metal catalysts.* Paper presented at the 2nd mercosur congress on chemical engineering, Rio de.

Johnk, C. T. A. (1975). Engineering electromagnetic fields and waves. *New York, John Wiley and Sons, Inc., 1975. 667 p., 1*.

Jolly, J. A. (1972). Financial techniques for comparing the monetary gain of new manufacturing processes such as microwave heating. *J. Microwave Power, 7*(1), 5-16.

Jolly, J. A. (1976). Economics and Energy Utilization Aspects of the Application of Microwaves: A Tutorial Review. *J. Microwave Power, 11*(3), 233-245.

Jones, A. C., & O'Brien, P. (2008). *CVD of compound semiconductors: Precursor synthesis, developmeny and applications*: John Wiley & Sons.

Jones, C. A., Leonard, J. J., & Sofranko, J. A. (1987). Fuels for the future: remote gas conversion. *Energy & Fuels, 1*(1), 12-16. doi:10.1021/ef00001a002

Jones, D. A., Lelyveld, T. P., Mavrofidis, S. D., Kingman, S. W., & Miles, N. J. (2002a). Microwave heating applications in enviromnental engineering - a review. *Resources Conservation and Recycling, 34*(2), 75-90. doi:10.1016/s0921-3449(01)00088-x

Jones, D. A., Lelyveld, T. P., Mavrofidis, S. D., Kingman, S. W., & Miles, N. J. (2002b). Microwave heating applications in environmental engineering—a review. *Resources, Conservation and Recycling, 34*(2), 75-90. doi:http://dx.doi.org/10.1016/S0921-3449(01)00088-X

Kalinski, J. (1978). An industrial microwave attenuation monitor (MAM) and its application for continuous moisture content measurements'. *J. Microwave Power, 13*, 275-281.

Khaghanikavkani, E., & Farid, M. M. (2013). Mathematical Modelling of Microwave Pyrolysis. *International Journal of Chemical Reactor Engineering, 11*. doi:10.1515/ijcre-2012-0060

Khajeh Talkhoncheh, S., & Haghighi, M. (2015). Syngas production via dry reforming of methane over Ni-based nanocatalyst over various supports of clinoptilolite, ceria and alumina. *Journal of Natural Gas Science and Engineering, 23*, 16-25. doi:http://dx.doi.org/10.1016/j.jngse.2015.01.020

Khalesi, A., Arandiyan, H. R., & Parvari, M. (2008). Effects of Lanthanum Substitution by Strontium and Calcium in La-Ni-Al Perovskite Oxides in Dry Reforming of Methane. *Chinese Journal of Catalysis, 29*(10), 960-968. doi:http://dx.doi.org/10.1016/S1872-2067(08)60079-0

Kim, G. J., Cho, D.-S., Kim, K.-H., & Kim, J.-H. (1994). The reaction of CO2 with CH4 to synthesize H2 and CO over nickel-loaded Y-zeolites. *Catalysis Letters, 28*(1), 41-52. doi:10.1007/bf00812468

Kim, S. W., Ahn, J. Y., Kim, S. D., & Hyun Lee, D. (2003). Heat transfer and bubble characteristics in a fluidized bed with immersed horizontal tube bundle. *International Journal of Heat and Mass Transfer, 46*(3), 399-409. doi:https://doi.org/10.1016/S0017-9310(02)00296-X

Knowlton, T. M. (1999). Pressure and Temperature Effects in Fluid-Particle Systems. In W. C. Yang (Ed.), *Fluidization, Solid Handling and Processing: Industrial Applications* (pp. 111-152). New Jersey: Noyes.

Koberstein, E. (1973). Model Reactor Studies of the Hydrogen Cyanide Synthesis from Methane and Ammonia. *Industrial & Engineering Chemistry Process Design and Development, 12*(4), 444-448. doi:10.1021/i260048a010

Kraszewski, A. (1980). Microwave aquametry: A review. *J. Microwave Power, 15*(4), 209-220.

Krishna, R., van Baten, J. M., & Ellenberger, J. (1998). Scale effects in fluidized multiphase reactors. *Powder Technology, 100*(2–3), 137-146. doi:http://dx.doi.org/10.1016/S0032-5910(98)00134-X

Kunii, D., & Levenspiel, O. (1991). *Fluidization Engineering*. Boston: Butterworth-Heinemann.

Latifi, M., Berruti, F., & Briens, C. (2014). A novel fluidized and induction heated microreactor for catalyst testing. *Aiche Journal, 60*(9), 3107-3122.

Latifi, M., & Chaouki, J. (2015). A novel induction heating fluidized bed reactor: Its design and applications in high temperature screening tests with solid feedstocks and prediction of defluidization state. *Aiche Journal, 61*(5), 1507-1523. doi:10.1002/aic.14749

Lavoie, J.-M. (2014). Review on dry reforming of methane, a potentially more environmentally-friendly approach to the increasing natural gas exploitation. *Frontiers in Chemistry, 2*, 81. doi:10.3389/fchem.2014.00081

Lee, C. H., Luan, H. F., Bai, W. P., Lee, S. J., Jeon, T. S., Senzaki, Y., . . . Kwong, D. L. (2000, 10-13 Dec. 2000). *MOS characteristics of ultra thin rapid thermal CVD ZrO/sub 2/ and Zr silicate gate dielectrics.* Paper presented at the Electron Devices Meeting, 2000. IEDM '00. Technical Digest. International.

Lee, S. (1996). *Methane and its Derivatives* (Vol. 70): CRC Press.

Lewis, W. K., Gilliland, E. R., & Reed, W. A. (1949). Reaction of methane with copper oxide in a fluidized bed. *Industrial & Engineering Chemistry, 41*(6), 1227-1237.

Li, J., Wen, L., Qian, G., Cui, H., Kwauk, M., Schouten, J. C., & Van den Bleek, C. M. (1996). Structure heterogeneity, regime multiplicity and nonlinear behavior in particle-fluid systems. *Chemical Engineering Science, 51*(11), 2693-2698. doi:Doi: 10.1016/0009-2509(96)00138-8

Li, M.-w., Xu, G.-h., Tian, Y.-l., Chen, L., & Fu, H.-f. (2004). Carbon Dioxide Reforming of Methane Using DC Corona Discharge Plasma Reaction. *The Journal of Physical Chemistry A, 108*(10), 1687-1693. doi:10.1021/jp037008q

Lide, D. R. (2004). *CRC handbook of chemistry and physics* (Vol. 85): CRC press.

Liu, M., Zhang, Y., Bi, H., Grace, J. R., & Zhu, Y. (2010). Non-intrusive determination of bubble size in a gas–solid fluidized bed: An evaluation. *Chemical Engineering Science, 65*(11), 3485-3493. doi:http://dx.doi.org/10.1016/j.ces.2010.02.049

Liu, X., Sun, H., Chen, Y., Lau, R., & Yang, Y. (2008). Preparation of large particle MCM-41 and investigation on its fluidization behavior and application in single-walled carbon nanotube production in a fluidized-bed reactor. *Chemical Engineering Journal, 142*(3), 331-336. doi:http://dx.doi.org/10.1016/j.cej.2008.04.035

Luikov, A. V. (1964). Capillary-Porous Bodies. *Advances in heat transfer, 1*.

Luo, J. Z., Yu, Z. L., Ng, C. F., & Au, C. T. (2000). CO2/CH4 Reforming over Ni–La2O3/5A: An Investigation on Carbon Deposition and Reaction Steps. *Journal of Catalysis, 194*(2), 198-210. doi:http://dx.doi.org/10.1006/jcat.2000.2941

Ma, J., Fang, M., Li, P., Zhu, B., Lu, X., & Lau, N. T. (1997). Microwave-assisted catalytic combustion of diesel soot. *Applied Catalysis A: General, 159*(1), 211-228. doi:http://dx.doi.org/10.1016/S0926-860X(97)00043-4

MacLatchy, C. S., & Clements, R. M. (1980). Simple Technique for Measuring High Microwave Electric Field Strengths. *J. Microwave Power, 15*(1), 7-14.

Martínez, J. D., Mahkamov, K., Andrade, R. V., & Silva Lora, E. E. (2012). Syngas production in downdraft biomass gasifiers and its application using internal combustion engines. *Renewable Energy, 38*(1), 1-9. doi:http://dx.doi.org/10.1016/j.renene.2011.07.035

Menéndez, J. A., Arenillas, A., Fidalgo, B., Fernández, Y., Zubizarreta, L., Calvo, E. G., & Bermúdez, J. M. (2010). Microwave heating processes involving carbon materials. *Fuel Processing Technology, 91*(1), 1-8. doi:http://dx.doi.org/10.1016/j.fuproc.2009.08.021

Menéndez, J. A., Domínguez, A., Fernández, Y., & Pis, J. J. (2007). Evidence of Self-Gasification during the Microwave-Induced Pyrolysis of Coffee Hulls. *Energy & Fuels, 21*(1), 373-378. doi:10.1021/ef060331i

Metaxas, A. C. (1988). *Industrial Microwave Heating Power and Energy* (pp. 1 online resource (376 p.)).

Metaxas, A. C., & Meredith, R. J. (1983). *Industrial microwave heating*. London, UK: P. Peregrinus on behalf of the Institution of Electrical Engineers.

Miccio, F. (2013). On the integration between fluidized bed and Stirling engine for micro-generation. *Applied Thermal Engineering, 52*(1), 46-53. doi:http://dx.doi.org/10.1016/j.applthermaleng.2012.11.004

Motasemi, F., & Afzal, M. T. (2013). A review on the microwave-assisted pyrolysis technique. *Renewable & Sustainable Energy Reviews, 28*, 317-330. doi:10.1016/j.rser.2013.08.008

Muradov, N. (2001). Catalysis of methane decomposition over elemental carbon. *Catalysis Communications, 2*(3–4), 89-94. doi:http://dx.doi.org/10.1016/S1566-7367(01)00013-9

Muradov, N. (2001). Hydrogen via methane decomposition: an application for decarbonization of fossil fuels. *International Journal of Hydrogen Energy, 26*(11), 1165-1175. doi:http://dx.doi.org/10.1016/S0360-3199(01)00073-8

Muradov, N., Smith, F., & T-Raissi, A. (2005). Catalytic activity of carbons for methane decomposition reaction. *Catalysis Today, 102–103*(0), 225-233. doi:http://dx.doi.org/10.1016/j.cattod.2005.02.018

Muradov, N. Z. (1998). CO2-free production of hydrogen by catalytic pyrolysis of hydrocarbon fuel. *Energy & Fuels, 12*(1), 41-48. doi:10.1021/ef9701145

Murray, E. P., Tsai, T., & Barnett, S. A. (1999). A direct-methane fuel cell with a ceria-based anode. *Nature, 400*(6745), 649-651.

Mushtaq, F., Mat, R., & Ani, F. N. (2014). A review on microwave assisted pyrolysis of coal and biomass for fuel production. *Renewable and Sustainable Energy Reviews, 39*(0), 555-574. doi:http://dx.doi.org/10.1016/j.rser.2014.07.073

Naslain, R., & Langlais, F. (1986). CVD-processing of ceramic-ceramic composite materials. In R. Tressler, G. Messing, C. Pantano, & R. Newnham (Eds.), *Tailoring Multiphase and Composite Ceramics* (pp. 145-164): Springer US.

Nematollahi, B., Rezaei, M., Lay, E. N., & Khajenoori, M. (2012). Thermodynamic analysis of combined reforming process using Gibbs energy minimization method: In view of solid carbon formation. *Journal of Natural Gas Chemistry, 21*(6), 694-702. doi:http://dx.doi.org/10.1016/S1003-9953(11)60421-0

Nikoo, M. K., & Amin, N. A. S. (2011). Thermodynamic analysis of carbon dioxide reforming of methane in view of solid carbon formation. *Fuel Processing Technology, 92*(3), 678-691. doi:http://dx.doi.org/10.1016/j.fuproc.2010.11.027

Oehr, C., & Suhr, H. (1988). Thin copper films by plasma CVD using copper-hexafluoro-acetylacetonate. *Applied Physics A, 45*(2), 151-154. doi:10.1007/BF02565202

Ohlsson, T. H., Bengtsson, N. E., & Risman, P. O. (1974). The frequency and temperature dependence of dielectric food data as determined by a cavity perturbation technique. *Journal of Microwave Power, 9*(2), 129-145.

Omae, I. (2006). Aspects of carbon dioxide utilization. *Catalysis Today, 115*(1–4), 33-52. doi:http://dx.doi.org/10.1016/j.cattod.2006.02.024

Ostrowski, T., Giroir-Fendler, A., Mirodatos, C., & Mleczko, L. (1998). Comparative study of the catalytic partial oxidation of methane to synthesis gas in fixed-bed and fluidized-bed membrane reactors: Part I: A modeling approach. *Catalysis Today, 40*(2), 181-190.

Oyama, S. T., Hacarlioglu, P., Gu, Y., & Lee, D. (2012). Dry reforming of methane has no future for hydrogen production: Comparison with steam reforming at high pressure in standard and membrane reactors. *International Journal of Hydrogen Energy, 37*(13), 10444-10450. doi:http://dx.doi.org/10.1016/j.ijhydene.2011.09.149

Pakhare, D., Shaw, C., Haynes, D., Shekhawat, D., & Spivey, J. (2013). Effect of reaction temperature on activity of Pt- and Ru-substituted lanthanum zirconate pyrochlores (La2Zr2O7) for dry (CO2) reforming of methane (DRM). *Journal of CO2 Utilization, 1*, 37-42. doi:http://dx.doi.org/10.1016/j.jcou.2013.04.001

Pakhare, D., & Spivey, J. (2014). A review of dry (CO2) reforming of methane over noble metal catalysts. *Chemical Society Reviews, 43*(22), 7813-7837. doi:10.1039/c3cs60395d

Pandit, R. B., & Prasad, S. (2003). Finite element analysis of microwave heating of potato—transient temperature profiles. *Journal of Food Engineering, 60*(2), 193-202. doi:http://dx.doi.org/10.1016/S0260-8774(03)00040-2

Papp, H., Schuler, P., & Zhuang, Q. (1996). CO2 reforming and partial oxidation of methane. *Topics in Catalysis, 3*(3), 299-311. doi:10.1007/bf02113856

Perkin, R. M. (1979). Prospects of drying with radio frequency and microwave electromagnetic fields. *Capenhurst Electr. Council Res. Centre Rep. ECRC/M 1235, 1979*.

Pert, E., Carmel, Y., Birnboim, A., Olorunyolemi, T., Gershon, D., Calame, J., . . . Wilson, O. C. (2001). Temperature measurements during microwave processing: The significance of

thermocouple effects. *Journal of the American Ceramic Society, 84*(9), 1981-1986. doi:10.1111/j.1151-2916.2001.tb00946.x

Philippe, R., Serp, P., Kalck, P., Kihn, Y., Bordère, S., Plee, D., . . . Caussat, B. (2009). Kinetic study of carbon nanotubes synthesis by fluidized bed chemical vapor deposition. *Aiche Journal, 55*(2), 450-464. doi:10.1002/aic.11676

Pimentel, D., & Patzek, T. W. (2008). Biofuels, solar and wind as renewable energy systems. *Benefits and risks. New York: Springer*.

Podkolzin, S. G., Stangland, E. E., Jones, M. E., Peringer, E., & Lercher, J. A. (2007). Methyl chloride production from methane over lanthanum-based catalysts. *Journal of the American Chemical Society, 129*(9), 2569-2576.

Poling, B. E., Prausnitz, J. M., & O'Connell, J. P. (2001). *The properties of gases and liquids* (Vol. 5): Mcgraw-hill New York.

Puschner, H. (1966). Heating with microwaves. *Fundamentals, Components, and Circuit Technique, Philips Gloeilampenfabrieken, Eindhoven, Netherlands*.

Puskas, I. (1995). Natural gas to syncrude: Making the process pay off. *CHEMTECH, 25*(12).

Reitmeier, R. E., Atwood, K., Bennett, H. A., & Baugh, H. M. (1948). Production of Synthesis Gas by Reacting Light Hydrocarbons Wit Steam and Carbon Dioxide. *Ind. Eng. Chem., 40*, 620-626.

Riedel, T., Claeys, M., Schulz, H., Schaub, G., Nam, S.-S., Jun, K.-W., . . . Lee, K.-W. (1999). Comparative study of Fischer–Tropsch synthesis with H2/CO and H2/CO2 syngas using Fe- and Co-based catalysts. *Applied Catalysis A: General, 186*(1–2), 201-213. doi:http://dx.doi.org/10.1016/S0926-860X(99)00173-8

Ross, J. R. H. (2005). Natural gas reforming and CO2 mitigation. *Catalysis Today, 100*(1–2), 151-158. doi:http://dx.doi.org/10.1016/j.cattod.2005.03.044

Rostrup-Nielsen, J. R. (1991). Promotion by poisoning. *Studies in Surface Science and Catalysis, 68*, 85-101.

Rostrup-Nielsen, J. R. (1994). Catalysis and large-scale conversion of natural gas. *Catalysis Today, 21*(2), 257-267. doi:http://dx.doi.org/10.1016/0920-5861(94)80147-9

Rostrup-Nielsen, J. R. (2000). New aspects of syngas production and use. *Catalysis Today, 63*(2–4), 159-164. doi:http://dx.doi.org/10.1016/S0920-5861(00)00455-7

Rostrup-Nielsen, J. R., & Hansen, J. H. B. (1993). CO2-Reforming of Methane over Transition Metals. *Journal of Catalysis, 144*(1), 38-49. doi:http://dx.doi.org/10.1006/jcat.1993.1312

Rostrup-Nielsen, J. R., Sehested, J., & Nørskov, J. K. (2002). Hydrogen and synthesis gas by steam- and C02 reforming *Advances in Catalysis* (Vol. Volume 47, pp. 65-139): Academic Press.

Roy, R., Agarwal, D., Chen, J. P., & Gedevanishvili, S. (1999). Full sintering of powdered-metal bodies in a microwave field. *Nature, 399*(6737), 668-670.

Rüdisüli, M., Schildhauer, T. J., Biollaz, S. M. A., & van Ommen, J. R. (2012). Scale-up of bubbling fluidized bed reactors — A review. *Powder Technology, 217*(0), 21-38. doi:10.1016/j.powtec.2011.10.004

Rudnev, V., Loveless, D., Cook, R. L., & Black, M. (2002). *Handbook of induction heating*: CRC Press.

Russell, A. D., Antreou, E. I., Lam, S. S., Ludlow-Palafox, C., & Chase, H. A. (2012). Microwave-assisted pyrolysis of HDPE using an activated carbon bed. *RSC Advances, 2*(17), 6756-6760. doi:10.1039/C2RA20859H

Rzepecka, M. A., & Pereira, M. (1974). Permittivity of some dairy products at 2450 MHz. *Journal of Microwave Power, 9*(4), 277-288.

Sabatier, P., & Senderens, J.-B. (1902). New synthesis of methane. *CR Acad. Sci. Paris, 134*, 514-516.

Saidur, R., Islam, M. R., Rahim, N. A., & Solangi, K. H. (2010). A review on global wind energy policy. *Renewable and Sustainable Energy Reviews, 14*(7), 1744-1762. doi:http://dx.doi.org/10.1016/j.rser.2010.03.007

Salameh, M. G. (2003). Can renewable and unconventional energy sources bridge the global energy gap in the 21st century? *Applied Energy, 75*(1), 33-42. doi:http://dx.doi.org/10.1016/S0306-2619(03)00016-3

Samih, S., & Chaouki, J. (2014). Development of a fluidized bed thermogravimetric analyzer. *Aiche Journal, 61*(1), 84-89. doi:10.1002/aic.14637

See, C. H., & Harris, A. T. (2008). CaCo3 supported Co-Fe catalysts for carbon nanotube synthesis in fluidized bed reactors. *Aiche Journal, 54*(3), 657-664. doi:10.1002/aic.11403

Serban, M., Lewis, M. A., Marshall, C. L., & Doctor, R. D. (2003). Hydrogen production by direct Contact pyrolysis of natural gas. *Energy & Fuels, 17*(3), 705-713. doi:10.1021/ef020271q

Shabanian, J., & Chaouki, J. (2015). Fluidization characteristics of a bubbling gas-solid fluidized bed at high temperature in the presence of interparticle forces. *Chem. Eng. J., Submitted for publication*.

Shafiee, S., & Topal, E. (2008). An econometrics view of worldwide fossil fuel consumption and the role of US. *Energy Policy, 36*(2), 775-786. doi:http://dx.doi.org/10.1016/j.enpol.2007.11.002

Shafiee, S., & Topal, E. (2009). When will fossil fuel reserves be diminished? *Energy Policy, 37*(1), 181-189. doi:http://dx.doi.org/10.1016/j.enpol.2008.08.016

Shah, N., Panjala, D., & Huffman, G. P. (2001). Hydrogen production by catalytic decomposition of methane. *Energy & Fuels, 15*(6), 1528-1534. doi:10.1021/ef0101964

Sheldon, R. (2012). *Metal-catalyzed oxidations of organic compounds: mechanistic principles and synthetic methodology including biochemical processes*: Elsevier.

Sheldon, R. A. (1991). Heterogeneous Catalytic Oxidation and Fine Chemicals. *Studies in Surface Science and Catalysis, 59*, 33-54. doi:http://dx.doi.org/10.1016/S0167-2991(08)61106-4

Shimizu, K.-I., Kaneko, T., Fujishima, T., Kodama, T., Yoshida, H., & Kitayama, Y. (2002). Selective oxidation of liquid hydrocarbons over photoirradiated TiO2 pillared clays. *Applied Catalysis A: General, 225*(1), 185-191. doi:http://dx.doi.org/10.1016/S0926-860X(01)00863-8

Sinha, A. K., Seelan, S., Tsubota, S., & Haruta, M. (2004). Catalysis by Gold Nanoparticles: Epoxidation of Propene. *Topics in Catalysis, 29*(3), 95-102. doi:10.1023/b:toca.0000029791.69935.53

Sinha, A. K., Seelan, S., Tsubota, S., & Haruta, M. (2004). A Three-Dimensional Mesoporous Titanosilicate Support for Gold Nanoparticles: Vapor-Phase Epoxidation of Propene with High Conversion. *Angewandte Chemie International Edition, 43*(12), 1546-1548. doi:10.1002/anie.200352900

Sloan, E. D. (2003). Fundamental principles and applications of natural gas hydrates. *Nature, 426*(6964), 353-363.

Sobhy, A., & Chaouki, J. (2010). Microwave-assisted Biorefinery. *Cisap4: 4th International Conference on Safety & Environment in Process Industry, 19*, 25-29. doi:Doi 10.3303/Cet1019005

Sodesawa, T., Dobashi, A., & Nozaki, F. (1979). Catalytic reaction of methane with carbon dioxide. *Reaction Kinetics and Catalysis Letters, 12*(1), 107-111. doi:10.1007/bf02071433

Solangi, K. H., Islam, M. R., Saidur, R., Rahim, N. A., & Fayaz, H. (2011). A review on global solar energy policy. *Renewable and Sustainable Energy Reviews, 15*(4), 2149-2163. doi:http://dx.doi.org/10.1016/j.rser.2011.01.007

Speight, J. G. (1993). *Gas processing: environmental aspects and methods*: Butterworth-Heinemann.

Steele, B. C. H., & Heinzel, A. (2001). Materials for fuel-cell technologies. *Nature, 414*(6861), 345-352.

Steele, D. J., & Kent, M. (1978). *Microwave stripline techniques applied to moisture measurement in food materials.* Paper presented at the Proc. 1978 IMPI Symp. On Microwave Power.

Steinberg, M. (1998). Production of hydrogen and methanol from natural gas with reduced CO2 emission. *International Journal of Hydrogen Energy, 23*(6), 419-425. doi:http://dx.doi.org/10.1016/S0360-3199(97)00092-X

Steinberg, M. (1999). Fossil fuel decarbonization technology for mitigating global warming. *International Journal of Hydrogen Energy, 24*(8), 771-777. doi:http://dx.doi.org/10.1016/S0360-3199(98)00128-1

Stuchly, S. S. (1970). Dielectric properties of some granular solids containing water. *J. Microwave Power, 5*(2), 62-68.

Tai, H.-S., & Jou, C.-J. G. (1999). Application of granular activated carbon packed-bed reactor in microwave radiation field to treat phenol. *Chemosphere, 38*(11), 2667-2680. doi:http://dx.doi.org/10.1016/S0045-6535(98)00432-9

Temur Ergan, B., & Bayramoğlu, M. (2011). Kinetic Approach for Investigating the "Microwave Effect": Decomposition of Aqueous Potassium Persulfate. *Industrial & Engineering Chemistry Research, 50*(11), 6629-6637. doi:10.1021/ie200095y

Terselius, B., & Ranby, B. (1978). Cavity perturbation measurements of the dielectric properties of vulcanizing rubber and polyethylene compounds. *J. Microwave Power, 13*, 327-335.

Teuner, S. (1987). A new process to make oxo-feed. *Hydrocarbon Process.;(United States), 66*(7).

Thostenson, E. T., & Chou, T. W. (1999). Microwave processing: fundamentals and applications. *Composites Part a-Applied Science and Manufacturing, 30*(9), 1055-1071. doi:Doi 10.1016/S1359-835x(99)00020-2

Timilsina, G. R., Kurdgelashvili, L., & Narbel, P. A. (2012). Solar energy: Markets, economics and policies. *Renewable and Sustainable Energy Reviews, 16*(1), 449-465. doi:http://dx.doi.org/10.1016/j.rser.2011.08.009

Timmons, D., Harris, J. M., & Roach, B. (2014). The economics of renewable energy. *Global Development And Environment Institute, Tufts University*, 52.

Tinga, W. R. (1970). *Multiphase dielectric theory applied to cellulose mixtures.*

Tinga, W. R., & Nelson, S. O. (1973). Dielectric properties of materials for microwave processing-tabulated. *J. Microwave Power, 8*(1), 23-66.

To, E. C., Mudgett, R. E., Wang, D. I. C., Goldblith, S. A., & Decareau, R. V. (1974). Dielectric properties of food materials. *J. Microwave Power, 9*(4), 303-315.

Treybal, R. E. (1981). *Mass-Transfer Operations* (Third Edition ed.). London: McGraw-Hill Book Company.

Tsai, H. L., & Wang, C. S. (2008). Thermodynamic equilibrium prediction for natural gas dry reforming in thermal plasma reformer. *Journal of the Chinese Institute of Engineers, 31*(5), 891-896.

Turner, J. A. (1999). A Realizable Renewable Energy Future. *Science, 285*(5428), 687-689. doi:10.1126/science.285.5428.687

Udengaard, N. R. (1992). Sulfur passivated reforming process lowers syngas H sub 2/CO ratio. *Oil and Gas Journal;(United States), 90*(10).

Uhlig, H. H., & Keyes, F. G. (1933). The Dependence of the Dielectric Constants of Gases on Temperature and Density. *The Journal of Chemical Physics, 1*(2), 155-159.

Undri, A., Frediani, M., Rosi, L., & Frediani, P. (2014). Reverse polymerization of waste polystyrene through microwave assisted pyrolysis. *Journal of Analytical and Applied Pyrolysis, 105*, 35-42. doi:http://dx.doi.org/10.1016/j.jaap.2013.10.001

Usman, M., Wan Daud, W. M. A., & Abbas, H. F. (2015). Dry reforming of methane: Influence of process parameters—A review. *Renewable and Sustainable Energy Reviews, 45*, 710-744. doi:http://dx.doi.org/10.1016/j.rser.2015.02.026

Vahlas, C., Caussat, B., Serp, P., & Angelopoulos, G. N. (2006). Principles and applications of CVD powder technology. *Materials Science and Engineering: R: Reports, 53*(1–2), 1-72. doi:http://dx.doi.org/10.1016/j.mser.2006.05.001

Vernon, P. D. F., Green, M. L. H., Cheetham, A. K., & Ashcroft, A. T. (1990). Partial oxidation of methane to synthesis gas. *Catalysis Letters, 6*(2), 181-186.

Von Hippel, A. R. (1954). *Dielectric materials and applications ; papers by twenty-two contributors*. Cambridge New York: Technology Press of M.I.T. ; Wiley.

Vos, B., Mosman, J., Zhang, Y., Poels, E., & Bliek, A. (2003). Impregnated carbon as a susceptor material for low loss oxides in dielectric heating. *Journal of Materials Science, 38*(1), 173-182. doi:10.1023/a:1021138505264

Wang, J., & Sun, X. (2012). Understanding and recent development of carbon coating on LiFePO4 cathode materials for lithium-ion batteries. *Energy & Environmental Science, 5*(1), 5163-5185. doi:10.1039/c1ee01263k

Wang, S., Lu, G. Q., & Millar, G. J. (1996). Carbon Dioxide Reforming of Methane To Produce Synthesis Gas over Metal-Supported Catalysts: State of the Art. *Energy & Fuels, 10*(4), 896-904. doi:10.1021/ef950227t

Warnecke, R. (2000). Gasification of biomass: comparison of fixed bed and fluidized bed gasifier. *Biomass and Bioenergy, 18*(6), 489-497. doi:http://dx.doi.org/10.1016/S0961-9534(00)00009-X

Weizhong, Q., Fei, W., Zhanwen, W., Tang, L., Hao, Y., Guohua, L., . . . Xiangyi, D. (2003). Production of carbon nanotubes in a packed bed and a fluidized bed. *Aiche Journal, 49*(3), 619-625. doi:10.1002/aic.690490308

White, G. A., Roszkowski, T. R., & Stanbridge, D. W. (1975). Predict carbon formation.[Synthesis gas and SNG operations]. *Hydrocarbon Process.;(United States), 54*(7).

White, J. R. (1970). Measuring the strength of the microwave field in a cavity. *Journal of Microwave Power, 5*(2), 145-147.

Wiesbrock, F., Hoogenboom, R., & Schubert, U. S. (2004). Microwave-assisted polymer synthesis: State-of-the-art and future perspectives. *Macromolecular Rapid Communications, 25*(20), 1739-1764. doi:10.1002/marc.200400313

Wilhelm, D. J., Simbeck, D. R., Karp, A. D., & Dickenson, R. L. (2001). Syngas production for gas-to-liquids applications: technologies, issues and outlook. *Fuel Processing Technology, 71*(1–3), 139-148. doi:http://dx.doi.org/10.1016/S0378-3820(01)00140-0

Wiser, R., Bolinger, M., Barbose, G., Darghouth, N., Hoen, B., Mills, A., . . . Widiss, R. 2015 Wind Technologies Market Report. *Energy Efficiency and Renewable Energy*.

Wu, K. T., Lee, H. T., Juch, C. I., Wan, H. P., Shim, H. S., Adams, B. R., & Chen, S. L. (2004). Study of syngas co-firing and reburning in a coal fired boiler. *Fuel, 83*(14–15), 1991-2000. doi:http://dx.doi.org/10.1016/j.fuel.2004.03.015

Wurzel, T., Malcus, S., & Mleczko, L. (2000). Reaction engineering investigations of CO2 reforming in a fluidized-bed reactor. *Chemical Engineering Science, 55*(18), 3955-3966. doi:http://dx.doi.org/10.1016/S0009-2509(99)00444-3

Xu, Y., & Yan, X.-T. (2010). Introduction to chemical vapour deposition. *Chemical Vapour Deposition: An Integrated Engineering Design for Advanced Materials*, 1-28.

Yadav, G. D., & Borkar, I. V. (2006). Kinetic modeling of microwave-assisted chemoenzymatic epoxidation of styrene. *Aiche Journal, 52*(3), 1235-1247. doi:10.1002/aic.10700

Yamazaki, O., Nozaki, T., Omata, K., & Fujimoto, K. (1992). Reduction of carbon dioxide by methane with Ni-on-MgO-CaO containing catalysts. *Chemistry letters, 21*(10), 1953-1954.

Yarlagadda, P. S., Morton, L. A., Hunter, N. R., & Gesser, H. D. (1990). Temperature oscillations during the high-pressure partial oxidation of methane in a tubular flow reactor. *Combustion and Flame, 79*(2), 216-218.

Yaws, C. L. (1999). *Chemical properties handbook*: McGraw-Hill.

Yen, Y.-w., Huang, M.-D., & Lin, F.-J. (2008). Synthesize carbon nanotubes by a novel method using chemical vapor deposition-fluidized bed reactor from solid-stated polymers. *Diamond and Related Materials, 17*(4–5), 567-570. doi:http://dx.doi.org/10.1016/j.diamond.2007.12.020

York, A. P., Xiao, T., & Green, M. L. (2003). Brief overview of the partial oxidation of methane to synthesis gas. *Topics in Catalysis, 22*(3-4), 345-358.

York, A. P. E., Xiao, T., & Green, M. L. H. (2003). Brief Overview of the Partial Oxidation of Methane to Synthesis Gas. *Topics in Catalysis, 22*(3), 345-358. doi:10.1023/A:1023552709642

Zabrodskiĭ, S. S. (1966). *Hydrodynamics and heat transfer in fluidized beds*: Massachusetts Institute of Technology.

Zhang, M., Tang, J., Mujumdar, A. S., & Wang, S. (2006). Trends in microwave-related drying of fruits and vegetables. *Trends in Food Science & Technology, 17*(10), 524-534. doi:10.1016/j.tifs.2006.04.011

Zhang, Z. L., & Verykios, X. E. (1994). Carbon dioxide reforming of methane to synthesis gas over supported Ni catalysts. *Catalysis Today, 21*(2), 589-595. doi:http://dx.doi.org/10.1016/0920-5861(94)80183-5

Zheludev, I. S., & Tybulewicz, A. (1971). *Physics of crystalline dielectrics* (Vol. 2): Plenum Press New York.

Zinn, S., & Semiatin, S. (1988). *Elements of induction heating: Design, control and applications*. Metals PArk, Ohio: ASM International.